

**THE SYNTHESIS, CATALYTIC TESTING, RECOVERY AND  
REUSE OF FLUOROUS AND NON-FLUOROUS  
ASYMMETRIC LIGANDS AND CATALYSTS**

Thesis submitted for the degree of

Doctor of Philosophy

At the University of Leicester

by

Andrew John West MChem (Leicester)

Department of Chemistry

University of Leicester



October 2004

UMI Number: U195284

All rights reserved

INFORMATION TO ALL USERS

The quality of this reproduction is dependent upon the quality of the copy submitted.

In the unlikely event that the author did not send a complete manuscript and there are missing pages, these will be noted. Also, if material had to be removed, a note will indicate the deletion.



UMI U195284

Published by ProQuest LLC 2013. Copyright in the Dissertation held by the Author.  
Microform Edition © ProQuest LLC.

All rights reserved. This work is protected against  
unauthorized copying under Title 17, United States Code.

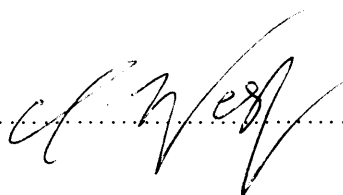


ProQuest LLC  
789 East Eisenhower Parkway  
P.O. Box 1346  
Ann Arbor, MI 48106-1346

## Statement of Originality

The experimental work in this thesis has been carried out by the author in the department of chemistry at the University of Leicester between September 2001 and July 2004. The work has not been submitted, and is not presently being submitted, for any other degree at this or any other university.

Signed.....



Date...13/12/04.....

Andrew West

University of Leicester

University Road,

Leicester.

LE1 7RH

## Acknowledgements

First of all, I would like to thank my family for their love and support over all the many years I have been in education. I hope I have done you all proud. Next I should thank my supervisors, Eric Hope and Alison Stuart, for their guidance over the three years and their help with the many problems a Ph. D. creates. I save the majority of my thanks and praise for the many people I have worked with in the lab over my time at Leicester. They make the lab the great place it is to work, kept me sane when things were going wrong and were always there with a friendly word and pints of lager when I was ready to give up. I give special thanks to James Bennett, Dan Duncan, Jose Vidal and Donna Palmer, our surrogate fluorine group member, for great friendships, advice and proofreading (sorry for boring you all!). Thanks also to Wayne Eltringham for useful discussions on the intricacies and inabilities of chiral GC (and beer!). I also owe an enormous debt to our talented post doc. and my good friend Dave Adams who, despite a full-time job, still proofread my thesis from start to finish in an impressive two weeks including time in transit. Better than I did...!

I must thank Dr. Graham Eaton, Dr. Gerry Griffiths and Dr. John Fawcett for mass spectrometry, NMR spectroscopy and X-ray crystallographic help. Without their input, this thesis would be considerably shorter. I should also thank all of the other technical support staff who have aided me throughout my research.

Also, I must thank the University of Leicester and Merck Speciality Chemicals for the money they have provided to allow me to do this work and Julian Vaughan-Spickers and Martin Pellatt, my industrial supervisors, for their help with ideas and the patent. I also thank Crystal Faraday for interest in my research towards the end of my project and for sending me to Rhode Island for a week!

Finally I'd like to end on a quote. According to Martin Van Buren, it is easier to do a job right than explain why you didn't. I hope I don't have any explaining to do...

**Contents**

	Page Number
Statement of Originality	i
Abstract	ii
Acknowledgements	iii
Contents	iv
List of Abbreviations	ix
 <b>Chapter One – Introduction</b>	
1.1	Heterogeneous and Homogeneous catalysis 1
1.2	Techniques for Facile Product Separation 2
1.2.1.1	Supercritical Fluids 2
1.2.1.2	Co-solvents, Surfactants and Solubilising Groups 3
1.2.1.3	Uses of Supercritical Fluids 4
1.2.1.4	Supercritical Fluids – Conclusions 6
1.2.2.1	Ionic Liquids 7
1.2.2.2	Properties of Ionic Liquids 8
1.2.2.3	Uses of Ionic Liquids in Synthesis 8
1.2.2.4	Ionic Liquids – Conclusions 10
1.2.3.1	Biphase Catalysis 11
1.2.3.2	Aqueous Biphase Systems 11
1.2.3.3	Uses of Aqueous Biphase Systems 12
1.2.3.4	Fluorous Biphase Systems 14
1.2.3.5	Uses of Fluorous Biphase Systems in Catalysis 15
1.2.3.6	Biphase Catalysis – Conclusions 17
1.2.4.1	Supported Catalysis Systems 17
1.2.4.2	Organic Supports for Catalysis 18
1.2.4.3	Inorganic Supports for Catalysis 18
1.2.4.4	Supported Solvents for Catalysis – Supported Aqueous Phase Catalysis 19
1.2.4.5	Supported Solvents for Catalysis – Supported Organic Phase Catalysis 21
1.2.4.6	Supported Solvents for Catalysis – Supported Fluorous Phase Catalysis 22
1.2.4.7	Supported Catalysis – Conclusions 23
1.2.5.1	Dendrimers 23
1.2.5.2	Examples of the Use of Dendrimers 23
1.2.5.3	Dendrimers – Conclusions 25
1.2.6.1	Other Methodologies for Catalyst Recycle 26
1.3	Catalyst Recovery by Column Chromatography 27
1.3.1	Fluorous Solid Phase Extraction 27

1.4	Outline of Research	29
1.5	References for Chapter One	31
<b>Chapter Two – BINAP</b>		
2.1	The Investigation of BINAP	36
2.1.1	BINAP in Catalysis	36
2.1.2	Examples of Recyclable BINAP	38
2.1.3	Fluorous BINAP	42
2.2	Synthesis and Coordination Chemistry	46
2.2.1	The Synthesis of Light Fluorous BINAP Ligands	46
2.2.2	Coordination Chemistry – The Bonding In M-PX <sub>3</sub> Ligands	54
2.2.3	Coordination Chemistry – Complexes	56
2.2.4	Complexes of Platinum(II)	56
2.2.5	Complexes of Palladium(II)	58
2.2.6	Phosphine Selenides	59
2.3	Catalytic Testing	61
2.3.1	Hydrogenation Reactions	61
2.3.2	Chiral Induction	64
2.3.3.	Catalytic Asymmetric Hydrogenation – Results	64
2.4	Separation Studies	67
2.4.1	Separation of ( <i>R</i> )-BINAP and ( <i>R</i> )-Rf-BINAP by Distillation	68
2.4.2	Separation of ( <i>R</i> )-BINAP using Silica Gel	68
2.4.3	Separation of ( <i>R</i> )-Rf-BINAP Using FRP Silica Gel	70
2.4.4	BINAP – Conclusions	71
2.5	References for Chapter Two	73
<b>Chapter Three – MonoPhos</b>		
3.1	The Investigation of MonoPhos	76
3.1.1	Introduction to MonoPhos	76
3.1.2	Examples of Recyclable MonoPhos	82
3.2	Synthesis and Coordination Chemistry	83
3.2.1	The Synthesis of Rf-MonoPhos	83
3.2.2	Coordination Chemistry – Complexes	85
3.2.3	Complexes of Platinum(II)	85
3.2.4	Complexes of Palladium(II)	87
3.2.5	Complexes of Rhodium(III)	88

<b>3.3</b>	<b>Catalytic Testing</b>	<b>91</b>
3.3.1	Hydrogenation Reactions	91
3.3.2	Chiral Induction	92
3.3.3	Catalytic Asymmetric Hydrogenation – Results	94
3.3.4	Catalyst Separation Using Solid Phase Extraction	95
<b>3.4</b>	<b>Supported MonoPhos</b>	<b>97</b>
<b>3.5</b>	<b>Light Fluorous MonoPhos - Conclusions</b>	<b>98</b>
<b>3.6</b>	<b>Heavy Fluorous MonoPhos</b>	<b>99</b>
3.6.1	Ligand Synthesis	99
3.6.2	Coordination Chemistry – Complexes	101
3.6.3	Catalysis Using Rf <sub>4</sub> -MonoPhos	102
3.6.4	Heavy Fluorous MonoPhos – Conclusions	104
<b>3.7</b>	<b>References for Chapter Three</b>	<b>106</b>

#### **Chapter Four – Ti-BINOL Chemistry**

<b>4.1</b>	<b>Introduction</b>	<b>108</b>
4.1.1	Ti-BINOL Systems	108
4.1.2	The Mechanism of Chiral Induction	111
4.1.3	Recyclable Ti-BINOL Systems	114
<b>4.2</b>	<b>Results and Discussion</b>	<b>118</b>
4.2.1	The Addition of Diethylzinc	119
4.2.2	Separation Studies	121
4.2.3	The Addition of Diethylzinc using Rf <sub>4</sub> -BINOL	122
4.2.4	The Addition of Allyltri- <i>n</i> -butyltin	123
4.2.5	Separation Studies	124
4.2.6	Alternative Solid Supports	129
4.2.7	Partition coefficients	130
<b>4.3</b>	<b>Conclusions</b>	<b>131</b>
<b>4.4</b>	<b>References for Chapter Four</b>	<b>133</b>

#### **Chapter Five – Investigation of Palladium BINAP Chemistry**

<b>5.1</b>	<b>Introduction</b>	<b>134</b>
5.1.1	Pd/BINAP Chemistry	134
5.1.2	Recyclable Pd(II)-Diaqua Catalysts	137
<b>5.2</b>	<b>The Synthesis of Non-Fluorous and Light Fluorous Palladium(II) Diaqua Catalysts</b>	<b>138</b>

<b>5.3</b>	Catalytic Testing and Recovery of Palladium(II)-Diaqua Catalysts	139
<b>5.4</b>	Palladium Diaqua Catalysts Based on MonoPhos	142
<b>5.5</b>	Palladium Diaqua Catalysts – Conclusions	143
<b>5.6</b>	References for Chapter Five	145

## Chapter Six – Experimental Details

<b>6.1</b>	General Experimental Details	146
6.1.1	Nuclear Magnetic Resonance Spectroscopy	146
6.1.2	Mass Spectrometry	146
6.1.3	Elemental Analysis	146
6.1.4	Optical Rotation	146
6.1.5	Enantiomeric Purity Determination	146
6.1.6	IR Analyses	147
6.1.7	X-Ray Crystallography	147
6.1.8	ICP Spectroscopy	147
6.1.9	Starting Materials	147
<b>6.2</b>	Experimental Details for Chapter Two	147
6.2.1	Synthesis of BINAP-based Molecules	147
6.2.2	Determination of BINAP Partition Coefficients	158
6.2.3	Preparation of Coordination Complexes and Selenides	159
6.2.4	Catalytic Testing	166
6.2.5	Hydrogenation Using Catalyst Recovered by Product Distillation	169
6.2.6	Solid Separation and Ligand Reuse	170
<b>6.3</b>	Experimental Details for Chapter Three	173
6.3.1	Synthesis of MonoPhos and Light Fluorous MonoPhos Molecules	173
6.3.2	Preparation of Coordination Complexes	174
6.3.3	Catalytic Testing	178
6.3.4	Solid Phase Separation	180
6.3.5	Supported Catalysis	180
6.3.6	Synthesis of Heavy Fluorous ( <i>R</i> )-Rf <sub>4</sub> -MonoPhos and complexes	180
<b>6.4</b>	Experimental Details for Chapter Four	185
6.4.1	General Procedure for the Determination of BINOL Partition Coefficients	185
6.4.2	Catalytic Testing	185
6.4.3	General Procedure for Attempted Separation of BINOL and 1-Phenyl-propan-1-ol	186
6.4.4	Asymmetric Addition of Diethylzinc to Benzaldehyde using ( <i>R</i> )-Rf <sub>4</sub> -BINOL	186
6.4.5	General Catalysis Procedure for the Addition of Allyltri- <i>n</i> -butyltin to Benzaldehyde	186

6.4.6	General Procedure for the Separation of BINOL and 4-Phenyl-1-buten-4-ol	188
6.5	Experimental Details for Chapter Five	189
6.5.1	Synthesis of Palladium(II)-Diaqua Catalysts	189
6.6	References for Chapter Six	191

## Appendix

A 1	Crystal Data for ( <i>R</i> )-6,6'-Bis(perfluoro- <i>n</i> -hexyl)-2,2'-di(trifluoromethane-sulphonyloxy)-1,1'-binaphthyl	I
A 2	Crystal Data for Rf-BINAP	II
A 3	Crystal Data for [PdCl <sub>2</sub> (( <i>R</i> )-BINAP)]	III
A 4	Crystal Data for [RhCp*Cl <sub>2</sub> (( <i>S</i> )-MonoPhos)]	IV
A 5	Crystal Data for ( <i>R</i> )-4,4'-6,6'-tetrabromo-2,2'-dihexyloxy-1,1'-binaphthyl	V
A 6	Crystal Data for Sn-BINOL Polymer	VI
A 7	Inorganic Seminar Programme (Autumn/Winter 2001)	VII
A 8	Inorganic Seminar Programme (Winter/Spring 2002)	VIII
A 9	Inorganic Seminar Programme (Spring/Summer 2002)	IX
A 10	Inorganic Seminar Programme (Autumn/Winter 2002)	X
A 11	Inorganic Seminar Programme (Spring/Summer 2003)	XI
A 12	Inorganic Seminar Programme (Autumn/Winter 2003)	XII
A 13	Inorganic Seminar Programme (Spring/Summer 2004)	XIII
A 14	Conferences Attended	XIV
A 15	Presentations	XV
A 16	Publications and Awards	XVI
A 17	Lecture Courses Attended	XVII

## Abbreviations

ABC	Aqueous biphasic catalysis
acac	Pentane-2,4-dionate
Ar	Aryl
BArF	Tetra(3,5-bis(trifluoromethyl)phenyl)-boronate anion
BINAP	2,2'-Bis(diphenylphosphino)-1,1'-binaphthyl
BINAPO	BINAP oxide
BINOL	1,1'-Bi-2-naphthol
Bipy	2,2'-Bipyridine
BMIM	1- <i>n</i> -Butyl-3-methyl-imidazolium ion
Bn	Benzyl fragment
bs	Broad singlet
BSA	Bis(trimethylsilyl)acetamide
CAMP	Cyclohexyl-2-anisylmethyl phosphane
cod	1,5-Cyclooctadiene
Cp*	Pentamethylcyclopentadienyl
d	Doublet
DABCO	1,4-Diazabicyclo[2.2.2]octane
dba	Dibenzanthracene
DCM	Dichloromethane
dd	Doublet of doublets
DEAD	Diethyl azodicarboxylate
Diop	2,3- <i>O</i> -Isopropylidene-2,3-dihydroxy-1,4-bis(diphenylphosphino)-butane
Dipamp	1,2-Bis[( <i>o</i> -methoxyphenyl)phenylphosphino]ethane
DMAP	Dimethylamino pyridine
DMF	<i>N,N</i> -Dimethylformamide
DMSO	Dimethyl sulphoxide
dppe	1,2-Bis(diphenylphosphino)ethane
dppf	1,1'-Bis(diphenylphosphino)ferrocene
dppomf	1,1'-Bis(diphenylphosphino)octamethylferrocene
dppp	1,2-Bis(diphenylphosphino)propane
EA	Elemental analysis
EDCL	3-ethylcarbodiimide-1-(3-dimethylaminopropyl) hydrochloride

ee	Enantiomeric excess
EI	Electron impact
ES	Electrospray
Et <sub>2</sub> O	Diethyl ether
FAB	Fast atom bombardment
FC-72	Perfluoro- <i>n</i> -hexane
FRP	Fluorous reverse phase
FSPCE	Fluorous solid phase catalyst extraction
FSPE	Fluorous solid phase extraction
GC	Gas chromatography
H <sub>8</sub> -BINOL	5,6-5',6'-bis(cyclohexyl)-1,1'-bi-2-phenol
Herrmann's catalyst	<i>Trans</i> -Di- $\mu$ -acetatobis[2-(di- <i>o</i> -tolylphosphino)benzyl]dipalladium(II)
hfacac	1,1,1,6,6,6-hexafluoropentane-2,4-dionate
HMPT	Hexamethylphosphorus triamide
HOBt	1-hydroxybenzotriazole
HPLC	High performance liquid chromatography
Hz	Hertz
ICP	Inductively-coupled plasma
IL	Ionic liquid
<i>J</i>	Coupling constant
MeOH	Methanol
MonoPhos	1,1'-Bi-2-naphthyl-dimethylphosphoramidite
M.p.	Melting point
MTPA	$\alpha$ -Methoxy- $\alpha$ -trifluoromethylphenyl acetyl
NMR	Nuclear magnetic resonance
OR	Optical rotation
P <sub>c</sub>	Critical pressure
Ph	Phenyl fragment
PP3	Perfluoro-1,3-dimethylcyclohexane
ppb	Parts per billion
RCM	Ring closing metathesis
Rf <sub>4</sub> -BINOL	4,4'-6,6'-tetra(perfluoro- <i>n</i> -hexyl)-1,1'-bi-2-naphthol
Rf-BINAP	6,6'-Bis(perfluoro- <i>n</i> -hexyl)-2,2'-bis(diphenylphosphino)-1,1'-binaphthyl
Rf-BINOL	6,6'-Bis(perfluoro- <i>n</i> -hexyl)-1,1'-bi-2-naphthol

Rf-C <sub>2</sub> H <sub>2</sub> -BINAP	6,6'-Bis(1 <i>H</i> ,2 <i>H</i> -perfluoro- <i>n</i> -hexyl)-2,2'-bis(diphenylphosphino)-1,1'-binaphthyl
Rf-C <sub>2</sub> H <sub>4</sub> -BINAP	6,6'-Bis(1 <i>H</i> ,1 <i>H</i> ,2 <i>H</i> ,2 <i>H</i> -perfluoro- <i>n</i> -hexyl)-2,2'-bis(diphenylphosphino)-1,1'-binaphthyl
Rf <sub>4</sub> -MonoPhos	4,4'-6,6'-Tetra(perfluoro- <i>n</i> -hexyl)-1,1'-bi-2-naphthyl-dimethylphosphoramidite
Rf-MonoPhos	6,6'-Bis(perfluoro- <i>n</i> -hexyl)-1,1'-bi-2-naphthyl-dimethylphosphoramidite
Rf-MOP	2-(Di- <i>para</i> -perfluorohexyl-phenylphosphino)-2'-(1 <i>H</i> ,1 <i>H</i> -perfluorooctyloxy)-1,1'-binaphthyl
rpm	Revolutions per minute
R <sub>t</sub>	Retention time
s	Singlet
ss	Singlet with satellites
SAPC	Supported aqueous phase catalysis
scCO <sub>2</sub>	Supercritical carbon dioxide
SCF	Supercritical fluid
SAPC	Supported aqueous phase catalysis
SFPC	Supported fluorous phase catalysis
SLPC	Supported liquid phase catalysis
SOPC	Supported organic phase catalysis
t	Triplet
T <sub>c</sub>	Critical temperature
THF	Tetrahydrofuran
TMS	Tetramethylsilane
TOF	Turnover frequency
TPPTS	Triphenylphosphine trisulphonate, sodium salt
um	Unresolved multiplet

## Introduction

### 1.1 Heterogeneous and Homogeneous Catalysis

The benefits and drawbacks of homogeneous catalysis versus heterogeneous catalysis have been investigated by scientists for over fifty years since the discovery by Bodien that the hydrogenation of alkenes could be achieved using a soluble cobalt catalyst. Homogeneous catalysis, where the catalyst and reactants are in the same phase, has become a very important process since this publication, and now covers vast areas of chemistry.

However, heterogeneous catalysis, where the catalyst and reactants are in different phases, has been used in the industrial for comparatively longer period. The catalyst is usually present as a solid and the reactants as liquids or, more commonly, gases. Diffusion occurs at the interface between the solid and the gas on the surface of the catalyst. Therefore, to maximize the rate of reaction, small particles of catalyst are used to maximize the catalytically active surface area. Heterogeneous catalysis generally have far higher thermal stabilities than their homogeneous counterparts. This means that under more forcing conditions giving rise to fast rates of reaction. Also, recycling the catalyst is easily achieved by separation of the phases.

# Chapter One



“Get your facts right first and then you can distort them as much as you please.”

- Mark Twain

A major drawback to heterogeneous catalysis is its general lack of specificity and flexibility. A homogeneous catalyst can be tailored to catalyze a reaction specifically at one site on a reactant molecule, whereas this tailoring is generally not possible in heterogeneous systems. Also, for a solid-state catalyst, there are many different surface sites due to the method of catalyst preparation. Often, only one type of these sites is catalytically active towards the desired product, while the other site types are either inactive or catalyze undesired side-reactions. This results in a lower activity per metal centre than in homogeneous catalysis.

The tuning of homogeneous catalysis has become a vast area of research. In homogeneous systems, the catalyst is a discrete entity consisting of a single complex or combination of complexes, rather than a large collection of active species as in heterogeneous systems. The hydrogenation of alkenes using Wilkinson's Catalyst,  $[\text{CpRh}(\text{PPh}_3)_3]^+$  is an excellent example of a crystalline metal homogeneous catalyst. The triphenylphosphine ligands confer solubility in organic solvents to the complex and help to stabilize the varying oxidation states of the metal during reaction. The substrate is added as either a liquid or a gas, along with hydrogen. Both are taken up

# 1 Introduction

## 1.1 Heterogeneous and Homogeneous Catalysis

The benefits and drawbacks of homogeneous catalysis *versus* heterogeneous catalysis have been investigated by scientists for over fifty years since the disclosure by Roelen that the hydroformylation of olefins could be achieved using a soluble cobalt catalyst.<sup>1</sup> Homogeneous catalysis, where the catalysts and reactants are in the same phase, has become a very important process since this publication, and now covers vast areas of research.

However, heterogeneous catalysis, where the catalyst and reactants are in different phases, has been used in the sciences for a significantly longer period. The catalyst is usually present as a solid and the reactants as liquids or, more commonly, gases. Reaction occurs at the interface between the solid and the gas on the surface of the catalyst. Therefore, to maximise the rate of reaction, small particles of catalyst are generally employed to maximise the catalytically active surface area. Heterogeneous catalysts generally have far higher thermal stabilities than their homogeneous counterparts. Thus, reactions can be run under more forcing conditions giving rise to fast rates of reaction. Also, isolating the product from the catalyst is easily achieved by separation of the phases.

A simple example of heterogeneous catalysis is the reduction of ethene on a platinum surface using hydrogen.<sup>2</sup> Ethene gas and hydrogen gas are adsorbed onto the surface of a platinum catalyst and the ethene molecule is hydrogenated stepwise by two hydrogen atoms to form ethane. The ethane is then desorbed from the surface and released back into the gas phase.

A major drawback for heterogeneous catalysis is its general lack of specificity and tuneability. A homogeneous catalyst can be tailored to catalyse a reaction specifically at one site in a reactant molecule, whereas this tailoring is generally not possible in heterogeneous systems. Also, in a solid-state catalyst, there are many different surface sites due to the method of catalyst preparation.<sup>3</sup> Often, only one type of these sites is catalytically active towards the desired product, while the other site types are either inactive or catalyse undesired side-reactions. This results in a lower activity per metal centre than in homogeneous catalysis.

The tuning of homogeneous catalysts has become a vast area of research.<sup>4</sup> In homogeneous systems, the catalyst is a discrete entity consisting of a single complex or combination of complexes, rather than a large collection of active species as in heterogeneous systems. The hydrogenation of olefins using Wilkinson's Catalyst,  $[\text{C}(\text{I})\text{Rh}(\text{PPh}_3)_3]$ ,<sup>5</sup> is an excellent example of a transition metal homogeneous catalyst. The triphenylphosphine ligands confer solubility in organic solvents to the complex and help to stabilise the varying oxidation states of the metal during reaction. The substrate is added as either a liquid or a gas, along with hydrogen. Both are taken up

into solution to give a single phase containing catalyst and reactants. One catalytic cycle produces hydrogenated product and regenerates the active catalyst.

Although homogeneous catalysis has the advantages of more specific and controllable systems that can be studied and improved, it suffers from a general inability to isolate catalysts from products at the end of reaction. This is of vital importance for two reasons. Firstly, the employment of transition metals, particularly precious metals, and the use of expensive and difficult to prepare ligands make separation and reuse of the catalysts desirable, if not imperative, if the process is to be industrially viable. Secondly, where the catalysts are used in the pharmaceutical or fine chemical industries, there must be no contamination of the product with heavy metal residues. These problems have severely restricted the use of homogeneous catalysis in industry, even though much higher selectivities and specificities are attainable.

It is evident that homogeneous catalysis would be largely the industrially-preferred system if the problem of catalyst separation could be overcome. To this end, much research has been invested into the perfection of various techniques which allow the industrial employment of homogeneous systems, but which can provide a method of catalyst re-isolation at the termination of the reaction. This type of research can be placed under the banner of 'green chemistry'; an approach that aims to improve the efficiency and safety of given systems encompassing ideas such as waste minimisation being superior to treatment, maximising atom economy, reduction of solvents and the preference for catalytic reagents over stoichiometric ones. For a process to be truly 'green', the catalyst should not be discarded after it is separated but instead recycled. This not only minimises waste but also financial costs.

A number of techniques for the heterogenisation of homogeneous catalysts that allow catalyst recovery post-reaction including non-conventional solvents, multiphase systems and supported systems are examined in detail over the following sections. Each methodology attempts to overcome the problems outlined above, using various techniques to maintain or increase catalyst activity, selectivity and specificity while allowing catalyst and product separation at the end of the reaction and reuse of the catalyst.

## **1.2 Techniques with Facile Product Separation**

### **1.2.1.1 Supercritical Fluids**

As outlined in the previous section, homogeneous systems can be tailored to specific reactions much more easily than heterogeneous systems and, by judicious design of the catalyst, high yields and selectivities can be obtained. For the best product yields, selectivities and specificities, therefore, it is logical to also employ a tuneable solvent. Supercritical fluids (SCFs) are such solvents.<sup>6</sup>

A SCF is defined as a substance above its critical temperature ( $T_c$ ) and critical pressure ( $P_c$ ). The critical point represents the highest temperature and pressure at which the substance can exist as a vapour and liquid in equilibrium. At the critical point, the density of the liquid and gas are the same; the distinction between gas and liquid disappears.

Although a range of SCFs have been employed in research,<sup>7,8</sup> supercritical carbon dioxide (scCO<sub>2</sub>) is generally the solvent of choice. It is non-toxic, cheap and readily available on a large scale. It is also relatively inert. However, scCO<sub>2</sub> has not been studied seriously until recently because of its low solubilising power. To be soluble in scCO<sub>2</sub>, a molecule must be non-polar and have a low molecular weight,<sup>9</sup> which restricts the choice of catalysts, reagents and substrates which can be used. Recent improvements in the uses of surfactants, co-solvents and solubilising reagents (see Section 1.2.1.2) is, however, likely to lead to greater use of the solvent.

Supercritical reactions can, in theory, overcome the problem of catalyst/substrate separation due to the differing solubilities of the catalysts, substrates and products. Below a 'crossover pressure', increasing the temperature of the system decreases the solubility because the SCF density is reduced. This is known as 'retrograde behaviour'. Above the crossover pressure, increasing the temperature increases the solubility because the volatility of the solutes is increased.<sup>10</sup> Assuming that the components of the system have suitably different solubilities, changing the pressure or temperature of the system could selectively precipitate each of the components, which could then be isolated and, in the case of the catalyst, reused. This process fits the goals set out above: The catalyst is in a homogeneous system during the reaction allowing for high activity and selectivity, but can be made heterogeneous and, therefore, recoverable by changing the recyclable conditions.

### 1.2.1.2 Co-solvents, Surfactants and Solubilising Groups

Most SCFs that have a  $T_c$  below 100 °C are non-polar.<sup>9</sup> The exceptions to this are either expensive or toxic and so their use is not favoured. Because of this solvent non-polarity, it is necessary to modify the catalyst so that it, too, has non-polar regions to aid solubility. To achieve this, aryl groups are replaced with alkyl groups or substituted with non-polar perfluoroalkyl groups or chains (e.g. CF<sub>3</sub>, C<sub>6</sub>F<sub>13</sub>). A good example of the success of this method is a comparison of the supercritical solubility of the copper complexes [Cu(acac)<sub>2</sub>] and [Cu(hfacac)<sub>2</sub>] (acac = pentane-2,4-dionate, hfacac = 1,1,1,6,6,6-hexafluoropentane-2,4-dionate). [Cu(hfacac)<sub>2</sub>] is two hundred times more soluble in scCO<sub>2</sub> than [Cu(acac)<sub>2</sub>].<sup>11</sup> Another example showing the differences in solubility between aryl, alkyl and perfluoroalkyl is the study of the solubility of [Rh(hfacac)(R<sub>2</sub>PCH<sub>2</sub>CH<sub>2</sub>PR<sub>2</sub>)].<sup>12</sup> When R = phenyl, the complex is insoluble in scCO<sub>2</sub> and becomes sparingly soluble when phenyl is changed for cyclohexyl. However, the solubility is increased by a

factor of seven when R is changed to *para*-(1*H*,1*H*,2*H*,2*H*-perfluorodecyl)phenyl, C<sub>6</sub>H<sub>4</sub>-*p*-C<sub>2</sub>H<sub>4</sub>C<sub>8</sub>F<sub>17</sub>.

Addition of co-solvents has been shown to increase solubility,<sup>9,13</sup> with the addition of small volumes of methanol being common. The addition of counterions has also been used to effect better solubility. The [(3,5-(CF<sub>3</sub>)<sub>2</sub>C<sub>6</sub>H<sub>3</sub>)<sub>4</sub>B]<sup>-</sup> (BArF) anion has been shown to enhance the solubility of cationic rhodium complexes,<sup>7</sup> and tetraalkylammonium cations can enhance the solubility of anions.<sup>9</sup> The final method of increasing solubility is to add surfactants. These create aqueous reverse micelles in scCO<sub>2</sub> and generally contain alkyl or perfluoroalkyl tails to help the solubility. Surfactants have been used to solubilise hydrophilic reagents like KMnO<sub>4</sub>.<sup>14</sup>

### 1.2.1.3 Uses of Supercritical Fluids

The uses of supercritical fluids still remain few, although the polymerisation of supercritical ethene is an important industrial process that is used in the production of millions of tonnes of polythene per annum.<sup>12</sup> To date, most studies have involved hydrogenation,<sup>15</sup> asymmetric hydrogenation,<sup>7,16</sup> hydroformylation<sup>8,12</sup> and the hydrogenation of CO<sub>2</sub>.<sup>17,18</sup> Pertinent examples of these uses are outlined below.

Most work has been carried out on hydrogenation reactions. Leitner *et al.* have studied the hydrogenation of isoprene using the rhodium catalyst [Rh(hfacac)(R<sub>2</sub>PCH<sub>2</sub>CH<sub>2</sub>PR<sub>2</sub>)] where R equals C<sub>6</sub>H<sub>4</sub>-*m*-(C<sub>2</sub>H<sub>4</sub>C<sub>6</sub>F<sub>13</sub>) (Figure 1.1).

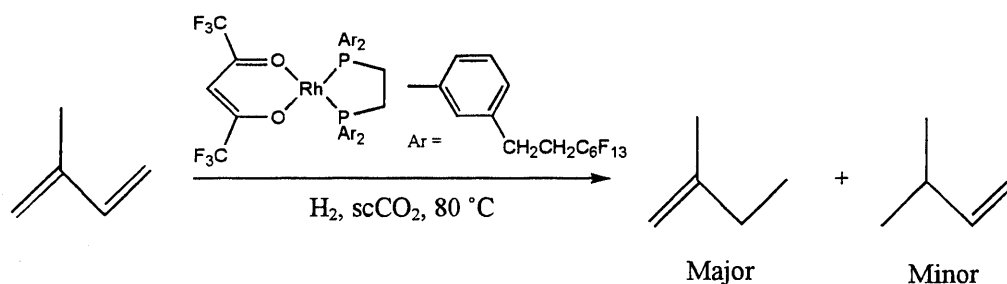


Figure 1.1. The hydrogenation of isoprene in scCO<sub>2</sub>

Whilst this reaction is successful, the rate is much slower than when the analogous 1,3-bis-(diphenylphosphino)propane (dppp) complex is used in common organic solvents.

Noyori *et al.* have used a ruthenium-based catalyst in the asymmetric hydrogenation of  $\alpha,\beta$ -unsaturated carboxylic acids such as tiglic acid<sup>16</sup> (Figure 1.2).

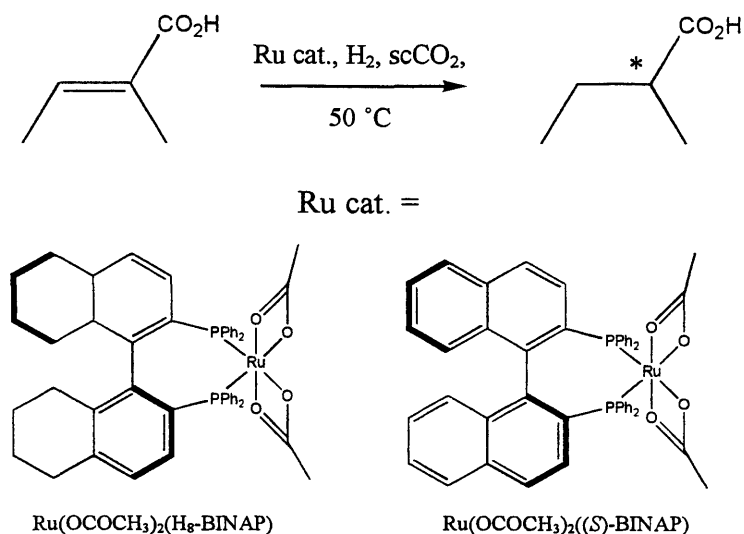


Figure 1.2. Asymmetric hydrogenation of tiglic acid

In  $\text{scCO}_2$  using  $\text{Ru}(\text{OCOCH}_3)_2(\text{H}_8\text{-BINAP})$ , an 81 % enantiomeric excess ( $ee$ ) was achieved. This was comparable with the value obtained in methanol (82 %) and better than the value achieved in hexane (73 %). Addition of a small amount of the fluorinated alcohol  $\text{F}_{15}\text{C}_7\text{CH}_2\text{OH}$  increased the enantioselectivity to 89 %  $ee$ , but it was not known whether this was due to increased solubility of the catalyst/substrate or a change in the reaction mechanism. The  $[\text{Ru}(\text{OCOCH}_3)_2((S)\text{-BINAP})]$  catalyst was much less active due to lower solubility. This clearly shows the effect that substituting aryl groups for alkyl groups has on the solubility of a ligand/catalyst.

Depending on the catalyst, the rate-limiting step in hydroformylation reactions can be the reaction of the active catalyst with hydrogen. Therefore, using SCFs as reaction media should lead to an increase in rates for these systems, as gas-to-liquid mass-transfer problems are not an issue. Rathke *et al.* described the first successful example of homogeneous hydroformylation in  $\text{scCO}_2$ <sup>8</sup> (Figure 1.3).

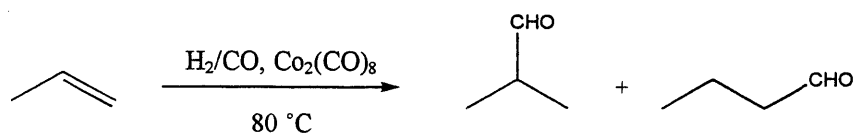


Figure 1.3. Hydroformylation of propene in  $\text{scCO}_2$

The hydroformylation of propene at 56 atm pressure of  $\text{H}_2$  and  $\text{CO}$  occurs at a slightly lower rate in  $\text{scCO}_2$  than in organic solvents like heptane. However, the selectivity towards the linear aldehyde is higher in  $\text{scCO}_2$  than in benzene (88 % *versus* 83 %). It was observed that, at constant

pressure, increasing the temperature decreased the percentage of linear aldehyde obtained whereas, at constant temperature, increasing the pressure increased the linear aldehyde percentage.

Leitner *et al.* more recently determined that a  $\text{scCO}_2$ -soluble rhodium complex containing fluorinated ligands was also a good hydroformylation catalyst. The hydroformylation of oct-1-ene was achieved in good yield and with 82 % selectivity towards the linear aldehyde<sup>12</sup> (Figure 1.4).

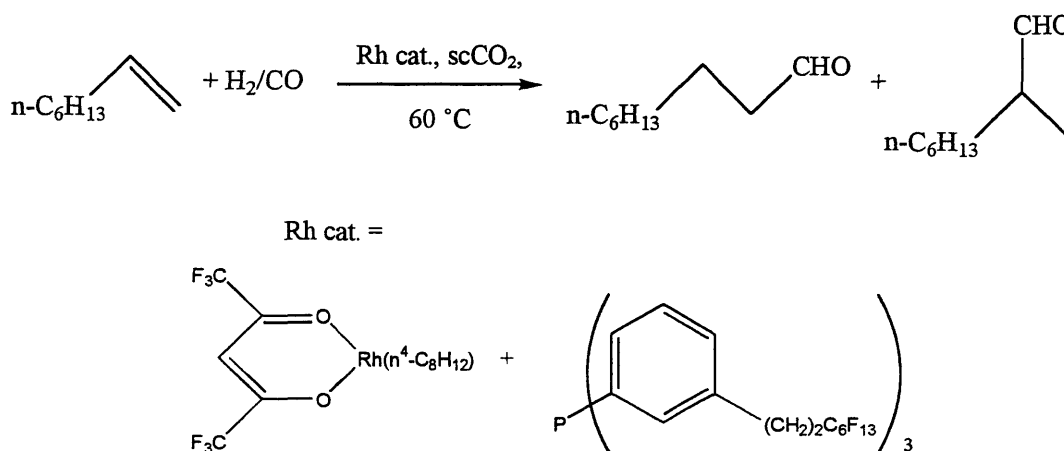


Figure 1.4. The hydroformylation of oct-1-ene and the catalyst used

When a rhodium/phosphine ratio of 1:6 was used, the reaction proceeded smoothly with the absence of any side reactions such as hydrogenation or isomerisation.

Asymmetric Diels-Alder reactions have also been carried out successfully in  $\text{scCO}_2$ <sup>19</sup> and, recently, Thomas Swan opened the world's first commercial-scale  $\text{scCO}_2$  plant for the synthesis of organic molecules.<sup>20</sup> Here, solid-supported catalysts are packed into a reactor and substrates dissolved in  $\text{scCO}_2$  are passed through the solid where reaction occurs. Using this methodology, continuous flow reactions can be carried out without problematic separation of the catalyst and products.

#### 1.2.1.4 Supercritical Fluids – Conclusions

The examples given in section 1.2.1.3 show that SCFs are useful reaction solvents with the advantages that there are no mass-transport concerns in reactions where diffusion is an issue and, if  $\text{CO}_2$  is employed, the solvent is cheap, non-toxic and non-flammable. The separation of the products and catalysts is easily achieved by reducing the pressure of the system and there are no problems with solvent residues.

It would seem that SCFs achieve the goals set out at the start, namely that they can be used as solvents to homogenise catalysts and substrates, but the catalyst can be made heterogeneous once

again, separated from products and reused in further catalysis. However, in practice there are a number of issues that hinder the widespread application of supercritical reactions. One problem with supercritical fluids is the required modification of ligands to achieve  $\text{scCO}_2$  solubility of catalysts, although this problem is not unique to supercritical systems. Where addition of solubilising groups to modifying ligands is not possible, supercritical reactions will be impossible to achieve and the system cannot be used. Addition of co-solvents and surfactants to reactions adds contaminants to the products that may be inseparable at the end of the reaction. In industrial terms, the costs associated with high-pressure reactions may prove to be the most prohibitive factor in the use of SCFs on a large scale. However, if high yields, selectivities and facile separation of the catalyst from the product can be realised in important industrial processes then the use of supercritical systems will become more attractive.

### 1.2.2.1 Ionic Liquids

Ionic liquids (ILs) consist of ion pairs that are liquid at temperatures lower than one hundred degrees centigrade. They are not associated with being corrosive and have a low viscosity which differentiates them from molten salts. These are high melting, high viscosity, highly corrosive liquids. The development of ionic liquids dates back to 1914 and the production of ethylammonium nitrate.<sup>21</sup> Ethylammonium nitrate is liquid at room temperature, but usually contains small amounts of water which makes it impure. The first truly ionic liquids were based around chloroaluminate ions and were designed for use as bath solutions for electroplating aluminium.<sup>22</sup> After this initial interest, they were largely forgotten until the 1970s, when room temperature chloroaluminate melts were prepared successfully.<sup>23</sup> Then, in 1980, Seddon and Hussey started to use these melts as nonaqueous polar solvents for the investigation of transition metal complexes.<sup>24</sup> Ionic liquids were used for the first time as solvents for homogeneous transition metal catalysis in 1990 by Chauvin<sup>25</sup> and Wilkes<sup>26</sup>. Chauvin *et al.* dissolved nickel-based catalysts in weakly acidic chloroaluminate melts and tested these ionic catalyst solutions in the dimerisation of propene. Wilkes used similar weakly acidic chloroaluminate melts to study ethylene polymerisation with Ziegler-Natta catalysts.

However, ionic liquids consisting of chloroaluminate ions are highly hygroscopic and labile towards hydrolysis making them difficult solvents to employ. In 1992, Wilkes *et al.* synthesised systems with dramatically enhanced stabilities towards hydrolysis that contained  $\text{BF}_4$  anions.<sup>27</sup> In addition to their enhanced stability, they also showed a greater functional group tolerance. This new class of ionic liquids was successfully used in the rhodium-catalysed hydroformylation of olefins,<sup>28</sup> showing ionic liquid-based catalysis was not limited to chloroaluminate melts. This discovery led to a sharp rise in research into the use of ILs in synthesis.

### 1.2.2.2 Properties of Ionic Liquids

Like supercritical fluids, the physical and chemical properties of ionic liquids can be specifically tailored over a wide range to suit the system in which they are employed by judicious choice of cation and anion. Ionic liquids have no vapour pressure and do not form azeotropes with organic products, so easy separation of the products of a reaction is possible by distillation or extraction.<sup>29</sup> The choice of the melt determines the maximum temperature which can be used. However, certain ionic liquids are stable up to 400 °C, much higher than the temperature at which most organic solvents degrade. Additionally, by altering the nature of the anion or cation employed, the density and viscosity of ionic liquids can be varied.

These factors seem to make ILs a good reaction medium for homogeneous catalysis where the catalyst can be recovered and reused. By anchoring the catalyst in the ionic liquid, using modifying ligands with appropriate functional groups, a reaction can be carried out homogeneously. The product can then either be extracted or distilled from the IL and the solvent containing the catalyst reused in further catalytic reactions.

### 1.2.2.3 Uses of Ionic Liquids in Synthesis

The differing solubilities of molecules in ionic liquids can be used to good effect. For example, Rogers *et al.* examined the solubility of acids and bases in a H<sub>2</sub>O/[BMIM]PF<sub>6</sub> biphasic system at varying pHs<sup>30</sup> ([BMIM] = 1-*n*-butyl-3-methyl-imidazolium ion). It was found that neutral substrates were preferentially soluble in the ionic liquid while ionic species dissolved in the aqueous layer. This investigation showed the biphasic system behaved in a similar manner to an organic/aqueous biphasic system (see section 1.2.3.2), but with the advantage that the volatile organic solvent had been removed.

Ionic liquids can be used purely as solvents or as co-catalysts. Among other processes, ionic liquids have been used in hydrogenations,<sup>31,32</sup> hydroformylations,<sup>33,34</sup> Heck reactions,<sup>35,36</sup> dihydroxylations<sup>37</sup> and oligomerisations.<sup>38,39,40</sup> Pertinent examples of some of these uses are outlined below.

The rhodium-catalysed hydrogenation of pent-1-ene to pentane was successfully achieved using ionic liquids with weakly coordinating anions (e.g. PF<sub>6</sub><sup>-</sup>, BF<sub>4</sub><sup>-</sup>, SbF<sub>6</sub><sup>-</sup>) under biphasic conditions (Figure 1.5), where the reactant and product formed the organic phase.<sup>28</sup>



As for the hydrogenation systems detailed above, the biphasic system could be separated and the catalytic ionic liquid phase reused. The turnover frequency (TOF) was relatively high ( $126 \text{ h}^{-1}$ ) and no leaching of the platinum catalyst into the organic phase was observed.

More recently, a higher melting phosphonium salt-based ionic liquid has been used in the hydroformylation of hex-1-ene using a rhodium catalyst.<sup>42</sup> At room temperature, the ionic liquid was solid and so after reaction, the system could be cooled and the organic phase poured off. After renewed heating to liquefy the solid, the ionic liquid phase could be reused with no loss of activity.

IL-supported catalysts have been investigated for use in ring-closing metathesis (RCM) reactions.<sup>43</sup> Modification to Hoveyda's catalyst to include an alkyl imidazolium salt attached to the carbene ligand led to the formation of a [BMIM]PF<sub>6</sub>-soluble catalyst. (Figure 1.8).

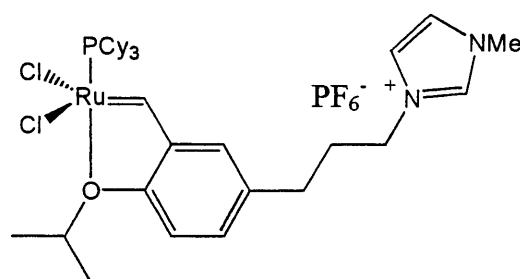


Figure 1.8. IL-soluble Hoveyda's catalyst

Addition of a small amount of this catalyst into the IL led to a system which was highly active for a range of RCM reactions and which, after extraction of the product with tetrahydrofuran, could be reused up to nine times with no loss of activity. When Hoveyda's catalyst, without the imidazolium salt, was used, significant leaching of the catalyst into the tetrahydrofuran used for extraction was observed and the IL phase could not be reused to give high substrate conversion.

Finally, Heck reactions sometimes show dramatically improved rates and selectivities in ionic liquids.<sup>36,44</sup> The coupling of bromobenzene to styrene is known to be a low-yielding reaction in organic solvents, (20 % yield in DMF using diiodo-(1,3-dimethylimidazolin-2-ylidene)-palladium(II) as a catalyst) with the production of large quantities of palladium black.<sup>36</sup> However, the use of molten [NBu<sub>4</sub>]Br in place of DMF dramatically improved the yield of stilbene to 99 % under otherwise identical conditions. The product could be distilled from the non-volatile ionic liquid catalyst and the latter could be reused up to 13 times without a significant drop in activity or production of palladium black.

#### 1.2.2.4 Ionic Liquids – Conclusions

Ionic liquid systems show benefits over scCO<sub>2</sub> systems because the solvents are easier to handle and no specialist equipment is required. However, the leaching of the catalyst from the ionic

liquid phase into the organic phase is an important factor in determining the applicability of ionic liquids to the system in question. Also, the low solubility of many organic molecules in ionic liquids is a major factor in determining how useful ionic liquid catalysis can be. For systems where the solubility is very low, reaction can only occur at the interface between the two solvents which is likely to produce an unacceptable rate of reaction. Finally, there is no data available for the toxicological or ecological impact of ionic liquids, although they are unlikely to be benign solvents. If safe disposal involves much processing of the waste ionic liquid, then the cost of disposal may prove to be prohibitive to use.

### 1.2.3.1 Biphasic Catalysis

As outlined in Section 1.2.2, the use of biphasic systems in catalysis can lead to simple separation of products from catalysts by decantation, providing the species to separate have suitably different solubilities in a specific solvent to overcome 'leaching'; loss of the compound from one phase into the other. It is possible to choose catalysts for use in ionic liquid systems that are preferentially soluble in the ionic liquid phase without ligand modification. For the biphasic systems considered here, however, the addition of solubilising groups to ligands is required to confer to the catalyst preferential solubility in a particular phase.

Although it is possible to produce biphasic systems with a wide-range of binary solvent combinations, the two systems which have been studied in the most detail are outlined below.

### 1.2.3.2 Aqueous Biphasic Systems

Aqueous biphasic catalysis works by employing an organic phase containing the reactants and an aqueous phase in which the catalyst is anchored. Clearly, for a biphasic system to form, the organic solvent must be immiscible with the aqueous phase, otherwise simple separation could not be achieved. This limits the system to the production of non-polar products which can be separated by decantation, although it is not necessary to use only non-polar reactants.

To confer aqueous solubility to the catalyst the component ligands are modified with highly polar substituents such as  $\text{SO}_3\text{H}$ ,<sup>45</sup>  $\text{CO}_2\text{H}$ <sup>46</sup> or their salts. These modified ligands have a reduced affinity for non-polar organic solvents and, therefore, subsequent catalysts are preferentially soluble in the aqueous phase. Examples of water-soluble ligands are shown in Figure 1.9.<sup>47</sup>

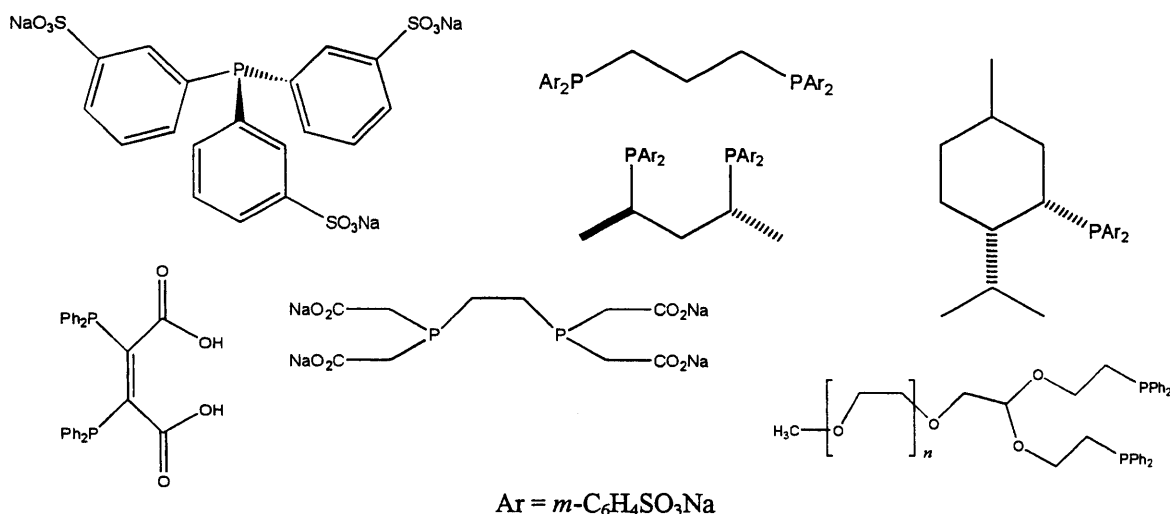


Figure 1.9. Water-soluble ligands used in catalysis

### 1.2.3.3 Uses of Aqueous Biphasic Systems

The hydrogenation of unsaturated compounds was the first application of water-soluble catalysts.<sup>48,49</sup> It was found that, for a range of substrates, although catalysis did occur the TOFs were generally low. These could be increased with the use of co-solvents but, in many cases, this led to increased leaching of the catalyst and loss of catalytic activity.

A large range of studies on the reduction by hydrogen of prochiral substrates have also been carried out.<sup>50,51,52</sup> Again, although the systems are catalytically active, the reaction rates are lower than with the homogeneous systems. For certain substrates, high *ee*'s can be obtained (Figure 1.10).<sup>51</sup>

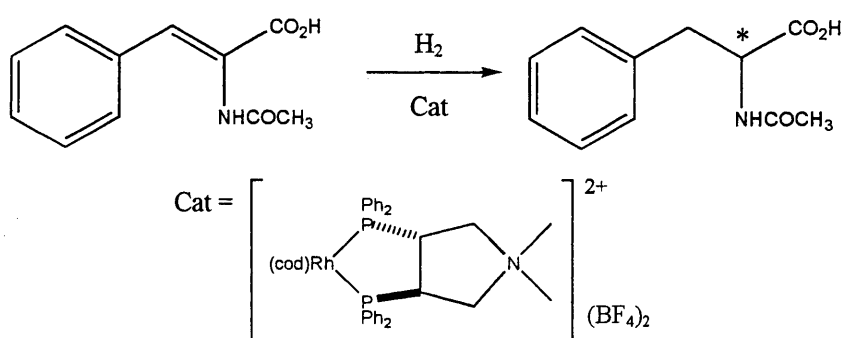


Figure 1.10. Asymmetric hydrogenation in an aqueous biphasic system and the catalyst used

For this system, an *ee* of 96 % could be achieved, with a TOF of around  $900 \text{ h}^{-1}$ . However, this highly active system is unusual, with most examples producing unacceptably low optical yields or low catalytic activities. Köckritz *et al.* have recently prepared a range of phosphorylated BINAP-

based ligands for use in hydrogenation and hydroformylation catalysis in aqueous biphasic systems (Figure 1.11).<sup>53</sup>

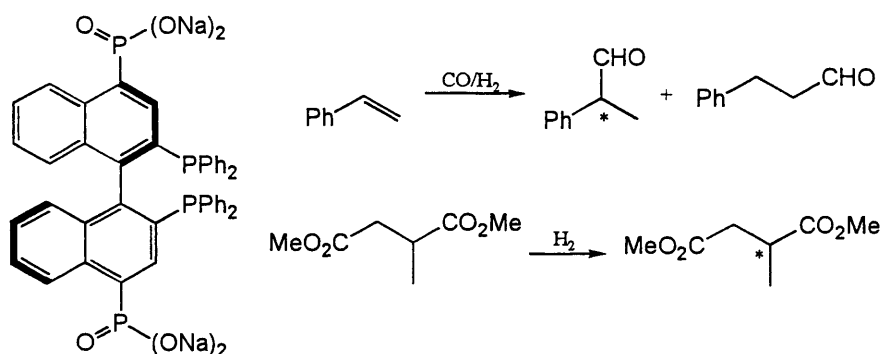


Figure 1.11. Aqueous-soluble BINAP-based ligand and hydroformylation of styrene and hydrogenation of dimethyl itaconate using the ligand and  $\text{Rh}(\text{CO})_2\text{acac}$

In a water:ethanol biphasic system, styrene could be hydroformylated under 20 bar syngas in 5 % conversion with an  $n:i$  ratio of 10:90. The product  $ee$  was also very low; just 26 %. The hydrogenation of dimethyl itaconate was more successful, with 99.4 % product yield being achieved in an ethanol/water/hexane biphasic system. However, a product  $ee$  of only 79.4 % was achieved, compared to 91.5 % for the parent BINAP ligand in ethanol. Additionally, no mention of reuse of the aqueous phase in further catalysis was made.

The most well known industrial application of an aqueous-organic biphasic system is the Ruhrchemie/Rhône-Poulenc process for the hydroformylation of propene.<sup>54</sup> The process uses a rhodium catalyst which contains triphenylphosphine ligands modified with sulphonate groups (Figure 1.12).

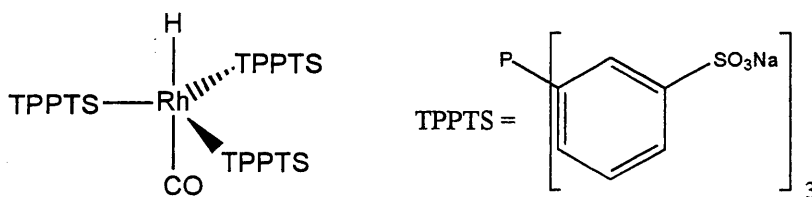


Figure 1.12. Rhodium-based catalyst used in the Ruhrchemie/Rhône-Poulenc process

The catalytic complex is totally insoluble in the organic product phase. This makes separation of the catalyst and product a simple matter of removing the organic phase and leaching of the catalyst into the aqueous phase. High  $n:i$  ratios are also obtained.

However, there are a number of disadvantages associated with aqueous biphasic processes, even though catalysts can often be re-isolated after high-yielding reactions and reused. Initially, the

rate of reaction is highly dependent on the solubility of the substrate in the aqueous phase. For low molecular weight olefins in the Ruhrchemie/Rhône-Poulenc process, mass transfer rates are high and the reaction proceeds at acceptable rates. For less miscible, higher molecular weight olefins however, the rate of diffusion can reduce the reaction rate to a non-viable level.<sup>55</sup> In the case of water-immiscible substrates, reaction can only occur at the limited interface between the solvents which can significantly reduce the reaction rate.

Another major drawback of the use of any biphasic system containing an aqueous phase is that moisture-sensitive reagents/catalysts/products cannot be used or produced, which reduces the applicability of the system in synthetic processes.

#### 1.2.3.4 Fluorous Biphasic Systems

From the sections above it is clear that biphasic catalysis chemistry can be useful for simple separation of products from catalysts, but the problems of low rates, low selectivities and solvent sensitivities greatly inhibit the use of aqueous-organic biphasic systems.

In 1994, the idea of replacing the aqueous phase with a perfluorocarbon or 'fluorous' phase was first suggested.<sup>56</sup> Fluorous biphasic catalysis has a number of advantages over aqueous biphasic catalysis. Firstly, water-sensitive moieties can be used/produced in catalysis without degradation. Secondly, with careful choice of the solvent used, the two immiscible liquid phases can be homogenised with heating and separated again upon cooling (Figure 1.13). This greatly improves mass transfer rates and the reaction is no longer limited to a small solvent-solvent interface, whilst facile catalyst/product separation is still achievable.

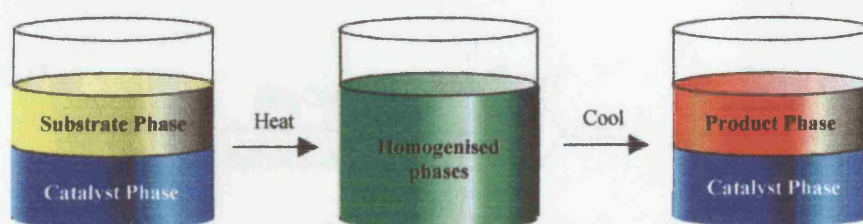


Figure 1.13. Diagram outlining fluorous biphasic methodology

Thirdly, the increased solubility of many gases in fluorous solvents leads to higher rates of reaction where gas diffusion is an important factor in controlling the rate.<sup>57</sup> Perfluorocarbon solvents are also recognised as being environmentally benign and generally non-toxic, although they are persistent in the environment and have been linked to the 'greenhouse effect'.

Like aqueous soluble catalysts, the constituent ligands require modifying groups to confer perfluorocarbon solubility to the complex. In fluoruous systems, however, organic functional groups cannot be used to confer this solubility. Here, perfluorocarbon chains or 'fluorous ponytails' such as  $-\text{C}_6\text{F}_{13}$ ,  $-\text{OCH}_2\text{C}_6\text{F}_{13}$  or  $-\text{CH}_2\text{CH}_2\text{C}_8\text{F}_{17}$  are required to provide solubilising power. Rendering the catalyst fluoruous soluble anchors the complex in the fluoruous phase, and organic molecules, having no fluoruous affinity, can thus be easily separated from the catalytic fluoruous phase and the catalyst reused.

Many different fluorinated ligands have been synthesised and studied, including alkyl and aryl phosphines,<sup>56,57,58</sup> phosphinites<sup>59</sup> and phosphites,<sup>56,60</sup>  $\beta$ -diketonates<sup>61</sup> and cyclopentadienes.<sup>62</sup> In all cases, the ligands have minimised intermolecular interactions and often contain spacer groups such as  $\text{C}_2\text{H}_4$  or  $\text{C}_6\text{H}_4$  to reduce the electron-withdrawing effect of the fluoruous ponytails on the donor atom.

### 1.2.3.5 Uses of Fluorous Biphase Systems in Catalysis

Fluorous Biphase Catalysis has been widely used for hydroformylations,<sup>56,63,64</sup> hydroborations,<sup>65,66</sup> hydrogenations,<sup>67,68</sup> oxidations,<sup>69,70</sup> epoxidations<sup>71,72,73</sup> transesterifications<sup>74</sup> and C-C bond formations.<sup>75</sup> Examples of these uses are outlined below.

The initial work on fluoruous biphases by Horváth and Rábai focused on the hydroformylation of oct-1-ene and dec-1-ene.<sup>56</sup> The reactions were carried out using a perfluoromethylcyclohexane/toluene biphasic system at 100 °C with a hydrogen/carbon monoxide pressure of 10 bar. The catalyst,  $[\text{HRh}(\text{CO})-(\text{P}(\text{C}_2\text{H}_4\text{C}_6\text{F}_{13})_3)_3]$ , was generated *in situ* from  $[\text{Rh}(\text{CO})_2(\text{acac})]$  and  $\text{P}(\text{C}_2\text{H}_4\text{C}_6\text{F}_{13})_3$  (Figure 1.14).

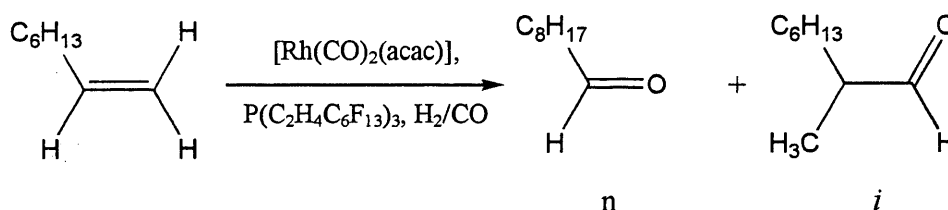


Figure 1.14. Hydroformylation of oct-1-ene in fluoruous biphase catalysis

GC analysis of the products of reaction showed 85 % conversion to nonanals had been achieved after twenty-four hours with an *n*:*i* ratio of 2.9. Reuse of the organic phase in a further catalytic reaction after the addition of fresh substrate produced only trace amounts of aldehydes, demonstrating that leaching of the catalytically active rhodium species into the organic phase had not occurred significantly.

The hydroformylation of dec-1-ene employing the same rhodium catalyst was further investigated<sup>63</sup> and the results obtained compared to the analogous homogeneous system with triphenylphosphine as ligand. Similar selectivities were observed in the two systems, but the activity in the fluorous system was an order of magnitude lower than the activity in the homogeneous case. The total loss of rhodium per mole of product due to leaching was calculated to be 1.18 ppm over nine consecutive reaction cycles.

The hydrogenation of alkenes has also been investigated using fluorous biphasic catalysis.<sup>69</sup> Horváth *et al.* applied the principle to the rhodium-catalysed hydrogenation of 2-cyclohexen-1-one, dodec-1-ene, cyclododecene and 4-bromostyrene, again in a perfluoromethylcyclohexane/toluene biphasic system. The Wilkinson's catalyst analogue,  $[\text{RhCl}(\text{P}(\text{C}_2\text{H}_4\text{-C}_6\text{F}_{13})_3)_3]$ , was used and the reactions carried out under 1 bar of  $\text{H}_2$  at 45 °C forming cyclohexanone, dodecane, cyclododecane and 4-bromoethylbenzene respectively in yields of 87 – 98 %. Three consecutive reaction cycles showed no significant loss of activity in any of the reactions.

The fluorous biphasic concept was adapted by Betzemeier and Knochel for use in C-C bond forming reactions by palladium-catalysed cross-coupling.<sup>75</sup> A fluorous-soluble palladium(0) catalyst prepared by reaction of  $[\text{Pd}(\text{dba})_2]$  with the perfluoroalkyl derivatised arylphosphine  $\text{P}(\text{C}_6\text{H}_4\text{-4-C}_6\text{F}_{13})_3$  was used to catalyse the coupling of arylzinc bromides and aryl iodides as shown in Figure 1.15.

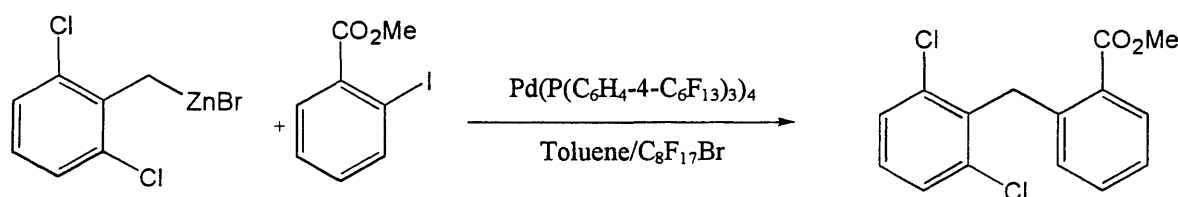


Figure 1.15. Cross-coupling reaction utilising fluorous biphasic catalysis

At a reaction temperature of 60 °C, the solvent mixture was monophasic allowing the reaction to proceed homogeneously and high yields of 87-99 % were attainable. Upon cooling, the two-phase system was regenerated and the fluorous phase containing the catalyst was reused several times with no significant loss of catalytic activity. The palladium catalytic complex was also found to be highly active, with only 0.15 mol % of catalyst required to produce high yields of the coupled product.

More recently, van Koten *et al.* have applied the fluorous biphasic methodology to the addition of diethylzinc to benzaldehyde using a fluorous zinc catalyst (Figure 1.16).<sup>76</sup>

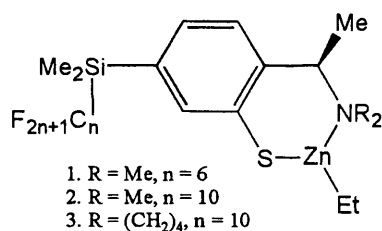


Figure 1.16. Fluorous catalysts used in the addition of diethylzinc to benzaldehyde

Using a hexane/perfluoromethylcyclohexane biphase, the enantioselective addition could be achieved in quantitative yield for up to five runs. However, for catalyst 1, the product *ee* had fallen from 84 % to just 3 % after five runs, and for catalyst 3 the *ee* had fallen from 92 % to 28 % after five runs. The authors attributed the loss to leaching of the catalyst into the organic phase.

### 1.2.3.6 Biphase Catalysis - Conclusions

Biphase systems provide a simple method of separation of the catalyst and product that is suitable for industrial use. However, catalyst leaching may be a major problem depending on the system used. Aqueous biphasic systems suffer from an incompatibility with water-sensitive substrates, catalysts and products and the low solubility of many organic substrates in water severely limits the rates of reaction for these reactions. Fluorous biphasic systems overcome these problems due to their ability to be homogenised under tuneable conditions and the removal of the requirement for an aqueous phase. However, fluorous solvents are very expensive which may prove prohibitive to their use in large quantities in industry. Also, for both systems, extensive ligand modification is required to achieve preferential solubility in a specific phase and, especially in fluorous systems, the ligand modification is often difficult, time consuming, costly and affects the rates/selectivities of the reactions in which they are used. Even so, if leaching levels are low and the fluorous solvent is carefully recycled, the cost of commercialising the system could be recovered and may be beneficial for certain systems.

### 1.2.4.1 Supported Catalysis Systems

It has been proposed that attaching homogeneous catalysts to an insoluble support *via* covalent bonding could lead to improvements in selectivity and reactivity in the system in which they are employed.<sup>77</sup> This would be due to the stereochemical conformation offered by the solid support, which is effectively a multidentate ligand, with the stabilisation of unstable species preventing dimerisation and other deactivation pathways. The catalyst can then be easily separated from a reaction mixture by isolation of the solid support by filtration.

The idea of solid supported catalysis was first developed in the late 1960s. In 1969, the first published work describing the support of cationic metal complexes (e.g. [Pt(NH<sub>3</sub>)<sub>4</sub>]<sup>2+</sup>) on

sulphonated polystyrenes appeared.<sup>78</sup> Much work on the attachment of catalysts to solid supports followed throughout the 1970s and 1980s,<sup>77</sup> some of which is detailed in the following sections.

Two types of support have been employed previously; organic and inorganic. The benefits and drawbacks of these two approaches are outlined below.

#### 1.2.4.2 Organic Supports for Catalysis

The most commonly used organic supports are polystyrene and styrene-divinylbenzene copolymer beads.<sup>79</sup> These polymers are modified to contain functional groups which can bind metal centres including diphenylphosphine,<sup>80</sup> tertiary amino<sup>81</sup> and thiol<sup>82</sup> groups. The properties of these polymers directly influence their performance as a catalyst support.<sup>79</sup> A low level of cross-linking leads to a polymer that is highly flexible, which can result in unfavourable interactions between functional groups. However, a polymer with too high a degree of cross-linking prevents entry of the substrate into the polymer matrix. It is clear, therefore, that the support must be tailored to suit the system in which it is used.

Investigations using organic polymer-supported catalysis have been carried out for many systems including hydrogenation, hydroformylation, hydrosilation and oligomerisation.<sup>77</sup> Although the results show that similar selectivities are observed in the polymer-supported systems and analogous homogeneous systems, the rates of reaction are generally much lower in polymer-supported systems. This is attributed to the influence of diffusion rates of reactants into the polymer support, a factor that is not applicable to the homogeneous system.<sup>83</sup> In addition, a high degree of bonding between the support and catalyst may inhibit the conformational changes necessary in a catalytic cycle making the catalyst inactive. As predicted by Hartley,<sup>77</sup> however, in certain systems the steric and electronic interactions are optimised and these systems show higher regio- and stereo-selectivities than the analogous homogeneous systems.

Despite some success in the use of organic supports, their employment is still generally research-based. This is mainly due to the lack of optimised systems and the properties of the supports which tend to be low mechanical strength and low thermal stability.

#### 1.2.4.3 Inorganic Supports for Catalysis

Inorganic polymers tend to give more robust supports that have higher thermal, solvent and ageing stabilities than their organic counterparts.<sup>84</sup> They also have a very rigid structure and well-defined pore network.

The most popular inorganic support is silica, which can be functionalised relatively easily. Surface silanol groups will react with chlorosilanes or alkoxy silanes to give a stable Si-O-Si linker (Figure 1.17).

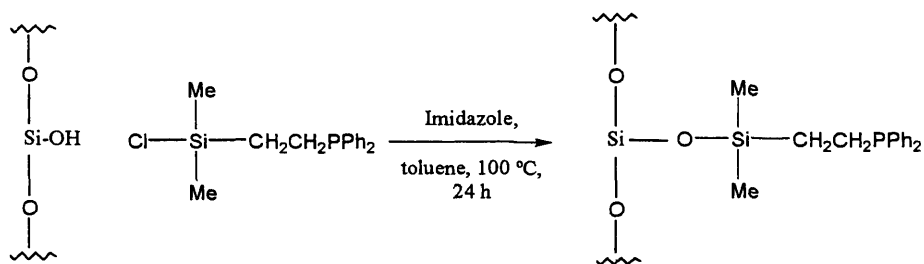


Figure 1.17. The synthesis of solid supports

The surface-bound coordinating ligands can be used to bind catalytically active metal centres or, in the case of metal carbonyls and alkoxides, the surface OH groups can be used as binding sites. In some cases, the presence of reactive surface silanol groups can be problematic, however, and so they are often ‘capped’ with a hydrocarbon chlorosilane to produce a more inert surface.<sup>85</sup>

The length of the organic spacer group has been shown to have an effect on the activity of a supported catalyst. When attached to longer spacer groups, rhodium(I) hydroformylation catalysts showed increased activity due to reduced interactions between the metal and surface hydroxy groups.<sup>86</sup> However, the use of spacer groups which are too long can also lead to reduced activity, as more flexible chains lead to intermolecular interactions, which result in coordinative blocking.<sup>87</sup>

Comparison of organic polystyrene and inorganic silica supports in hydrogenation<sup>88</sup> and hydrosilation<sup>89</sup> reactions showed that higher rates of reaction were observed when silica supports were employed. This was attributed to easier substrate access to the active sites on the more uniform silica surface. However, the activities were still lower than those for analogous homogeneous systems as a direct consequence of anchoring the catalytically active metal centre to the support, suppressing catalyst mobility and molecular rearrangements.

Although certain supported systems show improved activity, they are rare and so the use of these supports is unlikely to be commercially widespread.

#### 1.2.4.4 Supported Solvents for Catalysis – Supported Aqueous Phase Catalysis (SAPC)

Anchoring a catalyst to a solid support by a covalent bond restricts the mobility of the active species and may block coordination sites that are important for catalysis. As outlined above, the result of these factors is that support-bound catalyst molecules generally have reduced activity in catalysis, which may be inhibited altogether.

To overcome these problems, a system is required where the catalytic species is still held onto the support so that easy isolation is possible but which allows unrestricted mobility of the

catalyst moiety. To achieve this, Arhancet *et al* proposed the combination of biphasic catalysis and surface anchored catalysis to form supported liquid phase catalysis (SLPC).<sup>90</sup>

SLPC is a heterogeneous process in which a solution of the catalyst is distributed over a high surface area support. By employing a support and solvent that have similar properties, the solution can be made to adhere to the surface and effectively anchor the catalyst to the support *without covalent bonding*.

By using a hydrophilic support such as silica, a thin layer of water can be adhered to the surface and water-soluble catalysts (see Section 1.2.3.2) can be supported in this solvent. These 'activated' supports can then be used in catalysis with the advantages that the catalyst has relatively unrestricted mobility but isolation and reuse is still straightforward.

Controlled pore glass beads were used in the initial studies due to their very high surface areas. To prepare the supported aqueous phase catalysis (SAPC) catalyst, the support was degassed and an aqueous solution of the active species added. The water was then evaporated to produce dry support which had the catalyst adhered to its surface. This was rehydrated with controlled amounts of solvent by exposure to water vapour.<sup>91</sup>

The details of reaction for SAPC are much the same as for aqueous biphasic catalysis. When the hydrated support is placed in a non-polar organic solvent, the hydrophilic catalyst remains in the thin layer of supported water on the surface of the support. Reaction of organic molecules takes place at the interface between the aqueous and organic solvents (Figure 1.18).

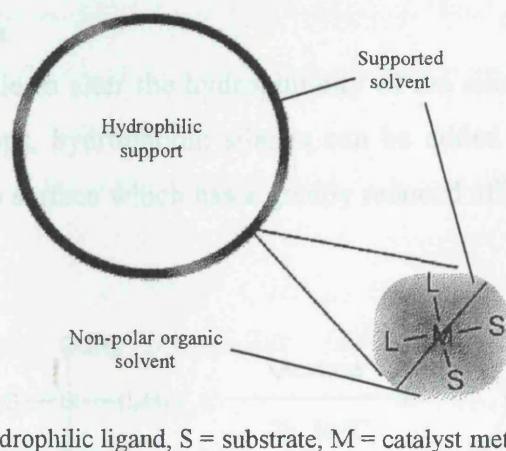


Figure 1.18. Diagram showing the nature of a supported aqueous phase system

Unlike in aqueous biphasic catalysis, however, due to the high surface area of the support, the aqueous/organic interface is very large. This leads to a system with much higher activities than for the simple biphasic case. In the hydroformylation of oleyl alcohol using  $[\text{HRh}(\text{CO})(\text{TPPTS})_3]$ , comparable selectivities in the biphasic and supported systems were obtained, but a higher activity was observed when the supported system was employed and no leaching of the rhodium catalyst

into the organic phase was observed. Filtration of the reaction mixture and reuse of the support in further catalysis produced product with no reduction of catalytic activity.<sup>90</sup>

The increased activity of the SAPC systems was attributed to the assumption that the catalyst retains its mobility in the supported aqueous phase allowing for structural changes during the catalytic cycle. This hypothesis is supported by liquid-phase <sup>31</sup>P NMR spectrum analysis of the supported metal complex, which suggests the catalyst is subject to the ‘tumbling’ effects of a species in solution. Dependence of catalytic activity on water content also supports this theory. If the water content is too low, the supported catalyst loses activity as its mobility is restricted. However, the catalytic activity is also decreased if the water content is too high, as the catalyst becomes less ‘concentrated’ at the aqueous/organic interface and the surface area:volume ratio is decreased.

#### 1.2.4.5 Supported Solvents for Catalysis – Supported Organic Phase Catalysis (SOPC)

As shown above, it is possible to support an aqueous layer on unmodified silica due to the hydrophilic hydroxyl groups on the surface of the silica. However, to achieve simple separation of the catalyst and product, the catalyst must be preferentially soluble in the aqueous layer and, to achieve this, the catalyst ligands must be modified. This modification may be troublesome, can affect the catalyst activity and may not be possible at all. In addition, the formation of polar products cannot occur if successful separation is desired as the product will dissolve in the supported aqueous phase and leaching of the catalyst could occur. These factors make SAPC unsuitable for certain systems.

However, it is possible to alter the hydrophilicity of the silica surface. Due to the reactive nature of the hydroxyl groups, hydrophobic silanes can be added which can be coupled to the hydroxyl groups to produce a surface which has a greatly reduced affinity for water (Figure 1.19).<sup>92</sup>

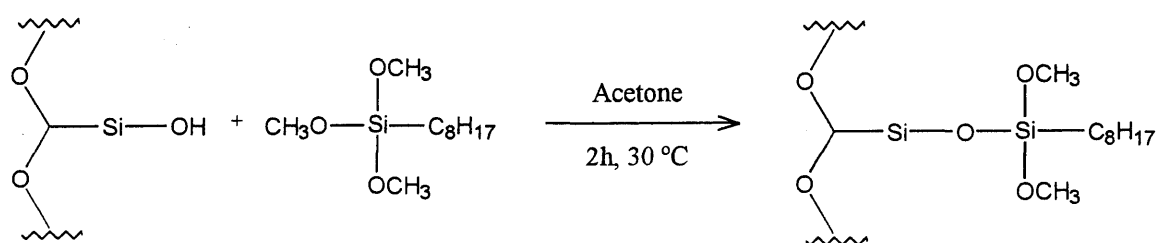


Figure 1.19. Synthesis of Reverse Phase silica gel

This material, known as reverse phase silica gel, shows a large affinity for organic rather than aqueous phases. Reverse phase silica gel can be used in an analogue of SAPC termed

Supported Organic Phase Catalysis (SOPC), where a thin layer of a non-polar organic solvent, such as cyclohexane, is supported on the surface of the silica. Unmodified, aqueous-insoluble catalysts can then be supported in the solvent while polar reactants/products reside in a bulk aqueous phase.

Such a system has been used by Williams *et al.*<sup>92</sup> in palladium-catalysed Heck reactions such as the coupling of 3-bromopyridine with styrene (Figure 1.20)

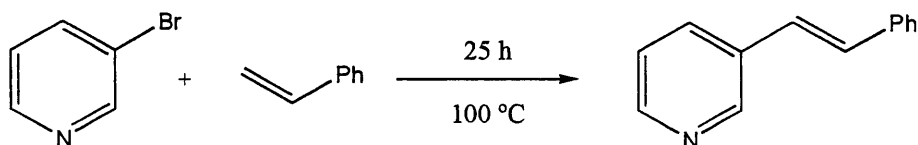


Figure 1.20. Palladium-catalysed coupling of *m*-bromopyridine with styrene

1 mole % [Pd(OAc)<sub>2</sub>] and 4 mole % P(*o*-Tol)<sub>3</sub> were dissolved in cyclohexane and the mixture added to reverse phase silica beads. The solvent was removed and then the beads were re-solvated with a controlled volume of cyclohexane and used in catalysis. In the styrene system, no additional solvent was required and, along with three equivalents of triethylamine, the reaction mixture was heated to 100 °C for 25 hours. A 77 % isolated yield was obtained with less than 0.1 % leaching.

Both SAPC and SOPC offer advantages over their simple biphase or covalently bound parents, such as increased activity due to increased surface area and free mobility which leads to rates approaching those in the homogeneous case. However, like aqueous/organic biphases, they both suffer from their incompatibility with water-sensitive reaction components.

#### 1.2.4.6 Supported Solvents for Catalysis – Supported Fluorous Phase Catalysis (SFPC)

As Fluorous Biphase Catalysis overcomes the problems of water sensitivity in the simple biphase case, so Supported Fluorous Phase Catalysis (SFPC) overcomes the problem in the supported catalysis case. Here, a fluorosoluble catalyst and a layer of fluorosolvent are supported on a fluorosol-modified solid support. As outlined in Section 1.2.4.5, the hydroxyl groups on the surface of silica can be coupled to silanes to change the affinity of the silica for various solvents. The SFPC concept uses a highly reactive fluorosilane to modify the silica surface.<sup>93</sup> The addition of fluorosilyl groups produces so-called Fluorous Reverse Phase (FRP) silica gel and allows a thin layer of fluorosolvent to adhere to the surface of the support. A fluorosol modified catalyst can then be dissolved in this layer of solvent and the active silica used in fluorosol/organic catalysis with the removal of water from the system.

Although, to date, there are no published examples of such supported systems, much work continues at the University of Leicester into adapting supported catalysis for use in synthesis using fluorinated solvents.<sup>94</sup> Added to the removal of water from the system, SFPC uses much less fluorinated solvent than its simple biphasic parent making the process much less expensive. However, the extensive modification of catalyst ligands with fluorinated ponytails is still required to make the catalyst preferentially soluble in the fluorinated phase and modification of the silica surface is also required.

#### 1.2.4.7 Supported Catalysis – Conclusions

Tethering the active catalyst species to a support has the potential to increase the specificity of the catalyst as fixed conformations are adopted which reduce side reactions. However, reducing the mobility of the catalyst can seriously affect its activity to the point where it is no longer active. Also, fixing the catalyst to the surface of a polymer introduces bulk through which substrates and products must diffuse. This reduces activity in the system and ultimately determines how effective the system can be.

Supporting a solvent rather than the catalyst leads to a large improvement. Combining the techniques of biphasic and supported catalysis provides a process that has a higher rate, due to a greatly increased solvent-solvent interface compared to biphasic catalysis and free mobility of the catalyst in the supported solvent. With optimisation, these systems could prove to be highly effective in industry as they are relatively cheap and the isolation and reuse of catalytic species is very easy. However, unless systems like SFPC can be developed, the technique will be limited to reactions which involve species which are not water sensitive, which is a severe limitation.

#### 1.2.5.1 Dendrimers

Many of the previous examples for the recovery and reuse of active catalysts include the use of functionalised ligands. Often, to aid synthesis and to reduce cost, the addition of modifying groups is kept to a minimum. For dendrimers, however, large numbers of modifying groups are added to change the solubility of the active catalyst or allow for catalyst recovery using membrane filtration. Dendrimers are novel macromolecules with regular molecular weights, precisely determined structures and a specific number of end-groups.<sup>95</sup>

#### 1.2.5.2 Examples of the Use of Dendrimers

The use of dendrimers in catalysis is rapidly increasing.<sup>96,97</sup> Togni *et al.* applied a dendritic Josiphos derivative (Figure 1.21) to the asymmetric hydrogenation of dimethyl itaconate in methanol using  $[\text{Rh}(\text{cod})_2]\text{BF}_4$  catalyst precursor.<sup>98</sup>

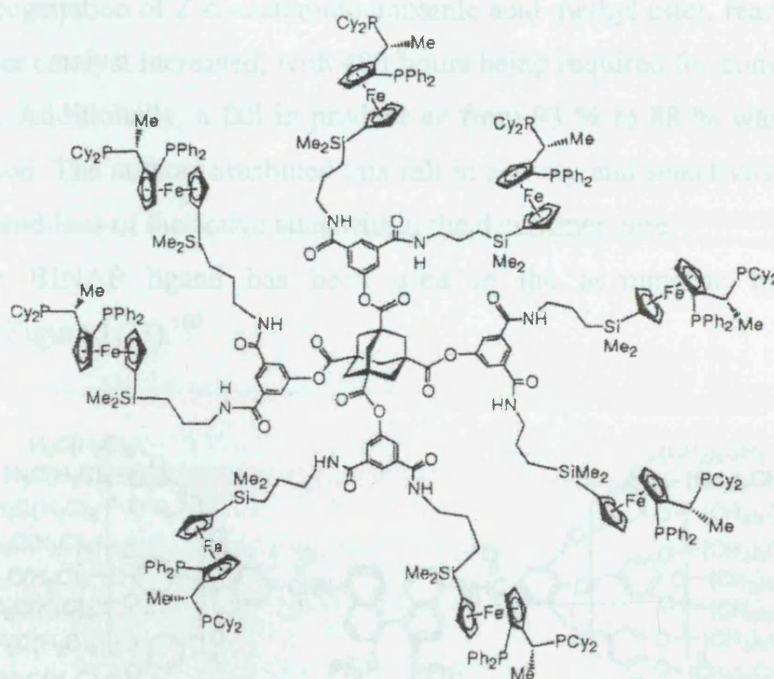


Figure 1.21. Dendrimer-bound Josiphos

100 % product conversion and 98 % *ee* were observed which was only slightly lower than for the non-dendritic Josiphos catalyst (99 %). In addition, the catalyst could be selectively retained using a commercial nanofiltration membrane (see section 1.2.6.1). Engle and Gade recently published the synthesis of a series of dendrimer-bound Rh(I) catalysts for use in asymmetric hydrogenation (Figure 1.22).<sup>99</sup>

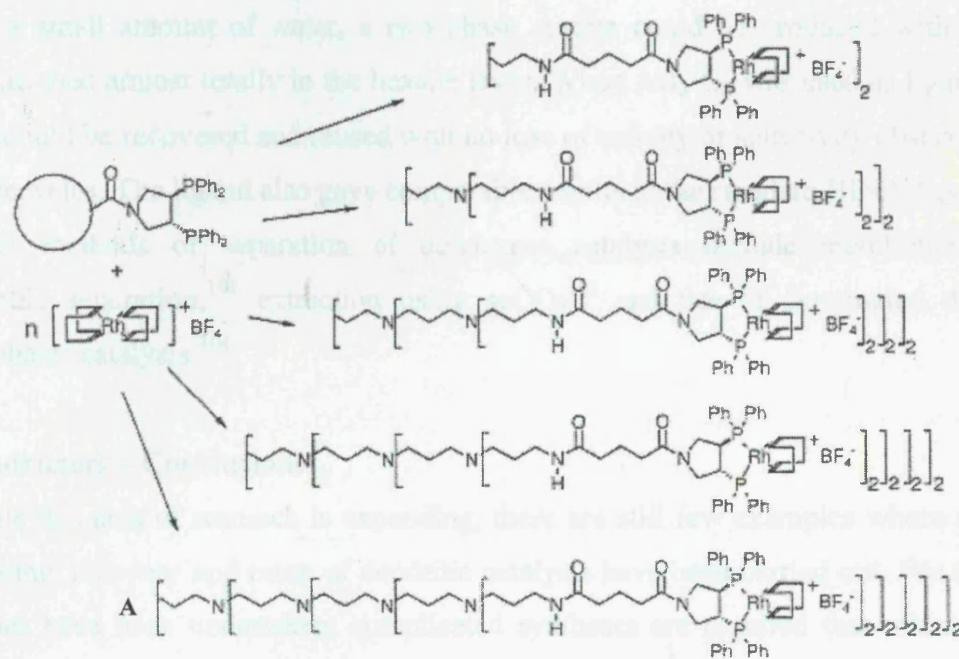


Figure 1.22. Five dendritic Rh(I) catalysts

For the hydrogenation of *Z*- $\alpha$ -acetamidocinnamic acid methyl ester, reaction rates fell as the size of the dendrimer catalyst increased, with 400 hours being required for complete hydrogenation using dendrimer **A**. Additionally, a fall in product *ee* from 93 % to 88 % was observed as larger dendrimers were used. The authors attributed this fall in activity and selectivity to the flexibility of the larger catalysts and loss of the active sites within the dendrimer core.

A dendritic BINAP ligand has been used in the asymmetric hydrogenation of 2-phenylacrylic acid (Figure 1.23).<sup>100</sup>

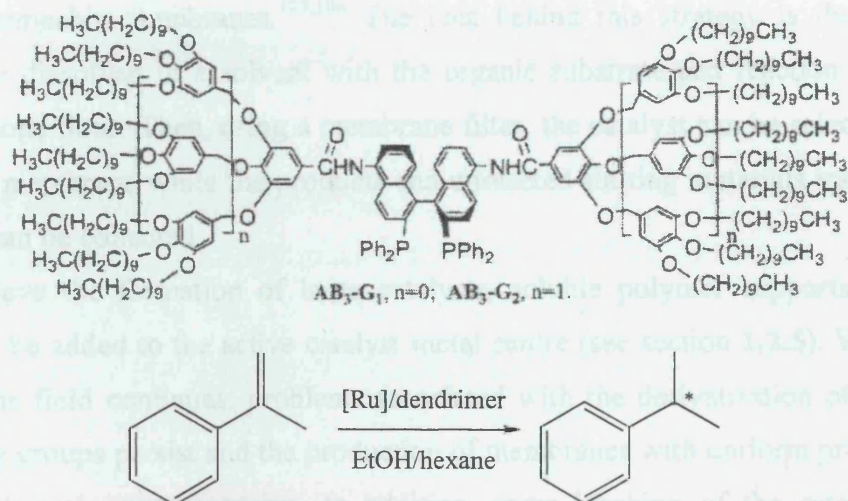


Figure 1.23. BINAP dendrimer and asymmetric hydrogenation of 2-phenylacrylic acid

Using equal volumes of ethanol and hexane, a monophasic reaction could be carried out with the catalyst and products in a homogenous mixture. At the end of reaction, however, with the addition of a small amount of water, a two phase system could be produced with the dendritic catalyst partitioned almost totally in the hexane layer. When AB<sub>3</sub>-G<sub>2</sub> was used as ligand, 99.3 % of the catalyst could be recovered and reused with no loss of activity or selectivity observed after three successive recycles. The ligand also gave comparable results to the standard BINAP system.

Other methods of separation of dendrimer catalysts include membrane filtration,<sup>101</sup> thermomorphic separation,<sup>102</sup> extraction using scCO<sub>2</sub><sup>103</sup> and use of fluorinated dendrimers in fluorous biphasic catalysis.<sup>104</sup>

### 1.2.5.3 Dendrimers – Conclusions

While this area of research is expanding, there are still few examples where the synthesis, catalytic testing, recovery and reuse of dendritic catalysts have been carried out. For those systems where studies have been undertaken, complicated syntheses are required that often result in low yields of the dendrimers that are very difficult to analyse spectroscopically. Subsequently formed

catalysts can be recovered and reused but, often due to heterogeneous conditions, dendrimer catalyst activities and selectivities are lower than the parent systems. As research continues, it is likely that more active and selective systems will be discovered and optimised but, due to complex and costly synthesis in many cases, it is unlikely that dendrimers will acquire widespread use.

#### 1.2.6.1 Other Methodologies for Catalyst Recycle

Ultra- and nanofiltration techniques have recently become more attractive due to improved synthesis of permeable membranes.<sup>105,106</sup> The idea behind this strategy is that relatively large catalysts can be dissolved in a solvent with the organic substrate and reaction carried out under homogeneous conditions. Then, using a membrane filter, the catalyst can be selectively retained on one side of the membrane while the products and unreacted starting materials travel through to the other side and can be collected.

To achieve the formation of large catalysts, soluble polymer supports can be used, or dendrimers can be added to the active catalyst metal centre (see section 1.2.5). Whilst, once more, research into the field continues, problems associated with the derivatisation of the catalyst with large modifying groups persist and the production of membranes with uniform properties on a large scale is difficult and very expensive. In addition, some leaching of the catalyst is also often observed which could not be tolerated on a large scale due to the cost of the catalyst. However, with optimisation, the method shows promise.

Ship-in-a-bottle catalysis makes use of catalysts which are trapped in a porous framework.<sup>107,108</sup> Here, the metal complexes are free to move around in the confines of the cavity but cannot leach out of the pore openings. This, theoretically, maximises the activity and selectivity of the catalyst while allowing its facile recovery and reuse.

Clearly, the type of framework employed is important and, most often used, are zeolites. To entrap the catalyst, a zeolite containing a metal in its pores is treated with the appropriate ligands. Once the catalyst is formed it is too large to escape the pores and a ship-in-a-bottle catalyst is obtained. This material can then be used in catalysis without loss of the catalyst species and be recovered by simple filtration.

It is evident that the most restricting part of this catalysis methodology is the type of catalyst which can be used. Only a relatively small number of catalysts can be employed which are bulky and cannot escape the pores of the zeolite. In addition, slow diffusion of reactants and products into and out of the pores can play a major role in the rate of reaction and bulky substrates cannot be used. However, for reactions such as oxidations employing bulky catalysts and small oxygen molecules,<sup>107</sup> the methodology can be applied successfully and the catalyst recovered and reused.

### 1.3 Catalyst Recovery by Column Chromatography

The above examples of processes that promote simple catalyst isolation have shown that catalyst/product separation is possible but, often, what is gained in simple separation is lost in reduced catalytic activity and selectivity, extensive and sometimes difficult ligand modification, the use of incompatible or expensive solvents or the use of specialised or expensive equipment.

What is still required, therefore, is a system which uses a minimum of ligand modification, a conventional non-aqueous solvent and a separation process which is simple yet extremely efficient. The main objective of this research is, therefore, to investigate a process which promises to incorporate these factors; the idea of Fluorous Solid Phase Catalyst Extraction (FSPCE).

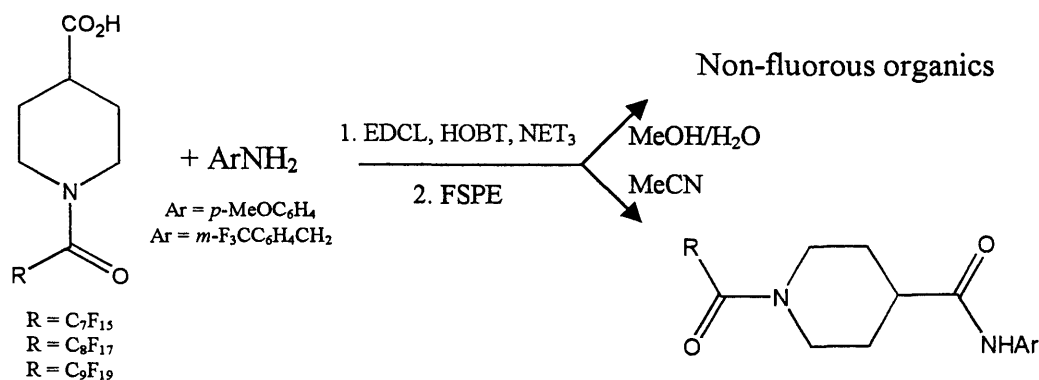
#### 1.3.1 Fluorous Solid Phase Extraction (FSPE)

The modification of silica to produce a fluorophilic surface was not originally prepared for use in supported catalysis (Section 1.2.4). Column chromatography has been used for decades to effect the separation of organic/aqueous molecules due to their differing affinities towards the solid support and the eluting solvent. Recently, however, the concept of fluorous solid phase extraction (FSPE) has emerged, using column chromatography and a fluorous solid phase to isolate fluorous molecules from non-fluorous species. The approach works due to interactions between fluorinated chains that are present in the molecules to be separated and the highly fluorinated surface of the support. These interactions slow the passage of the fluorinated molecule through the column of fluorinated solid support, while molecules that are not fluorinated show no affinity for the solid support and so travel through the column more rapidly, providing separation.

Although applications of FSPE are still emerging, currently there are two main types of use of the system in the literature; the separation of fluorous-tagged reagents/products from reaction mixtures<sup>109</sup> or the separation of fluorinated metal compounds from reaction mixtures.<sup>110</sup>

The isolation of fluorinated reagents/products has been termed 'light fluorous synthesis' and employs organic substrates that have been 'tagged' with a minimum number of fluorous ponytails. These tags provide the molecule with a fluorous affinity and, on passage through a column of FRP silica gel, the fluorinated species are selectively retained and can be isolated, while non-fluorous molecules pass straight through. The advantage of this process over fluorous biphasic (section 1.2.3) is that a perfluorocarbon solvent is not required and so extensive ligand modification is unnecessary; often a single fluorous ponytail is sufficient to effect adequate separation on a fluorous column.

One example of such a system involves the tagging and separation of a fluorous amide after reaction of a fluorous acid with a non-fluorous amine (Figure 1.24).<sup>109</sup>



EDCL = 3-ethylcarbodiimide-1-(3-dimethylaminopropyl) hydrochloride, HOBT = 1-hydroxybenzotriazole

Figure 1.24. Separation of fluoros labelled molecules from non-fluorous molecules by fluoros solid phase extraction

Elution of the reaction mixture with an 80 % methanol/water elutant selectively isolated the organic impurities, including unreacted starting materials and any products from side reactions. The fluoros product molecule was retained on the column and collected by elution with acetonitrile after complete removal of the non-fluorous materials. In contrast, using a non-fluorous amine led to a system where the product could not be isolated using solid phase extraction, the product, starting materials and by-products all being eluted in the 80 % methanol/water solvent.

Curran *et al* have also investigated the separation of fluoros metal compounds from reaction mixtures. The removal of fluoros-tagged heavy metal contaminants from a reaction mixture was achieved using FSPE and standard organic solvents (Figure 1.25).<sup>110</sup>

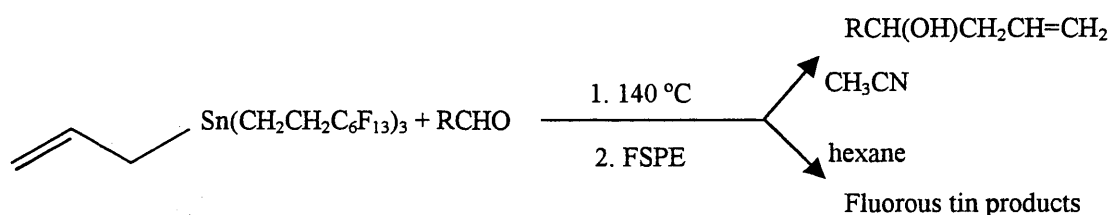


Figure 1.25. Isolation of fluoros by-products utilising fluoros solid phase extraction

Here, the organic products were selectively separated from the fluoros tin waste products by placing the reaction mixture on the top of a FRP silica gel column and eluting with acetonitrile. Again, having isolated the desired molecules, the spent tin catalyst could be re-isolated by elution with a non-polar solvent such as hexane. This is a very useful process as the toxic heavy metal can be completely removed from the product by a simple method. Also, theoretically, the tin catalyst

could be regenerated and reused in further syntheses eliminating waste tin, although this has yet to be demonstrated.

#### 1.4 Outline of Research

The method of Light Fluorous Synthesis, as described in section 1.3, shows that the tagging of organic molecules with fluorous ponytails does not seriously affect their solubility in common organic solvents, but does provide an effective handle for simple separation on FRP silica gel. These results suggest that the idea of 'Light Fluorous Catalysis' is also possible using Fluorous Solid Phase Catalyst Extraction. Here, the catalyst would be rendered 'lightly' fluorinated by the addition of a small number of fluorous ponytails to the modifying ligands.

For an ideal FSPCE system, a minimum number of fluorous ponytails should be incorporated into a catalyst for asymmetric synthesis *via* its ligands. Addition of a small number of ponytails would, ideally, only slightly affect the solubility of the catalyst in common organic solvents, requiring little/no modification to the solvent system used during reaction, whilst providing an effective handle for catalyst re-isolation. After the reaction is complete, the reaction mixture could be passed down a column of FRP silica gel and the products eluted with a polar solvent for which the fluorous catalyst has little/no affinity. After complete removal of the products, the catalyst could then be eluted with a solvent for which it has a strong affinity, re-isolated by removal of the elutant and reused in further catalysis with no loss of activity or selectivity.

Once again, work within the group at the University of Leicester has shown that such a technique is possible using fluorinated derivatives of acetoacetate ligands.<sup>111</sup> Using  $[\text{Ni}(\text{F}_{13}\text{C}_6\text{COCHCOC}_6\text{F}_{13})_2]$ , 2,4-pentanedione could be converted to the corresponding enaminodione after reaction with ethyl cyanoformate in 99 % yield, compared to only 74 % yield when  $[\text{Ni}(\text{acac})_2]$  was used as catalyst. After separation using FRP silica gel, the catalyst could be reused three times before any significant loss of activity was observed. This investigation aimed to extend this success into asymmetric catalysis using catalysts and ligands that could be employed in a broader range of reactions.

The work presented in this thesis describes the investigation of a number of catalytic systems. For each system, the following aims are discussed:

- The synthesis of light fluorous analogues of common chiral organic ligands with a broad range of catalytic applications and full characterisation.
- The investigation of the effect of the perfluorocarbon chains on the abilities of the ligands to coordinate to 'informative' metal centres

- The production of light fluorinated and non-fluorinated analogues of known asymmetric catalysts and comparison of their activities/selectivities in known asymmetric syntheses.
- The evaluation of the ability to isolate the light fluorinated/non-fluorinated catalysts by separation using solid phase extraction and other means.
- The reuse of any isolated material in further catalysis and determination of its subsequent activity and selectivity.

## 1.5 References For Chapter One

1. Roelen, O., *Angew. Chem.*, 62, 1948, 60.
2. Aria, M., Guo, S. L., Nishiyama, Y., Shirai, M., Torii, K., *J. Catal.*, 161, 1996, 704.
3. *A Molecular View of Heterogeneous Catalysis*, Ed. E. G. Derouane, DeBoeck Université, Paris, 1996.
4. Masters, C., *Homogeneous Transition-metal Catalysis*, Chapman and Hall, Cambridge, 1981.
5. Jardine, F. H., Osborne, J. A., Wilkinson, G. J., Young, J. F., *J. Chem. Soc., Chem. Commun.*, 1965, 131.
6. Ikariya, T., Jessop, P. G., Noyori, R., *Science*, 269, 1995, 1065.
7. Burk, M. J., Feng, S., Gross, M. F., Tumas, W., *J. Am. Chem. Soc.*, 117, 1995, 8277.
8. Klinger, R. J., Krause, T. R., Rathke, J., *Organometallics*, 11, 1991, 585.
9. Ikariya, T., Jessop, P. G., Noyori, R., *Chem. Rev.*, 99, 1999, 475.
10. Sako, T., Sato, M., Yamane, S., *J. Chem. Eng. Jpn.*, 23, 1990, 770.
11. Laintz, K. E., Smith, R. D., Yonker, C. R., Wai, C. M., *J. Supercrit. Fluids*, 4, 1991, 194.
12. Baumann, W., Kainz, S., Koch, D., Leitner, W., *Angew. Chem. Int. Ed. Engl.*, 36, 1997, 1628.
13. Gouw, T. H., Jentoft, R. E., *Anal. Chem.*, 44, 1972, 681.
14. Ikariya, T., Jessop, P. G., Noyori, R., *Chem. Rev.*, 95, 1995, 259
15. Ikariya, T., Jessop, P. G., Noyori, R., *Organometallics*, 14, 1995, 1510
16. Ikariya, T., Jessop, P. G., Noyori, R., Sylvia, C. A., Xiao, J., *Tetrahedron Lett.*, 37, 1996, 2813
17. Ikariya, T., Jessop, P. G., Noyori, R., *Nature*, 368, 1994, 231.
18. Hsiao, Y., Ikariya, T., Jessop, P. G., Noyori, R., *J. Am. Chem. Soc.*, 118, 1996, 344.
19. Fukuzawa, S.-I., Metoki, K., Esumi, S.-I., *Tetrahedron*, 59, 2003, 10445.
20. 'Swan Unveil Supercritical Processing', *Process Intensification Newsletter*, 7, 2002.
21. Sugden, S., Wilkins, H., *J. Chem. Soc.*, 1929, 1291.
22. Hurley, F. H., Wier, T. P., *J. Electrochem. Soc.*, 98, 1951, 207.
23. Chum, H. L., Koch, V. R., Miller, L. L., Osteryoung, R. A., *J. Am. Chem. Soc.*, 97, 1975, 3264.
24. Armitage, P. D., Hussey, C. L., Kear, C. M., Scheffler, T. B., Seddon, K. R., *Inorg. Chem.*, 22, 1983, 2099.
25. Chauvin, Y., Gilbert, B., Guibard, I., *J. Chem. Soc., Chem. Commun.*, 1990, 1715.

26. Carlin, R. T., Wilkes, J. S., *J. Mol. Catal.*, 63, 1990, 125.
27. Wilkes, J. S., Zaworotko, M. J., *J. Chem. Soc., Chem. Commun.*, 1992, 965.
28. Chauvin, Y., Mussmann, L., Olivier, H., *Angew. Chem. Int. Ed. Engl.*, 34, 1995, 2698.
29. Keim, W., Wasserscheid, P., *Angew. Chem. Int. Ed. Engl.*, 39, 2000, 3772.
30. Huddleston, J. G., Rogers, R. D., Swatloski, R. P., Visser, A. E., Willauer, H. D., *Chem. Commun.*, 1998, 1765.
31. Dullius, E. L., Dupont, J., Einloft, S., de Souza, R. F., Suarez, P. A. Z., *Polyhedron*, 15, 1996, 1217.
32. Dullius, E. L., Dupont, J., Einloft, S., de Souza, R. F., Suarez, P. A. Z., *Inorg. Chim. Acta*, 255, 1997, 207.
33. Parshall, G. W., *J. Am. Chem. Soc.*, 94, 1972, 8716.
34. Waffenschmidt, H., Wasserscheid, P., *J. Mol. Catal.*, 164, 2000, 61.
35. Henze, H., Kaufmann, D. E., Nouroozian, M., *Synlett*, 1996, 1091.
36. Böhm, V. P. W., Herrmann, W. A., *J. Org. Chem.*, 572, 1999, 141.
37. Branco, L. C., Afonso, C. A. M., *J. Org. Chem.*, 69, 2004, 4381.
38. Brassat, I., Englert, U., Keim, W., Keitel, D. P., Killat, S., Suranna, G.-P., Wang, R., *Inorg. Chim. Acta*, 280, 1998, 150.
39. Dietrich, F. K., Dupont, J., Einloft, S., de Souza, R. F., *Polyhedron*, 15, 1996, 3257.
40. Dupont, J., Simon, L. C., de Souza, R. F., *Applied Catalysis A: General*, 175, 1998, 215.
41. Dupont, J., Montiero, A. L., de Souza, R. F., Zinn, F. K., *Tetrahedron: Asymmetry*, 2, 1997, 177.
42. Andersen, J.-A., Guise, S., Karodia, N., Newlands, C., *Chem. Commun.*, 1998, 2341.
43. Audic, N., Clavier, H., Mauduit, M., Guillemin, J.-C., *J. Am. Chem. Soc.*, 125, 2003, 9248.
44. Böhm, V. P. W., Herrmann, W. A., *Chem. Eur. J.*, 6, 2000, 1017.
45. Alario, F., Amrani, Y., Colleuille, Y., Dang, T. P., Jenck, J., Morel, D., Sinou, D., *J. Chem. Soc., Chem. Commun.*, 1986, 202.
46. Avery, A., Schut, D. M., Weakley, T. J. R., Tyler, D. R., *Inorg. Chem.*, 32, 1993, 233.
47. Herrmann, W. A., Kohlpaintner, C. W., *Angew. Chem. Int. Ed. Engl.*, 32, 1993, 1524.
48. Dror, Y., Manassen, J., *J. Mol. Catal.*, 2, 1977, 219.
49. Beck, M. T., Joó, F., Tóth, Z., *Inorg. Chim. Acta*, 25, 1977, L61.
50. Amrani, Y., Benhazma, R., Sinou, D., *J. Organomet. Chem.*, 288, 1985, C37.
51. Kinzel, E., Nagel, U., *Chem. Ber.*, 119, 1986, 1731.
52. Davis, M. E., Hanson, B. E., Tóth, I., *Tetrahedron: Asymmetry*, 1, 1990, 913.
53. Köckritz, A., Bischoff, S., Kant, M., Siefken, R., *J. Mol. Catal. A.*, 174, 2001, 119.

54. Cornils, B., Kuntz, E., *J. Organomet. Chem.*, 502, 1995, 177.
55. Bachmann, H., Herrmann, W. A., Kohlpaintner, C. W., *J. Mol. Catal.*, 1992, 73.
56. Horváth, I. T., Rábai, J., *Science*, 266, 1994, 72.
57. Horváth, I. T., *Acc. Chem. Res.*, 31, 1998, 641.
58. Bhattacharyya, P., Gudmunsen, D., Hope, E. G., Kemmitt, R. D. W., Paige, D. R., Stuart, A. M., *J. Chem. Soc. Perkin Trans. 1*, 1997, 3609.
59. Bhattacharyya, P., Croxtall, B., Fawcett, J., Gudmunsen, D., Hope, E. G., Kemmitt, R. D. W., Paige, D. R., Russell, D. R., Stuart, A. M., Wood, D. R., *J. Fluorine Chem.*, 101, 2000, 247.
60. Adams, D. J., Gudmunsen, D., Hope, E. G., Stuart, A. M., West, A. J., *J. Fluorine Chem.*, 121, 2003, 213.
61. Klement, I., Knochel, P., Lutjens, H., *Angew. Chem. Int. Ed. Engl.*, 36, 1997, 1454.
62. Hughes, R. P., Trujillo, H. A., *Organometallics*, 15, 1996, 286.
63. Bond, J., Cook, R., Horváth, I. T., Kiss, G., Mozeleski, E., Rábai, J., Stevens, P., *J. Am. Chem. Soc.*, 120, 1998, 3133.
64. Adams, D. J., Cole-Hamilton, D., Foster, D., Gudmunsen, D., Hope, E. G., Pogorzelec, P., Schwartz, G., Stuart, A. M., *Tetrahedron*, 58, 2002, 3901.
65. Gladysz, J., Horváth, I. T., Juliette, J. J., *Angew. Chem. Int. Ed. Engl.*, 36, 1997, 1610.
66. Gladysz, J., Horváth, I. T., Juliette, J. J., Rutherford, D., *J. Am. Chem. Soc.*, 121, 1999, 2696.
67. Gladysz, J., Horváth, I. T., Juliette, J. J., Rocaboy, C., Rutherford, D., *Catalysis Today*, 42, 1998, 381.
68. Paige, D. R., *'The Synthesis, Co-ordination Chemistry and Catalytic Applications of Phosphine Ligands Containing Long-Chain Perfluoroalkyl Groups.'*, Ph.D. Thesis, University of Leicester, 1998.
69. Banfi, S., Manfredi, A., Montanari, F., Pozzi, G., Quici, S., *Tetrahedron*, 52, 1996, 11879.
70. Colombani, I., Miglioli, M., Montanari, F., Pozzi, G., Quici, S., *Tetrahedron*, 53, 1997, 6145.
71. Montanari, F., Pozzi, G., Quici, S., *Chem Commun.*, 1997, 69.
72. Barbier, F., Begue, J.-P., Bonnetdelpon, D., Ravikumar, K., *Tetrahedron*, 54, 1998, 7457.
73. Cavazzini, M., Manfredi, A., Montanari, F., Quici, S., Pozzi, G., *Chem. Commun.*, 2000, 2171.
74. Xiang, J., Orita, A., Otera, J., *Adv. Synth. Catal.*, 344, 2002, 84.

75. Betzemeier, B., Knochel, P., *Angew. Chem. Int. Ed. Engl.*, **36**, **1997**, 2623.
76. Kleijn, H., Rijnberg, E., Jastrzebski, J. T. B. H., van Koten, G., *Org. Lett.*, **6**, **1999**, 853.
77. Hartley, F., *Supported Metal Complexes: A New Generation of Catalysts*, Wiley-VCH, **1985**, 4.
78. Haag, W., Whitehurst, D., 'Ion Exchange Resin Containing Zero-Valent Metal', US Patent No. 3578609, May 11, **1971**.
79. Cornils, B., Herrmann, W. A., *Applied Homogeneous Catalysis with Organometallic Compounds*, Wiley-VCH, Bench Ed., **2000**, 68.
80. Evans, G., Pitmann, C., McMillan, R., Beach, R., *J. Organomet. Chem.*, **67**, **1974**, 295.
81. Capka, M., Svoboda, P., Krauss, M., *Chem. Ind.*, **1972**, 650.
82. Rollmann, L., *Inorg. Chim. Acta*, **6**, **1972**, 137.
83. Haines, R., Pittmann, G., Smith, L., *J. Am. Chem. Soc.*, **97**, **1975**, 1742.
84. Grubbs, R., Kroll, L., Stuart, E., *J. Makromol. Sci. Chem.*, **7**, **1973**, 1047.
85. Corey, E. J., Venkateswarla, A. J., *J. Am. Chem. Soc.*, **94**, **1972**, 6190.
86. Boucher, L. J., Murrell, L. L., Oswald, A. A., *Preprints, Petrol Div. ACS Meeting*, Los Angeles, Mar. **1974**, 162.
87. Capka, M., *Collect. Czech Chem. Commun.*, **55**, **1990**, 2803.
88. Grubbs, R., Kroll, L., *J. Am. Chem. Soc.*, **93**, **1971**, 3062.
89. Michalska, M., *J. Mol. Catal.*, **3**, **1977/78**, 125.
90. Arhancet, J. P., Davis, M. E., Merola, J. S., *Nature*, **334**, **1989**, 454.
91. Arhancet, J. P., Davis, M. E., Merola, J. S., *Nature*, **334**, **1989**, 455.
92. Anson, M. S., Mirza, A. R., Tonks, L., Williams, J. M., *Tetrahedron Lett.*, **40**, **1999**, 7147.
93. Curran, D. P., Luo, Z., *J. Am. Chem. Soc.*, **121**, **1999**, 9069.
94. Sherrington, J., *Synthesis and Characterisation of Fluorophilic Materials for Use as Catalytic Supports*, Ph.D. First/Second Year Reports, University of Leicester, **1999-2001**.
95. Newkome, G. R., Moorefield, C. N., Vögtle, F., *Dendritic Molecules: Concepts, Synthesis, Perspectives*, VCH, Weinheim, **1996**.
96. Ribourdouille, Y., Engel, G. D., Gade, L. H., *C. R. Chimie*, **6**, **2003**, 1087.
97. King, A. S. H., Twyman, L. J., *J. Chem. Soc. Perkin Trans. 1*, **2002**, 2209.
98. Kollner, C., Pugin, B., Togni, A., *J. Am. Chem. Soc.*, **120**, **1998**, 10274.
99. Engel, G. D., Gade, L. H., *Chem. Eur. J.*, **8**, **2002**, 4319.
100. Deng, G.-J., Fan, Q.-H., Chen, X.-M., Liu, D.-S., Chan, A. S. C., *Chem. Commun.*, **2002**, 1570.

101. De Groot, D., de Waal, B. F. M., Reek, J. N. H., Schenning, A. P. H. J., Kamer, P. C. J., Meijer, E. W., van Leeuwen, P. W. N. M., *J. Am. Chem. Soc.*, 123, **2001**, 8453.
102. Mizugaki, T., Murata, M., Ooe, M., Ebitani, K., Kaneda, K., *Chem. Commun.*, **2002**, 52.
103. Goetheer, E. L. V., Baars, M. W. P. L., van den Broeke, L. J. P., Meijer, E. W., Keurentjes, J. T. F., *Ind. Eng. Chem. Res.*, 39, **2000**, 4634.
104. Caminade, A.-M., Turrin, C.-O., Sutra, P., Majoral, J.-P., *Current Opinion in Colloid and Interface Science*, 8. **2003**, 282.
105. Dijkstra, H. P., van Klink, G. P. M., van Koten, G., *Acc. Chem. Res.*, 35, **2002**, 798
106. Kragl, U., Dwars, T., *Trends in Biotechnology*, 19, **2001**, 442.
107. Balkus Jr., K. J., Khanmamedova, A. K., Dixon, K. M., Bedioui, F., *Applied Catalysis A: General*, 143, **1996**, 159.
108. Sheldon, R. A., Arends, I. W. C. E., Lempers, H. E. B., *Catalysis Today*, 14, **1998**, 387.
109. Curran, D. P., Luo, Z., *J. Am. Chem. Soc.*, **1999**, 121, 9069.
110. Curran, D. P., Hadida, S., He, M., *J. Org. Chem.*, **1997**, 62, 6714.
111. Croxtall, B., Hope, E. G., Stuart, A. M., *Chem. Commun.*, **2003**, 2430.

## 2 The Investigation of BINAP

### 2.1 Introduction

#### 2.1.1 BINAP in Catalysis

There are many examples of asymmetric catalysts which produce both high enantioselectivity and high yields of desired products.<sup>1-10</sup> To study the synthesis of light fluorescent materials of all of these systems would take time well beyond the scope of this text. Therefore, to investigate the light fluorescent approach to synthesis of separation polymers, examples of highly effective asymmetric catalytic systems have been selected.

The first example of a ligand that is employed in such systems is the C<sub>2</sub>-symmetric 1,1'-binaphthalene-2,2'-diylbis(diphenylphosphino)ethane, more commonly referred to as BINAP (R) and (S)-D.

# Chapter Two



**“The great tragedy of science – the slaying of a beautiful hypothesis with an ugly fact.”**

**- Thomas Huxley**

The efficacy and selectivity of application of BINAP is difficult to overstate. There are hundreds of examples of asymmetric catalysts that employ the ligand and yield products of high enantioselectivity and in high yield. BINAP has been used as an effective ligand in many asymmetric systems including hydrogenations,<sup>11,12</sup> hydroformylations,<sup>13</sup> arylations,<sup>14</sup> hydroborations<sup>15</sup> and allylations.<sup>16</sup>

Specific examples of the uses of BINAP include the hydroboration of  $\alpha$ -acylimine/cyclic amide or esters employing the Rh(D) BINAP catalyst  $[(\text{BINAP})\text{Rh}(\text{D})\text{Cl}(\text{OAc})\text{C}(\text{O})\text{R}]$  (figure 2.1).

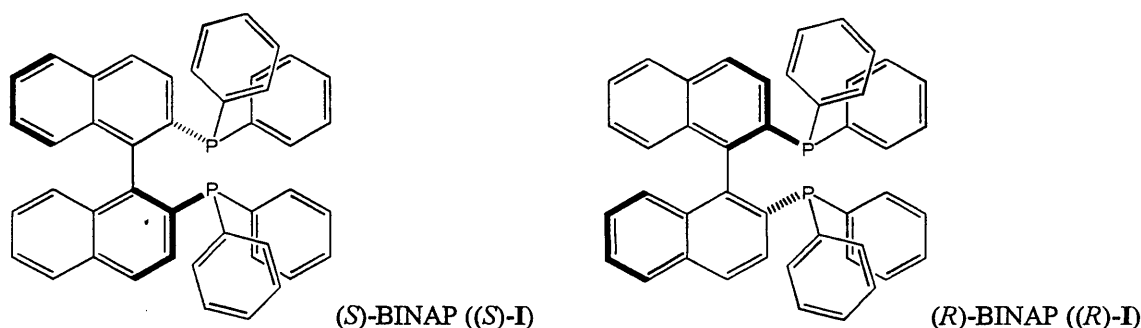
## 2 The Investigation of BINAP

### 2.1 Introduction

#### 2.1.1 BINAP in Catalysis

There are many examples of asymmetric catalysts which produce both high enantioselectivities and high yields of desired products.<sup>1,2,3,4</sup> To study the synthesis of light fluoruous analogues of all of these systems would take many years and is well beyond the scope of this report. Therefore, to investigate the light fluoruous approach to synthesis and separation, pertinent examples of highly effective asymmetric catalytic systems have been selected.

The first example of a ligand that is employed in such systems is the C<sub>2</sub>-symmetric 2,2'-bis(diphenylphosphino)-1,1'-binaphthyl, more commonly referred to as BINAP ((*R*) and (*S*)-I).



BINAP is possibly the most well known example of an axially chiral diphosphine and was first synthesised by Noyori and Takaya.<sup>5</sup> Asymmetry in products is induced by steric interactions between the bulky triarylphosphine system and the reactants bound to the active metal centre of the catalyst. The arrested rotation in BINAP forces the ligand to coordinate in one orientation and interconversion between the (*R*) and (*S*) enantiomers is not possible at room temperature. Upon coordination of a prochiral substrate, the bulky phenyl groups attached to each of the phosphorus atoms effectively block one face of the substrate molecule to reaction. Activation of the prochiral substrate molecule by the catalyst metal centre leads to an increased rate of reaction with greatly enhanced enantioselective productivity.

The efficacy and widespread application of BINAP is difficult to overstate. There are hundreds of examples of asymmetric catalysts that employ the ligand and yield products of high enantiopurity and in high yield. BINAP has been used as an effective ligand in many asymmetric systems including hydrogenations,<sup>6,7,8</sup> hydroformylations,<sup>9</sup> arylations,<sup>10</sup> hydroborations<sup>11</sup> and allylations.<sup>12</sup>

Specific examples of the uses of BINAP include the hydrogenations of  $\alpha$ -(acylamino)acrylic acids or esters employing the Rh(I) BINAP catalyst [Rh(BINAP)(norbornadiene)]ClO<sub>4</sub><sup>13</sup> (Figure 2.1).

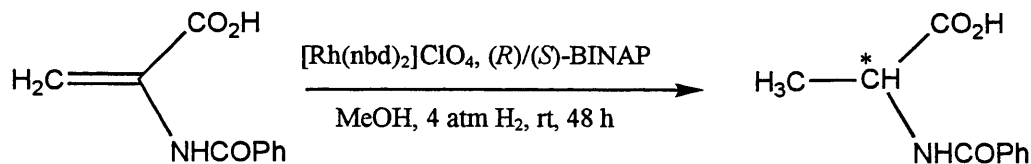


Figure 2.1. Asymmetric hydrogenation using BINAP as a ligand

Here, for a range of starting materials, yields of up to 99 % were achieved with enantioselectivities as high as 100 % under exceptionally mild reaction conditions using only 1 mol % catalyst concentrations. Even complex molecules could be hydrogenated specifically with comparable yields and selectivities, showing the tolerance and scope of the ligand and catalyst.

The arylation of  $\gamma$ -butyrolactones using a nickel-based catalyst also shows how effective BINAP can be as a ligand<sup>14</sup> (Figure 2.2).

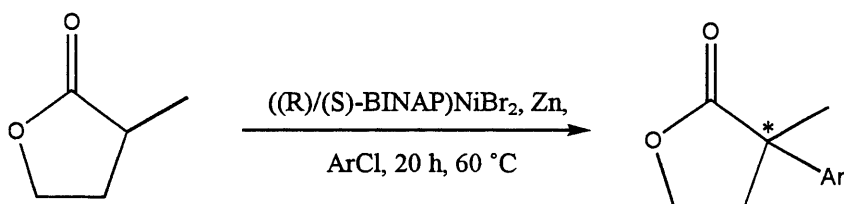


Figure 2.2. Asymmetric arylation using BINAP as a ligand

Reduction of the nickel(II) metal centre by zinc *in situ* led to a catalyst with enantioselectivities as high as 96 % depending on the aryl chloride used, although 15 mol % of the ligand was required. A variety of electron-rich and electron-poor aryl chlorides could be employed, including bulky 2-chloronaphthalene, chlorobenzene and *ortho*- and *meta*-methoxychlorobenzene. The presence of ethyl esters and silyl ethers could be tolerated and the yields of products were good, ranging between 80 and 95 %.

A final example of the usefulness of BINAP as an asymmetric ligand concerns the formation of chiral organoboron compounds, again by asymmetric hydrogenation.<sup>15</sup> Such compounds can be oxidised to form chiral “building blocks” for use in organic synthesis (Figure 2.3).

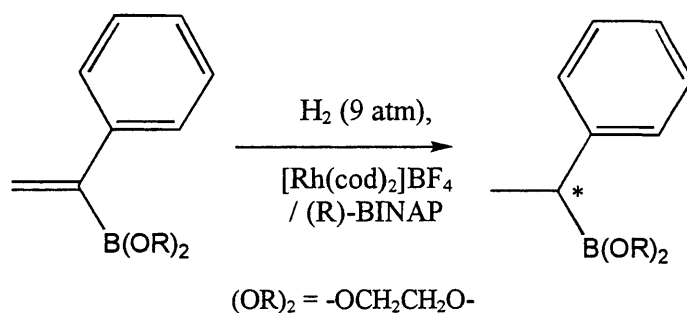


Figure 2.3. The production of chiral organic “building blocks” using BINAP as a ligand

A relatively high catalyst loading of 3.6 mol% was used. Hydrogenation of the double bond produced yields as high as 75 % and an enantiomeric excess of 80 % was achieved. It was noted that enantioselectivity was strongly related to temperature during reaction, with lower temperatures producing higher enantiomeric purities. Due to the long reaction period, a TOF of only 0.13 h<sup>-1</sup> was observed.

These examples and countless others show BINAP to be an exceptionally useful ligand in asymmetric catalysis with many wide-ranging applications. However, in almost all cases, no indication is made as to whether there were any attempts to recover and reuse the catalysts prepared. Whilst the primary issue in the majority of examples was to prepare and evaluate the effectiveness of BINAP-metal complexes as asymmetric catalysts, making no study of the ability to isolate the catalyst and reuse it in further catalysis leaves the experiments seemingly incomplete. Clearly, for products which are to be used in the fine chemical or pharmaceutical industries, there can be no heavy metal or ligand contamination. In addition, the cost of the catalyst precursors and BINAP itself is not trivial and so the isolation and reuse of the catalyst and/or ligand is of vital importance in these systems if they are to become commercially viable.

### 2.1.2 Examples of Recyclable BINAP

Examples of the use of recoverable and recyclable BINAP-based catalysts are limited. However, it would seem that the reason for the scarcity of literature on the reuse of such systems is not due to the inability to recover the ligand or catalyst; more that the ability to recover the catalyst species is simply not investigated.

Recently, Lemaire *et al.* have looked at the recycling of a water-soluble *diam*BINAP-based catalyst after an asymmetric hydrogenation reaction (Figure 2.4).<sup>16</sup>

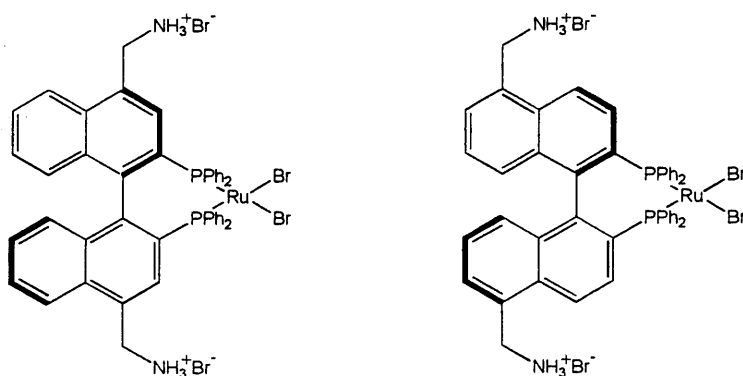


Figure 2.4. Water-soluble Ru(II) hydrogenation catalysts ((*R*)-enantiomers shown)

When (*R*)-BINAP was used in the hydrogenation of ethyl acetoacetate, complete conversion and 98 % product *ee* could be achieved after 15 hours in ethanol under 40 bar H<sub>2</sub>. Using the two water-soluble catalysts shown in Figure 2.4 in independent reactions, ethyl acetoacetate could be completely hydrogenated in water at 50 °C after 15 hours under 40 bar H<sub>2</sub> using either ligand. The product *ee* was determined to be greater than 97 % after each run, with up to eight recycles being possible for both ligands. The ligands could also be used in the hydrogenation of other ketoesters with similar results. However, long reaction times were required due to the relatively low solubility of hydrogen in water.

Saluzzo *et al.* have reported a range of BINAP derivatives with polyamide or urea functionalities in the 6,6'-positions.<sup>17</sup> These substitutions either render the BINAP ligand insoluble and so make re-isolation of the ligand by filtration straight forward, or allow recovery of the ligand by precipitation with the addition of an appropriate solvent. All of the ligands prepared used *diam*-BINAP as a starting material (**II**) and some of the ligands are shown in Figure 2.5.

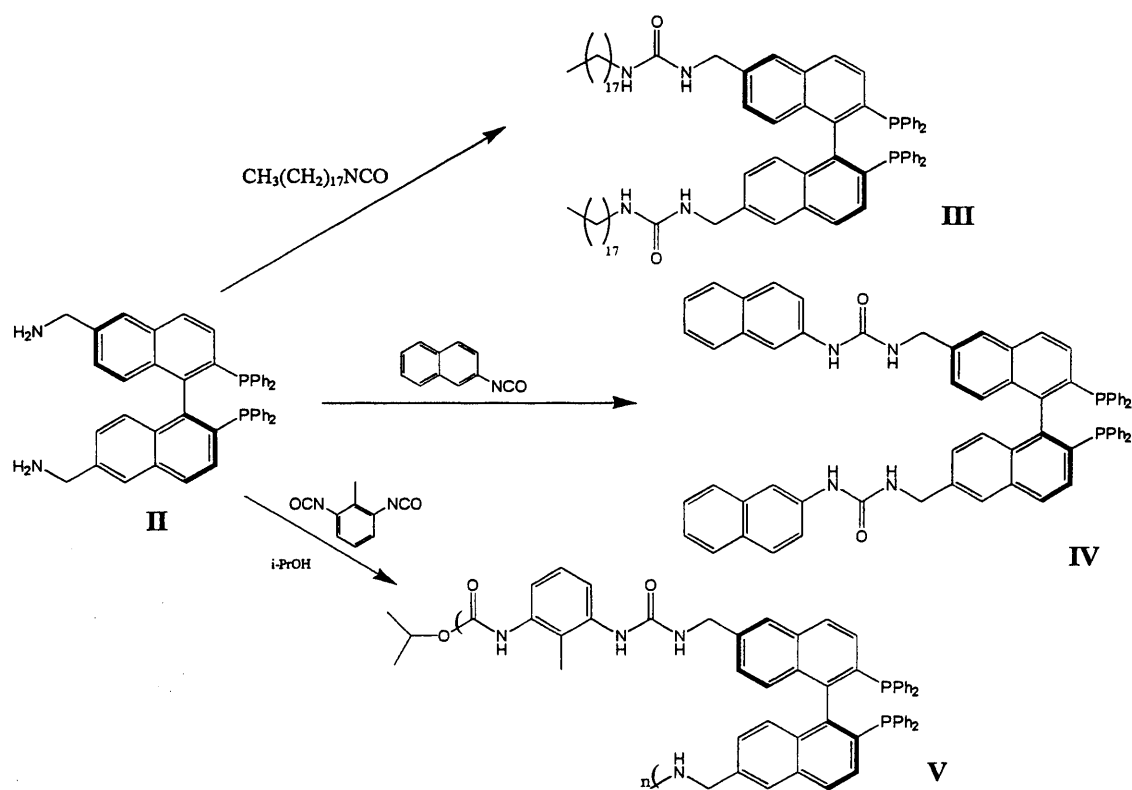


Figure 2.5. The synthesis of selected heterogeneous BINAP ligands

In the hydrogenation of methyl acetoacetate using  $[\text{RuCl}_2(\text{benzene})]_2$ , ligand **III** gave conversions and product *ee*'s of 100 %. However, the catalyst was homogeneous and so could not be recovered by filtration. Ligand **IV** also led to *ee*'s and conversions of 100 % in the first catalytic run, but subsequent reuse of the recovered catalyst led to reduced conversions and

enantioselectivities. (99 % conversion, 97 % *ee* run 2; 54 % conversion, 33 % *ee* run 3). The final ligand shown (**V**) proved to be the best ligand for recovery and reuse, continually giving 100 % conversion and 99 % *ee* after three runs. The ligand could be easily recovered by filtration under argon and reused without purification. However, as expected for heterogeneous systems, the rate of reaction was much slower by comparison to the system using ligand **III**, and 18 hours were required for full conversion of the methyl acetoacetate to methyl 3-hydroxybutyrate.

Ruthenium-BINAP catalysts have been immobilised in ionic liquids and used in the hydrogenation of 2-phenylacrylic acid (Figure 2.6).<sup>18</sup>

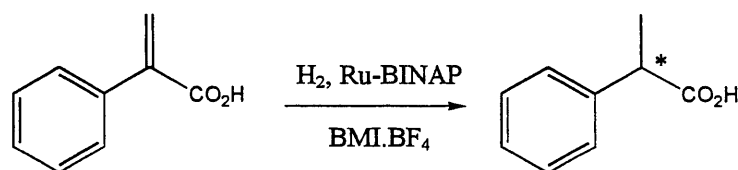


Figure 2.6. Asymmetric hydrogenation of 2-phenylacrylic acid

After hydrogenation, when isopropanol and 1-*n*-butyl-3-methylimidazolium tetrafluoroborate (BMIMBF<sub>4</sub>) were used as solvents, the 2-phenylpropionic acid product could be isolated from the [RuCl<sub>2</sub>(*S*)-BINAP]<sub>2</sub>.NEt<sub>2</sub> catalyst, which was preferentially soluble in the ionic liquid phase, by simple decantation of the organic phase from the ionic liquid phase. The ionic liquid phase could then be reused in further catalysis with no loss of activity or enantioselectivity. 100 % conversion to the desired product was achieved with good product *ee*'s of between 70 and 85 %.

Better product conversions and *ee*'s were observed in the asymmetric hydrogenation of a range of  $\beta$ -keto esters using the ionic-liquid-immobilised Ru-based catalysts shown in Figure 2.7.<sup>19</sup>

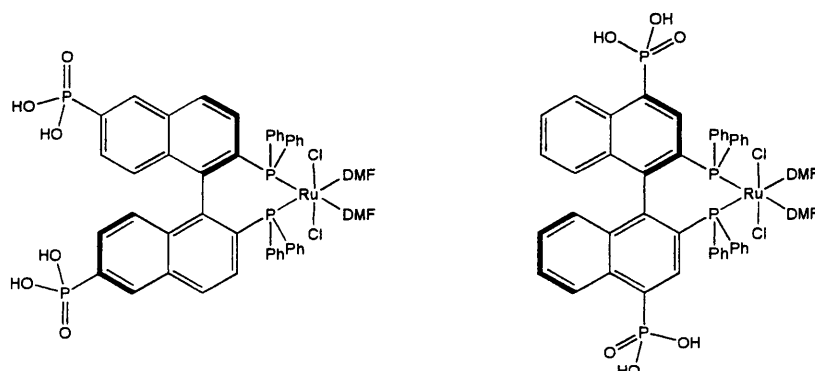


Figure 2.7. Derivatised BINAP catalysts soluble in room temperature ionic liquids

In a range of room temperature ionic liquids, methyl acetoacetate could be hydrogenated in high conversion and high *ee* and extracted from the ionic liquid/methanol homogeneous phase using hexane. The ionic liquid phase could then be used in further catalysis. When BMIMBF<sub>4</sub> was used as

ionic liquid solvent, high product *ee*'s of greater than 95 % could still be achieved after 4 runs, but the conversion fell from 99 % to 75 % and fell to only 45 % after a fifth recycle. However, when propyl-2,3-dimethylimidazolium bis(trifluoromethylsulphonyl)amide was used instead, product *ee*'s of greater than 97 % could still be achieved after four runs with conversions of greater than 99 %. It was not until the fifth run using this solvent that the conversion started to fall.

Soluble polymer-supported BINAP-based catalysts have been investigated as candidates for facile recycling.<sup>20</sup> Chan *et al.* have synthesised short-chain BINAP-containing polymers for use in ruthenium-catalysed asymmetric hydrogenation of 2-(6'-methoxy-2'-naphthyl)acrylic acid, the precursor to the anti-inflammatory drug naproxen (Figure 2.8).<sup>21</sup>

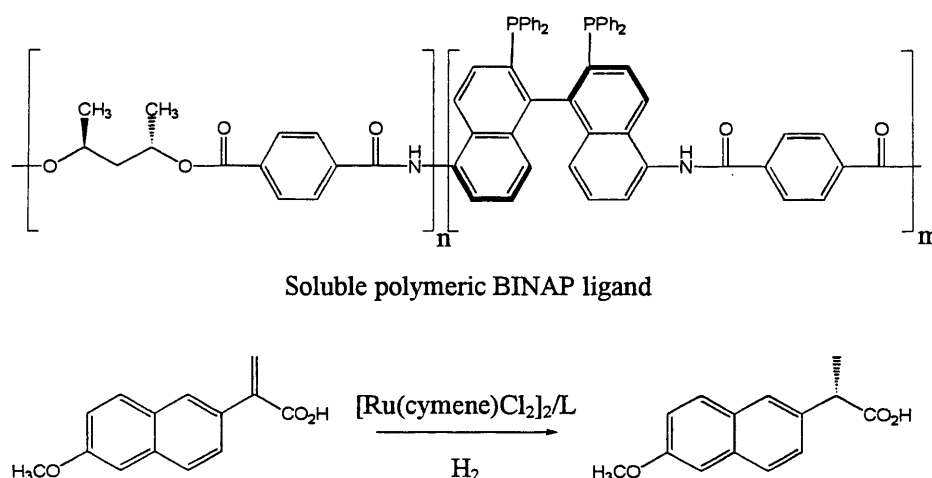


Figure 2.8. Soluble polymer-supported BINAP and formation of naproxen by Ru-catalysed asymmetric hydrogenation

The catalysis was carried out in methanol/toluene (2:3 v/v) under 110 bar H<sub>2</sub> and 95.4 % conversion and 87.7% *ee* obtained after four hours at room temperature. Interestingly, under the same conditions using (*S*)-BINAP as ligand only 56.5 % conversion was achieved, although the product *ee*'s were comparable. This rate acceleration was attributed to the added steric bulk of the polymer support which affects the dihedral angle of the binaphthyl rings. The active catalyst was recycled by simple precipitation and filtration ten times with no loss of activity or enantioselectivity.

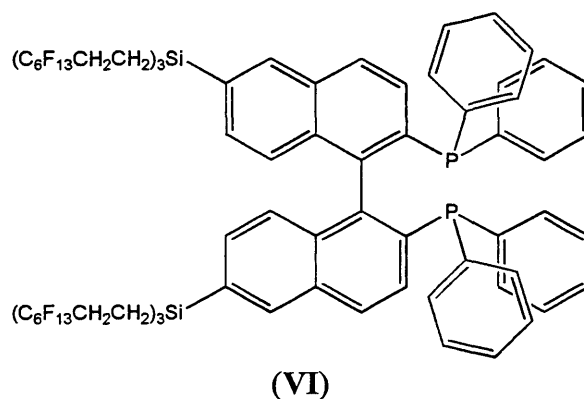
Other notable examples of systems for the recycling of BINAP-based catalysts include sol-gel entrapped rhodium and ruthenium hydrogenation catalysts<sup>22</sup>, dendritic BINAP-based catalysts<sup>23,24</sup> and porous hybrid solids containing Ru-based catalysts for asymmetric hydrogenation.<sup>25</sup> All of these examples show innovative ways in which BINAP can be used and recycled after asymmetric catalysis but, as stated before, they are a minority in the literature. They

also serve to show that the isolation and recovery of BINAP after catalysis is possible and that the investigation of other methods of recovery and reuse are pertinent.

### 2.1.3 Fluorous BINAP

Because BINAP is such an impressive ligand in a wide range of asymmetric catalyses and because the study of the recovery and reuse of its catalysts has been largely overlooked, the investigation of light fluorous versions of BINAP seems logical and appropriate.

Fluorous analogues of BINAP have been prepared previously, but extensive attempts to separate the ligands from reaction mixtures by any method and reuse them have not commonly been undertaken. Nakamura, Takeuchi and co-workers have prepared a BINAP analogue with six fluorous ponytails attached to the binaphthyl backbone in the 6,6'- positions *via* a silicon atom<sup>26</sup> (VI).



This ligand contains an additional  $C_2H_4$  spacer unit in the fluorous ponytail to further insulate the phosphorus atom from the electron withdrawing effect of the fluorine atoms and contains 53.7 % fluorine by weight. Partition coefficients, determined by stirring a known amount of ligand in equal amounts of a perfluorocarbon solvent and organic solvent and then analysing the contents of each layer, showed that the BINAP was preferentially soluble in the fluorous solvent. However, judicious choice of the organic solvent was required to maximize the separation. A mixture of FC-72 (perfluoro-*n*-hexane) and acetonitrile gave a partition coefficient (defined as (concentration of species in fluorous layer) / (concentration of species in organic layer)) of 49.0, whereas an FC-72/benzene mixture only yielded a partition coefficient of 2.9.

The ligand was used in an asymmetric Heck reaction of 2,3-dihydrofuran with 4-chlorophenyl triflate (Figure 2.9).

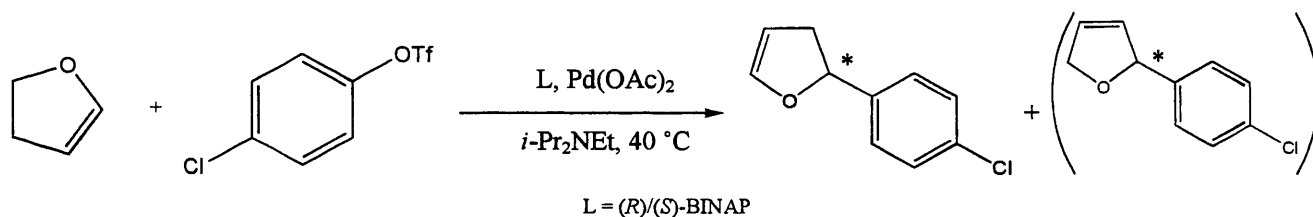


Figure 2.9. Palladium-catalysed cross-coupling reaction using BINAP as a ligand<sup>26</sup>

The enantioselectivity of the catalyst was excellent and compared favourably with the non-fluorinated analogue. However, the yield of the product was reduced when the fluorinated ligand was employed in comparison to the yields achieved for the non-fluorinated system (67 % *versus* 59 %). Attempted separation of the fluorinated BINAP by using fluorinated reverse phase (FRP) silica gel was only partially successful. Much of the ligand had been converted to the phosphine-oxide (BINAPO) during reaction and would require a reduction step before it could be reused. In addition, the catalytically active metal centre was not retained. Further, carrying out the reaction in a benzene-FC-72 biphasic system lowered the yield even more and attempted reuse of the catalyst-containing fluorinated solvent in subsequent catalytic runs produced no additional product, presumably due to ligand oxidation.

Pozzi and co-workers have synthesised a BINAP-related light fluorinated ligand which can be employed in asymmetric allylic alkylations.<sup>27</sup> 2-(Di-*para*-perfluorohexyl-phenylphosphino)-2'-(1*H*,1*H*-perfluorooctyloxy)-1,1'-binaphthyl (Rf-MOP), (VII), was used as ligand in the palladium(0)-catalysed alkylation of 1,3-diphenylprop-2-enyl acetate (Figure 2.10).

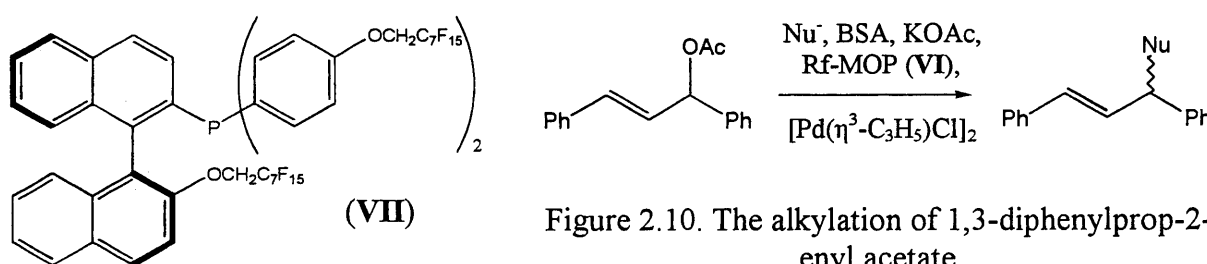


Figure 2.10. The alkylation of 1,3-diphenylprop-2-enyl acetate

Four different carbon nucleophiles were used, three of which lead to high yields of product (> 70 %) with enantiomeric excesses of greater than 81 %. When toluene was used as the reaction solvent, the fluorinated ligand and palladium complexes could be completely recovered by two 5 ml extractions using *n*-perfluorooctane. However, once again this recovered material showed no catalytic activity in subsequent reactions.

The addition of fluorous ponytails to BINAP ligands is not limited to substitutions on the binaphthyl backbone. Pozzi, Sinou and co-workers recently demonstrated that ponytails could also be added to the phenyl rings of the diphenylphosphine unit.<sup>28</sup> Using an 8-step synthesis, ligand **VIII** (Figure 2.11) could be isolated in 4 % overall yield

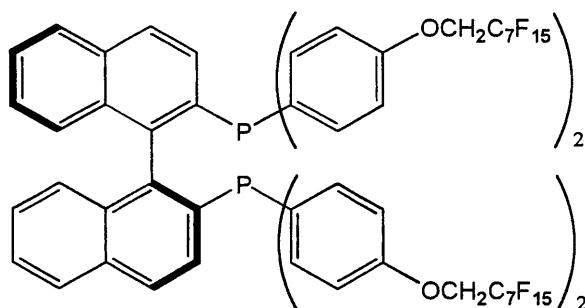


Figure 2.11. Ligand **VIII**

The ligand was shown to be effective in a range of asymmetric catalysed reactions. However, it gave consistently lower product conversions and *ee*'s than BINAP or fluorous analogues of BINAP that had been substituted at the 6,6'-positions. The ligand was also not sufficiently fluorous to be preferentially soluble in a perfluorocarbon solvent, but it could be removed from products by liquid-liquid extraction using FC-72. However, the recovered material was not catalytically active in further reactions, presumably due to phosphine oxidation. Due to the extensive chemistry required to achieve ponytail addition on the phenyl rings and the binaphthyl backbone, it would be unfeasible to produce a BINAP ligand with substitution at both the PPh<sub>2</sub> and 6,6'-positions.

These results are, needless to say, disappointing. With optimisation, the fall in overall yields of products obtained in fluorous systems in comparison to non-fluorous systems could possibly be reduced. In addition, the ability to separate the ligand and heavy metal from the product by simple extraction or column chromatography is advantageous. However, unless the catalyst can be recovered and recycled, the cost associated with preparing a fluorinated ligand and the difficult syntheses which are often involved means that these systems are unlikely to acquire widespread use.

It is, however, also unlikely that an analogue of BINAP completely suitable for fluorous biphasic catalysis could ever be successfully prepared. Combining the work of Pozzi, Sinou,<sup>28</sup> Nakamura and Takeuchi<sup>26</sup> to maximise the fluorine content of the ligand would still only yield a fluorous BINAP (**A**) with 60 % fluorine by weight (Figure 2.12). The synthesis of such a ligand would be prohibitively expensive, difficult and low yielding and the ligand would also weigh 4150 gmol<sup>-1</sup>, making it highly insoluble in most solvents. Even following successful synthesis, the

electron-withdrawing effect of so many fluororous ponytails would be likely to make the ligand so sensitive to oxidation that it could not be used. An alternative fluororous BINAP (**B**), also shown in Figure 2.11, would contain 62 % by weight fluorine but, once again, its complex and expensive synthesis would be prohibitive and the ligand would be likely to be even more sensitive to oxidation than ligand (**A**). It is for these reasons that light fluororous analogues of BINAP are much more appropriate for recovery and reuse.

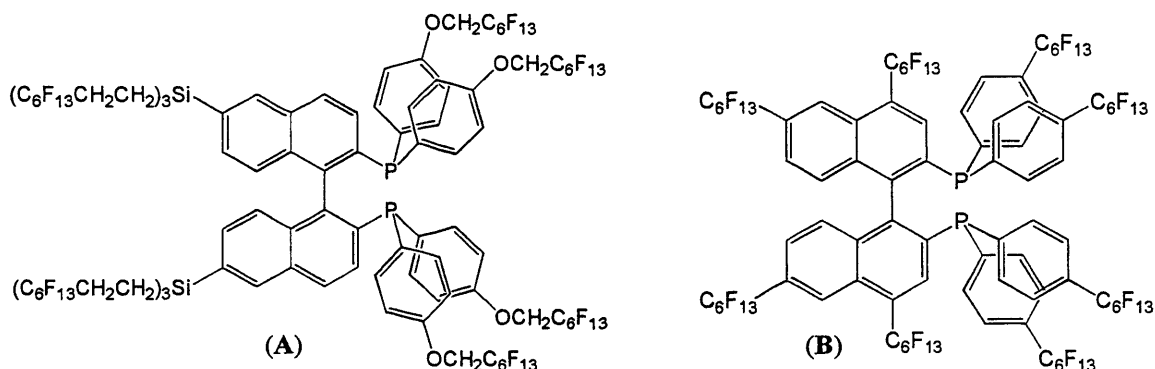
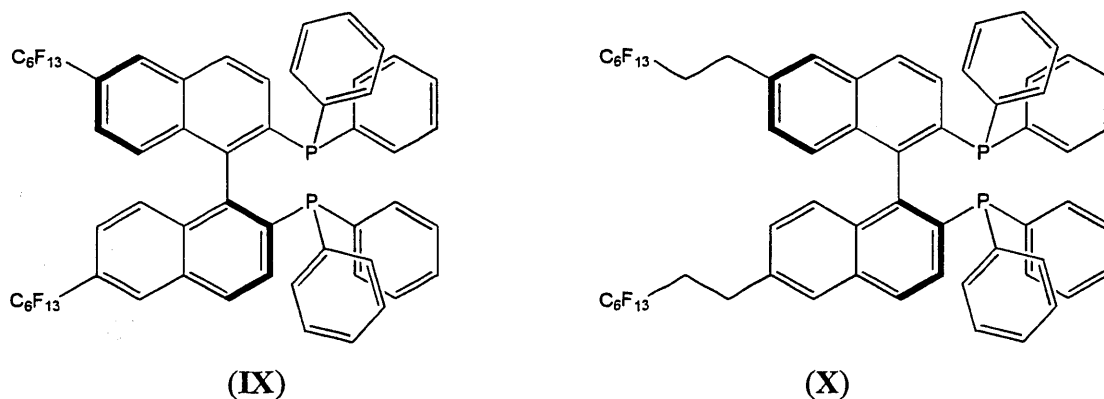


Figure 2.12. Fluororous BINAP ligands with > 60 % by weight fluorine content

It had been proposed that a light fluororous BINAP would be of use in reactions carried out under supercritical conditions<sup>29</sup> (see Chapter One). This previous work, carried out at the University of Leicester, prepared two light fluororous analogues of BINAP, (**IX**) and (**X**), ((*S*)-enantiomers shown) for use in supercritical fluid hydrogenation reactions.



Here, the perfluoroalkyl chains attached to the binaphthyl backbone were present to promote the solubility of the ligand and subsequently formed catalysts in the supercritical fluid. However, initial testing of catalysts employing the two light fluororous BINAP ligands was carried out in standard organic solvents. The results of these experiments showed that the fluororous ponytails had no effect on the enantioselectivity of the catalyst but, when (**IX**) was used, the yield of product was reduced to 42 % in comparison to 88 % in the non-fluororous system if the same conditions were

used. The additional  $C_2H_4$  spacer unit in (X) helped shield the metal centre from the electron-withdrawing effect of the ponytails more effectively and the yield of the product was virtually the same as the non-fluorous system (83 %). No attempts were made to recover the catalysts after reaction, and further study into the applicability of the ligands under supercritical conditions has yet to be carried out.

Very recently, similar ligands to those prepared at the University of Leicester have been synthesised for use in supercritical  $CO_2$  for the hydrogenation of methyl and ethyl acetoacetate and methyl-2-acetamidoacrylate (Figure 2.13).<sup>30</sup>

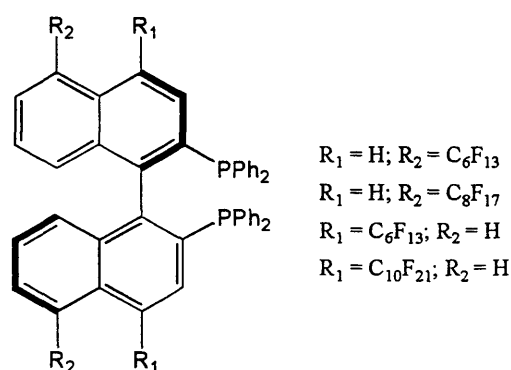


Figure 2.13. Derivatised BINAP for  $scCO_2$  asymmetric hydrogenation reactions

In methanol, both ethyl and methyl acetoacetate could be hydrogenated with 100 % conversion and, on average, 98 % *ee* with all the ligands prepared. However, the hydrogenation of methyl-2-acetamidoacrylate in  $scCO_2$  could not be achieved without the addition of a fluorinated co-solvent. 100 % conversion to product could then be achieved with *ee*'s as high as 74 %, although standard BINAP gave the same conversion and similar product *ee*'s.

The results from this preliminary work were promising, as they showed that light fluorous ligands could be employed in common organic solvents without being detrimental to enantioselectivities of products. With optimisation, it was also likely that the yields of products could be improved using the ligands prepared within the group. The expansion of the study of (IX) and (X) into light fluorous synthesis and separation was, therefore, an ideal place to commence investigation.

## 2.2 Synthesis and Coordination Chemistry

### 2.2.1 The Synthesis of Light Fluorous BINAP Ligands

A full synthetic route for the preparation of 6,6'-bis(perfluoro-*n*-hexyl)-2,2'-bis(diphenylphosphino)-1,1'-binaphthyl (Rf-BINAP), (IX) had already been prepared from previous work within the group<sup>29</sup> but problems associated with the deprotection of 6,6'-bis(perfluoro-*n*-

hexyl)-2,2'-diacetoxy-1,1'-binaphthyl (step (iv), Figure 2.14) led to improvements being made to the procedure. The use of sodium hydride in mineral oil as deprotecting agent led to contamination of the product with the mineral oil, which proved exceptionally difficult to remove completely. It was decided that the use of a different deprotecting agent was necessary to produce cleaner product. Previous work within the group had raised concerns about the use of sodium methoxide not generated *in-situ* as a deprotecting agent, as loss of fluoros ponytails had been observed following the addition of sodium ethoxide. However, the deprotection of acetoxy-protected fluoros biphenols could be achieved using sodium ethoxide in ethanol without any apparent degradation of the fluoros ponytails.<sup>31</sup> In the binaphthyl system, the use of either sodium ethoxide or sodium methoxide also had no effect on the ponytails and the acetoxy protecting groups were cleanly removed. Switching away from sodium hydride meant that the removal of the troublesome mineral oil from the deprotected product was no longer required and the free alcohol could be used in the next synthetic step after a simple recrystallisation. This full synthesis was therefore achieved as outlined in Figure 2.14.

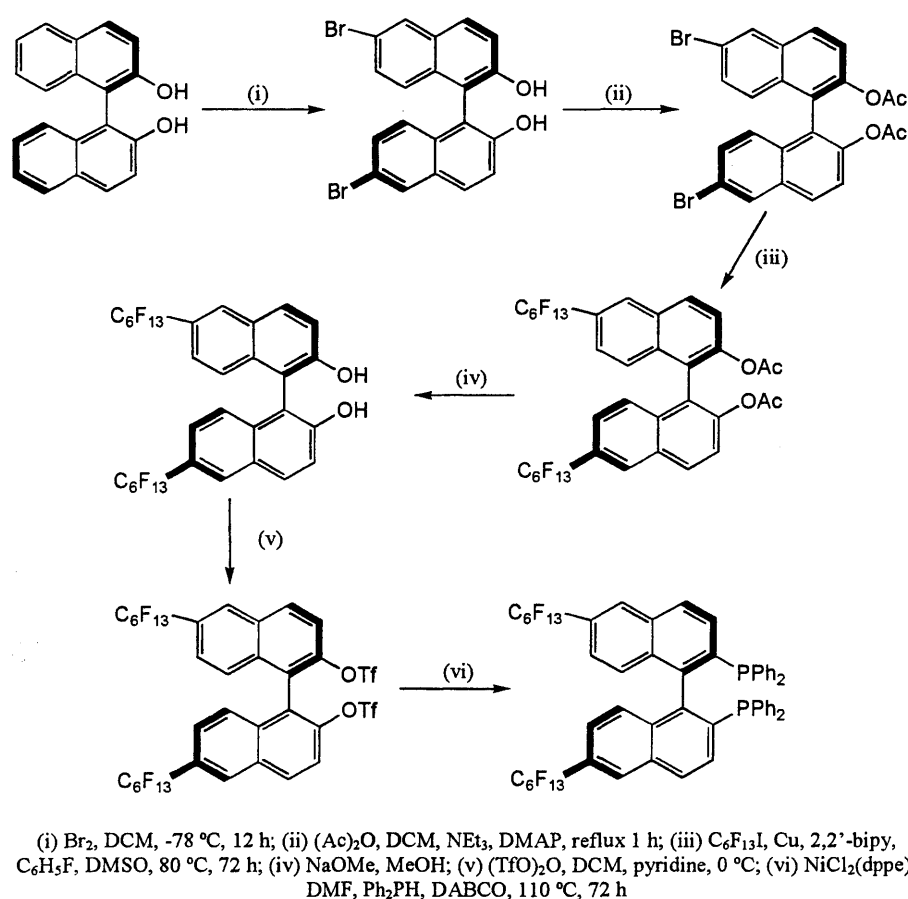


Figure 2.14. Modified literature route for the synthesis of Rf-BINAP<sup>29</sup>

To attach fluoros ponytails, a copper-mediated cross-coupling reaction was undertaken (Reaction 2.3). The cross-coupling of iodofluoroalkanes with iodoarenes in the presence of copper

powder in an aprotic solvent was first examined in detail by McLoughlin and Thrower.<sup>32</sup> This reaction was extended further by Chen *et al.* to include a variety of bromoarenes,<sup>33</sup> as employed here.

As a consequence of the large electron-withdrawing effect of the perfluoroalkyl group, the iodine-carbon bond in perfluoroalkyl iodides is polarised to give a partial positive charge at iodine. This allows interaction between the iodine and polar aprotic solvents such as DMSO and DMF. In such solvents, a perfluoroalkylcopper reagent is formed and this can react with aryl bromides or iodides (Figure 2.15).

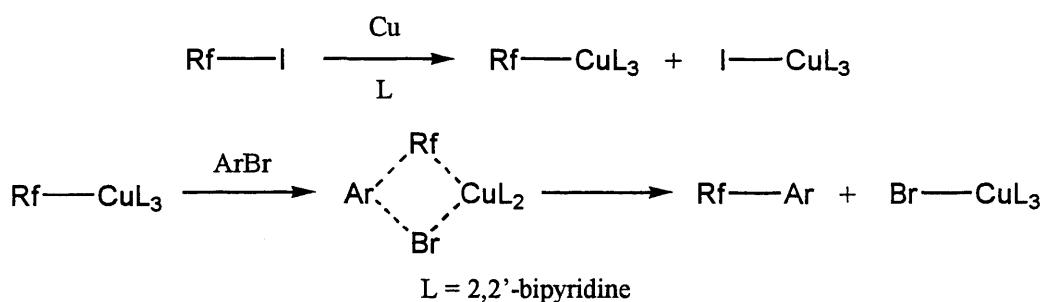
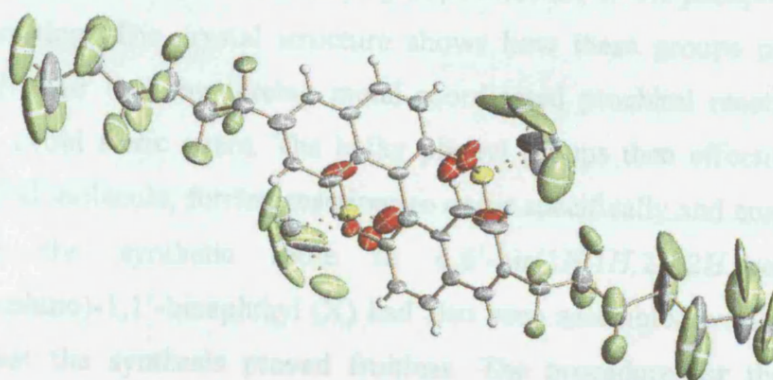


Figure 2.15. Mechanism of copper-catalysed cross-coupling reactions using aryl bromides and perfluoroalkyl iodides

For the synthesis towards (IX), DMSO was used as a polar aprotic solvent, along with an equal volume of fluorobenzene to help to dissolve the perfluoro-*n*-hexyl iodide. 2,2'-bipyridine was used in a catalytic amount to act as a complexing ligand for the perfluoroalkylcopper intermediate formed during reaction. The reaction mixture was worked up by hydrolysis, filtered to remove any solid copper species and extracted with diethyl ether. The organic extracts were washed repeatedly with aqueous hydrochloric acid and water to remove soluble copper compounds and traces of DMSO. The organic layer was then dried and the solvent removed under reduced pressure to yield a green-brown oil which would not solidify even after prolonged drying under vacuum. Extraction of the product into PP3 was unsuccessful, the product having too little fluorous character to be soluble. However, re-dissolving the semi-solid in methanol and adding an equal volume of PP3 formed a biphasic system in which the product, 6,6'-bis(perfluoro-*n*-hexyl)-2,2'-diacetoxy-1,1'-binaphthyl, crystallised at the interface as a white, crystalline solid.

The overall yield for the complete synthesis of Rf-BINAP is only 15 % due to the number of steps and the low yielding copper-mediated cross-coupling and phosphination stages.

Crystals of (*R*)-6,6'-bis(perfluoro-*n*-hexyl)-2,2'-di(trifluoromethane-sulphonyloxy)-1,1'-binaphthyl suitable for X-ray analysis were obtained after slow evaporation of dichloromethane solvent. The crystal structure is shown below (Figure 2.16), with data for the crystal given in the appendix.



Crystal structure showing 50% displacement ellipsoids. Even with disordered sites (dashed bonds) the terminal F atoms exhibit highly anisotropic behaviour.

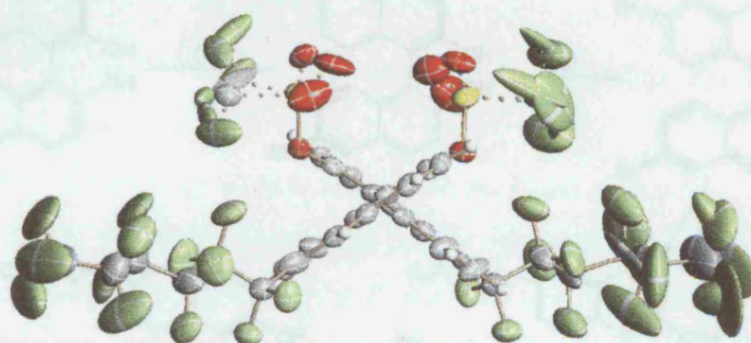
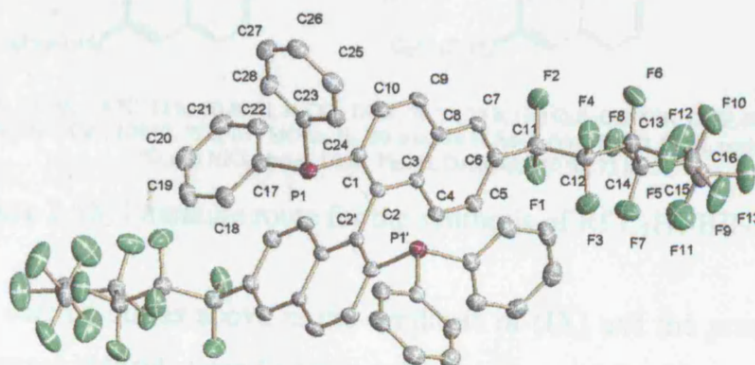


Figure 2.16. Crystal Structure of (*R*)-6,6'-bis(perfluoro-*n*-hexyl)-2,2'-di(trifluoromethanesulphonyloxy)-1,1'-binaphthyl

Crystals of racemic Rf-BINAP suitable for single crystal X-ray diffraction studies were also obtained by slow evaporation of a solution of the ligand in diethyl ether and hexane (1:6) (Figure 2.17)



Structure 2.17. Crystal structure of racemic Rf-BINAP

The molecular structures, viewed down the C1-C1' pivot, clearly show the non-planar geometry of the two naphthyl ring systems in both crystal structures and indicates that the

perfluoroalkyl chains adopt a conformation in the solid state that minimises their interaction with each other. The conformation of the phenyl groups attached to the phosphorus atoms in Structure 2.2 is also interesting. The crystal structure shows how these groups produce enantioselective catalysts through their bulk by forcing metal-coordinated prochiral reactants to adopt a certain conformation to avoid steric strain. The bulky phenyl groups then effectively block certain sites within the prochiral molecule, forcing reactions to occur specifically and enantioselectively.

Although the synthetic route to 6,6'-bis(1*H*,1*H*,2*H*,2*H*,-perfluoro-*n*-octenyl)-2,2'-bis(diphenylphosphino)-1,1'-binaphthyl (**X**) had also been assembled within the group<sup>29</sup>, extensive attempts to repeat the synthesis proved fruitless. The procedure for the synthesis of (**X**), as published previously, is outlined in Figure 2.18.

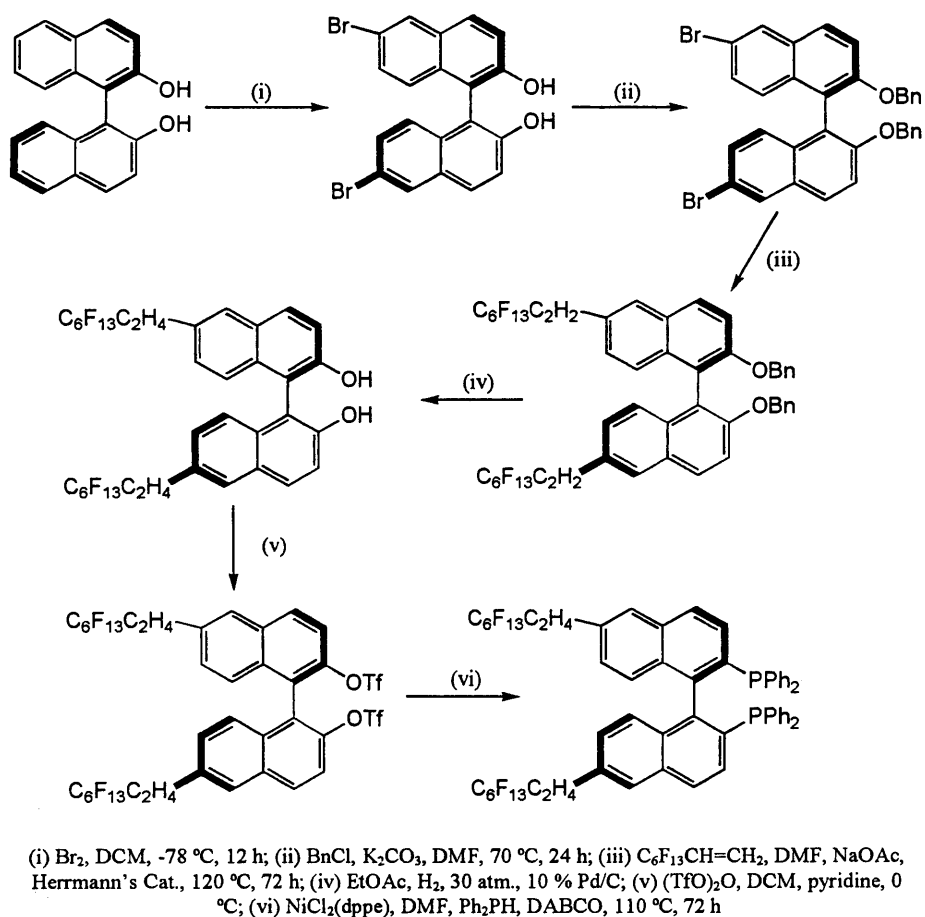


Figure 2.18. Literature route for the synthesis of Rf-C<sub>2</sub>H<sub>4</sub>-BINAP<sup>29</sup>

Step (i) was carried out as above in the synthesis of (**IX**) and the protection of the phenol groups employing benzyl chloride (step (ii)) was achieved successfully. However, Heck coupling of the 1*H*,1*H*,2*H*-perfluoro-1-octene to the protected binaphthyl derivative using Herrmann's Catalyst was extremely troublesome. Repeated attempts to successfully carry out step (iii) in high yield failed, even though a yield of over 90 % had been reported previously.<sup>29</sup> Analysis of the crude

product that was obtained after reaction showed the majority of the material to be benzyl-protected binaphthol with only one perfluoroalkyl tail attached. The mass spectrum of the mixture showed that some of the desired product had been formed, but the crude mix also contained the monosubstituted product seen by  $^1\text{H}$  NMR spectroscopic analysis, the same molecule with hydrogen substituted for bromine and the starting material (Figure 2.19). The highest yield that was obtained after intensive purification was 5 %, which clearly made the synthesis unfeasible.

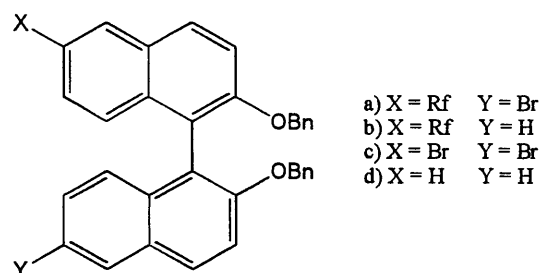


Figure 2.19. Mixture of products observed after step iii

Heck reactions employing palladacycle catalysts have previously been shown to produce higher yields when small, non-bulky groups are present within the aryl halide.<sup>33</sup> This is suggested to be a consequence of more favourable coordination of the aryl halide to the palladium catalyst with smaller steric interactions and, therefore, a more rapid turnover of the catalytic cycle (Figure 2.20).<sup>35</sup>

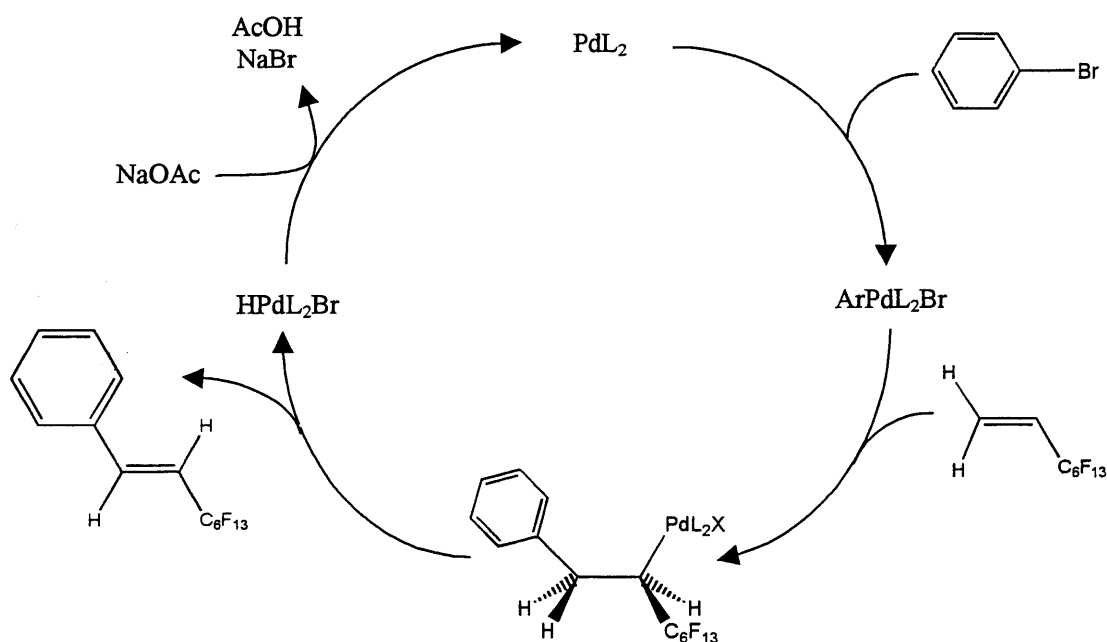


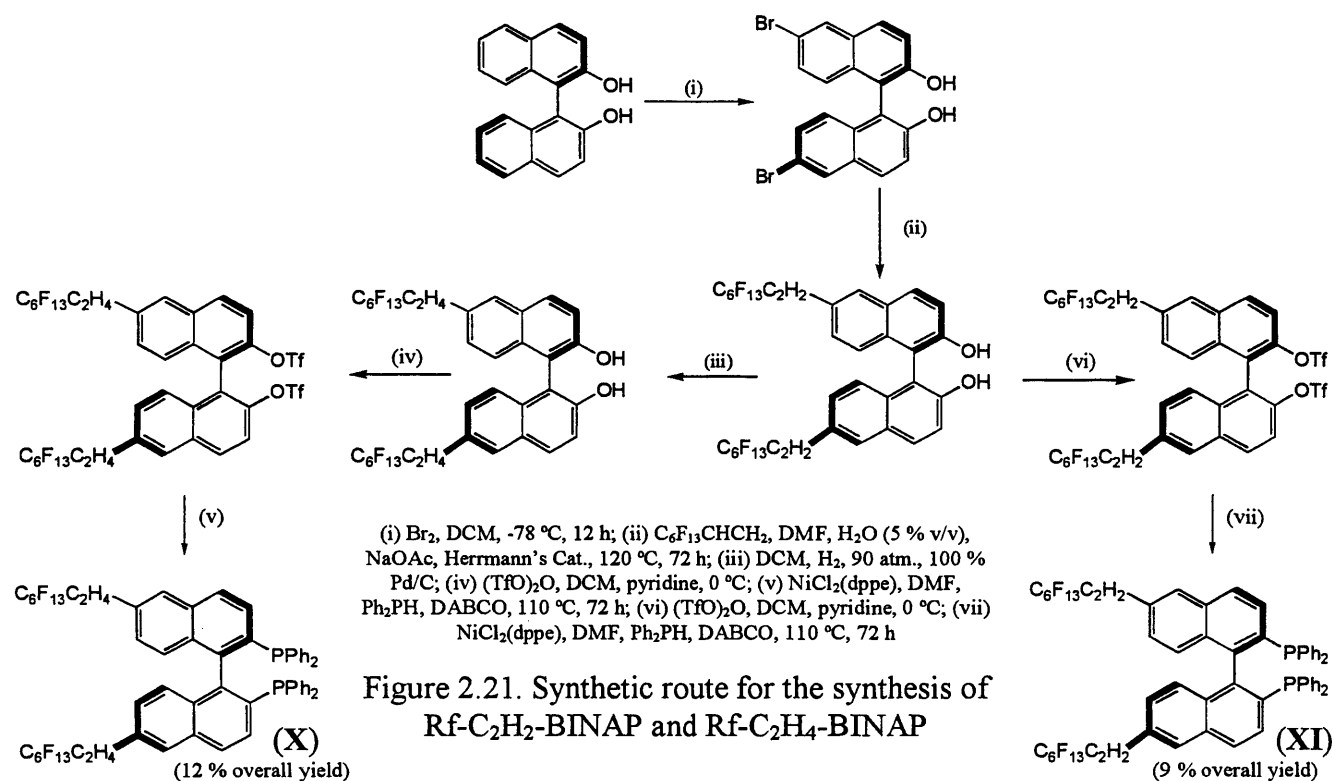
Figure 2.20. Catalytic cycle for palladium-catalysed Heck reactions

A benzyl protecting group was chosen previously because it protected the OH group from any side reactions which may occur and was removed during the hydrogenation of the double bond contained in the coupled perfluoroalkyl chain. This negated the necessity of a deprotecting agent and removed one step from the overall synthesis of the fluoros BINAP. Changing the protecting group from a benzyl group to the much less bulky acetyl group produced a profound effect on the yield of the reaction. The product could be collected in 70 % yield and easily purified by recrystallisation from hexane, although it was thought that an additional step would be required to deprotect the binaphthyl derivative. However, during the reaction the acetyl groups were cleaved from the molecule producing the free OH groups. It was unclear whether this was happening before or after the Heck coupling had occurred, and so the reaction was repeated using 6,6-dibromo-1,1'-bi-2-naphthol with no protecting groups. Pleasingly, the reaction proceeded smoothly, with 6,6'-bis(1*H*,2*H*-perfluoro-*n*-1-octenyl)-1,1'-bi-2-naphthol being the major product. This was again purified by recrystallisation from hexane. The discovery that a protecting group is not required in this coupling reaction is beneficial because one synthetic step is removed from the complete synthesis of the final molecule.

However, problems with reproducibility of the reaction led to its further modification, as the solubility of sodium acetate in DMF is sufficiently low to seriously reduce the rate and yield of reaction. Following the procedure given above without using benzyl protecting groups, a significant amount of bi-2-naphthol possessing only one fluoros ponytail was still often isolated after step (iv). Sodium acetate is required to regenerate the active catalyst during the catalytic cycle and if it is insoluble in the solvent then catalyst regeneration will be slow and the addition of the second fluoros tail hampered. However, the addition of a small amount of water to the reaction mixture helped solubilise the sodium acetate, making regeneration of the catalyst more facile. Adding 5 % (v/v) water to the DMF increased the yields of reaction dramatically from around 40 % to upwards of 70 % reproducibly.

The hydrogenation of the alkene spacer group was also altered (step (iv)). Using the conditions employed in the literature procedure, hydrogenation of the double bond was often incomplete after reaction or, worse, did not occur at all. Contamination of the high-pressure reactor from other users was cited as a factor in the problem as often, after two or three hydrogenation attempts, the ligands would change from being only 2-3 % hydrogenated to 100 % alkane. However, extensive cleaning of the reactor vessel did not always rectify the problem and alterations to the procedure were, therefore, undertaken. It was found that, after testing different solvents and conditions, dichloromethane was the best solvent to use as full hydrogenation occurred after each reaction. Also, a higher pressure was required to achieve 100 % alkene conversion and the hydrogen pressure was increased from 30 bar to 90 bar. Finally, the palladium catalyst loading was

increased. Although lower loadings were examined, to ensure complete hydrogenation and to avoid multiple product hydrogenations, 100 % by weight Pd/C catalyst loadings were used. These conditions, although harsh, led to full conversion of the starting alkene to the alkane after every individual reaction without damage to the binaphthyl backbone or racemisation. The modified full synthesis of the two fluorous BINAP ligands with alkene or alkane spacers is given in Figure 2.21.



For comparative purposes, 2,2'-bis(diphenylphosphino)-1,1'-binaphthyl (BINAP) was prepared from 1,1'-bi-2-naphthol in two steps ((i) reaction with  $(\text{TfO})_2\text{O}$ ; (ii) Ni-catalysed reaction with  $\text{Ph}_2\text{PH}$ ) in 40 % overall yield.

Although the ligands were not synthesised for use in fluorous biphasic catalysis, the partition coefficients in a  $\text{PP}_3$ /toluene biphasic system were determined to allow comparison to other systems. Sixty milligrams of the (*R*)-enantiomers of each of the BINAP ligands were stirred in the  $\text{PP}_3$ /toluene biphasic system, allowed to stand and then aliquots of each phase taken, the solvent removed under reduced pressure and the residue analysed gravimetrically. The data obtained is outlined in Table 2.1

Ligand <sup>a</sup>	Observation <sup>b</sup>	Undissolved Ligand (mg)	Ligand in Toluene (mg)	Ligand in PP3 (mg)	Partition Coefficient <sup>c</sup>
VIII	Ligand not fully dissolved	23	38	2	95 %
X	Ligand not fully dissolved	16	40	2	95 %
IX	Ligand not fully dissolved	20	38	2	95 %
BINAP	Ligand dissolved fully	/	56	0	100 %

<sup>a</sup> (R)-enantiomers used in all cases; 2 ml PP3, 2 ml toluene, rt, stir = 20 mins, settle = 20 mins, 1 ml of each layer analysed

<sup>b</sup> Ligand at interface <sup>c</sup> % in toluene phase

Table 2.1. Partition coefficient data for BINAP ligands in a toluene/PP3 biphasic system

It is clear from the data that, as expected, the ligands are not preferentially perfluorocarbon soluble and reside mostly in the toluene phase, although the saturation point of the organic solvent is low leaving around one third of the BINAP ligands undissolved.

### 2.2.2 Coordination Chemistry – The Bonding In M-PX<sub>3</sub> Complexes

Traditionally, the Dewar-Chatt model has been used to describe the bonding between a metal centre and a phosphorus(III) (PX<sub>3</sub>) ligand.<sup>36</sup> Here, the ligand donates charge through the lone pair on phosphorus to the metal centre, and the metal centre provides  $\pi$ -back-donation of charge from its *d* orbitals into vacant 3*d* orbitals on phosphorus. However, critics of this model argued that, in many cases, the *d* orbitals of phosphorus were too high in energy to overlap efficiently with filled metal *d* orbitals.<sup>36</sup> It was proposed that phosphorus ligands could accept  $\pi$ -electron density without the participation of high energy *d* orbitals if lower energy P-X  $\sigma^*$  orbitals were employed instead.<sup>37</sup> *Ab initio* calculations employing no *d* orbitals on phosphorus showed significant  $\pi$ -back-bonding still occurred between various metal centres and the phosphorus ligands. The overlap of metal *d* and phosphorus  $\sigma^*$  orbitals is outlined in Figure 2.22.

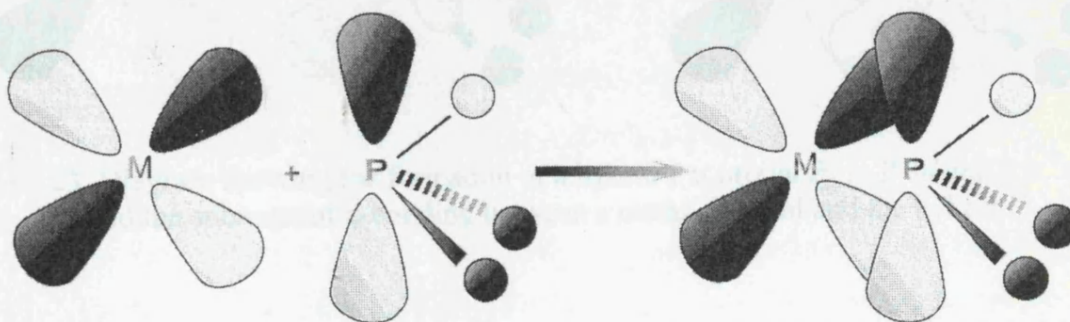


Figure 2.22. The interaction of metal *d* and phosphorus  $\sigma^*$  orbitals (P placed on *z* axis, M *d*<sub>yz</sub> and *d*<sub>xz</sub> orbitals used for overlap)

The computational calculations, omitting  $d$  orbitals from phosphorus, predicted that increasing the  $\pi$ -back-donation between the metal centre and  $PX_3$  ligand would result in a lengthening of the P-X bond as electron density was added to the  $\sigma^*$  orbitals. Adding a phosphorus  $d$  orbital to the calculations caused only a minor variation in the electron densities obtained, again suggesting that  $d$  orbitals are not significantly involved in  $\pi$ -back-bonding. Experimental observations helped to support these calculations.<sup>38</sup> Analysis of bond lengths in various M- $PX_3$  complexes as determined by X-ray crystallography showed that, for metals in high oxidation states, longer M-P bonds and shorter P-X bonds were observed than for metals in low oxidation states, where the reverse was true. This evidence suggested that P-X  $\sigma^*$  orbitals did act as  $\pi$ -acceptors. More recent computational calculations have, however, shown that stronger interactions between phosphorus ligands and metal centres are observed when  $d$  orbitals are included in the calculations.<sup>39,40</sup> Hybridisation of a P-X  $\sigma^*$  orbital and a P  $3d$  orbital forms a doubly-degenerate P  $\pi$ -acceptor orbital of the correct geometry to overlap with metal  $d$  orbitals (Figure 2.23). The phosphorus lone pair forms a  $\sigma$ -bond to the metal centre, while the metal back-donates from its filled  $d$  orbitals into the hybridised phosphorus  $3d\sigma^*$  orbitals to form a  $\pi$ -bond.

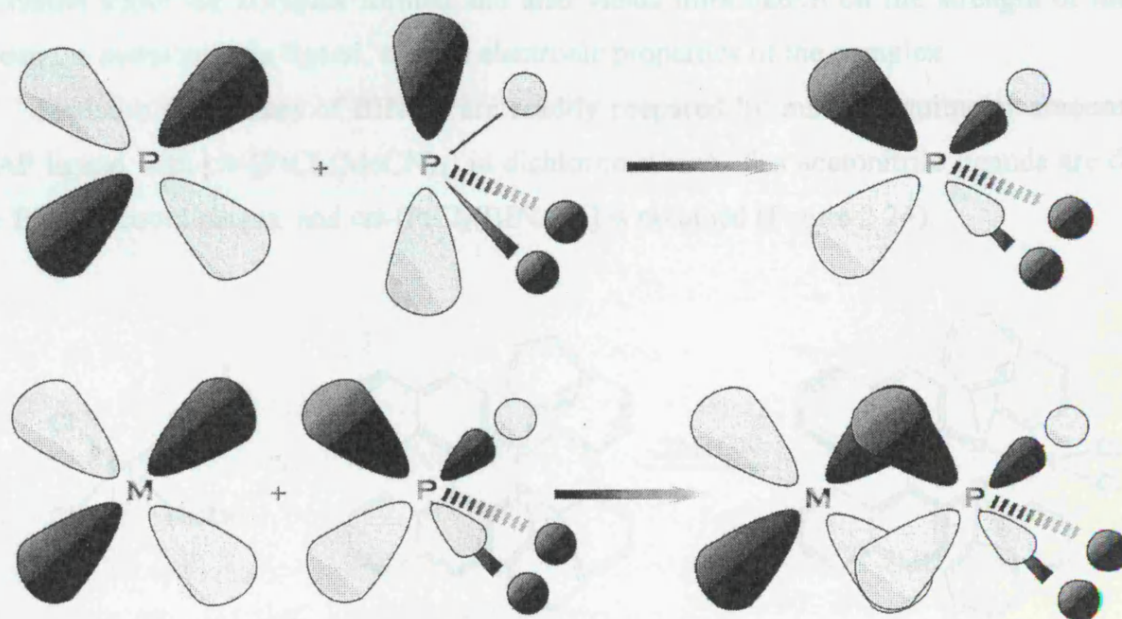


Figure 2.23. Diagram showing the formation of a hybrid P  $\pi$  orbital from P  $3d$  and P  $\sigma^*$  orbitals and the subsequent  $\pi$ -bonding between a metal  $d$  orbital and the hybrid.

These data suggest that electron-withdrawing groups attached to the binaphthyl backbones or phenyl rings should increase the  $\pi$ -acceptor ability of the BINAP ligand. This is due to an increase in the energetic accessibility of the  $\sigma^*$  orbitals due to a decrease in their overall energy.<sup>38</sup>

### 2.2.3 Coordination Chemistry – Complexes

The BINAP ligand is conformationally flexible due to restricted rotation around the C(1)-C(1') pivot and unhindered rotation around the C(2 or 2')-P bonds. As a consequence, a wide range of transition metals can be accommodated without a serious increase in torsional strain, which helps to explain why BINAP is such a successful ligand in a wide range of catalysis. To determine the influence of the perfluoroalkyl ponytails on the  $\pi$ -acceptor ability of the light fluorinated BINAP ligands prepared in this work, a variety of coordination complexes were synthesised. Any differences in the electronic properties of the ligands and subsequent complexes give rise to spectroscopic variations that could then be used to investigate the effect of the ponytails on the electron density at phosphorus and the suitability of the ligands in catalysis.

The complexes described below have been analysed by  $^1\text{H}$ ,  $^{19}\text{F}\{^1\text{H}\}$  and  $^{31}\text{P}\{^1\text{H}\}$  NMR spectroscopy, mass spectrometry, melting point, optical rotation and elemental analysis.

### 2.2.4 Complexes of Platinum(II)

The platinum isotope  $^{195}\text{Pt}$  (spin  $\frac{1}{2}$ , 33 % natural abundance) exhibits coupling to the phosphorus atoms of BINAP in  $^{31}\text{P}$  NMR spectroscopy. This coupling provides useful structural information about the complex formed and also yields information on the strength of interaction between the metal and the ligand, and the electronic properties of the complex.

Platinum complexes of BINAP are readily prepared by mixing equimolar amounts of the BINAP ligand with *cis*-[PtCl<sub>2</sub>(MeCN)<sub>2</sub>] in dichloromethane. The acetonitrile ligands are displaced upon BINAP coordination, and *cis*-[PtCl<sub>2</sub>(BINAP)] is obtained (Figure 2.24).

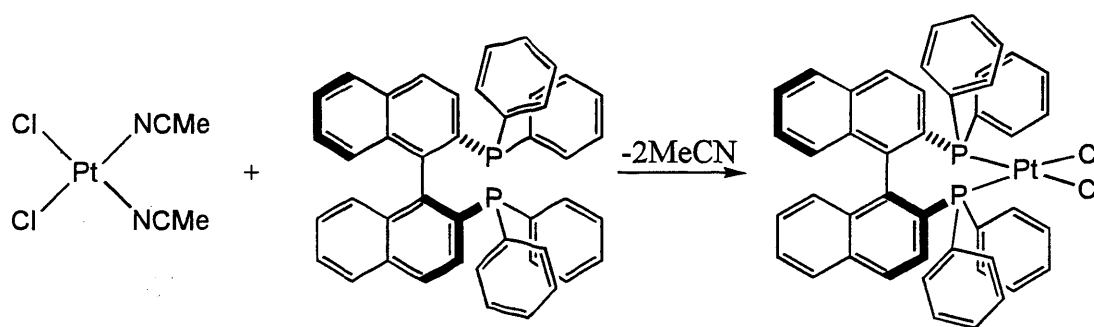


Figure 2.24. The synthesis of [PtCl<sub>2</sub>(BINAP)] complexes

Eight complexes of this type, employing the (*R*)- and (*S*)-enantiomers of BINAP, Rf-BINAP (**IX**), Rf-C<sub>2</sub>H<sub>4</sub>-BINAP (**X**) and Rf-C<sub>2</sub>H<sub>2</sub>-BINAP (6,6'-bis(1*H*,2*H*-perfluoro-*n*-1-octenyl)-2,2'-bis(diphenylphosphino)-1,1'-binaphthyl) (**XI**), were prepared and analysed. All of the complexes proved to be air- and moisture-stable and yields of between 50 and 60 % were obtained in all cases. Optical rotation measurements showed the ligands all had similar optical properties, with all (*R*)-

enantiomers giving equal magnitude but opposite sign optical rotation values to the corresponding (*S*)-enantiomers. The  $^1\text{H}$  NMR spectra of all the complexes were largely uninformative, showing only a complex mass of peaks in the aromatic region of the spectrum. For complexes of (**IX**), (**X**) and (**XI**), the  $^{19}\text{F}$  NMR spectra were also of little interest as they remained relatively the same as for the free ligands. The  $^{31}\text{P}$  NMR spectra were, however, far more informative. These data are outlined in Table 2.2.

Ligand	$^{31}\text{P}$ NMR data (ligand) (ppm) <sup>a</sup>	$^{31}\text{P}$ NMR data (complex) (ppm) <sup>a</sup>	$^1J_{\text{Pt-P}}$ coupling (Hz)
( <i>R</i> )-BINAP	s, -15.5	ss, 9.8	3665
( <i>S</i> )-BINAP	s, -15.1	ss, 9.7	3665
( <i>R</i> )-( <b>IX</b> )	s, -13.8	ss, 10.8	3636
( <i>S</i> )-( <b>IX</b> )	s, -13.5	ss, 10.8	3638
( <i>R</i> )-( <b>XI</b> )	s, -14.5	ss, 10.3	3647
( <i>S</i> )-( <b>XI</b> )	s, -14.5	ss, 10.3	3644
( <i>R</i> )-( <b>X</b> )	s, -15.6	ss, 9.8	3665
( <i>S</i> )-( <b>X</b> )	s, -15.6	ss, 9.8	3660

<sup>a</sup>NMR spectroscopic data from complexes dissolved in  $\text{CDCl}_3$

Table 2.2.  $^{31}\text{P}\{^1\text{H}\}$  NMR data for  $[\text{PtCl}_2\text{BINAP}]$  complexes

As expected, attaching electron-withdrawing perfluoroalkyl ponytails to the binaphthyl backbone (**IX**) shifts the peak in the  $^{31}\text{P}$  NMR spectrum for free ligand down-field relative to BINAP as the phosphorus atom is more deshielded, and subsequent platinum complexes show smaller coupling constants. This effect is less pronounced when an additional  $\text{C}_2\text{H}_2$  spacer unit is inserted into the ponytails (ligand **XI**). Finally, the data shows that insertion of a  $\text{C}_2\text{H}_4$  spacer unit between the fluorinated ponytail and the binaphthyl backbone removes any electronic effect of the fluorine atoms on the phosphorus centre, as the coupling constants for platinum complexes of  $\text{Rf-C}_2\text{H}_4\text{-BINAP}$  (**X**) are identical to those for BINAP complexes.

Comparison of this data shows that BINAP and  $\text{Rf-C}_2\text{H}_4\text{-BINAP}$  ligands are the strongest  $\sigma$  donors, as they yield the higher  $^1J_{\text{Pt-P}}$  coupling constants indicating a stronger M-P bond. Removing electron density from the phosphorus atoms (ligands **IX**) and **XI**) makes them weaker  $\sigma$  donors than BINAP as the phosphorus centre is less-willing to donate its lone pair of electrons, leading to a reduction in the  $^1J_{\text{Pt-P}}$  coupling constants.

## 2.2.5 Complexes of Palladium(II)

Although no common isotopes of palladium are NMR active, useful information regarding the coordination and bonding of phosphines to the metal centre can still be obtained without phosphorus-palladium coupling.

Once again, complexes of BINAP are easily prepared by stirring a mixture of  $[\text{PdCl}_2(\text{MeCN})_2]$  and the BINAP ligand in a 1:1 molar ratio in dichloromethane under an atmosphere of nitrogen. Both acetonitrile ligands are displaced upon coordination of the BINAP ligand to yield *cis*- $[\text{PdCl}_2(\text{BINAP})]$  (Figure 2.25).

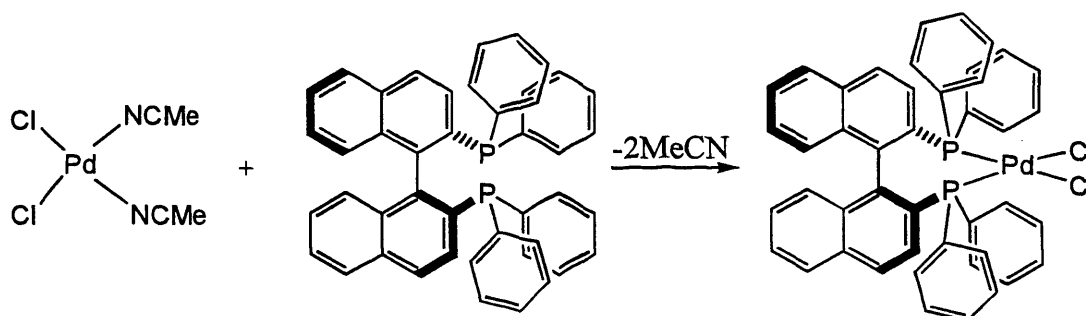


Figure 2.25. The synthesis of  $[\text{PdCl}_2(\text{BINAP})]$  complexes

Again, eight complexes of the type  $[\text{PdCl}_2(\text{L})]$  were prepared, where L equalled (*R*)- or (*S*)-BINAP, Rf-BINAP (**IX**), Rf-C<sub>2</sub>H<sub>4</sub>-BINAP (**X**) and Rf-C<sub>2</sub>H<sub>2</sub>-BINAP (**XI**). These complexes were air- and moisture-stable and gave characteristic shifts in the <sup>31</sup>P NMR spectra (Table 2.3). Optical rotation measurements again showed the ligands all had similar optical properties, with all (*R*)-enantiomers giving equal magnitude but opposite sign optical rotation values to the corresponding (*S*)-enantiomers.

Ligand	<sup>31</sup> P NMR data (ligand) (ppm) <sup>a</sup>	<sup>31</sup> P NMR data (complex) (ppm) <sup>a</sup>
( <i>R</i> )-BINAP	s, -15.5	s, 28.5
( <i>S</i> )-BINAP	s, -15.1	s, 28.5
( <i>R</i> )-( <b>XI</b> )	s, -15.5	s, 33.5
( <i>S</i> )-( <b>XI</b> )	s, -13.5	s, 33.5
( <i>R</i> )-( <b>IX</b> )	s, -14.5	s, 32.7
( <i>S</i> )-( <b>IX</b> )	s, -14.5	s, 32.6
( <i>R</i> )-( <b>X</b> )	s, -15.6	s, 28.4
( <i>S</i> )-( <b>X</b> )	s, -15.6	s, 28.4

<sup>a</sup> NMR spectroscopic data from complexes dissolved in CDCl<sub>3</sub>

Table 2.3. <sup>31</sup>P{<sup>1</sup>H} NMR spectroscopic data for  $[\text{PdCl}_2\text{BINAP}]$  complexes

The complexes of palladium showed the same general trend as for platinum complexes of the BINAP ligands. Rf-BINAP (IX) complexes showed a significant down-field shift to BINAP complexes, with Rf-C<sub>2</sub>H<sub>4</sub>-BINAP (X) complexes giving similar chemical shift values to BINAP and Rf-C<sub>2</sub>H<sub>2</sub>-BINAP (XI) complexes being intermediate between IX and X. This data is in agreement with the data observed for platinum complexes of the BINAP ligands and again suggests that BINAP and Rf-C<sub>2</sub>H<sub>4</sub>-BINAP ligands are the strongest  $\sigma$  donors, while Rf-BINAP ligands are the weakest donors and Rf-C<sub>2</sub>H<sub>2</sub>-BINAP ligands come somewhere between the two extremes.

The mass spectra obtained by positive ion mode FAB mass spectrometry also showed that complexation had occurred, with  $[M-Cl]^+$  peaks clearly visible for the complexes. Elemental analyses of all of the complexes provided data that was in agreement with the values predicted in all cases.

Crystals of the  $[PdCl_2((R)-BINAP)]$  complex suitable for X-ray diffraction were obtained and the structure determined (Figure 2.26).

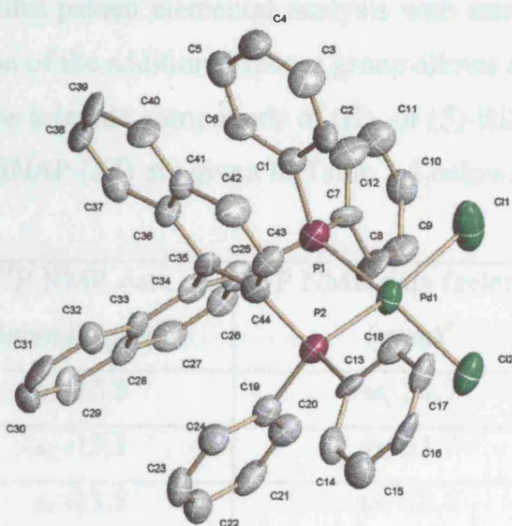


Figure 2.26.  $[PdCl_2((R)-BINAP)]$  (H atoms omitted for clarity)

Although the crystals were poor quality, the structure was refined and shows the *cis*-arrangement of the BINAP ligand and chlorine atoms. The structure was found to have one dichloromethane molecule in bonding distance to the chlorine atoms of the complex that was disordered.

### 2.2.6 Phosphine Selenides

BINAP can be reacted with selenium powder to form phosphine selenide compounds. Se (spin  $\frac{1}{2}$ , 8 % natural abundance) exhibits coupling to phosphorus centres that can be observed in  $^{31}P$  NMR spectra and used as a further probe of the effects of fluoros ponytails on the environment around phosphorus.

It has been shown previously that  $^1J_{\text{Pt-P}}$  coupling constants in platinum complexes of phosphines are influenced by both the electronic and steric effects of modifying groups on the ligand.<sup>42,43</sup> Phosphine selenides are much less susceptible to the steric influence of modifying groups and, therefore, supply information only on the electronic effect of the modifying group on the  $\sigma$ -donor properties of the phosphine ligand.<sup>44,45</sup>

Eight selenium compounds employing each of the synthesised BINAP ligands were prepared and characterised by NMR spectroscopy and mass spectrometry. Due to the instability of the selenides, satisfactory elemental analyses could not, however, be obtained for all of the compounds. The selenides decompose after short periods of time to form red selenium and BINAP oxide. (*R*)- and (*S*)-BINAP and (*R*)- and (*S*)-Rf-BINAP selenides could be isolated and purified, but repeated attempts to obtain accurate elemental analysis data for the compounds failed. Even when commercially available (*R*)- and (*S*)-BINAP was used to form the selenide compounds, accurate elemental analysis values could not be obtained. Interestingly, both enantiomers of Rf-C<sub>2</sub>H<sub>2</sub>-BINAP and Rf-C<sub>2</sub>H<sub>4</sub>-BINAP selenides passed elemental analysis with satisfactory component values. It is not known why the inclusion of the additional spacer group allows accurate elemental analysis.

<sup>31</sup>P NMR data for the selenide compounds of (*R*)- or (*S*)-BINAP, Rf-BINAP (**IX**), Rf-C<sub>2</sub>H<sub>4</sub>-BINAP (**X**) and Rf-C<sub>2</sub>H<sub>2</sub>-BINAP (**XI**) are given in Table 2.4 below.

Ligand	<sup>31</sup> P NMR data (ligand) (ppm) <sup>a</sup>	<sup>31</sup> P NMR data (selenide) (ppm) <sup>a</sup>	<sup>1</sup> J <sub>Pt-P</sub> coupling (Hz)
( <i>R</i> )-BINAP	s, -15.5	ss, 33.7	739
( <i>S</i> )-BINAP	s, -15.1	ss, 33.7	739
( <i>R</i> )-( <b>IX</b> )	s, -13.8	ss, 32.7	749
( <i>S</i> )-( <b>IX</b> )	s, -13.5	ss, 32.7	749
( <i>R</i> )-( <b>XI</b> )	s, -14.5	ss, 32.8	746
( <i>S</i> )-( <b>XI</b> )	s, -14.5	ss, 32.8	746
( <i>R</i> )-( <b>X</b> )	s, -15.6	ss, 32.8	743
( <i>S</i> )-( <b>X</b> )	s, -15.6	ss, 32.8	743

<sup>a</sup>NMR spectroscopic data from complexes dissolved in CDCl<sub>3</sub>

Table 2.4. <sup>31</sup>P{<sup>1</sup>H} NMR spectroscopic data for selenide compounds

The data shows that the electronic environment around the phosphorus centres in each of the selenide compounds remains relatively unchanged, with the <sup>31</sup>P chemical shift remaining almost constant for each of the component ligands. As for complexes of platinum, directly attaching fluororous ponytails to the binaphthyl backbone (ligands (*R*)- and (*S*)-(**IX**)) has the largest effect on

the  $^{31}\text{P}$  coupling constants, with both enantiomers of ligands (X) and (XI) giving intermediate values between ligands (*R*)- and (*S*)-(IX) and (*R*)- and (*S*)-BINAP. Unlike previously for the complexes of platinum, however, Rf-C<sub>2</sub>H<sub>4</sub>-BINAP ligands (X) do not give identical coupling constant values to those of non-fluorous BINAP ligands. The implication of this observation is that phosphine selenides are a more sensitive technique for probing the effect of the electronegativity of fluorine ponytails on phosphorus centres than complexes of platinum. It is pleasing to note, however, that in all cases, the effects of the fluorine ponytails on the bonding ability of the BINAP ligands prepared are small and are unlikely to dramatically affect the coordinating ability of the light fluorine analogues of BINAP to catalyst metal centres.

## 2.3 Catalytic Testing

### 2.3.1 Hydrogenation Reactions

Although BINAP has been used as a ligand in many catalytic syntheses, much study has centred on the use of the ligand in asymmetric hydrogenations.<sup>6-8,13,15,46</sup> Consequently, it was decided that a basic asymmetric hydrogenation reaction would first be studied to determine the effect of the perfluoroalkyl tails on selectivity, specificity and rate of reaction.

Previous work within the group<sup>29</sup> studied the hydrogenation of dimethyl itaconate in methanol using BINAP and the ruthenium catalyst precursor [RuCl<sub>2</sub>(benzene)]<sub>2</sub>. The reactions were carried out at ambient temperature and a hydrogen pressure of 20 bar. For comparison, the same reaction was carried out using the same conditions with Rf-BINAP (IX), and Rf-C<sub>2</sub>H<sub>4</sub>-BINAP (X). As stated previously, the addition of fluorine ponytails to the BINAP ligands had no effect on the enantioselectivities of the catalysts. This is as expected, since the perfluoroalkyl chains are sufficiently removed from the phenyl groups attached to the phosphorus atoms to have no effect on their conformation and subsequent enantiomeric induction. However, attaching the fluorine tails did have an effect on the yields of the reactions, with ponytails directly attached to the binaphthyl backbone more than halving the activity of the catalyst. (88 % yield of product using BINAP as ligand, 42 % yield of product using Rf-BINAP under the same conditions.)

This work provides a useful comparison for other studies into the effects of the perfluoroalkyl chains on yields/conversions and enantioselectivities. Investigation of the literature concerning BINAP as a productive and successful ligand in catalytic asymmetric hydrogenation reactions uncovered a highly effective system using the same catalyst precursor as studied above.<sup>47</sup> In these studies, the hydrogenation of a range of functionalised ketones had been investigated with the production of high yields of products with high enantiomeric excesses (Figure 2.27).

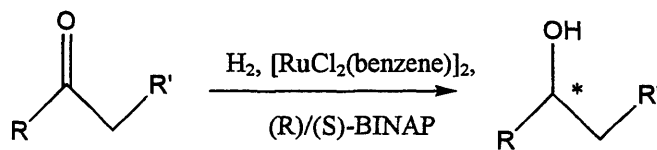


Figure 2.27. Asymmetric hydrogenation of functionalised ketones<sup>47</sup>

For the functionalised ketone methyl acetoacetate ( $R = \text{CH}_3$ ,  $R' = \text{CO}_2\text{CH}_3$ ), high yields and enantiomeric excesses could be achieved under relatively mild conditions, so this prochiral substrate was chosen as the initial test reactant. It was suggested from the previous work that preformation of the active catalyst was required before the hydrogenations could be carried out. This was achieved by heating the BINAP ligand and the catalyst precursor at  $100\text{ }^\circ\text{C}$  in dry DMF for ten minutes under argon followed by cooling and removal of the solvent. It was believed that the preforming of the catalyst would allow spectroscopic analysis and so the procedure was carried out using Rf-BINAP to yield a red-orange solid. However, analysis of the solid by  $^{31}\text{P}$  NMR spectroscopy showed only a small amount of a species different to the free ligand had been prepared. Two small doublets were observed at  $54.3\text{ ppm}$  ( $J = 39.7\text{ Hz}$ ) and  $58.4\text{ ppm}$  ( $J = 40.7\text{ Hz}$ ) and a large peak corresponding to free Rf-BINAP was observed at  $-13.6\text{ ppm}$  (Figure 2.28).

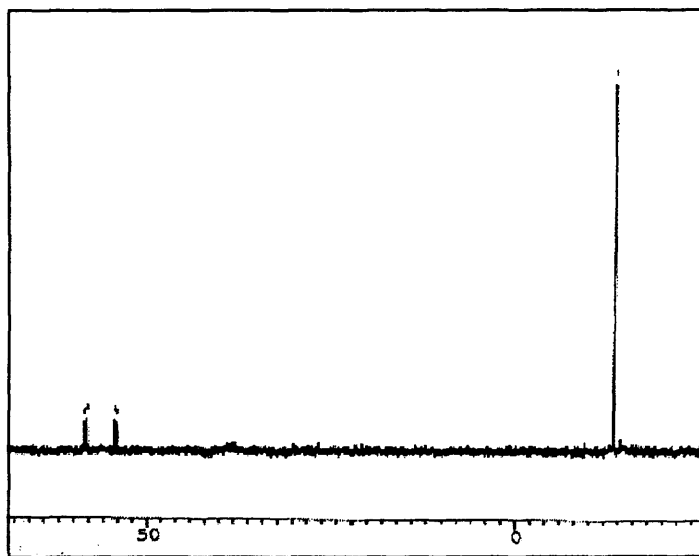


Figure 2.28.  $^{31}\text{P}\{^1\text{H}\}$  NMR spectrum of  $[\text{RuCl}_2(\text{benzene})]_2$  / Rf-BINAP after heating for 10 minutes in DMF followed by solvent removal

The  $^{31}\text{P}$  NMR spectrum indicated bonding to the ruthenium centre (due to the chemical shift) and an inequivalence of the two phosphorus atoms in the Rf-BINAP ligand. If symmetrical coordination were achieved, then the phosphorus atoms would be equivalent and would not couple to each other. Six-coordinate octahedral complexes, formed by the coordination of two solvent ligands, could give rise to more peaks as isomers could be introduced. In the previous work, many

more peaks were observed in the  $^{31}\text{P}$  NMR spectrum which were attributed to a mixture of  $[\text{RuCl}_2(\text{BINAP})(\text{DMF})_2]$  and  $[\text{RuCl}_2(\text{BINAP})(\text{DMF})]_n$  moieties. Here, additional peaks were not observed even after prolonged heating in DMF. Figure 2.28 does show, however, that the conditions employed to pre-form the catalyst do not lead to complete coordination, an equilibrium exists in the system or an equilibrium exists in the NMR solvent which causes ligand dissociation.

Reported in the same literature was the use of a different ruthenium catalyst precursor,  $[\text{RuCl}_2(\text{SbPh}_3)_3]$ , which could be prepared by reaction between triphenyl antimony and ruthenium trichloride.<sup>48</sup> The air- and moisture-stable catalyst precursor could then be used to form an enantioselective catalyst containing BINAP by heating molar equivalents of the two moieties in dry 1,2-dichlorobenzene at 160 °C for ten minutes. Again, in an attempt to pre-form a catalyst which could be analysed by spectroscopic methods, this preparation was followed using Rf-BINAP to yield a pink-brown solid. However, the  $^{31}\text{P}$  NMR spectrum was almost identical to the spectrum obtained previously for the  $[\text{RuCl}_2(\text{benzene})]_2/\text{Rf-BINAP}$  system (Figure 2.29).

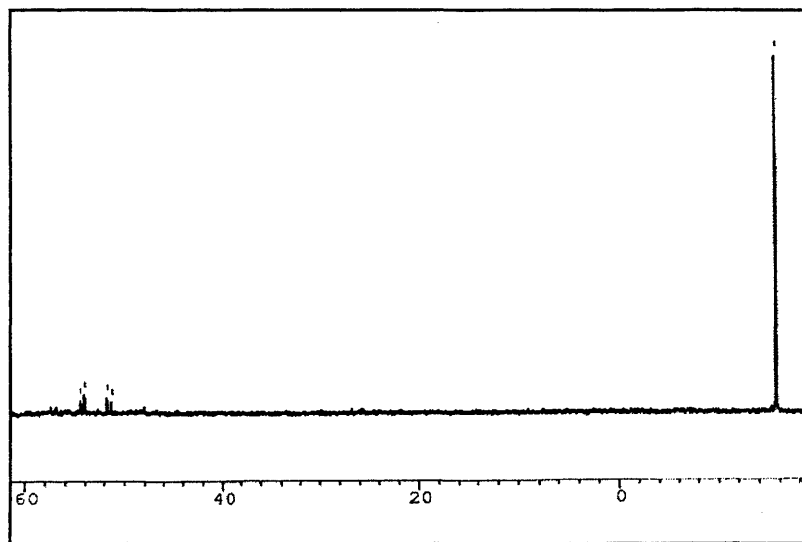


Figure 2.29.  $^{31}\text{P}\{^1\text{H}\}$  NMR spectrum of  $[\text{RuCl}_2(\text{SbPh}_3)_3] / \text{Rf-BINAP}$

A slight shift in the position of the two doublets was observed, with the first doublet situated at 53.3 ppm and the second at 56.0 ppm. This was expected as the catalyst contained  $\text{SbPh}_3$  as a ligand and so a change in the chemical shift was likely. However, once again, no other peaks due to solvent coordination were visible and much of the Rf-BINAP ligand added remained uncoordinated, indicating the presence of an equilibrium or incomplete coordination.

Using this information, it was decided that pre-forming the catalyst might not be necessary. If an equilibrium existed, then it would occur during the hydrogenation reaction and the catalyst would form as the reaction proceeded. To test this hypothesis, the hydrogenation of methyl acetoacetate using (*R*)-BINAP and the  $[\text{RuCl}_2(\text{benzene})]_2$  precursor was attempted without pre-

formation of the catalyst, otherwise using the same conditions as employed previously. Analysis of the solution obtained at the end of the reaction showed > 99 % conversion of the starting material to methyl 3-hydroxybutyrate with a product *ee* of 84 %, negating the need for the pre-formation step. Subsequently, all catalytic testing was carried out using a catalyst formed *in situ*.

### 2.3.2 Chiral Induction

The BINAP ligand in this system induces enantioselectivity in the product as a consequence of its steric bulk (Figure 2.30).

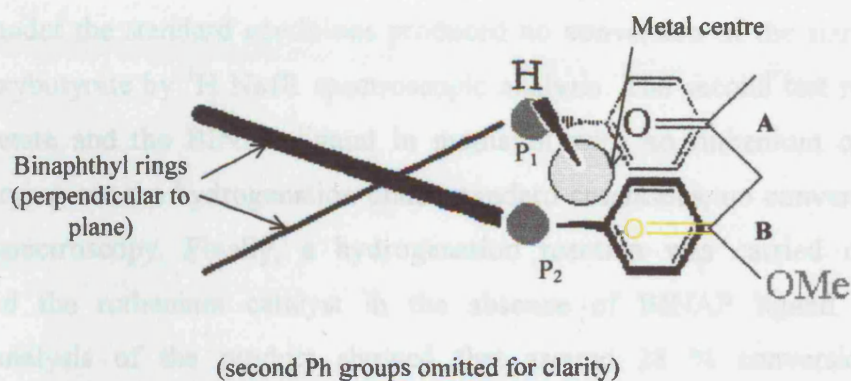


Figure 2.30. Proposed coordination orientation of a BINAP ligand and functionalised ketone, showing how steric bulk leads to enantioselective reduction

It can be envisaged that, upon coordination of the methyl acetoacetate starting material, the metal-coordinated hydrogen can only attack at position A as the Ph group of the second phosphorus atom ( $P_2$ ) blocks attack at position B. Due to the reactivity of the substrate, the ester functionality is not reduced, which explains the chemoselectivity: If the substrate binds with the ester group at position A then no reduction occurs. To achieve stereoselective reduction, the starting material has to coordinate with the ketone group at position A, forcing addition of hydrogen to only one face of the substrate.

The diagram shown employs (*R*)-BINAP and, using this theoretical model, the (*R*)-enantiomer of the product is produced upon completion of the reaction. This is in agreement with experimental observations for this reaction.<sup>47</sup>

### 2.3.3 Catalytic Asymmetric Hydrogenation – Results

The standard conditions for these reactions were taken from the previous work and adapted slightly.<sup>47</sup> Previously, the hydrogenation reactions had been carried out with a preformed catalyst at 100 °C using methanol or dichloromethane as solvent and a hydrogen pressure of 100 bar for thirty minutes. The reactor to be used for hydrogenation studies had a pressure limit of 100 bar and so it

was decided that, instead, the reaction would be carried out at 50 bar for one hour. Dry and degassed solvents were to be used to avoid ligand/catalyst degradation and so dichloromethane was used as solvent to negate the problems associated with large-scale methanol degassing. Finally, for reasons given above, the catalyst precursor was not preformed. However, before hydrogen gas was introduced to the reactor, the ligand, catalyst and substrate were stirred in the solvent under one atmosphere of nitrogen at 100 °C for twenty minutes. It was thought this initial mixing before the addition of hydrogen would allow the formation of the catalyst precursor species *in situ*.

Before catalyst testing was begun, three blank runs were carried out. The first contained the starting material in methanol with no BINAP ligand or ruthenium catalyst. Running the hydrogenation under the standard conditions produced no conversion of the starting material into methyl 3-hydroxybutyrate by <sup>1</sup>H NMR spectroscopic analysis. The second test reaction employed methyl acetoacetate and the BINAP ligand in methanol with no ruthenium catalyst precursor. Again, after carrying out the hydrogenation under standard conditions, no conversion was detected by <sup>1</sup>H NMR spectroscopy. Finally, a hydrogenation reaction was carried out using methyl acetoacetate and the ruthenium catalyst in the absence of BINAP ligand. Here, <sup>1</sup>H NMR spectroscopic analysis of the product showed that around 28 % conversion to methyl 3-hydroxybutyrate had occurred. However, as expected, analysis of the product by optical rotation showed that the catalyst had not shown any enantioselectivity during the hydrogenation. These tests show that the ruthenium catalyst precursor and BINAP ligand are both necessary to catalyse the reaction enantioselectively.

Additionally, to confirm that no reaction occurred during the twenty-minute *in situ* precatalyst formation period, BINAP, the ruthenium catalyst precursor and methyl acetoacetate were heated to 100 °C for 20 minutes in the reactor, allowed to cool and the mixture analysed by <sup>1</sup>H NMR spectroscopy. Once again, no conversion to methyl 3-hydroxybutyrate had occurred.

Although chiral GC was attempted to determine product enantiomeric purity, the two enantiomers of methyl-3-hydroxybutyrate formed during asymmetric hydrogenation could not be sufficiently resolved to obtain accurate enantiomeric excess values. As a result, diastereomers of the enantiomers were formed using (*R*)- $\alpha$ -methoxy- $\alpha$ -trifluoromethylphenylacetyl chloride<sup>49</sup> (Mosher's Acid Chloride) (Figure 2.31) and the enantiomeric purity determined by <sup>1</sup>H NMR spectroscopy.<sup>47</sup>

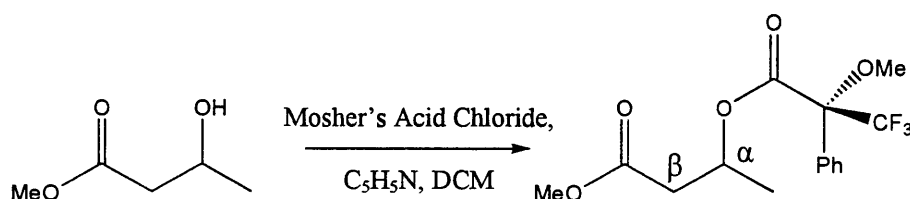


Figure 2.31. Formation of diastereoisomers using (*R*)- $\alpha$ -methoxy- $\alpha$ -trifluoromethylphenylacetyl chloride

The protons *beta* to the ester functionality show characteristic doublets formed by coupling to the *alpha* proton at the ester linkage, which is diastereotopic. Measurement of the integration of the two doublets allows elucidation of the enantiomeric purity of the product, with the enantiomeric excess being the percentage difference between the two integration values. The absolute configuration of the product was determined by formation of Mosher's acid esters of enantiomerically pure methyl-3-hydroxybutyrate samples, which were obtained commercially, followed by comparison of the <sup>1</sup>H NMR spectra. Results of the hydrogenation reactions are detailed in Table 2.5.

Ligand <sup>a</sup>	Conversion (%) <sup>b</sup>	Run 1 <i>ee</i> (%)	Run 2 <i>ee</i> (%)	Run 3 <i>ee</i> (%)	Average <i>ee</i> (%) <sup>c</sup>
( <i>R</i> )-BINAP	> 95	80	74	80	78
( <i>S</i> )-BINAP	> 95	76	72	80	76
( <i>R</i> )-Rf-BINAP (IX)	> 95	86	70	72	76
( <i>S</i> )-Rf-BINAP (IX)	> 95	68	76	72	72
( <i>R</i> )-C <sub>2</sub> H <sub>2</sub> -BINAP (XI)	> 95	72	80	76	76
( <i>S</i> )-C <sub>2</sub> H <sub>2</sub> -BINAP (XI)	> 95	74	74	76	75
( <i>R</i> )-C <sub>2</sub> H <sub>4</sub> -BINAP (X)	> 95	91	68	82	80
( <i>S</i> )-C <sub>2</sub> H <sub>4</sub> -BINAP (X)	> 95	78	80	68	75

<sup>a</sup> [RuCl<sub>2</sub>(benzene)]<sub>2</sub> catalyst precursor used in all cases <sup>b</sup> By <sup>1</sup>H NMR spectroscopy for all runs <sup>c</sup> By <sup>1</sup>H NMR spectroscopy of (*R*)-MTPA ester

Table 2.5. Hydrogenation results

Table 2.4 shows some interesting results. Primarily, in this system, the data shows that the direct addition of fluoros ponytails to the binaphthyl backbone has no detrimental effect on the total conversion of substrate to product. This is not in agreement with the itaconic acid system<sup>29</sup> and indicates that the inclusion of additional spacer groups in the BINAP ligand is not always necessary to ensure high product yields. The product enantiomeric excesses observed are lower than those reported previously<sup>47</sup> but, under these conditions, they are consistent. It is known that the pressure of hydrogen used in asymmetric hydrogenation reactions can have a dramatic effect on product enantiopurity.<sup>50</sup> Here, the hydrogen pressure is half that used in the previous study. In addition, reactor type, solvent, volume and rate of stirring are all likely to affect the enantiomeric excess of the product and, with optimisation, it is likely that the *ee* values determined could be improved. For this study, however, such improvement is not required as proof that the ligands are active is more important than absolute product conversions or enantiopurities.

Successive runs show fluctuations in the enantiomeric purity observed, but these can be attributed to errors associated with the method used for *ee* determination rather than changes observed in the selectivity of the catalysts.

A biphasic system was also employed to test the solubility and retention of the catalytic complex in a fluorinated solvent. Equal volumes of PP3 and methanol were added to the reaction vessel along with the catalyst precursor, (*R*)-Rf-BINAP and methyl acetoacetate starting material and the hydrogenation carried out under standard conditions. The organic layer was decanted from the fluorinated solvent layer and fresh methanol and starting material added. A second hydrogenation reaction was then carried out. The results of these experiments are outlined in Table 2.6.

Run <sup>a</sup>	Solvent	Conversion (%) <sup>b</sup>	ee (%) <sup>c</sup>
1	Methanol/PP3	> 95	80
2 <sup>d</sup>	Methanol <sup>e</sup>	0	n.d. <sup>f</sup>

<sup>a</sup> Catalyst precursor used – [RuCl<sub>2</sub>(benzene)]<sub>2</sub> <sup>b</sup> Determined by <sup>1</sup>H NMR spectroscopy <sup>c</sup> determined by <sup>1</sup>H NMR spectroscopic analysis of (*R*)-MTPA ester <sup>d</sup> PP3 layer from run 1 reused after decantation <sup>e</sup> No additional PP3 solvent added <sup>f</sup> Not determined

Table 2.6. Hydrogenation results using a fluorinated biphasic

This data showed that, as expected, the fluorinated phase is inactive after the first catalytic run. Due to its low fluorine content, the catalytic complex is likely to be preferentially soluble in the organic phase and, therefore, removed during the decantation of the product after Run 1. Thus, this catalytic complex could not be employed in Fluorinated Biphasic Catalysis.

## 2.4 Separation Studies

Although determining the effect of fluorinated ponytails on the abilities of Rf-BINAP ligands to induce enantioselectivity and produce high product yields in catalysis is important, the ability to isolate and reuse the ligands and catalysts was a major factor in this investigation. This was of critical importance to the project and would determine the usefulness of light-fluorinated BINAP ligands since, if the catalysts could not be preferentially separated and reused, there was no benefit in adding ponytails to the binaphthyl backbone.

It was decided that, as there were no observable differences between the catalytic abilities of the light fluorinated BINAP ligands in this system, separation studies would be carried out using (*R*)-BINAP and (*R*)-Rf-BINAP only. It was unlikely that the separation of the light fluorinated BINAP ligands with additional spacer units would be significantly different to Rf-BINAP and so the time consuming study of their individual separations was not attempted. Additionally, both enantiomers of the same ligand were not tested for separation ability, as again, their ease of separation from the product was unlikely to be any different.

### 2.4.1 Separation of (*R*)-BINAP and (*R*)-Rf-BINAP by Distillation

Even though novel and sometimes complex ways to recover and reuse BINAP-based catalysts have been investigated, there are no literature reports on the attempted simple and relatively cheap isolation of products by distillation followed by reuse of BINAP-based catalysts. Here, fluoros ponytails were added to the BINAP ligands to supply a handle for their separation on FRP silica gel. However, should it be possible to remove the products/reactants by distillation and then reuse an active catalyst, these perfluorocarbon chains may not actually be required.

Two standard asymmetric hydrogenation reactions were carried out using (*R*)-BINAP and (*R*)-Rf-BINAP as ligands. After reaction, the reaction mixture was removed from the reactor *via* syringe and added to a flame-dried flask under nitrogen. The product was then distilled along with the dichloromethane solvent under high vacuum to yield a dark red-brown semi-solid. This residue was dried and then used in further catalytic reactions. The results of these reactions are given in Table 2.7.

Run <sup>a</sup>	Ligand	Conversion (%) <sup>b</sup>	<i>ee</i> (%) <sup>c</sup>
1	( <i>R</i> )-BINAP	> 95	78
2 <sup>d</sup>	( <i>R</i> )-BINAP	> 95	2
3 <sup>d</sup>	( <i>R</i> )-BINAP	> 95	0
4	( <i>R</i> )-Rf-BINAP	> 95	78
5 <sup>d</sup>	( <i>R</i> )-Rf-BINAP	> 95	20
6 <sup>d</sup>	( <i>R</i> )-Rf-BINAP	> 95	0

<sup>a</sup>Standard catalytic conditions <sup>b</sup>by <sup>1</sup>H NMR spectroscopy <sup>c</sup>by <sup>1</sup>H NMR spectroscopy of (*R*)-MTPA ester  
<sup>d</sup>catalysis carried out using residue from previous run

Table 2.7. Results of catalysis using catalytic material recovered by distillation

It is clear from the data that distillation cannot be used to isolate a product and allow the recovery of an active catalyst in BINAP-based asymmetric systems. Although the conversion of the reactant is constant, the product *ee*'s are dramatically affected and show that the high temperatures needed to distill the product, even under high vacuum, racemise the BINAP ligands and destroy their enantioselectivity.

### 2.4.2 Separation of (*R*)-BINAP Using Silica Gel

Initially, a range of solvents were screened which solubilised the methyl-3-hydroxybutyrate while maximising the interaction of the BINAP ligands with either silica gel or FRP silica gel. It was determined that methanol was the best solvent for both the fluoros and non-fluoros systems,

with (*R*)-BINAP and (*R*)-Rf-BINAP both being almost insoluble while the product was highly soluble.

After carrying out a standard hydrogenation reaction using (*R*)-BINAP as ligand, the reaction mixture was concentrated *in vacuo* and then passed down a short 3 cm long column of silica gel using methanol as the eluting solvent.  $^1\text{H}$  and  $^{31}\text{P}$  NMR spectroscopic studies of the product obtained after removal of the methanol solvent showed that conversion to product was > 95 % and the *ee* was 82 %. More importantly, there was no evidence of ligand contamination, with no obvious proton peaks in the aromatic region of the  $^1\text{H}$  NMR spectrum of the product or phosphine peaks in the  $^{31}\text{P}$  NMR spectrum.

Next, dichloromethane was used as the eluting solvent to attempt to recover the catalyst from the column. However, even after a large volume of solvent had been passed down the column, a dark red band was still present on the top of the silica and the solvent collected was not coloured. As the catalyst precursor was red-brown, this was not a good sign. Removal of the dichloromethane *in vacuo* produced a white powder which was analysed by  $^1\text{H}$  and  $^{31}\text{P}$  NMR spectroscopy and mass spectrometry and determined to be BINAP oxide.

This result suggested that a ruthenium metal-containing species had stuck to the surface of the hydroxyl-rich silica and become irreversibly bound. It was not possible to remove the metal-containing species with any solvent tried. However, it was possible to re-isolate the BINAP ligand as BINAP oxide with an 85 % recovered yield. The optical activity of the recovered ligand was compared with that of pure BINAP oxide and found to be almost equal in sign and magnitude, suggesting that very little ligand racemisation had occurred. As a result, this ligand could theoretically be reduced and reused in further catalysis without loss of enantioselectivity or activity. As it was not possible to remove any metal-containing species from the column, it was decided that it was unlikely that the product contained any ruthenium metal contamination, and so analysis of the isolated product for metal content was not sought.

As the catalysis had been carried out under anaerobic conditions, it was unlikely that the BINAP ligand had oxidised during reaction. However, as the BINAP was recovered as oxide, it was hypothesised that the ligand must have been oxidised whilst on the silica column, either by the silica itself, the non-degassed solvents or the air. To avoid this, a ligand recovery was attempted also under anaerobic conditions. Silica gel was dried and degassed at 150 °C under high vacuum for 24 hours and then packed in a column in a dry box under nitrogen. The hydrogenation reaction mixture was concentrated *in vacuo* as before and then placed on the column of degassed silica and the product eluted with dry and degassed methanol. Once all of the product had been removed, dry and degassed dichloromethane was used as elutant and a white powder was again collected leaving a dark red band on the silica surface.  $^1\text{H}$  and  $^{31}\text{P}$  NMR spectroscopic analysis of the powder showed

it was unoxidised (*R*)-BINAP with a recovered yield of 82 %. Determination of the optical purity of the ligand by optical rotation showed it was not racemised and gave a value similar to pure (*R*)-BINAP, although it had fallen slightly.

The ligand was reused in a further standard asymmetric hydrogenation reaction and reisolated in a similar way. The results are given in Table 2.8.

Run <sup>a</sup>	Conversion (%) <sup>b</sup>	<i>ee</i> (%) <sup>c</sup>
1	> 95	82
2 <sup>d</sup>	> 95	68

<sup>a</sup>Standard catalytic conditions <sup>b</sup>by <sup>1</sup>H NMR spectroscopy <sup>c</sup>by <sup>1</sup>H NMR spectroscopy of (*R*)-MTPA ester  
<sup>d</sup>catalysis carried out using (*R*)-BINAP from previous run

Table 2.8. Results of catalysis using (*R*)-BINAP recovered by chromatography

The data shows that the re-isolated BINAP ligand can be used successfully in further catalysis to give high conversion to product and high product *ee*'s. However, only 65 % of the BINAP could be recovered after the second run, meaning half of the ligand had been lost after only two recovery attempts. Mechanical losses along with degradation of the ligand and problems associated with working under nitrogen with such tiny amounts of material were the likely causes of the loss. With so tiny an amount of material, it was not possible to carry out a third catalytic run accurately. Even so, the results are very promising and suggest that it would be possible to reuse the BINAP ligand successfully in a number of catalytic runs on a larger scale.

#### 2.4.3 Separation of (*R*)-Rf-BINAP Using FRP Silica Gel

Although it was possible to isolate and reuse (*R*)-BINAP using standard silica gel, it was hoped that, using FRP silica gel and (*R*)-Rf-BINAP, both the ligand and a catalytically active species could be re-isolated. As stated previously, it was thought that the ruthenium-containing species bound irreversibly to the hydroxyl groups on the surface of the silica gel and, therefore, could not be recovered. FRP silica gel has a fluorinated surface with many of the hydroxyl groups capped, which should reduce the amount of ruthenium that binds irreversibly to the silica and may allow re-isolation of an active species.

Once again, a standard asymmetric hydrogenation reaction was carried out and the solvent removed under reduced pressure. FRP silica gel, which had been dried for 24 hours at 150 °C under high vacuum, was packed under nitrogen in a glove box into a short column 3 cm long and the reaction mixture residue added to the top. The product was then eluted with dry and degassed methanol.

The product was analysed by  $^1\text{H}$ ,  $^{31}\text{P}$  and  $^{19}\text{F}$  NMR spectroscopy after removal of the solvent and found to be free of starting material contamination. In addition, there were no signs of aromatic protons in the  $^1\text{H}$  NMR spectrum due to (*R*)-Rf-BINAP contamination, and the  $^{19}\text{F}$  and  $^{31}\text{P}$  NMR spectra also contained no signs of the fluororous ligand. The product was converted to the Mosher's acid ester and its enantiomeric excess determined to be 84 %.

Dry and degassed dichloromethane was then used to wash the column in an attempt to recover the catalyst. However, once again, a red-brown band remained at the top of the column and a colourless solution was obtained which was found to contain (*R*)-Rf-BINAP after removal of the solvent *in vacuo*. The ligand gave a similar optical rotation value to the pure ligand and was used in further asymmetric hydrogenation reactions. The results of these hydrogenations are given in Table 2.9.

Run <sup>a</sup>	Conversion (%) <sup>b</sup>	ee (%) <sup>c</sup>
1	> 95	84
2 <sup>d</sup>	> 95	72
3 <sup>d</sup>	> 95	68

<sup>a</sup> Standard catalytic conditions <sup>b</sup> by  $^1\text{H}$  NMR spectroscopy <sup>c</sup> by  $^1\text{H}$  NMR spectroscopy of (*R*)-MTPA ester  
<sup>d</sup> catalysis carried out using (*R*)-Rf-BINAP from previous run

Table 2.9. Results of catalysis using (*R*)-Rf-BINAP recovered by chromatography

Once more, the data shows that re-isolated (*R*)-Rf-BINAP can be reused successfully in further catalysis without significant loss of activity or selectivity. However, as with (*R*)-BINAP, losses of ligand after each successive recycle are significant and, after three recycles, only one third of the original ligand could be isolated. At this point, the amount of ligand was too small to be reused accurately in further catalysis. However, as for (*R*)-BINAP above, the ability to isolate and recycle the ligand is a very promising result and again could be used on a larger scale with the losses due to handling significantly reduced.

#### 2.4.4 BINAP – Conclusions

It is perhaps not that surprising that the light fluororous approach could not be applied to this system. Initial attempts to pre-form the catalytic complex containing the BINAP ligands were unsuccessful, leading to the conclusion that the active species is only formed under the reaction conditions. This would suggest that, after depressurisation and cooling of the reaction, the complex breaks down into free BINAP ligand and a ruthenium-containing moiety. Passing the reaction mixture down a column of silica gel then successfully removes the free ligand from the product but,

as the ligand is no longer coordinated to the catalyst metal centre, only the ligand can be recovered and the metal is lost.

Clearly, the addition of fluorinated ponytails to the BINAP ligand cannot overcome this problem. To successfully retain a catalytically active species on FRP silica gel and then recover and reuse it requires the ligand to stay coordinated to the metal centre. If this does not occur, then it is likely that the metal will be lost in any system.

However, the fact that the fluorinated ponytails have no effect on product conversion or catalyst enantioselectivity when Rf-BINAP ligands are used under the conditions employed here is a very positive observation, as this result shows addition of perfluoroalkyl chains is not always detrimental to the outcome of an asymmetric catalytic reaction. This data implies that use of a fluorinated BINAP ligand in a different system where the ligand-catalyst complex is more stable may well lead to good yields and selectivities and the ability to separate the complex from the products. In addition, this recycling protocol for the fluorinated BINAP ligands is likely to be applicable to a wide variety of substrates in ruthenium-catalysed asymmetric hydrogenation reactions as it is selectively retained on FRP silica gel. Due to the differing solubility of underivatized BINAP in alternative substrates, there is no guarantee the ligand could be isolated and reused without resorting to column chromatography.

## 2.5 References for Chapter Two

1. Guiry, P., McCarthy, M., *Tetrahedron*, 57, 2001, 3809.
2. Jacobsen, E. N., *Acc. Chem. Res.*, 33, 2000, 421.
3. Vogl, E. M., Harald, G., Shibasaki, M., *Angew. Chem. Int. Ed. Engl.*, 38, 1999, 1570.
4. Lin, P., *Tetrahedron: Asymmetry*, 9, 1998, 1457.
5. Ito, T., Miyashita, A., Noyori, R., Souchi, T., Takaya, H., Toriumi, K., Takaya, H., Yasuda, A., *J. Am. Chem. Soc.*, 102, 1980, 7932.
6. Bender, D., Cai, D., Hughes, D., Payack, J., Reider, P., Verhoeven, T., *J. Org. Chem.*, 59, 1994, 7180.
7. Kitamura, M., Nagai, K., Noyori, R., Ohta, T., Takaya, H., *J. Org. Chem.*, 52, 1987, 3176.
8. Kitamura, M., Noyori, R., Ohkuma, T., *Tetrahedron Lett.*, 31, 1990, 5509.
9. Åhman, J., Buchwald, S., Palucki, M., Troutman, M., Wolfe, J., *J. Am. Chem. Soc.*, 120, 1998, 1918.
10. Hoegaerts, D., Jacobs, P., *Tetrahedron: Asymmetry*, 10, 1999, 3039.
11. Hayashi, T., Ito, Y., Matsumoto, Y., *Tetrahedron: Asymmetry*, 2, 1991, 601.
12. Ishiba, A., Nakashima, H., Yamamoto, Yanagisawa, A., *J. Am. Chem. Soc.*, 118, 1996, 4723.
13. Miyashita, A., Takaya, H., *Tetrahedron*, 40, 1984, 1245.
14. Buchwald, S., Spielvogel, D., *J. Am. Chem. Soc.*, 124, 2002, 3500.
15. Miyaura, N., Ueda, M., Saitoh, A., *J. Organomet. Chem.*, 642, 2002, 145.
16. Berthod, M., Saluzzo, C., Mignani, G., Lemaire, M., *Tetrahedron: Asymmetry*, 15, 2004, 639.
17. Saluzzo, C., Lamouille, T., Le Guyader, F., Lemaire, M., *Tetrahedron: Asymmetry*, 2002, 13, 1141.
18. Monteiro, A. L., Zinn, F. K., de Souza, R. F., Dupont, J., *Tetrahedron: Asymmetry*, 8, 1997, 177.
19. Ngo, H. L., Hu, A., Lin, W., *Chem. Commun.*, 2003, 1912.
20. Bayston, D. J., Fraser, J. L., Ashton, M. R., Baxter, A. D., Polywka, M. E. C., Moses, E., *J. Org. Chem.*, 63, 1998, 3137.
21. Fan, Q-h., Ren, C-y., Yeung, C-h., Hu, W-h., Chan, A. S. C., *J. Am. Chem. Soc.*, 121, 1999, 7407.
22. Gelman, F., Avnir, D., Schumann, H., Blum, J., *J. Mol. Catal. A*, 146, 1999, 123.
23. Deng, G-j., Fan, Q-h., Chen, X-m., Liu, G-h., *J. Mol. Catal. A*, 193, 2003, 21.

24. Deng, G-j., Fan, Q-h., Chen, X-m., Liu, D-s., Chan, A. S. C., *Chem. Commun.*, **2002**, 1570.
25. Hu, A., Ngo, H. L., Lin, W., *Angew. Chem. Int. Ed. Engl.*, **42**, **2003**, 6000.
26. Nakamura, Y., Ohgo, Y., Okumura, K., Takeuchi, S., Zhang, S., *Tetrahedron Lett.*, **43**, **2002**, 3053.
27. Cavazzini, M., Maillard, D., Pozzi, G., Quici, S., Sinou, D., *Chem. Commun.*, **2001**, 1220.
28. Bayardon, J., Cavazzini, M., Maillard, D., Pozzi, G., Quici, S., Sinou, D., *Tetrahedron: Asymmetry*, **14**, **2003**, 2215.
29. Birdsall, D., Chen, W., Hope, E., Hu, Y., Stuart, A., Xiao, J., *Tetrahedron Lett.*, **42**, **2001**, 8551.
30. Berthod, M., Mignani, G., Lemaire, *Tetrahedron: Asymmetry*, **15**, **2004**, 1121.
31. Adams, D., *private communication*, **2002**.
32. McLoughlin, V., Thrower, J., *Tetrahedron*, **25**, **1969**, 5921.
33. Chen, G., Tamborski, C., *J. Fluorine Chem.*, **43**, **1989**, 207.
34. Beller, M., Brossmer, C., Herrmann, W., Öfele, K., Reisinger, C-P., Riermeier, T., *Chem. Eur. J.*, **3**, **1997**, 1357.
35. Amatore, C., Jutand, A., *J. Organomet. Chem.*, **576**, **1999**, 254.
36. Chatt, J., Duncanson, L., *J. Chem. Soc.*, **1953**, 2939.
37. Berkovitch-Yellin, Z., Ellis, D., Trogler, W., Xiao, S-X., *J. Am. Chem. Soc.*, **105**, **1983**, 7033.
38. Marynick, D., *J. Am. Chem. Soc.*, **106**, **1984**, 4064.
39. Connelly, N., Orpen, A., *J. Chem. Soc., Chem. Commun.*, **1985**, 1310.
40. Bagus, P., Pacchioni, G., *Inorg. Chem.*, **31**, **1992**, 4391.
41. Lyne, P., Mingos, D., *J. Org. Chem.*, **478**, **1994**, 141.
42. Hope, E. G., Kemmitt, R. D. W., Paige, D. R., Stuart, A. M., Wood, D. R. W., *Polyhedron*, **18**, **1999**, 2913.
43. Croxtall, B., Fawcett, J., Hope, E. G., Russell, D. R., Stuart, A. M., *J. Chem. Soc., Dalton Trans.*, **1999**, 491.
44. Howell, J. A. S., Fey, N., Lovatt, J. D., Yates, P. C., McArdle, P., Cunningham, D., Sadeh, E., Gottlieb, H. E., Goldschmidt, Z., Hursthouse, M. B., Light, M. E., *J. Chem. Soc. Dalton Trans.*, **1999**, 3015.
45. Adams, D. J., Cole-Hamilton, D. J. Hope, E. G., P. J. Pogorzelec, Stuart, A. M., *J. Organomet. Chem.*, **689**, **2004**, 1413.
46. Kumobayashi, H., Miura, T., Sayo, N., Saito, T., Zhang, X., *Synlett*, **SI**, **2001**, 1055.

47. Kitamura, M., Noyori, R., Ohkuma, T., Tokunaga, M., *Tetrahedron Lett.*, 32, **1991**, 4163.
48. Stephenson, T., Wilkinson, G., *J. Inorg. Nucl. Chem.*, 28, **1966**, 945.
49. Goldberg, Y., Alper, H., *J. Org. Chem.*, 51, **1992**, 3731.
50. Noyori, R., *Asymmetric Catalysis in Organic Synthesis*, Wiley & Sons, New York, **1994**, Chapter 2.

## 3 The Investigation of Monodentate

### 3.1 Introduction

#### 3.1.1 Monodentate Ligands and Monophos

Enantioselective hydrogenation of substrates using monodentate phosphorus-containing ligands was first investigated nearly thirty-five years ago by Horner and Knowles *et al.*<sup>1,2</sup> These first attempts used chiral Rhodium's type catalysts, but low product enantioselectivities were observed, with enantiomeric excesses ( $e.e.$ ) between only 3 and 15 %. Subsequent attempts to develop monodentate ligands which would produce a high enantiomeric excess of product met with limited success, the best ligand being (S)- $1^{\circ}$ -(1R), cyclohexyl- $\alpha$ -amidoethylphosphane, which gave  $e.e.$ 's up to 90 % in the hydrogenation of chiral iron(III) acids.<sup>3</sup>

# Chapter Three



However, further study of monodentate phosphorus-containing ligands for asymmetric hydrogenation was largely abandoned after the discovery that bidentate chelating phosphorus ligands, which were easier to synthesize, produced products with much higher  $e.e.$  However, it was noted that a rhodium complex containing Dap with a chiral backbone gave  $e.e.$ 's of up to 90 %. Shortly thereafter, Knowles *et al.* demonstrated that a rhodium complex containing a chiral bidentate phosphorus ligand with three phosphorus atoms (carosap) also produced  $e.e.$ 's of over 90 %.<sup>4</sup> Further, Doyle *et al.* have introduced phosphine-1,2-diamines<sup>5</sup> was introduced as a highly efficient ligand for asymmetric hydrogenations (see Chapter 5). The broad applicability of these chelating bidentate ligands, along with their more straightforward preparation and higher enantioselectivities, has caused a systematic shift in research away from monodentate ligands for enantioselective hydrogenation, which remained largely forgotten for over thirty years.

Recent interest in monodentate phosphorus ligands have once more been receiving much attention. This interest was first indicated very recently by Doyle and Feringa *et al.* in 1999 that a rhodium complex of 1,2-diphenylphosphinane, prepared in their research group, had achieved the highest  $e.e.$  of 99 % in the hydrogenation of chiral iron(III) acids (Figure 3.1).<sup>6</sup>

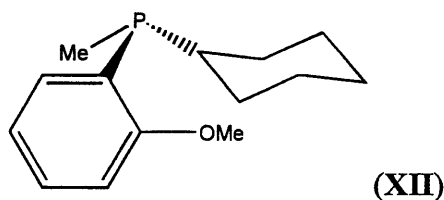
Figure 3.1. Hydrogenation of chiral iron(III) acids using a rhodium complex of 1,2-diphenylphosphinane.  $e.e.$  = 99 %.

### 3 The Investigation of MonoPhos

#### 3.1 Introduction

##### 3.1.1 Monodentate Ligands and MonoPhos

Enantioselective hydrogenation of substrates using monodentate phosphorus-containing ligands was first investigated nearly thirty-five years ago by Horner and Knowles *et al.*<sup>1,2</sup> These first examples used chiral Wilkinson's type catalysts, but low product enantioselectivities were observed, with enantiomeric excesses (*ee*'s) of between only 3 and 15 %. Subsequent attempts to develop monodentate ligands which would produce a high enantiomeric excess of product met with limited success, the best ligand being CAMP (XII), cyclohexyl-*o*-anisylmethylphosphane, which gave *ee*'s up to 90 % in the hydrogenation of dehydroamino acids.<sup>3</sup>



However, further study of monodentate ligands for use in asymmetric hydrogenations was largely abandoned after the discovery that bidentate chelating phosphorus ligands, which were easier to synthesise, produced products with much higher *ee*'s. Kagan *et al.* showed that a rhodium complex containing diop with a chiral backbone gave enantioselectivities of greater than 70 %.<sup>4</sup> Shortly afterwards, Knowles *et al.* demonstrated that a rhodium complex containing a chelating bidentate phosphane ligand with chiral phosphorus atoms (dipamp) also produced *ee*'s of over 90 %.<sup>5</sup> Further, BINAP (2,2'-bis(diphenylphosphino)-1,1'-binaphthyl) was introduced as a highly efficient ligand in asymmetric hydrogenations (see Chapter 2). The broad applicability of these chelating bidentate species, coupled with their more straightforward preparation and higher enantioselectivities, led to a dramatic shift in research away from monodentate ligands for enantioselective synthesis, which remained largely forgotten for over thirty years.

Recently, however, monodentate phosphorus ligands have once more been receiving much attention. This is largely due to the disclosure by Guillen and Fiaud *et al.* in 1999 that a rhodium complex of 1,2,5-triphenylphospholane, prepared in their research group, had reduced the methyl ester of (*Z*)-*N*-acetylaminoacinnamic acid in 82 % *ee*<sup>6</sup> (Figure 3.1).

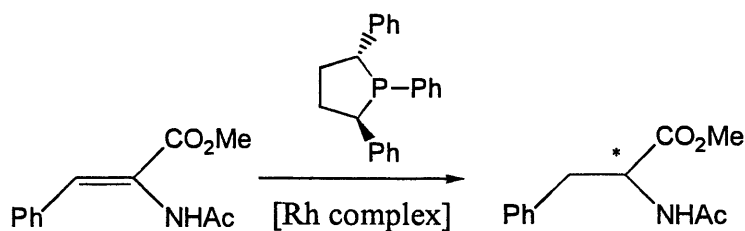


Figure 3.1. Asymmetric hydrogenation using a chiral monodentate phosphine ligand

This result has led to the investigation of other monodentate ligands, several of which use binaphthyl backbones to provide their chiral component, rather than a chiral phosphorus atom.

Initially, Orpen and Pringle *et al.* reported studying a range of monodentate phosphonites which contained binaphthyl backbones.<sup>7</sup> Rhodium(I) complexes of these ligands were shown to hydrogenate methyl-2-acetamido acrylates with up to 100 % conversion and 92 % *ee* (Figure 3.2).

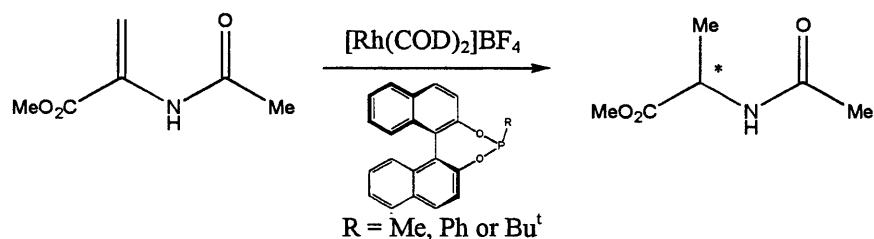


Figure 3.2. Asymmetric hydrogenation using an axially chiral monodentate phosphonite ligand

Almost concurrently, Reetz and Sell published similar results for this reaction,<sup>8</sup> with the inclusion of data for an ethyl R group. Use of a rhodium(I) catalyst with an ethyl group attached to the phosphonite led to 100 % conversion to the product with 94 % *ee*. This work was followed swiftly by the publication of data on the hydrogenation of itaconic acid dimethyl ester using a phosphite with an (*R*)-OCH(Me)Ph substituent<sup>9</sup> (Figure 3.3).

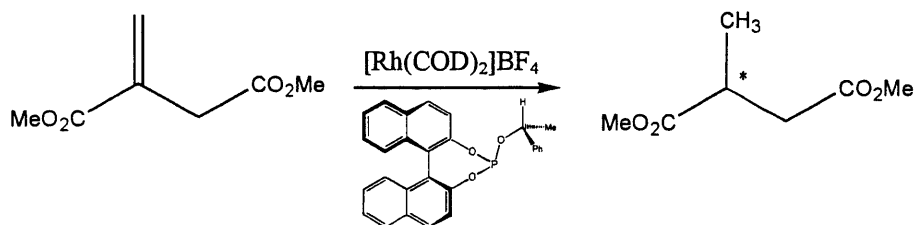


Figure 3.3. Asymmetric hydrogenation using an axially chiral monodentate phosphite

This ligand proved to be exceptional, yielding conversions to product of 100 % and *ee*'s greater than 99 %. Also, a substrate:rhodium ratio as high as 5000:1 could be employed, still yielding complete conversion in twenty hours under atmospheric pressures of hydrogen.

Interestingly, the stereochemistry of the R group had no influence on the stereochemistry of the product.

During this time, the use of monodentate phosphoramidites had been examined in copper-catalysed dialkylzinc additions to enones,<sup>10,11</sup> producing excellent enantioselectivities. Subsequently, Feringa *et al.* studied the use of binaphthylphosphoramidite<sup>12</sup> (MonoPhos, (XIII)) in enantioselective hydrogenations (Figure 3.4).

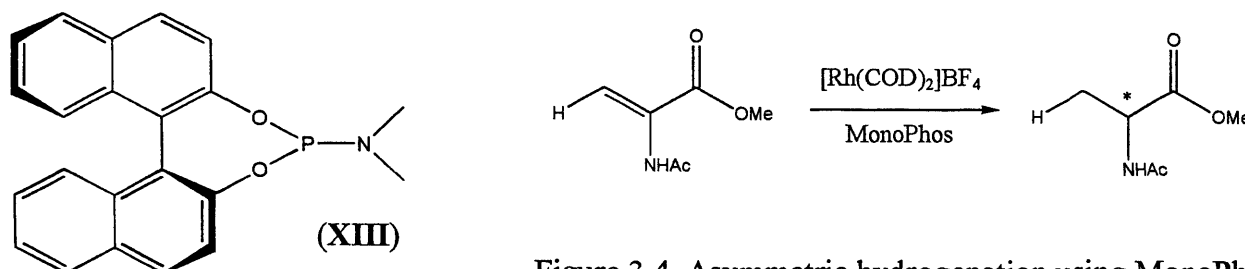


Figure 3.4. Asymmetric hydrogenation using MonoPhos

It was shown that, for a large range of substrates based on dehydroamino acid (methyl ester shown in Figure 3.4), 100 % yields and up to 100 % *ee*'s could be obtained. It was also shown that the solvent used during hydrogenation had an effect on the *ee*, dichloromethane producing the greatest enantioselectivity, whereas the hydrogen pressure had little effect on the *ee*. Most interestingly, a bidentate derivative of (XIII), which would be expected to give better enantioselectivities due to chelation and a more rigid structure, only yielded 56 % conversion to the product with 72 % *ee*.

Since this publication, the study of MonoPhos and other monodentate phosphorus-based ligands with binaphthyl backbones has continued steadily. Chen and Xiao have studied a monodentate phosphite bearing an L-menthol R group<sup>13</sup> in asymmetric synthesis. The study is unique in that racemic binaphthol is used as a starting material and coupled to dichloro-L-menthol-phosphinite. The racemic mixture is then fractionally crystallised from diethyl ether to obtain both diastereomers separately. This negates the use of expensive, resolved (*R*)- or (*S*)- binaphthol. The product conversions and *ee*'s are once again excellent, with itaconic acid dimethyl ester being hydrogenated by the [Rh(COD)(phosphite)<sub>2</sub>]BF<sub>4</sub> catalyst in 100 % yield and up to 95 % *ee*.

Chan *et al.* have employed rhodium-MonoPhos catalysts in the enantioselective hydrogenation of a range of enamides (Figure 3.5).<sup>14</sup>

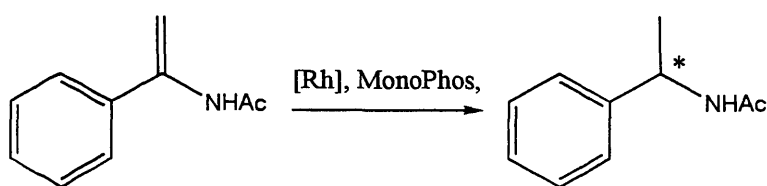


Figure 3.5. Asymmetric hydrogenation of enamides using Rh-MonoPhos

For the enamide shown, conversions to the asymmetric product were quantitative with *ee*'s of 95 % when dichloromethane was used as solvent. For other enamides studied, conversions of 100 % were also observed when non-bulky substituents were present with product *ee*'s of between 85 and 95 %.

Novel variations of the MonoPhos ligand have also been studied by Chen *et al.* Using  $H_8$ -BINOL (5,6-5',6'-bis(cyclohexyl)-1,1'-bi-2-phenol), it was possible to synthesis  $H_8$ -MonoPhos and study its activity in the asymmetric hydrogenation of  $\alpha$ -dehydroamino acids (Figure 3.6).<sup>15</sup>

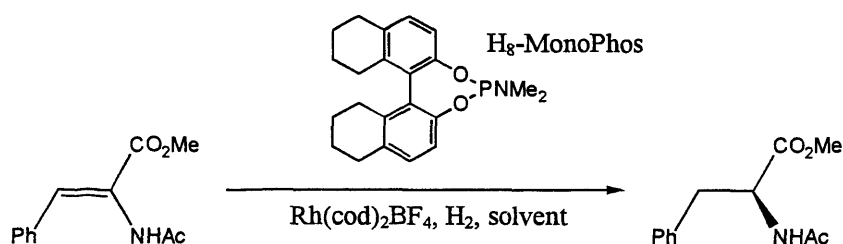


Figure 3.6. Asymmetric hydrogenation of methyl (*Z*)-acetoamidocinnamate using  $H_8$ -MonoPhos

When methyl (*Z*)-acetoamidocinnamate was used as substrate, 99 % product conversion and 94 % *ee* was observed when dichloromethane was used as solvent. When ethyl acetate was used as solvent, the product *ee* could be increased to 96 %, although the conversion fell to 97 %. By comparison, when MonoPhos was used as ligand for the same reaction, the product *ee*'s were similar, but the conversions fell to 26 % and 57 % respectively. The result shows that, when  $H_8$ -MonoPhos is employed in this hydrogenation, the resulting catalyst is more active. The study of  $H_8$ -MonoPhos has since been extended to a larger range of substrates and R-groups on the ligand nitrogen by the same research group.<sup>16</sup>

Feringa *et al.* have recently shown that alteration of the R-groups attached to the nitrogen atom of MonoPhos can significantly alter its ability to catalyse reactions enantioselectively.<sup>17</sup> A range of different MonoPhos-style ligands were tested, three of which are shown below (Figure 3.7).

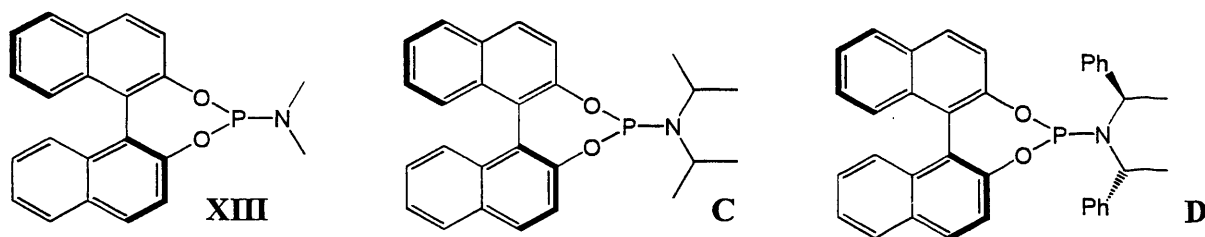


Figure 3.7. MonoPhos-derived Ligands

In a one-pot, multi-substrate copper-catalysed enantioselective conjugate addition of diethylzinc to a range of nitroalkenes (Figure 3.8), all of the ligands gave 100 % conversions to product. However, of the three ligands shown, MonoPhos (**XIII**) gave consistently the lowest product *ee*'s (5 – 35 %), followed by **C** (33 – 57 %) and then **D** (52 – 69 %).

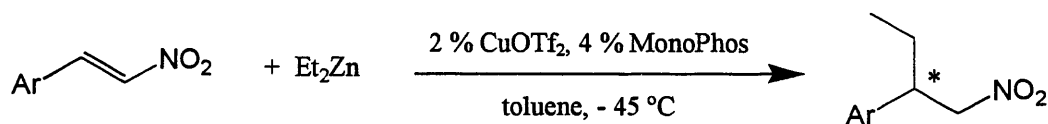


Figure 3.8. Conjugate Addition of Diethylzinc to Nitroalkenes

This study shows that for these conjugate additions, bulky R groups on the amine are required to give moderate to high product *ee*'s. For other systems where the transferral of small molecules occurs during catalysis, these more bulky MonoPhos-type ligands may yield higher enantiomeric excesses than standard MonoPhos.

Zhou and co-workers have also published work on modifications to phosphoramidites which lead to the formation of better ligands than MonoPhos in enantioselective synthesis.<sup>18</sup> In the asymmetric hydrogenation of  $\alpha$ -phenylethenylamine using  $[\text{Rh}(\text{cod})_2]\text{BF}_4$ , MonoPhos proved to have similar activity to the other two ligands tested (Figure 3.9). However, the enantioselectivity of MonoPhos was less than for the two alternatives. The use of MonoPhos led to the formation of a product with an enantiomeric excess of 93 %. When H<sub>8</sub>-MonoPhos (ligand **E**) was used, this enantioselectivity was increased to 96 % and increased again to 99 % when ligand **F** was used.

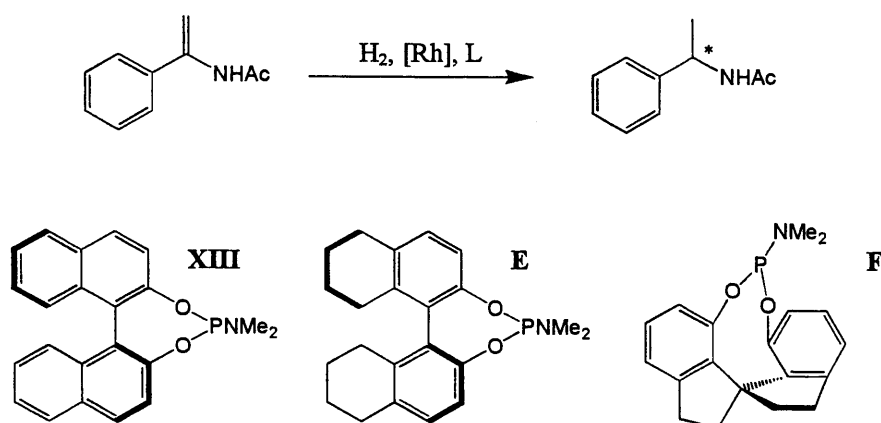


Figure 3.9. Asymmetric Hydrogenation using Phosphoramidites

Asymmetric hydrogenations of the same substrate using a MonoPhos derivative with an  $\text{NEt}_2$  group replacing the  $\text{NMe}_2$  group also led to higher enantioselectivities.<sup>19</sup> At  $5^\circ\text{C}$ , the use of the former led to product with an *ee* of 99 %, whereas the *ee* was only 90 % with the latter.

MonoPhos has also been used recently for the chemical resolution of secondary alcohols using diethyl azodicarboxylate (DEAD).<sup>20</sup> The enantioselectivity of a range of secondary alcohols could be enriched when MonoPhos was used as the enantiomer differentiating ligand. (Figure 3.10).

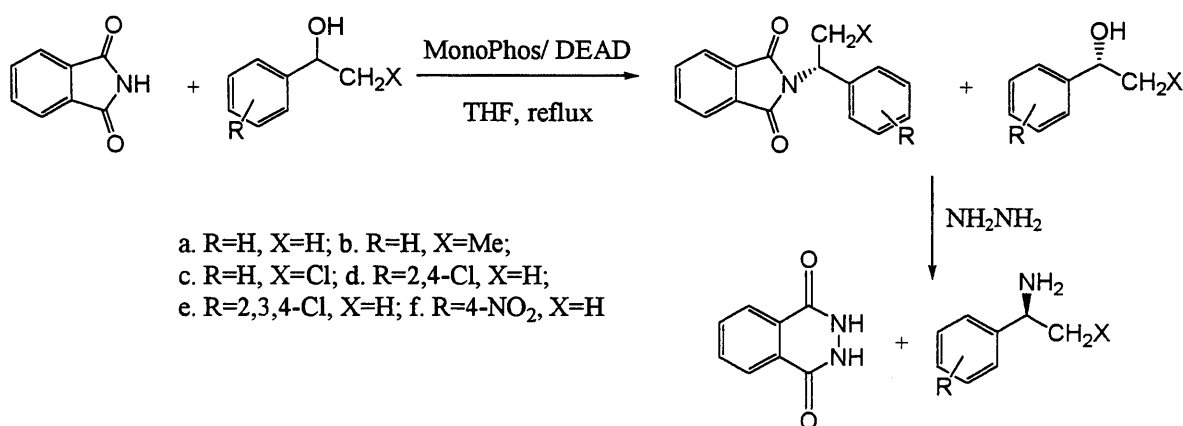


Figure 3.10. Resolution of secondary alcohols using MonoPhos

The (*S*)-enantiomers of the alcohols reacted preferentially with the phthalimide to leave the (*R*)-enantiomers in excess. The (*S*)-enantiomers could then be obtained in moderate enantiomeric excesses by reacting with hydrazine hydrate to release the material as the secondary amine. Moderate *ee*'s could be obtained between 13 and 30 % for the (*R*)-enantiomers and between 26 and 45 % for the (*S*)-enantiomers as their amine analogues.

Of the ligands outlined above, MonoPhos is by far the most simple enantioselective monodentate ligand to prepare. Comparison of all of the data obtained for monodentate phosphorus-based ligands also shows MonoPhos to be one of the best chiral inducing ligands, although most of

the ligands have comparable abilities. However, it is in terms of stability where MonoPhos shows the greatest advantage. Phosphonites and phosphites are susceptible to hydrolysis and phosphines are susceptible to oxidation. MonoPhos has proven to be a shelf-stable compound which is resistant to both oxidation and hydrolysis,<sup>21</sup> making it extremely useful for asymmetric homogeneous catalysis.

In comparison to BINAP, MonoPhos has a much lower mass, weighing roughly half the amount of BINAP. This makes MonoPhos a prospective ligand for use in light fluorous catalysis. Containing less organic bulk, the ligand should require less fluorous character to be selectively retained on FRP silica gel and so the attachment of perfluoroalkyl chains, catalysis, separation and reuse of the ligand in asymmetric hydrogenations was investigated.

### 3.1.2 Examples of Recyclable MonoPhos

The examples given above which concern MonoPhos focus solely on the study and improvement of the ligand and not on its recovery after catalysis. However, to date, there is only one example of a study of the isolation and reuse of a MonoPhos-based catalyst. Doherty and co-workers have recently published work on polymer-supported phosphoramidite ligands which can be easily recycled by precipitation and filtration.<sup>22</sup> In the study of asymmetric hydrogenation reactions of dimethyl itaconate and dehydroamino acid derivatives, MonoPhos was consistently better at giving rise to products with high enantiomeric excesses than polymer bound analogues. However, a polymer-bound MonoPhos ligand (Figure 3.11) could be easily recycled four times with no loss of activity or selectivity.

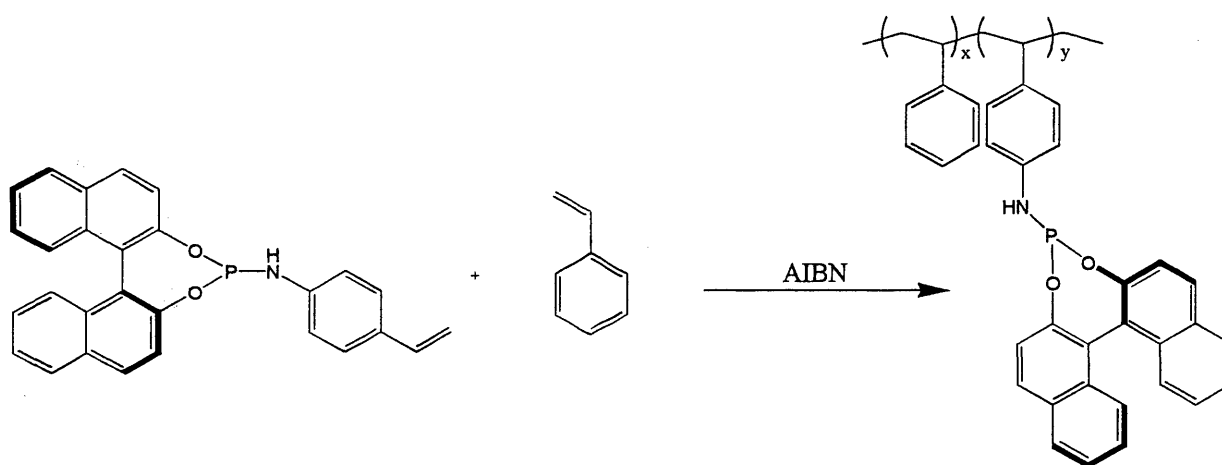


Figure 3.11. Synthesis of a polymer-bound phosphoramidite ligand.

For example, in the asymmetric hydrogenation of dehydroamino acid derivatives using  $[\text{Rh}(\text{cod})_2]\text{BF}_4$  and MonoPhos, 100 % conversion and > 99 % product *ee* could be obtained. Using a

polymer-supported MonoPhos, the product *ee* fell to 80 %, but the catalyst could be recycled four times with the same product *ee* achieved after each recycle. In addition, ICP-AES analysis of the organic product showed no sign of rhodium leaching into the product. This work shows the reuse of  $[\text{Rh}(\text{cod})_2]\text{BF}_4$  catalyst systems is possible and suggests that the use of non-polymer-supported MonoPhos ligands should give rise to higher product yields and enantiomeric excesses.

## 3.2 Synthesis and Coordination Chemistry

### 3.2.1 The Synthesis of Rf-MonoPhos

There have been no reported syntheses of fluorous analogues of MonoPhos, but the preparation of such ligands is relatively straightforward. MonoPhos is easily prepared by reaction of (*R*)- or (*S*)-2,2'-binaphthol with hexamethylphosphorous triamide (HMPT) in diethyl ether<sup>23</sup> (Reaction 3.1), (Figure 3.12).

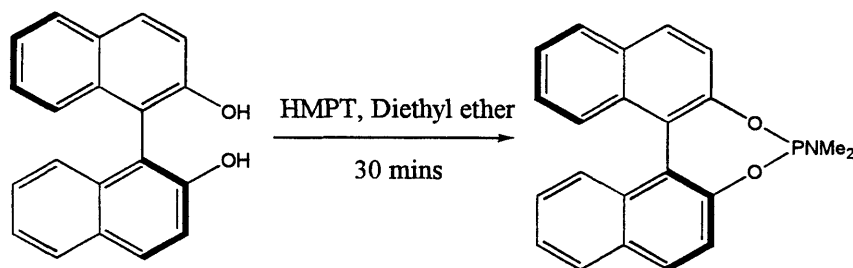


Figure 3.12. The synthesis of (*S*)-MonoPhos

This white solid was isolated and purified by recrystallisation from hexane.  $^1\text{H}$  and  $^{31}\text{P}\{^1\text{H}\}$  NMR spectroscopic data were in agreement with the data obtained previously for the molecule and the mass spectrum, elemental analysis and the melting points of the (*R*)- and (*S*)-enantiomers were as expected for MonoPhos. However, optical rotation measurements gave values which were equal in magnitude but opposite in sign to those reported previously. Positive optical rotations were observed for MonoPhos prepared from (*S*)-1,1'-bi-2-naphthol and negative rotations observed when (*R*)-1,1'-bi-2-naphthol was employed. Repeated synthesis within the group achieved the same results and so it was concluded that the observed rotations published previously were in error.

Having successfully prepared non-fluorous MonoPhos, synthesis of fluorous-derivatised analogues of the ligand was attempted. It was decided that, since the inclusion of additional spacer groups between the fluorous ponytails and binaphthyl backbone in BINAP-based ligands had no beneficial effect on subsequent catalyst activity or selectivity in these studies (see Chapter Two), only fluorous analogues of MonoPhos with ponytails directly bound to the binaphthyl backbone would be synthesised. This was achieved in the first part by the separate synthesis of (*R*)- and (*S*)-6,6'-bis-(perfluoro-*n*-hexyl)-1,1'-bi-2-naphthol as outlined in Section 2.2.1. Reaction of this

binaphthol with HMPT in dry diethyl ether produced (*R*)- and (*S*)-6,6'-bis(perfluoro-*n*-hexyl)-1,1'-bi-2-naphthyl-dimethyl-phosphoramidite ((*R*)- and (*S*)-Rf-MonoPhos (Figure 3.13)) as pale yellow oils. After washing the oils with acetonitrile and triturating with hexane, phosphorus-containing impurities were removed to yield the products as yellow solids.

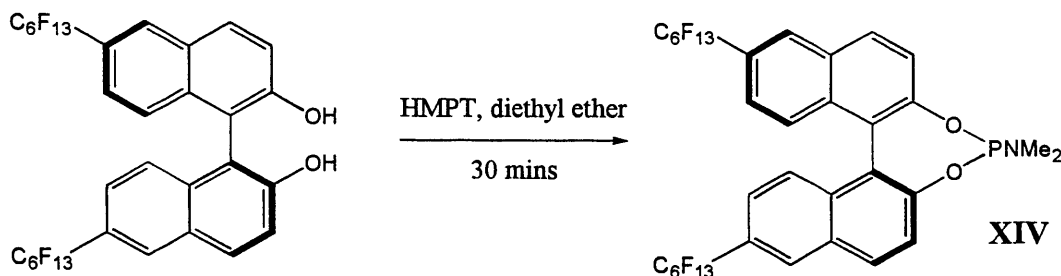


Figure 3.13. The synthesis of (*S*)-Rf-MonoPhos

The fluorous and non-fluorous MonoPhos ligands are air- and moisture-stable but degraded in sunlight over a period of one month. Analysis of the resulting pink solids showed a range of peaks in the  $^{31}P$  NMR spectra, indicating breakdown of the chelate ring and oxidation of the phosphorus centre. Subsequently, all samples were stored in the dark.

(*R*)- and (*S*)-enantiomers of the two ligands were prepared and fully characterised by  $^1H$  and  $^{31}P$  NMR spectroscopy,  $^{19}F$  NMR spectroscopy where appropriate, melting point, mass spectrum, optical rotation and elemental analyses.

Once again, although the ligands were not synthesised for use in fluorous biphasic catalysis, the partition coefficients in a PP3/toluene biphasic system were determined to allow comparison to other systems. Around 60 mg of (*S*)-MonoPhos and (*S*)-Rf-MonoPhos were separately stirred in the PP3/toluene biphasic system, allowed to stand and then portions of each phase taken, the solvent removed *in vacuo* and the residue analysed gravimetrically. The data obtained is outlined in Table 3.1.

Ligand <sup>a</sup>	Observation	Undissolved Ligand (mg)	Ligand in Toluene (mg)	Ligand in PP3 (mg)	Partition Coefficient <sup>c</sup>
( <i>S</i> )-MonoPhos (XIII)	Ligand not fully dissolved <sup>b</sup>	20	32	0	100 %
( <i>S</i> )-Rf-MonoPhos (XIV)	Ligand dissolved fully	/	34	42	45 %

<sup>a</sup> Conditions: 2.0 ml PP3, 2.0 ml toluene, rt, stir = 20 mins, settle = 20 mins, 1.0 ml of each layer analysed <sup>b</sup> Ligand at interface <sup>c</sup> % in toluene phase

Table 3.1. Partition coefficient data for MonoPhos ligands in a toluene/PP3 biphasic system

As expected, neither ligand was highly soluble in PP3, although (*S*)-Rf-MonoPhos was more soluble in PP3 than (*S*)-MonoPhos, which shows that the fluorous ponytails do add significant fluorous character to the light fluorous ligand.

### 3.2.2 Coordination Chemistry – Complexes

MonoPhos can be coordinated to a wide range of transition metals as, unlike bidentate phosphorus ligands, there is no ‘pocket’ in which the metal must be able to fit. As for Rf-BINAP (see Chapter Two), a variety of coordination complexes were synthesised to determine the effect of the perfluoroalkyl ponytails on the  $\pi$ -acceptor ability of the light fluororous MonoPhos ligands prepared. The complexes were fully characterised and changes in spectra were interpreted in terms of the effect of the ponytails on the electron density at phosphorus.

### 3.2.3 Complexes of Platinum(II)

Platinum(II) complexes of MonoPhos can be easily prepared by stirring *cis*-platinum dichloride bis-acetonitrile and MonoPhos in a 1:2 ratio in dichloromethane. Removal of most of the solvent and precipitation with petroleum ether produced the complex which could be isolated by filtration (Figure 3.14).

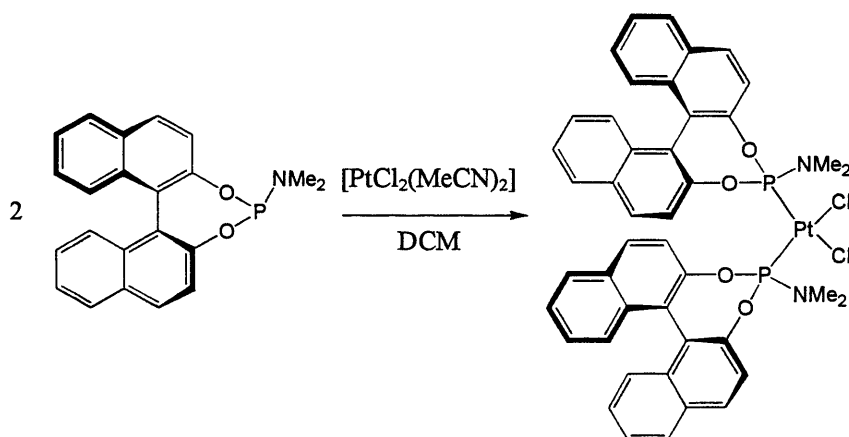


Figure 3.14. The synthesis of  $[\text{PtCl}_2(\text{MonoPhos})_2]$  complexes

It is evident from Figure 3.14 that having the MonoPhos ligands mutually *cis* may lead to steric crowding within the complex. However, a *cis*-geometry has been assigned to the complexes formed on the basis of their  $^1J_{\text{Pt-P}}$  coupling constants. Due to the symmetry of the metal *d* orbitals, the opportunity for metal-phosphorus  $\pi$ -back-bonding is increased when the ligands have a *cis* arrangement, as there is a greater interaction between the phosphorus  $\pi$ -acceptor orbitals and metal *d* orbitals than for *trans*-coordination.<sup>24</sup> Pt-P coupling constants obtained here are over 5000 Hz, indicating the phosphorus atom is *trans* to chlorine and, therefore, *cis* to the other MonoPhos ligand.

Four complexes of the type  $\text{PtCl}_2(\text{L})_2$  have been prepared, employing (*R*)- and (*S*)-MonoPhos and (*R*)- and (*S*)-Rf-MonoPhos. All of the complexes prepared proved to be air- and moisture-stable and yields of between 50 and 60 % were obtained in all cases. Mass spectra of the complexes showed no parent ion peaks, but peaks corresponding to  $[\text{M-Cl}]^+$  were observed for all

complexes by positive ion mode FAB mass spectrometry. The  $^1\text{H}$  NMR spectra of the complexes were largely uninformative, showing only a complex mass of peaks in the aromatic region of the spectrum corresponding to the protons on the binaphthyl backbone and a doublet at around 2.5 ppm corresponding to the methyl protons of the amine. The  $^{19}\text{F}$  NMR spectra of fluorine-containing complexes were also of little interest, as they remained relatively the same as for the free ligands. The  $^{31}\text{P}$  NMR spectra were, however, far more informative. The data from these spectra are outlined in Table 3.2

Ligand	$^{31}\text{P}$ { $^1\text{H}$ } NMR data (ligand) (ppm) <sup>a</sup>	$^{31}\text{P}$ NMR data (complex) (ppm) <sup>a</sup>	$^1J_{\text{Pt-P}}$ coupling (Hz)
( <i>R</i> )-MonoPhos (XIII)	s, 148.7	ss, 93.2	5604
( <i>S</i> )-MonoPhos (XIII)	s, 148.7	ss, 93.2	5604
( <i>R</i> )-Rf-MonoPhos (XIV)	s, 150.0	ss, 95.3	5582
( <i>S</i> )-Rf-MonoPhos (XIV)	s, 150.0	ss, 95.4	5578

<sup>a</sup>NMR spectroscopic data from complexes dissolved in  $\text{CDCl}_3$

Table 3.2.  $^{31}\text{P}\{^1\text{H}\}$  NMR spectroscopy data for  $[\text{PtCl}_2(\text{MonoPhos})_2]$  complexes

Comparison of this data shows that, as was true for the BINAP ligands, the non-fluorinated MonoPhos ligands are the stronger  $\sigma$  donors, as they yield the highest  $^1J_{\text{Pt-P}}$  coupling constants (see Section 2.2.2). Again, as expected, attaching electron-withdrawing fluorous ponytails to the binaphthyl backbone shifts the peak in the  $^{31}\text{P}$  NMR spectrum for free ligand down-field as the phosphorus atom is more deshielded. Removing electron density from the phosphorus atom in the ligand makes it a weaker  $\sigma$  donor than MonoPhos and leads to a reduction in the  $^1J_{\text{Pt-P}}$  coupling constant.

It is interesting to note that the fall in  $^1J_{\text{Pt-P}}$  coupling constants is around 20 Hz, which is less than the reduction in value when Rf-BINAP ligands are used in place of BINAP in platinum complexes of the same form. This is likely to be due to the presence of the oxygen atoms in the Rf-MonoPhos ligands, which supply extra shielding of the phosphorus centre from the electron-withdrawing ponytails, while the Rf-BINAP ligands do not have these oxygen atoms. It was shown in Chapter Two that, despite the electron-withdrawing effect of the ponytails observed by investigation of the coordination chemistry of Rf-BINAP ligands, the light fluorous Rf-BINAPs performed similarly to non-fluorous BINAPs in catalysis in the reaction studied. Therefore, as the effect of the ponytails on the electronic environment around the phosphorus atom is less in the case of MonoPhos than for BINAP, as shown by the data obtained from the platinum complexes above, this suggests that Rf-MonoPhos will also perform similarly to non-fluorous MonoPhos in catalysis.

### 3.2.4 Complexes of Palladium(II)

As stated in Section 2.2.5, palladium(II) complexes of the form  $[\text{PdCl}_2(\text{L})_2]$  can be easily prepared. For MonoPhos ligands, the complexes can be synthesised by stirring  $[\text{PdCl}_2(\text{MeCN})_2]$  and MonoPhos in a 1:2 ratio in dichloromethane at room temperature for one hour. (Figure 3.15).

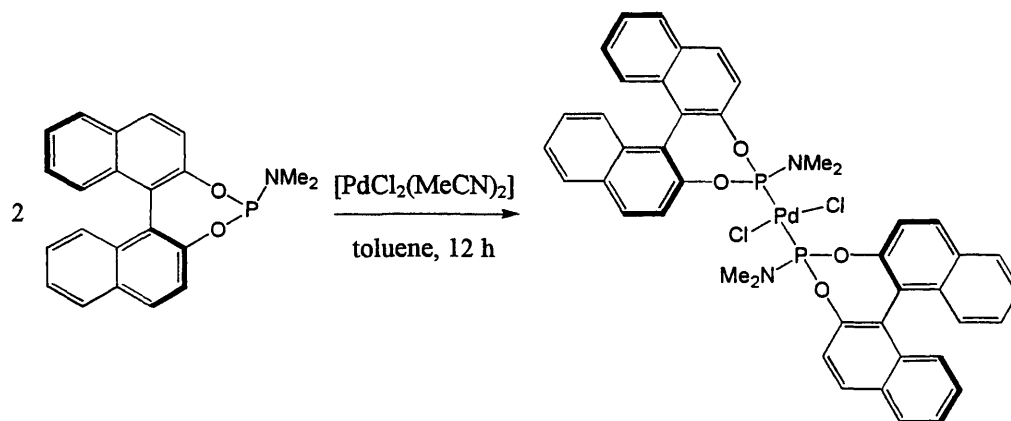


Figure 3.15. The synthesis of  $[\text{PdCl}_2(\text{MonoPhos})_2]$  complexes

Again, a range of MonoPhos complexes were prepared and analysed. The complex has been assigned a *trans* orientation in Figure 3.15 on the basis of comparison of IR data obtained for the complexes and *trans*- $[\text{PdCl}_2(\text{MeCN})_2]$  and  $^1\text{H}$  NMR spectroscopic analysis; upon coordination, the sharp doublet indicative of the two methyl groups attached to the MonoPhos ligand changes to a broad virtual triplet, indicating *trans*  $^3J_{\text{P-H}}$  and  $^5J_{\text{P-H}}$  coupling. The  $^{31}\text{P}$   $\{^1\text{H}\}$  NMR spectra again showed differences when fluoros ponytails were present. These data are outlined in Table 3.3.

Ligand	$^{31}\text{P}$ $\{^1\text{H}\}$ NMR data (ligand) (ppm) <sup>a</sup>	$^{31}\text{P}$ NMR data (complex) (ppm) <sup>a</sup>
( <i>R</i> )-MonoPhos (XIII)	s, 148.7	s, 118.5
( <i>S</i> )-MonoPhos (XIII)	s, 148.7	s, 118.5
( <i>R</i> )-Rf-MonoPhos (XIV)	s, 150.0	s, 119.9
( <i>S</i> )-Rf-MonoPhos (XIV)	s, 150.0	s, 119.9

<sup>a</sup>NMR spectroscopy data from complexes dissolved in  $\text{CDCl}_3$

Table 3.3.  $^{31}\text{P}$   $\{^1\text{H}\}$  NMR spectroscopic data for  $[\text{PdCl}_2(\text{MonoPhos})_2]$  complexes

The data show that, upon coordination, significant back-bonding occurs between the ligand and metal. The phosphorus chemical shift moves up-field, showing that the phosphorus atom is become more electron rich and so more shielded. For complexes of palladium, however, the effect of the fluoros ponytail is much less visible than for complexes of platinum, with the peak in the  $^{31}\text{P}$  NMR spectra corresponding to the complex being only slightly further down-field than the non-

fluorinated analogues. Once more, this data suggests that the influence of the fluororous ponytails on the phosphorus centre is negligible.

### 3.2.5 Complexes of Rhodium(III)

Rhodium complexes of the form  $[\text{RhCp}^*\text{Cl}_2(\text{MonoPhos})]$  are easily prepared by reaction of a MonoPhos ligand with the chloro-bridged dimeric rhodium starting material  $[\text{RhCl}(\mu\text{-Cl})(\eta^5\text{-C}_5\text{Me}_5)]_2$ .<sup>25</sup> Characterisation of the complexes is aided by coupling between the phosphorus atom of the ligands and the rhodium metal centre which is 100 % natural abundance spin  $\frac{1}{2}$ .

Formation of the complexes can be achieved by stirring the MonoPhos ligand and dimeric rhodium starting material in a 2:1 ratio in dichloromethane for one hour. The two equivalents of MonoPhos coordinate to the two monomeric rhodium species formed in solution (Figure 3.16).

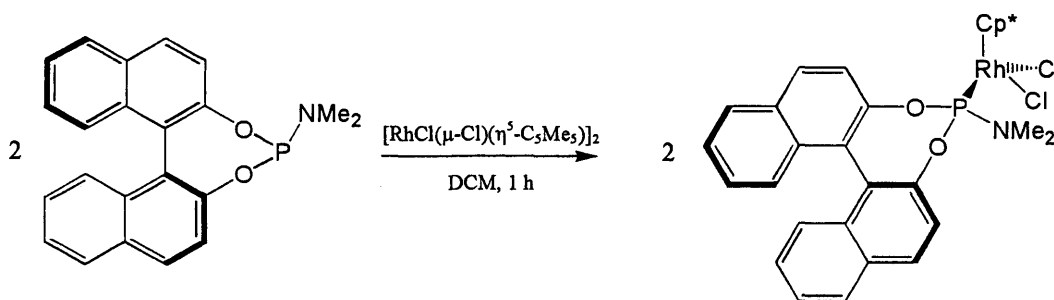


Figure 3.16. The synthesis of  $[\text{RhCp}^*\text{Cl}_2(\text{MonoPhos})]$  complexes

Once again, this procedure was carried out for the four MonoPhos moieties, and the complexes analysed by NMR spectroscopy, mass spectrometry, elemental analysis, optical rotation and melting point. Crystals of  $[\text{RhCp}^*\text{Cl}_2((S)\text{-MonoPhos})]$  suitable for X-ray analysis were obtained after slow evaporation of hexane/dichloromethane solvents. The crystal structure is outlined below (Figure 3.17) and data for the crystal is given in the appendix.

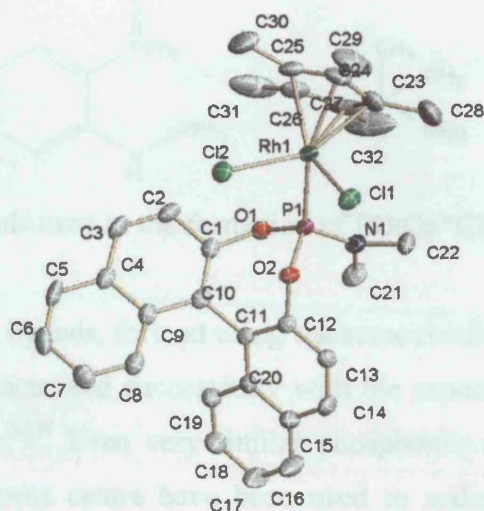


Figure 3.17. Crystal structure of  $[\text{RhCp}^*\text{Cl}_2((S)\text{-MonoPhos})]$

The structure shows the non-planar arrangement of the binaphthyl rings, the tetrahedral geometry of the phosphorus centre and the piano stool-shaped geometry adopted by the rhodium metal centre.

The aromatic region of the complexes in the  $^1\text{H}$  NMR spectra obtained at room temperature was interesting. Broad peaks corresponding to only eleven of the twelve aromatic protons could be observed in the case of non-fluorous MonoPhos, with a very broad ridge corresponding to the twelfth proton appearing in the middle of the other peaks. This pattern was similar for the fluorous MonoPhos derivative where peaks corresponding to only nine of the ten protons were clearly visible. The  $^{31}\text{P}$  NMR spectra were also unusual. Running the analysis using the standard 256 scans produced spectra with no peaks. Using concentrated solutions of the complexes still did not yield peaks in their phosphorus NMR spectra and only when 1500-scan analyses were carried out with these concentrated solutions did peaks appear. The peaks were very broad in all cases and consisted of a singlet in the region of the free ligand and a doublet slightly down-field. Due to the large number of scans which were required and the peaks which were obtained, it was suggested that the MonoPhos ligand was fluxional and did not remain coordinated through phosphorus at room temperature. Changing the NMR solvent did not change the outcome of the experiments and, to our knowledge, analysis of similar rhodium systems has not been carried out in the literature. The rhodium starting material has previously been used extensively for probing the electronic environment around phosphorus in monodentate ligands by our group and others at room temperature without such problems arising.<sup>26,27</sup>

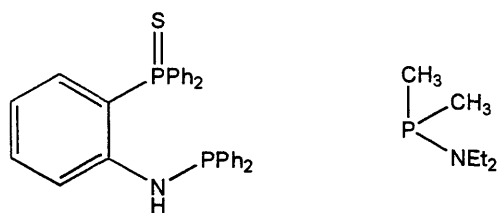


Figure 3.17. P-N ligands used in the formation of  $[\text{RhCp}^*\text{Cl}_2(\text{L})]$  complexes<sup>28,29</sup>

Additionally, rhodium-P-N type ligands, formed using the same rhodium starting material as above, have been synthesised and characterised successfully with the expected doublets appearing in the  $^{31}\text{P}$  NMR spectra (Figure 3.17).<sup>28,29</sup> Even very similar phosphonite and phosphite ligands with a nitrogen atom close to phosphorus centre have been used to make similar rhodium complexes without difficulty (Figure 3.18).<sup>30</sup>

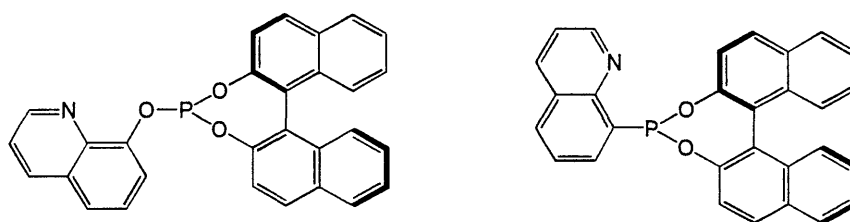


Figure 3.18. Phosphonite and phosphite ligands used to form of  $[\text{RhCp}^*\text{Cl}_2(\text{L})]$  complexes.<sup>30</sup>

As the complexes prepared here provide satisfactory elemental analysis data and, in the case of non-fluorous MonoPhos, a crystal structure has been obtained, it was possible to conclude that the complexes could be formed and were stable in the solid state. It was finally possible to obtain the expected doublet in the  $^{31}\text{P}$  NMR spectrum by running the analysis at  $-20\text{ }^\circ\text{C}$ . At this reduced temperature, a doublet corresponding to the phosphorus centre coupling to the rhodium metal centre was visible, and the proton spectra for both MonoPhos and Rf-MonoPhos contained the requisite number of peaks for the compounds. The requirement for low-temperature analysis is consistent with observations made within the group when an alternative rhodium-based starting material was used.<sup>31</sup> The  $^{31}\text{P}$  data for the complexes is outlined in Table 3.4.

Ligand	$^{31}\text{P}$ { $^1\text{H}$ } NMR data (ligand) (ppm) <sup>a</sup>	$^{31}\text{P}$ NMR data (complex) (ppm) <sup>a</sup>	$^1J_{\text{Rh-P}}$ (Hz)
( <i>R</i> )-MonoPhos (XIII)	s, 148.7	d, 141.7	223
( <i>S</i> )-MonoPhos (XIII)	s, 148.7	d, 141.7	223
( <i>R</i> )-Rf-MonoPhos (XIV)	s, 149.9	d, 143.4	225
( <i>S</i> )-Rf-MonoPhos (XIV)	s, 149.9	d, 143.4	225

<sup>a</sup>NMR spectroscopic data from complexes dissolved in CDCl<sub>3</sub> at -20 °C

Table 3.4. NMR spectroscopic data for selected MonoPhos ligands and Rh complexes

As was observed for the coordination complexes with other metal centres, the Rf-MonoPhos ligands are slightly more down-field than the non-fluorous MonoPhos ligands, as expected due to the electron-withdrawing effect of the perfluoroalkyl ponytails. However, the shift is very small and could be quoted as the same within experimental error. The same can be said of the coupling constants, where the values are almost identical. These data agree with the data for the platinum and palladium complexes, which all suggest that the effect of the fluoruous ponytails on the electronic environment around phosphorus is negligible.

### 3.3 Catalytic Testing

#### 3.3.1 Hydrogenation Reactions

Although there has been some study on systems which use MonoPhos ligands in other catalytic systems,<sup>32,33</sup> the majority of study has been carried out on the use of the ligand in asymmetric hydrogenation reactions.<sup>12,14,15,16</sup> However, little study of the ability to re-isolate and reuse the ligand after catalysis has been carried out. It was, therefore, decided that asymmetric hydrogenations would also be studied here using Rf-MonoPhos ligands with a view to recycling and reuse.

Itaconic acid and its dimethyl ester have been used extensively as a test substrates for asymmetric hydrogenation reactions.<sup>1,2</sup> So that comparison to other uses of the MonoPhos ligand would be possible, it was decided that testing would be carried out using dimethyl itaconate (Figure 3.20).

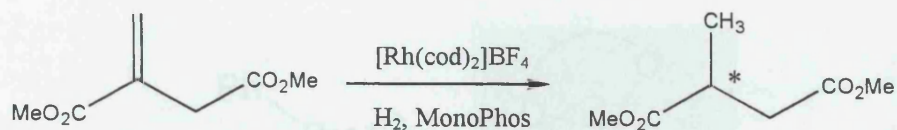


Figure 3.20. Asymmetric hydrogenation of dimethyl itaconate using MonoPhos

This substrate had been used in the only published example of a re-isolable example of a MonoPhos-type ligand, allowing a direct comparison of results.<sup>22</sup> As mentioned previously, bonding of the ligand to a polymer support and addition of a rhodium catalyst precursor lead to the formation of a catalyst which had the same activity but reduced selectivity compared to those for the analogous non-polymer-bound catalyst. It was hoped that, by using a homogeneous system, the selectivity of the subsequent catalyst could be improved and still be isolated and reused after reaction.

### 3.3.2 Chiral Induction

The abilities of MonoPhos as an asymmetric ligand in catalysis are clear, but the method in which the MonoPhos imparts its stereochemical information is not fully understood. Orpen, Pringle *et al.*<sup>34</sup> have used crystal structure analysis to determine the solid-state conformation of phosphonite-platinum complexes (Figure 3.21) and used this information to suggest the mechanism of chiral induction.

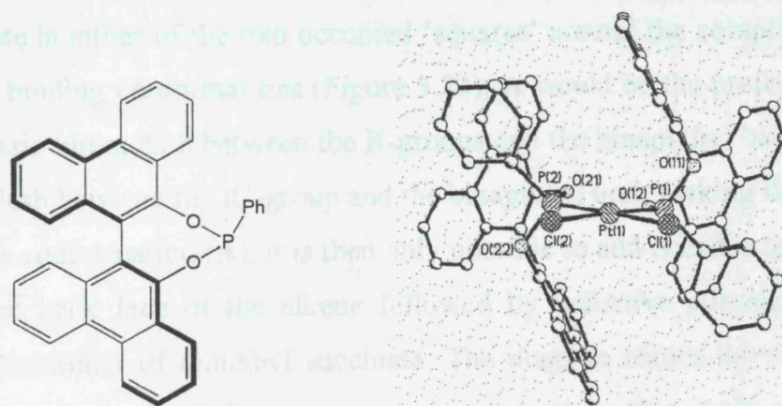


Figure 3.21. 9,9'-Biphenanthryl-phenyl-phosphonite and the crystal structure of the platinum complex  $[\text{PtCl}_2(\text{L})_2]$

As shown in the crystal structure, the sterically demanding monophosphonites adopt a *cis*-conformation around the metal centre that is extremely stable. In the conformation shown (Fig. 3.21), rotation around the P-O bonds and P-Ph bond is restricted, and the biaryl fragments adopt an edge-on arrangement while the Ph groups adopt a face-on arrangement. This coordination leaves two diagonally opposing squares occupied in a virtual coordination system (Figure 3.22).

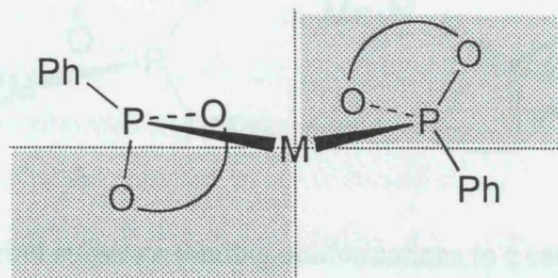


Figure 3.22. Stereoselective occupation of squares by two monophosphorus ligands around a metal centre

Investigations using chelating diphosphorus ligands have shown that such an edge/face arrangement can lead to diastereo-differentiating coordination of a prochiral substrate, through the minimisation of repulsive interactions.<sup>35,36</sup>

It is highly likely that MonoPhos coordinates in a similar manner to the phosphonites studied, with the phenyl groups substituted for  $\text{NMe}_2$  groups and binaphthyl units in place of the biphenanthryl backbones. The observation that there was restricted rotation around the P-Ph bond in the phosphonite system is also seen in MonoPhos metal complexes, where the methyl groups attached to the nitrogen are inequivalent in the  $^1\text{H}$  NMR spectra of the complexes due to restricted bond rotation.

The prochiral substrate can, in theory, bind to a catalytically active metal centre in four different ways but, with the addition of the two bulky chiral MonoPhos ligands, binding with the bulk of the substrate in either of the two occupied 'squares' around the complex is disfavoured. Of the two remaining binding conformations (Figure 3.23), **A** would be the preferred structure, with a minimisation of steric interaction between the R-groups and the binaphthyl backbone. In **B**, there is significant steric clash between the R'-group and the binaphthyl unit, making this conformation also disfavoured. In this conformation (**A**), it is then only possible to add coordinated hydrogen from the metal centre to the back face of the alkene followed by reductive elimination of the product, creating the (*S*)-enantiomer of dimethyl succinate. The diagram shows the use of (*S*)-MonoPhos and, experimentally, the use of this enantiomer does lead to the production of (*S*)-dimethyl succinate, supporting this binding model.

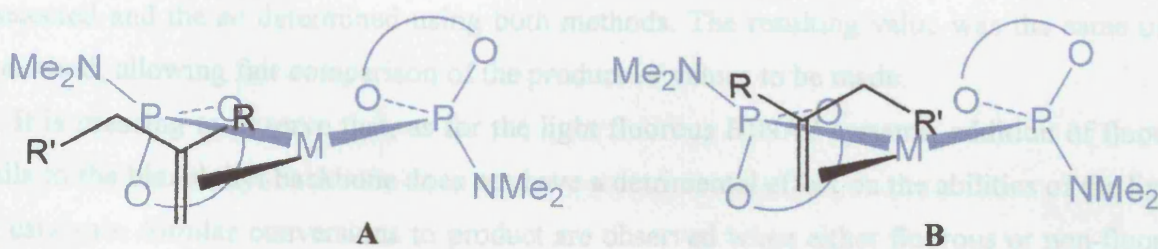


Figure 3.23. Prochiral substrate binding conformations to a catalyst complex.

### 3.3.3 Catalytic Asymmetric Hydrogenation - Results

The general hydrogenation procedure was taken from the previous work<sup>22</sup> and used with the MonoPhos and Rf-MonoPhos ligands synthesised here (Figure 3.24). Compared to BINAP systems, a relatively small substrate:catalyst ratio of 1:0.05 was used, indicating that the catalyst is less active than Ru-BINAP hydrogenation catalysts. It was not necessary to pre-form the catalyst species and it was generated *in situ* during the catalytic reaction.

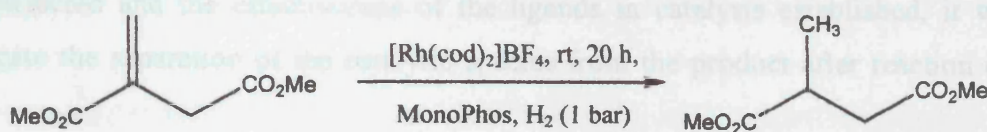


Figure 3.24. Asymmetric hydrogenation of dimethyl itaconate

Percentage product conversions were determined by <sup>1</sup>H NMR spectroscopy and product *ee*'s were determined by Chiral HPLC and GC, using pure dimethyl (*R*)-methylsuccinate as a standard which was obtained commercially.

The hydrogenation reactions were carried out three times for each ligand, and the results of these reactions are detailed in Table 3.5.

Ligand <sup>a</sup>	Conversion (%) <sup>b</sup>	Run 1 <i>ee</i> (%)	Run 2 <i>ee</i> (%)	Run 3 <i>ee</i> (%)	Average <i>ee</i> (%)
( <i>R</i> )-MonoPhos	95	78 <sup>c</sup>	90 <sup>c</sup>	98 <sup>c</sup>	89
( <i>S</i> )-MonoPhos	95	95 <sup>d</sup>	95 <sup>d</sup>	95 <sup>d</sup>	95
( <i>R</i> )-Rf-MonoPhos	90	90 <sup>c</sup>	85 <sup>c</sup>	75 <sup>c</sup>	83
( <i>S</i> )-Rf-MonoPhos	85	85 <sup>d</sup>	95 <sup>d</sup>	90 <sup>d</sup>	90

<sup>a</sup> [Rh(cod)<sub>2</sub>]<sub>2</sub>BF<sub>4</sub> catalyst precursor used in all cases <sup>b</sup> Average by <sup>1</sup>H NMR spectroscopy <sup>c</sup> By chiral GC <sup>d</sup> By chiral HPLC

Table 3.5. Asymmetric hydrogenation results

Due to problems with equipment, it was not possible to determine product *ee*'s using only chiral HPLC. However, to confirm that data obtained by chiral GC was comparable, two samples

were selected and the *ee* determined using both methods. The resulting value was the same using either method, allowing fair comparison of the product *ee* values to be made.

It is pleasing to observe that, as for the light fluoruous BINAP systems, addition of fluoruous ponytails to the binaphthyl backbone does not have a detrimental effect on the abilities of the ligand during catalysis. Similar conversions to product are observed when either fluoruous or non-fluoruous MonoPhos is used and the product *ee* is also comparable in all cases. This is, once again, a very important observation, as the implication of this result is that the ligand could be used successfully in a wide range of asymmetric reactions without a dramatic effect on product conversions or enantiomeric excesses. The results are also much better than those obtained in the previous system, which aimed to allow recovery and reuse of the MonoPhos ligand using a polymer support,<sup>22</sup> where conversions to product of 100 % were achieved, but the product *ee* was only 67 %.

### 3.3.4 Catalyst Separation Using Solid Phase Extraction

Once the synthetic strategy for the synthesis of light fluoruous analogues of MonoPhos had been perfected and the effectiveness of the ligands in catalysis established, it was necessary to investigate the separation of the catalytic species from the product after reaction using FRP silica gel.

The asymmetric hydrogenation reactions had been carried out in ethyl acetate and, although sufficiently soluble in the solvent, both the fluoruous and non-fluoruous catalytic species were not highly soluble. It was decided that, for this system, the reaction solvent would be an adequate elutant for the product while the catalysts, in their resting states, would be retained on the solid supports.

A catalytic asymmetric hydrogenation of dimethyl itaconate was carried out using a catalyst substituted with an (*R*)-MonoPhos ligand. After the reaction, the reaction mixture was concentrated *in vacuo* and, under a nitrogen atmosphere, placed *via* pipette onto the top of a short column of silica gel, which had been dried and degassed at 150 °C under high vacuum for two days. Using dry and degassed ethyl acetate to avoid degradation of the catalyst by the solvent, the product was eluted and shown to be free of catalyst contamination by <sup>1</sup>H and <sup>31</sup>P NMR spectroscopy, while a dark red-brown band remained on the top of the column.

Subsequently, recovery of the catalytic species was attempted. Dry and degassed dichloromethane was used as elutant, as it was known that the catalyst complex was highly soluble in this solvent, and a large volume passed down the column of silica gel. However, evaporation of the solvent yielded no material, with a red-brown band remaining at the top of the column. Dry and degassed methanol was also used as elutant, but no material, either ligand or catalyst, could be recovered from the column.

This loss of the transition-metal-containing species was assigned to irreversible binding to the hydroxyl units on the surface of the silica support. In this system, however, coordination of the MonoPhos ligands to the metal centre must have been retained after catalysis, making re-isolation of the ligand also impossible.

To recover the ligand, it was suggested that a weakly acidic solution could be used to destroy the coordination complex and free the ligand for elution with an organic solvent. However, when the column of silica was washed with 0.1 M hydrochloric acid and eluted with dichloromethane, the resulting solid obtained showed a large collection of peaks in the  $^{31}\text{P}$  NMR spectrum and, in the  $^1\text{H}$  NMR spectrum, a complex array of overlapping peaks in the aromatic region and a loss of the methyl group protons. This data suggested decomposition of the MonoPhos ligand, presumably by hydrolysis of the phosphorus-nitrogen bond. Washing this material with 0.1 M sodium hydroxide cleaved the phosphorus-oxygen bonds and yielded free binaphthol starting material in around 60 % recovery. Destruction of the chiral phosphorus-containing ligand was, clearly, not advantageous and so use of acid solutions to recover the ligand was abandoned.

Recovery of the non-fluorous catalyst was also attempted using FRP silica gel. As stated previously, FRP silica gel should be a more successful solid support for catalyst recovery, as the number of hydroxyl groups on the surface of the support has been reduced and replaced with non-reactive fluorine ponytails. A standard asymmetric catalytic hydrogenation reaction was carried out and the reaction mixture concentrated *in vacuo*. The mixture was then placed *via* pipette onto a 3 cm long column of FRP silica gel, which had been dried and degassed at 150 °C under high vacuum for 24 hours, in a glove box under nitrogen. Again, dry and degassed ethyl acetate was used to elute the product, which was shown by  $^1\text{H}$  and  $^{31}\text{P}$  NMR spectroscopic analysis to be free of ligand contamination, leaving a dark red-brown band on the top of the column. However, once again, elution with dry and degassed dichloromethane did not allow recovery of any material. This outcome was not good, as it suggested that the Rf-MonoPhos system may prove to be equally as unsuccessful.

As the non-fluorous system could not be recovered using silica gel, it was decided that it was not necessary to carry out a separation attempt using the light fluorine system on silica gel. Recovery of light fluorine MonoPhos-based catalysts was, however, attempted using FRP silica gel. A catalytic hydrogenation reaction of dimethyl itaconate was carried out using (*R*)-Rf-MonoPhos and the rhodium catalyst precursor and, after reaction, the mixture was concentrated *in vacuo*. In a dry box under a nitrogen atmosphere, the concentrated mix was then placed onto the top of a 3 cm long column of FRP silica gel which had been dried and degassed under high vacuum at 150 °C for 24 hours. Dry and degassed ethyl acetate was then passed down the column and the

product eluted. This was analysed by  $^1\text{H}$ ,  $^{19}\text{F}$  and  $^{31}\text{P}$  NMR spectroscopy and showed no sign of ligand/catalyst contamination.

A range of dry and degassed solvents was then tried in an attempt to elute the ligand/catalyst. However, as for the non-fluorous study, re-isolation of the ligand or catalyst was not possible. A red-brown band stayed on the top of the column after elution with dichloromethane, acetone, diethyl ether, methanol and acetonitrile, and removal *in vacuo* of the solvents collected after passage through the column yielded no isolated material. Once again, the inference from this result is that the catalyst resting state is not stable to isolation and recovery even on FRP silica gel, presumably due to irreversible binding of the rhodium metal to surface hydroxyl groups. In addition, unlike for Ru-BINAP systems, the ligand remains coordinated to the metal centre after catalysis, making recovery of the MonoPhos and Rf-MonoPhos ligands unattainable in this system.

### 3.4 Supported MonoPhos

As the work above had shown the Rh-MonoPhos catalyst could not be recovered by solid phase extraction, it was suggested that it might be possible to use FRP silica gel as a solid support in the catalytic asymmetric hydrogenation reaction. In this method, the rhodium catalyst precursor and light fluorine MonoPhos ligand would be mixed together in a suitable solvent in the presence of FRP silica gel and then the solvent removed *in vacuo*, forming an FRP silica gel-supported catalyst. This could then be used in a hydrogenation reaction and the catalyst recovered by simple filtration at the end of the reaction.

FRP silica gel was dried and degassed under high vacuum for 1 hour at 150 °C and then  $[\text{Rh}(\text{cod})_2]\text{BF}_4$  catalyst precursor and (*R*)-Rf-MonoPhos ligand added in a 1:2 ratio and the mixture stirred in dichloromethane. The solvent was removed and the resulting yellow solid used in the asymmetric hydrogenation of dimethyl itaconate. At the end of the reaction, the reaction mixture was concentrated *in vacuo*, filtered under nitrogen and the solid dried and reused in further catalysis. The results for this methodology are given in Table 3.6.

Run <sup>a</sup>	Conversion (%) <sup>b</sup>	ee (%)
1	5	n.d. <sup>c</sup>
2 <sup>d</sup>	0	/

<sup>a</sup>  $[\text{Rh}(\text{cod})_2]\text{BF}_4$  catalyst precursor used in all cases <sup>b</sup> by  $^1\text{H}$  NMR spectroscopy <sup>c</sup> not determined

<sup>d</sup> Using solid recovered from previous run

Table 3.6. Data for the asymmetric hydrogenation of dimethyl itaconate using a supported catalyst

It is evident from the data that the Rh-MonoPhos catalyst used here cannot be employed in this methodology. It is likely that the catalyst is deactivated by the solid support and, therefore,

leads to little conversion in the first run and no conversion after re-isolation. Due to such low yields, it was decided that determination of the product *ee* and rhodium leaching levels were unnecessary.

### 3.5 Light Fluorous MonoPhos - Conclusions

The recovery and reuse of Rh-MonoPhos-based hydrogenation catalysts initially seemed to be a much more attainable goal than Rh-BINAP-based catalysts, as the ligand was much less sensitive to oxidation than BINAP and additionally, analysis of the catalyst precursor and resting state by NMR spectroscopic studies showed the complex did not exist in an equilibrium, suggesting the rhodium metal would stay coordinated to the ligands throughout catalysis. If this were true then the metal centre would be better 'protected' by the ligands from deactivation on silica gel. The modifying fluorinated ponytails should retain the resting-state catalyst on the solid support during product elution and then allow re-isolation of an active catalyst after elution with a fluorophilic solvent.

However, this initial hypothesis was proven not to be true. Once more, a catalytic asymmetric hydrogenation could be carried out and the product isolated free of ligand/catalyst contamination by solid phase extraction. However, both non-fluorous and fluorinated catalyst could not be recovered and were retained on the silica gel. In this system, due to retained coordination, the MonoPhos ligands also could not be recovered and reused.

Even though the outcome of this investigation is not as positive as it was hoped, the study has, once again, been very informative. Firstly, it has proved that the synthesis of fluorinated analogues of MonoPhos is possible, and subsequent coordination chemistry has shown that the electronic environment around phosphorus and coordinating ability of the fluorinated and non-fluorous analogues are comparatively identical. The study has also shown that fluorinated analogues of MonoPhos are active and efficient in asymmetric hydrogenation reactions, giving similar product conversions and *ee*'s to their non-fluorous counterparts. Finally, the study has shown that the ligands stay coordinated to the metal centre in the catalyst precursor and resting state. This is important, as, for successful catalyst recovery, this must be the case. If the ligand dissociates then the catalyst metal centre will either be deactivated on the solid support or washed off the column with the product. The implication of this inference is that, for more stable catalyst resting states, it would be possible to isolate and reuse Rh-MonoPhos-based catalysts using FRP silica gel, while non-fluorous catalysts may not be selectively retained on silica gel and would be eluted with the product.

Finally, due to sensitivity towards FRP silica gel, supported catalysis based on this Rh-MonoPhos system cannot be used to produce high product conversions or *ee*'s, or allow re-isolation of an active catalyst species after a catalytic run.

### 3.6 Heavy Fluorous MonoPhos

#### 3.6.1 Ligand Synthesis

Whilst the investigation of light fluorous analogues of MonoPhos was underway, it was also surmised that it might be possible to synthesise a 'heavy fluorous' analogue of the ligand suitable for fluorous biphasic catalysis. The accepted figure for preferential perfluorocarbon solubility of a molecule is greater than 60 % by weight fluorine content.<sup>37</sup> It was, theoretically, possible to achieve this by derivatising the MonoPhos ligand with 4 perfluoroalkyl chains (Figure 3.25). This R<sub>f</sub>-MonoPhos ligand would contain 61 % by weight fluorine, which might make subsequent catalysts formed using the ligand preferentially fluorous soluble.

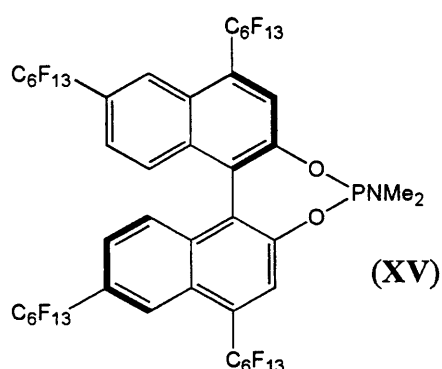
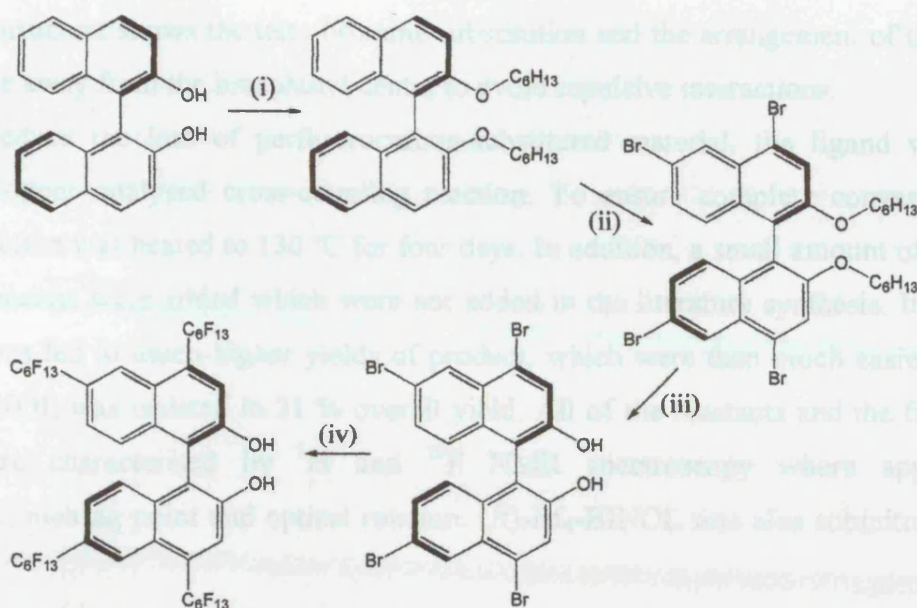


Figure 3.25. Heavy fluorous (*R*)-MonoPhos

To achieve the synthesis of this ligand, a 4,4'-6,6'-tetra(perfluoro-*n*-hexyl)-1,1'-bi-2-naphthol (R<sub>f</sub>-BINOL) starting material would be required, which could then be converted to the MonoPhos ligand by reaction with HMPT in the same way as for R<sub>f</sub>-MonoPhos. The synthesis of a similar tetra-substituted binaphthol with -C<sub>8</sub>F<sub>17</sub> ponytails had already been reported in the literature,<sup>38</sup> and so this experimental procedure was taken and adapted for this system. A full synthetic route is given in Figure 3.26.



- (i) 1-bromohexane,  $K_2CO_3$ , acetone, reflux, 72 h; (ii)  $Br_2$ ,  $MeCO_2H$ , rt, 12 h; (iii)  $BBr_3$ , DCM,  $-78^\circ C$ , rt;  
 (iv)  $C_6F_{13}I$ , DMSO,  $C_6H_5F$ , 2,2'-bipy, Cu powder,  $130^\circ C$ , 96 h.

Figure 3.26. The synthetic route to (*R*)- $Rf_4$ -binaphthol (adapted from reference 38)

It was first necessary to protect the hydroxyl groups with hexyl chains to allow successful substitution for bromine on the binaphthyl backbone. Without the addition of the hexyl chains it was not possible to achieve tetra-substitution, and a complex mixture of isomeric products was collected. Crystals suitable for X-ray analysis were obtained by slow evaporation of a solution of (*R*)-4,4'-6,6'-tetrabromo-2,2'-dihexyloxy-1,1'-binaphthyl in a 1:10 dichloromethane:hexane solvent mix. The structure obtained is shown in Figure 3.27 and data for the complex is given in the appendix.

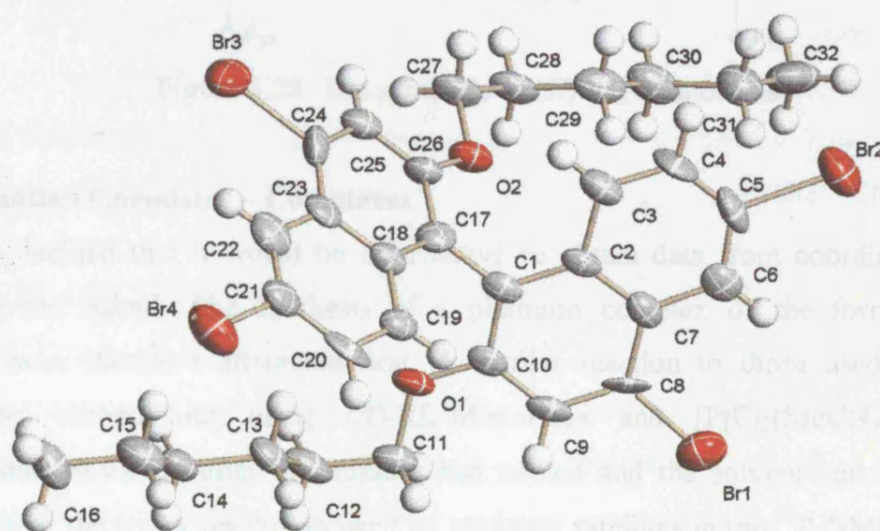


Figure 3.27. Structure of (*R*)-4,4'-6,6'-tetrabromo-2,2'-dihexyloxy-1,1'-binaphthyl showing 50 % displacement ellipsoids

The structure shows the tetra-bromine substitution and the arrangement of the hexyl chains, which radiate away from the binaphthyl centre to avoid repulsive interactions.

To reduce the loss of perfluorocarbon-substituted material, the ligand was deprotected before the copper-catalysed cross-coupling reaction. To ensure complete conversion, the cross-coupling reaction was heated to 130 °C for four days. In addition, a small amount of 2,2'-bipyridine and fluorobenzene were added which were not added in the literature synthesis. It was found that these additions led to much higher yields of product, which were then much easier to purify. The final Rf<sub>4</sub>-BINOL was isolated in 21 % overall yield. All of the reactants and the final Rf<sub>4</sub>-BINOL product were characterised by <sup>1</sup>H and <sup>19</sup>F NMR spectroscopy where appropriate, mass spectrometry, melting point and optical rotation. (*R*)-Rf<sub>4</sub>-BINOL was also submitted for elemental analysis.

To complete the synthesis of (*R*)-Rf<sub>4</sub>-MonoPhos (XV), (*R*)-Rf<sub>4</sub>-BINOL was reacted with HMPT in dry diethyl ether (Figure 3.28), and the Rf<sub>4</sub>-MonoPhos ligand fully characterised.

Partition coefficient data for the Rf<sub>4</sub>-MonoPhos ligand in toluene and PP3 was obtained and the ligand found to be 97 % partitioned in the fluorous phase. This result implied the ligand and subsequent catalysts should be appropriate for use in fluorous biphasic catalysis.

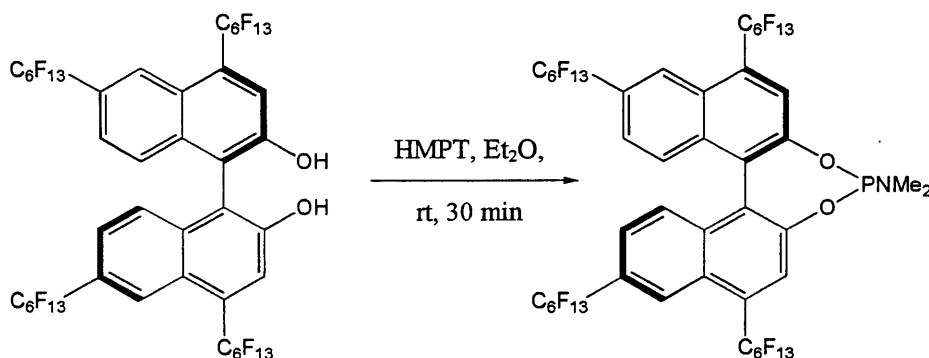


Figure 3.28. The synthesis of (*R*)-Rf<sub>4</sub>-MonoPhos

### 3.6.2 Coordination Chemistry – Complexes

It was decided that it would be informative to obtain data from coordination complexes formed using the ligand. The synthesis of a platinum complex of the form [PtCl<sub>2</sub>((*R*)-Rf<sub>4</sub>-MonoPhos)<sub>2</sub>] was, therefore attempted first. A similar reaction to those used in the previous syntheses was carried out using (*R*)-Rf<sub>4</sub>-MonoPhos and [PtCl<sub>2</sub>(MeCN)<sub>2</sub>] in refluxing dichloromethane. However, after the mixture had cooled and the solvent had been removed *in vacuo*, analysis of the sticky residue showed no platinum satellites in the <sup>31</sup>P NMR spectrum and a peak shifted up-field in comparison to (*R*)-Rf<sub>4</sub>-MonoPhos. It was assumed that the ligand was temperature-sensitive and had degraded during the synthesis. To test this hypothesis, (*R*)-Rf<sub>4</sub>-

MonoPhos was heated in refluxing dichloromethane and then recovered by removal of the solvent. The resulting  $^{31}\text{P}$  NMR spectrum showed the same peak as observed in the previous experiment, at around 14 ppm, indicating the ligand was very temperature-sensitive.

This result was quite limiting, as fluorous biphasic catalysis uses the temperature-dependent miscibilities of solvents to increase the rate of reaction whilst still allowing ligand/catalyst recovery. As the ligand degrades at only slightly elevated temperatures, catalysis would have to be carried out under biphasic conditions, which was likely to reduce the rate of reaction.

The coordination of the ligand to palladium and rhodium centres was far more successful as the reactions did not require heating. (*R*)-Rf<sub>4</sub>-MonoPhos could be reacted with *trans*-[PdCl<sub>2</sub>(MeCN)<sub>2</sub>] and [RhCl<sub>2</sub>Cp\*]<sub>2</sub> to form the corresponding coordination complexes as yellow and red solids respectively. The  $^{31}\text{P}$  NMR spectroscopic data for these complexes is given in Table 3.7.

Complex <sup>a</sup>	Free Ligand (ppm)	Coordinated Ligand (ppm)	Coupling Constant (Hz)
[Pd-( <i>R</i> )-MonoPhos]	s, 148.7	s, 118.5	/
[Pd-( <i>R</i> )-Rf-MonoPhos]	s, 150.0	s, 119.9	/
[Pd-( <i>R</i> )-Rf <sub>4</sub> -MonoPhos]	s, 152.8	s, 122.9	/
[Rh-( <i>R</i> )-MonoPhos]	s, 148.7	d, 141.7	223
[Rh-( <i>R</i> )-Rf-MonoPhos]	s, 150.0	d, 143.4	225
[Rh-( <i>R</i> )-Rf <sub>4</sub> -MonoPhos]	s, 152.8	d, 146.6	229

<sup>a</sup> Complexes either of the form [RhCp\*Cl<sub>2</sub>(MonoPhos)] or [PdCl<sub>2</sub>(MonoPhos)<sub>2</sub>]

Table 3.7.  $^{31}\text{P}$  NMR spectroscopic data for coordination complexes of MonoPhos ligands

The data shows the phosphorus centre of the Rf<sub>4</sub>-MonoPhos ligand is more electron deficient than the phosphorus centre of the Rf-MonoPhos ligand, which, in turn, is more electron deficient than the phosphorus centre of MonoPhos. However, the data indicates that the difference in the electronic environment around phosphorus for each of the ligands is not dramatic. This observation is encouraging as it suggests that the Rf<sub>4</sub>-MonoPhos ligand should behave similarly to the MonoPhos and Rf-MonoPhos ligands, which are both successful in the asymmetric hydrogenation reaction studied above.

### 3.6.3 Catalysis Using Rf<sub>4</sub>-MonoPhos

Due to the apparent sensitivity of the rhodium-based hydrogenation catalyst examined above using MonoPhos and Rf-MonoPhos, it was decided that this system would be an ideal test for a simple liquid-liquid extraction system using a fluorous solvent or fluorous biphasic system, where in both cases the catalyst could be handled exclusively under nitrogen in the absence of moisture.

To begin with, a standard catalytic reaction was attempted using the conditions set out above for the light fluorous approach to catalyst recovery. It was hoped that, post reaction, a small volume of PP3 could be added and the catalyst partitioned exclusively in the fluorous phase. The layers could then be separated, the PP3 removed *in vacuo* and the catalyst reused in further catalysis. However, upon addition of the ligand and catalyst precursor to dry and degassed ethyl acetate solvent, a thick oil was formed and the ethyl acetate turned only pale yellow even after prolonged stirring, indicating the oil was largely insoluble. Further, the oil did not become completely soluble upon the addition of the substrate and the ethyl acetate layer remained pale yellow. Clearly, catalysis would be unsuccessful using this system as the majority of the catalyst was not dissolved and so fluorous biphasic catalysis was attempted.

The same reaction conditions were used, with the addition of an equal volume of PP3 to the ethyl acetate organic solvent. The rhodium precursor and ligand were stirred in dry and degassed ethyl acetate for one hour and then the PP3 fluorous solvent added. After stirring for twenty minutes, the yellow colour in the organic solvent had disappeared and the layer was colourless, with the fluorous layer becoming coloured. This was a very good sign, suggesting that the catalyst precursor had partitioned itself in the fluorous phase.

This organic/fluorous mixture was transferred to a glove box under nitrogen and dimethyl itaconate added. The flask was then placed briefly under vacuum and refilled with one atmosphere of hydrogen. After 24 hours, the flask was transferred back to the glove box, the organic layer separated and the fluorous phase reused in three catalytic runs. The data is given in Table 3.8.

Run <sup>a</sup>	Conversion (%) <sup>b</sup>	ee (%) <sup>c</sup>	Rh leaching (ppm, % of total)
1	53	25	2.23 (0.6)
2 <sup>d</sup>	80	22	1.21 (0.3)
3 <sup>d</sup>	70	15	0.37 (0.09)
4 <sup>d</sup>	80	15	0.18 (0.04)

<sup>a</sup> [Rh(cod)<sub>2</sub>]BF<sub>4</sub> catalyst precursor used in all cases <sup>b</sup> by <sup>1</sup>H NMR spectroscopy <sup>c</sup> By chiral GC <sup>d</sup> Using PP3 layer from previous run

Table 3.8. Results for the asymmetric hydrogenation of dimethyl itaconate using Rf<sub>4</sub>-BINOL

It is clear from the data that anchoring the catalyst in the fluorous phase does have an effect on the product conversions, but it not as dramatic as was first envisaged. The slight fall in conversion in comparison to the homogeneous systems is most likely due to the low contact area between the two solvents and so lower interaction of the reactants and catalyst compared to a homogeneous system. Alternatively, the lower reactivity could be due to the bulky and highly electron withdrawing Rf<sub>4</sub>-MonoPhos ligand affecting the reactivity of the metal centre. The

rhodium leaching levels are excellent and only 1 % of the total rhodium added is lost to the product over the four runs. Additionally, no ligand is observed in the product by NMR spectroscopic analysis. Most seriously affected, however, is the enantioselectivity of the catalyst. The product is obtained in very low *ee* compared to the previous systems studied and begins to fall after the PP3 layer is reused in further catalysis.

There may be a number of reasons for this observation. To obtain good enantioselectivity, two monodentate ligands must be attached to the metal centre in a *cis* configuration as discussed above. A MonoPhos ligand substituted with four bulky fluoruous ponytails may well hinder the formation of such a structure or seriously affect the binding and subsequent reactivity of the substrate. It was also possible that ligand racemisation occurred, either during formation of the (*R*)-Rf<sub>4</sub>-MonoPhos itself or during reaction, although both suggestions seem unlikely. There is very little ligand racemisation observed during reaction in the systems using MonoPhos or Rf-MonoPhos. It was not possible to evaluate the enantiopurity of the (*R*)-Rf<sub>4</sub>-MonoPhos ligand itself, as there was no ligand on which an optical rotatory power comparison could be based, chiral GC was not possible due to ligand sensitivity and, to our knowledge, no HPLC column was available which could separate the enantiomers. However, it was assumed that similar optical rotation values would be observed for the enantiomerically pure parent tetra-substituted-C<sub>8</sub>F<sub>17</sub> BINOL (synthesised previously<sup>37</sup>) and the tetra-tridecafluorohexyl-substituted BINOL prepared here if the ligand was also enantiomerically pure. Optical rotation values in ethyl acetate were, therefore, obtained for (*R*)-Rf<sub>4</sub>-BINOL and the value compared to that for the previously prepared tetra-substituted-C<sub>8</sub>F<sub>17</sub> BINOL. The two figures proved to be almost identical, indicating that the (*R*)-Rf<sub>4</sub>-BINOL synthesised here was highly enantiomerically enriched. The fall in *ee* after four runs in this system was, therefore, most likely due to solvent effects. It is well-known that the solvent used in asymmetric reactions can have a dramatic effect on the enantiomeric excess of products.<sup>14</sup> Here, the system required the use of a highly non-polar fluoruous solvent to dissolve the ligand/catalyst, whereas it had been observed that polar solvents were needed to induce high enantioselectivity.<sup>14,15,16</sup> Because of this limitation, it seems unlikely that fluoruous biphasic catalysis will be of use in such reactions.

### 3.6.4 Heavy Fluoruous MonoPhos – Conclusions

An example of a highly fluorinated MonoPhos ligand with four perfluoroalkyl chains was successfully synthesised and characterised for the first time, and its coordination chemistry investigated. Catalysis in conventional solvents followed by liquid-liquid extraction to recover the catalyst was not possible due to the low solubility of the ligand and catalyst in organic solvents. The ligand was active in the hydrogenation of dimethyl itaconate under fluoruous biphasic catalysis

conditions and rhodium leaching levels were very low, but low product *ee*'s were observed. This is most likely due to changing from a polar solvent to a non-polar solvent and renders this system inappropriate for the catalysis studied. Further investigation into other systems which are active and selective in non-polar solvents would be worthwhile due to very low levels of ligand leaching from the fluorous phase into the organic phase, coupled with low leaching of rhodium catalyst metal into the organic phase.

### 3.6 References for Chapter Three

1. Büthe, H., Horner, L., Siegel, H., *Angew. Chem. Int. Ed. Engl.*, **7**, 1968, 942.
2. Knowles, W., Sabacky, M., *Chem. Commun.*, **1968**, 1445.
3. Knowles, W., Sabacky, M., Vineyard, B., *J. Chem. Soc., Chem. Commun.*, **1972**, 10.
4. Dang, T., Kagan, H., *J. Chem. Soc., Dalton Trans.*, **1971**, 481.
5. Knowles, W., Sabacky, M., Vineyard, B., Weinkauff, D., *J. Am. Chem. Soc.*, **97**, 1975, 2567
6. Fiaud, J.-C., Guillen, F., *Tetrahedron Lett.*, **40**, 1999, 2939.
7. Claver, C., Fernandez, E., Gillon, A., Heslop, K., Hyett, D., Martorell, A., Orpen, A., Pringle, P., *Chem. Commun.*, **2000**, 961.
8. Reetz, M., Sell, T., *Tetrahedron Lett.*, **41**, 2000, 6333.
9. Mehler, G., Reetz, M., *Angew. Chem. Int. Ed. Engl.*, **39**, 2000, 3889.
10. Feringa, B., *Acc. Chem. Res.*, **33**, 2000, 346.
11. Arnold, L., Feringa, B., Mandoli, A., Salvadori, P., de Vries, A., *Tetrahedron: Asymmetry*, **12**, 2001, 1929.
12. van den Berg, M., van Esch, J., Feringa, B., Minnaard, A., Schudde, E., de Vries, A., de Vries, J., *J. Am. Chem. Soc.*, **122**, 2000, 11539.
13. Chen, W., Xiao, J., *Tetrahedron Lett.*, **42**, 2001, 2897.
14. Jia, X., Guo, R., Li, X., Yao, X., Chan, A. S. C., *Tetrahedron Lett.*, **43**, 2002, 5541
15. Zeng, Q., Liu, H., Mi, A., Jiang, Y., Li, X., Choi, M. C. K., Chan, A. S. C., *Tetrahedron*, **58**, 2002, 8799.
16. Li, X., Jia, X., Lu, G., Au-Yeung, T.T.-L., Lam, K.-H., Lo, T. W. H., Chan, A. S. C., *Tetrahedron: Asymmetry*, **14**, 2003, 2687.
17. Duursma, A., Minnaard, A. J., Feringa, B. L., *Tetrahedron*, **58**, 2002, 5773.
18. Hu, A.-G., Fu, Y., Xie, J.-H., Zhou, H., Wang, L.-X., Zhou, Q.-L., *Angew. Chem. Int. Ed. Engl.*, **41**, 2002, 2348.
19. Jia, X., Li, X., Xu, L., Shi, Q., Yao, X., Chan, A. S. C., *J. Org. Chem.*, **68**, 2003, 4539.
20. Li, Z., Zhou, Z., Wang, L., Zhou, Q., Tang, C., *Tetrahedron: Asymmetry*, **13**, 2002, 145.
21. van den Berg, M., van Esch, J., Feringa, B., Minnaard, A., Schudde, E., de Vries, A., de Vries, J., *Chemistry Today - Chirals*, **2001**, 12.
22. Doherty, S., Robins, E. G., Pál, I., Newman, C. R., Hardacre, C., Rooney, D., D. Mooney, A., *Tetrahedron: Asymmetry*, **14**, 2003, 1517.
23. Feringa, B., Hulst, R., de Vries, N., *Tetrahedron: Asymmetry*, **5**, 1994, 699.
24. Gilheany, D., *Chem. Rev.*, **94**, 1994, 1339.

25. Kang, J., Maitus, P., Moseley, K., *J. Am. Chem. Soc.*, 91, **1969**, 5970.
26. Corcoran, C., Fawcett, J., Friedrichs, S., Holloway, J. H., Hope, E. G., Russell, D. R., Saunders, G. C., Stuart, A. M., *J. Chem. Soc., Dalton Trans.*, **2000**, 161
27. Atherton, M. J., Fawcett, J., Hill, A. P., Holloway, J. H., Hope, E. G., Russell, D. R., Saunders, G. C., Stead, R. M. J., *J. Chem. Soc., Dalton Trans.*, **1997**, 1137.
28. Werner, H., Klingert, B., Rheingold, A. L., *Organometallics*, 7, **1988**, 911.
29. Aucott, S. M., Slawin, A. M. Z., Wollins, J. D., *Polyhedron*, 22, **2003**, 361.
30. Drommi, D., Faraone, F., Franciò, G., *Organometallics*, 21, **2002**, 761.
31. Thesis of Thingy
32. Bartels, B., Helmchen, G., *Chem. Commun.*, **1999**, 741.
33. Feringa, B. L., Pineschi, M., Arnold, L. A., Imbos, R., de Vries, A. H. M., *Angew. Chem. Int. Ed. Engl.*, 36, **1997**, 2620.
34. Claver, C., Fernandez, E., Gillon, A., Heslpo, K., Hyett, D., Martorell, A., Orpen, G., Pringle, P., *Chem. Commun.*, **2000**, 961.
35. Vineyard, B., D., Knowles, W. S., Sabacky, M. J., Bachman, G. L., Weinkauff, D. L., *J. Am. Chem. Soc.*, 99, **1977**, 5946.
36. Brunner, H., Winter, A., Breu, J., *J. Organomet. Chem.*, 553, **1998**, 285.
37. Kiss, L. E., Kövesdi, I., Rábai, J., *J. Fluorine Chem.*, 108, **2001**, 95.
38. Tian, Y., Yang, Q. C., Mak, T. C. W., Chan, K. S., *Tetrahedron*, 58, **2002**, 3951.

## 4 Ti/BINOL Chemistry

### 4.1 Introduction

#### 4.1.1 Ti/BINOL Systems

Lewis acid catalysed reactions are numerous, extensive in their applications and diverse in their nature. However, commonly in asymmetric systems, 1,1'-bi-2-naphthol (BINOL, Figure 4.1) is used as an auxiliary ligand to introduce asymmetry in products.

# Chapter Four



There are a large number of examples of reactions where BINOL-based catalysts have been used in asymmetric synthesis. In 2001, the groups of N. M. Williams and M. J. Fréchet have independently investigated the asymmetric allylation of aldehydes using BINOL-coordinated Ti complexes (Figure 4.2).

- “New ideas pass through three periods:  
 - It can't be done  
 - It probably can be done but it's not worth doing  
 - I knew it was a good idea all along...”

- Arthur C Clarke

Figure 4.2. The addition of diethylzinc to vanillin aldehyde.

When benzaldehyde was used as substrate, yields higher than 85% could be achieved with product ee's of between 80 and 85% depending on the conditions used. It was found that an excess of both titanium tetrachloride and diethylzinc was required to produce good yields and enantioselectivities, although only 0.1 equivalents of BINOL ligand were required. A range of substituted aldehydes could be allylated using the same catalyst with good product yields and enantioselectivities obtained.

Koch and Fréchet have used a similar catalyst in the allylation of aldehydes bearing a variety of functional groups (Figure 4.3).

## 4 Ti/BINOL Chemistry

### 4.1 Introduction

#### 4.1.1 Ti/BINOL Systems

Lewis acid catalysed reactions are common, extensive in their applications and diverse in their nature.<sup>1</sup> However, commonly in asymmetric systems, 1,1'-bi-2-naphthol (BINOL, Figure 4.1) is used as an exceptional ligand to introduce asymmetry in products.

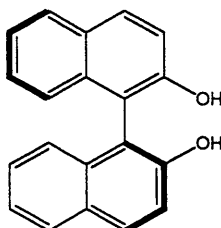


Figure 4.1 (*S*)-BINOL

There are a large number of examples in the literature where BINOL-based catalysts have been used in asymmetric synthesis.<sup>2,3,4</sup> Chan<sup>5</sup> and Nakai<sup>6</sup> have independently investigated the asymmetric alkylation of aldehydes catalyzed by Ti/BINOL complexes (Figure 4.2).

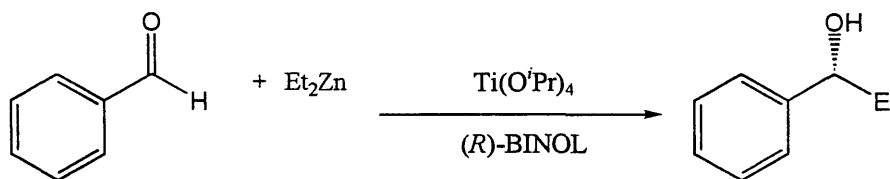


Figure 4.2. The addition of diethylzinc to benzaldehyde

When benzaldehyde was used as substrate, yields higher than 98 % could be achieved with product *ee*'s of between 80 and 85 % depending on the conditions used. It was found that an excess of both titanium tetraisopropoxide and diethylzinc was required to produce good yields and enantioselectivities, although only 0.1 equivalents of BINOL ligand were required. A range of substituted aldehydes could be alkylated using the same catalyst with good product yields and enantioselectivities obtained.

Keck and Geraci have used the same catalyst in the addition of allyltri-*n*-butyltin to a range of functionalised aldehydes (Figure 4.3).<sup>7</sup>

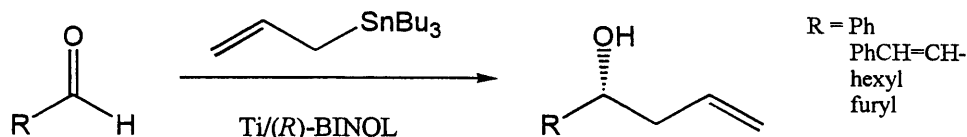


Figure 4.3. Addition of allyltri-*n*-butyltin to functionalised aldehydes

When R equalled phenyl, 98 % yield and 93 % product *ee* could be achieved. The other R groups showed a fall in yield and enantiomeric excess when used, but still gave product yields of between 60 and 85 % and product *ee*'s of between 70 and 93 %. Interestingly, in this example, the reactions were carried out both at room temperature and 0 °C, but the temperature difference did not dramatically affect the product *ee*.

Walsh *et al.* have used the same catalyst for the addition of allyltri-*n*-butyltin to a range of functionalised ketones with high success.<sup>8</sup> *Para*-methoxyphenylmethyl ketone could be allylated in 99 % yield with a product *ee* of 89 %, while 4-phenyl-but-3-ene-2-one could be converted to the corresponding alcohol product in 99 % yield and 90 % *ee*. Even 1-chloro-3-phenyl-but-3-one could be allylated successfully with no loss of the chlorine group with 99 % product yield and 76 % *ee*.

Both these examples show the applicability of the catalyst system for addition reactions for a range of substrates.

Ti/BINOL systems have also been used in aldol reactions.<sup>9,10</sup> Scettri and co-workers have used titanium tetraisopropoxide and BINOL as catalyst in the aldol condensation of silyloxydiene XVI with benzaldehyde (Figure 4.4).<sup>11</sup>

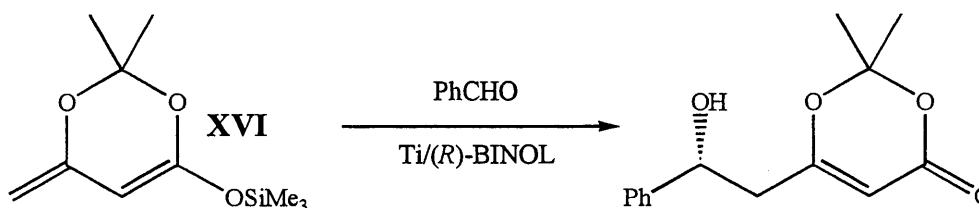


Figure 4.4. Aldol condensation using a masked acetoacetic ester

Interestingly for this system, pronounced positive non-linear effects were observed, where the use of enantiomerically enriched Ti/BINOL complexes led to products with high enantiopurity. BINOL with an *ee* of only 35 % could be used to yield a product with an *ee* of up to 72 %. Additionally, changing the method of catalyst preparation also dramatically affected the product enantiopurity. Using enantiopure Ti/(*R*)-BINOL and Ti/(*S*)-BINOL prepared separately and mixed in appropriate ratios, a catalyst with an (*R*)-BINOL *ee* of 35 % gave rise to product with an *ee* of 90 % in 64 % yield. The cause of these non-linear effects was not clear, although the authors noted that

dilute catalyst solutions must be used to ensure high enantiomeric excesses, otherwise poorly enantioselective titanium multiaggregates were formed.<sup>12,13</sup>

Asymmetric catalytic cyanosilylation has also been achieved using Ti/BINOL systems.<sup>14</sup> For a range of aliphatic aldehydes, a cyano group could be added in high yield and relatively high *ee* (Figure 4.5).

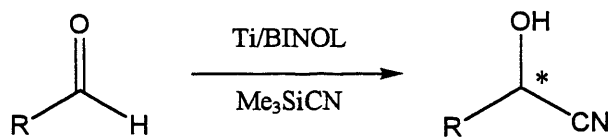


Figure 4.5. Cyanation of functionalised aldehydes.

Although the yields of products were greater than 90 % in all cases, bulky or long-chain aldehydes gave the best product *ee*'s, such as *tert*-butanal (75 %) and 1-nonanal (72 %). Smaller aldehydes gave much lower product *ee*'s, with propanal, benzaldehyde and 4-chlorobenzaldehyde all leading to products with less than 10 % enantiopurity.

Ding, Wang and Guo have recently used dimeric BINOL ligands and titanium tetraisopropoxide for carbonyl-ene reactions (Figure 4.6).<sup>15</sup>

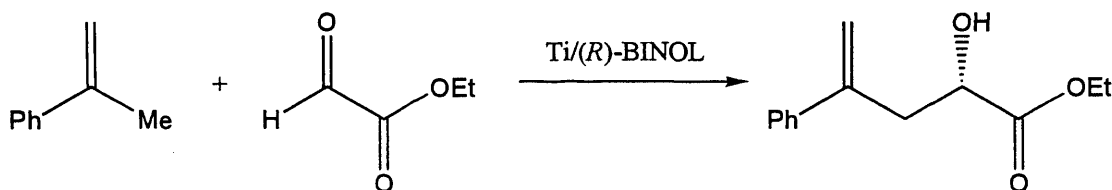


Figure 4.6. Asymmetric carbonyl-ene reaction using dimeric BINOL ligands

Three different linked BINOL ligands were prepared and used in the reaction with a very low catalyst loading of 1 mol %. These ligands are shown in Figure 4.7. Considering the similarity of the ligands, marked differences were observed in their catalyst-promoting abilities. Catalysts derived from **XVII** and **XIX** consistently gave high product yields and *ee*'s above 90 % under varying conditions. However, catalysts derived from **XVIII** gave much lower yields of, on average, only 20 % and very low product *ee*'s; 17 % on average. The authors suggest that the dramatic change in the abilities of the ligands to promote catalytic activity were due to the change of the linker and the subsequent change in supramolecular structure of the assemblies.

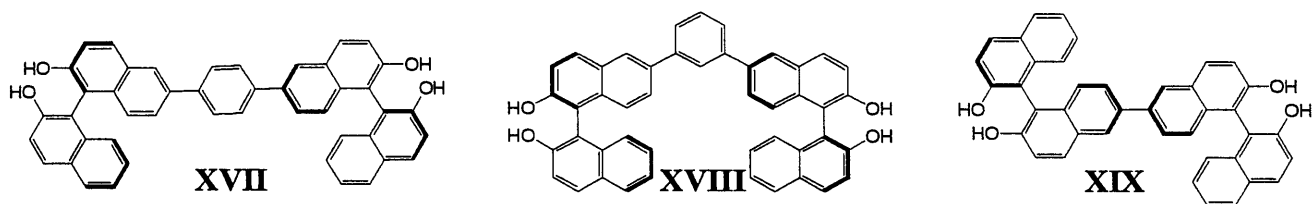


Figure 4.7. Dimeric BINOL ligands

These catalytic procedures show the Ti/BINOL system to be very effective, but the examples given above concentrate solely on the abilities of the catalytic system and not on the recovery and reuse of the ligand/catalyst. Due to the expensive nature of the resolved BINOL ligand recovery is desirable, and a range of methods to recover and reuse the ligand/catalyst have been investigated in the literature.

#### 4.1.2 The Mechanism of Chiral Induction

Although much study into the use of Ti/BINOL systems has been carried out, until recently the mechanism of reaction and chiral induction had not been studied in any detail. Mori and Nakai proposed an active catalyst structure in 1997<sup>6</sup> and a plausible catalytic cycle, but provided little experimental evidence to support their propositions. However, in 2001, Walsh *et al.*<sup>16</sup> carried out a detailed study of the system.

Study of the reaction mechanism is complicated by the fact that stoichiometric amounts of  $\text{Ti}(\text{iOPr})_4$  and BINOL, when used as catalyst, react differently to catalysts formed using catalytic amounts of BINOL compared to  $\text{Ti}(\text{iOPr})_4$ . From reports by Mori and Nakai,<sup>6</sup> Kagan<sup>17</sup> and Heppert<sup>18</sup>, a list of possible catalyst intermediates were assembled (Figure 4.8) and studied for their ability to catalyse the asymmetric addition of dialkylzinc reagents to aldehydes.

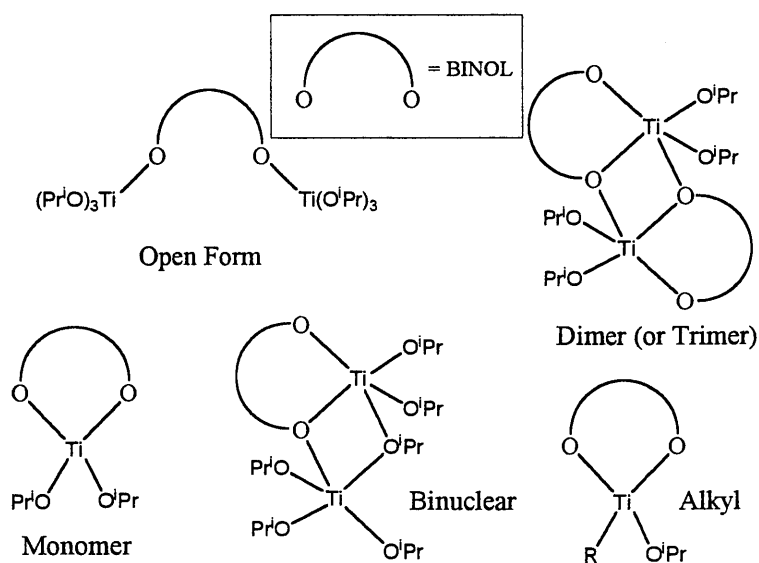


Figure 4.8. Possible Ti/BINOL catalyst intermediates

To discount the open form as a catalyst, the authors used monoalkylated BINOL as ligand, which was shown not to coordinate to titanium through the ether oxygen. Comparison of this ligand to BINOL in a standard diethylzinc addition to benzaldehyde showed that the ligand was much less active than BINOL, taking 24 hours to yield product conversions of only 75 % by comparison to BINOL, which gave 100 % conversion after just 4 hours. The monoalkylated BINOL also led to product with *ee*'s much less than the *ee*'s obtained using BINOL (20 % versus 89 %). The result showed the open form, (BINOLate)[Ti(<sup>i</sup>PrO)<sub>3</sub>]<sub>2</sub>, could not be the active catalyst.

To study the structure of the active species when catalytic amounts of BINOL were used, the ligand and Ti(<sup>i</sup>PrO)<sub>4</sub> were mixed in a 1:2 ratio and the dichloromethane solvent removed by slow evaporation to yield crystals suitable for X-ray diffraction. The structure is given in Figure 4.13 (G). In this structure, two titanium centres are present, one of which interacts with both of the oxygens of the BINOLate ligand significantly decreasing the torsional angle between the two naphthyl groups. Mixing BINOL and Ti(<sup>i</sup>PrO)<sub>4</sub> in a 1:6 ratio, as used in most experimental procedures, and slow evaporation of the solvent led to the formation of crystals which were also solved by X-ray analysis (Figure 4.9, (H)).

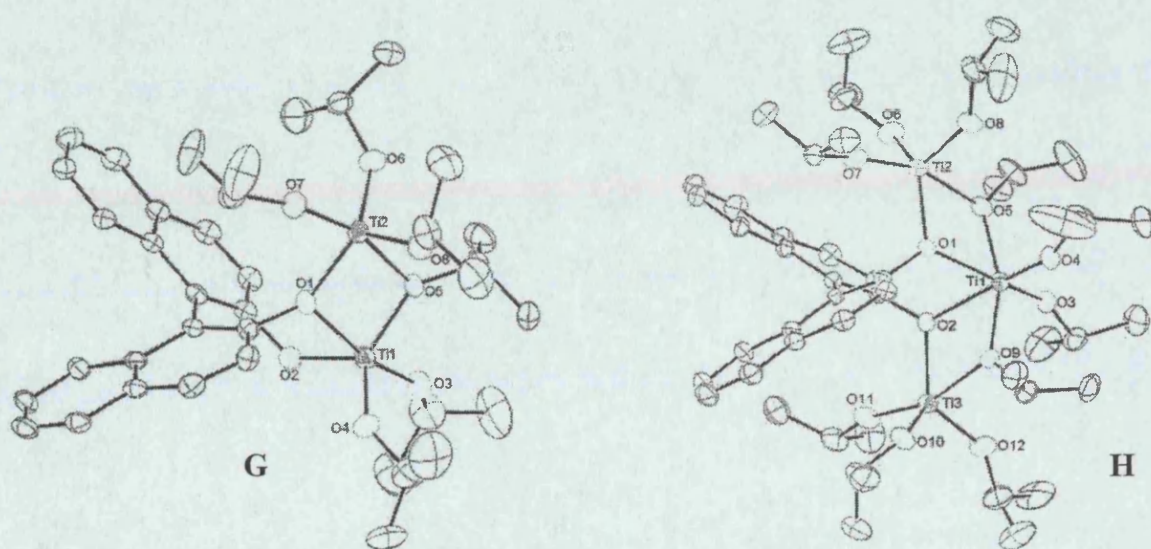


Figure 4.9. Crystal structures of catalytic Ti/BINOL complexes

H consists of a trinuclear arrangement of titanium centres bonded to a single BINOLate ligand. This is the structure that would be expected if G were to bind to another Ti(<sup>i</sup>PrO)<sub>4</sub> molecule. This species was unlikely to be an active catalyst, as the central titanium atom which would pass on the chiral information from the BINOL ligand was pseudo-octahedral and, therefore, unlikely to bind the aldehyde substrate. Indeed, it was shown by NMR studies that, in solution, the complex broke down to form species G. These structures indicate that the monomer (BINOLate)Ti(<sup>i</sup>PrO)<sub>2</sub> is sufficiently Lewis acidic that it does not remain in this form in the presence of other titanium

alkoxides. In addition, formation of the complexes shows the monomer preferentially coordinates  $\text{Ti}(\text{iPrO})_4$ , rather than a second molecule of monomer.

Use of complex **G** in a catalytic reaction led to product in the same yield and with the same *ee* to that formed using BINOL and  $\text{Ti}(\text{iPrO})_4$  (99 % conversion after 4 hours, 89 % *ee*), indicating that, in the catalytic BINOL-content reactions, species **G** is an active species.

When a stoichiometric addition of BINOL and  $\text{Ti}(\text{iPrO})_4$  was carried out, crystals suitable for X-ray diffraction were obtained and the structure is shown in Figure 4.10.

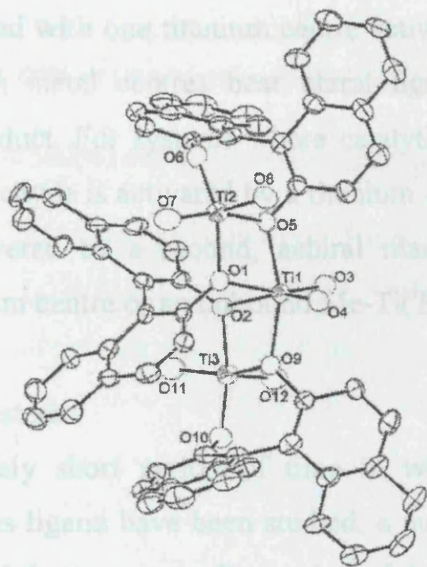


Figure 4.10. Crystal structure of stoichiometric Ti/BINOL complexes

This structure is trimetallic and, again, contains a titanium centre in a distorted octahedral geometry and two centres with distorted trigonal-bipyramidal geometries. Here, only naphthylate oxygens bridge the titanium centres and all the isopropoxy groups are terminal. This species is known to be dimeric in solution.<sup>16</sup> When a 1:1 ratio of BINOL and  $\text{Ti}(\text{iPrO})_4$  was used in stoichiometric reactions, significant non-linear effects were observed; when catalysts with low enantiopurity were used in the reactions, products with higher enantiopurities than the catalyst were isolated. This indicated the presence of two chiral inducing groups within the active species. Similar results were also observed by Scettri *et al.* when a 1:1 ratio of BINOL: $\text{Ti}(\text{iPrO})_4$  was used.<sup>11</sup> The result also indicated that the active species in the stoichiometric systems and catalytic systems were not the same, as no non-linear effects were observed in the catalytic system. It was determined by comparison of results that the catalytic BINOL system was around twice as active in the addition of diethylzinc to a range of aldehydes than the stoichiometric system, with 95 % *versus* 50 % conversion after ten minutes, but the product *ee*'s obtained were very similar in all cases.<sup>16</sup>

Finally, to determine the interaction of the metal alkyl reagent with the substrate and the catalyst species, the authors investigated the use of dimethylzinc and  $\text{Me-Ti}(\text{iPrO})_3$  as separate alkylating agents. It was shown that, when  $\text{Me-Ti}(\text{iPrO})_3$  was used as the methyl source, similar product yields and *ee*'s could be achieved to when dimethylzinc was used as the alkylating agent. This result shows that the metal alkyl reagent is not directly involved in the carbon-carbon bond forming reaction and must, instead, transfer the alkyl group to titanium for addition to the substrate.

All of these experiments show that two titanium centres are involved in the asymmetric addition of alkyl groups to aldehydes. When stoichiometric amounts of BINOL and  $\text{Ti}(\text{iPrO})_4$  are used, a dimeric species is formed with one titanium centre activating the aldehyde while the other delivers the alkyl group. Both metal centres bear chiral ligands and so both can affect the enantiomeric excess of the product. For systems where catalytic amounts of BINOL are used in comparison to  $\text{Ti}(\text{iPrO})_4$ , the aldehyde is activated by a titanium atom bearing the chiral ligand. The alkyl group can then be delivered by a second, achiral titanium centre; either one which is associated with the chiral titanium centre or an unbound  $\text{Me-Ti}(\text{iPrO})_3$  species.

#### 4.1.3 Recyclable Ti/BINOL Systems

Considering the relatively short period of time in which reactions involving titanium tetraisopropoxide and BINOL as ligand have been studied, a number of studies have been carried out on the recovery and reuse of these systems. Ikegami *et al.* have used insoluble, polymer-bound Ti/BINOL catalysts in a carbonyl-ene reaction (Figure 4.11).<sup>19</sup>

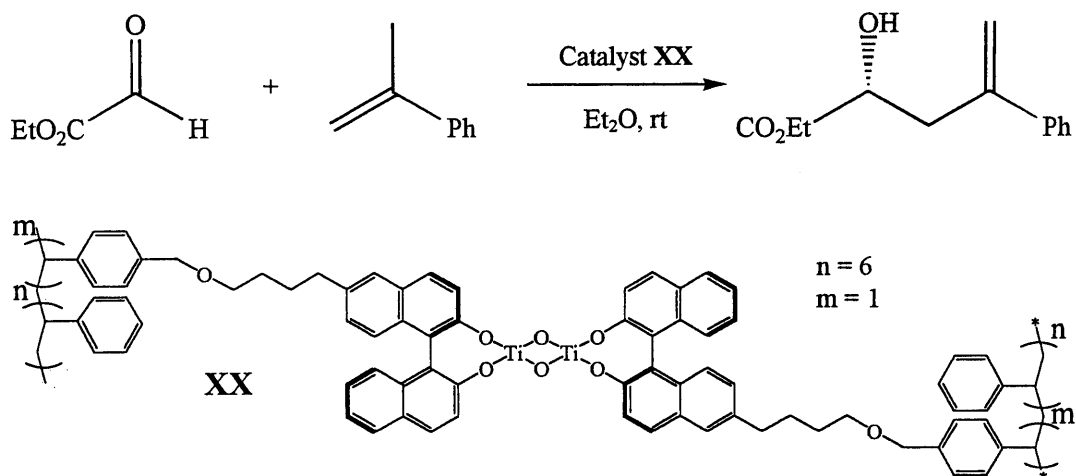


Figure 4.11. Carbonyl-ene reaction using polymer-supported catalyst XX

Using 20 mol % of catalyst, the product could be isolated in 85 % yield and 88% *ee*. The catalyst could be recovered by simple filtration and reused four times with no loss of activity or

selectivity. However, due to the heterogeneity of the catalyst, the activity was much less than that for non-supported Ti/BINOL.

Soluble polymer supports have also been used by Sasai and Jayaprakash in the addition of diethylzinc to benzaldehyde.<sup>20</sup> Here, yields of around 60 % could be achieved with product *ee*'s of between 70 and 80 %, depending on the solvent employed. It is noteworthy that the activity of the soluble polymer-supported Ti/BINOL catalyst was much higher, with reactions normally carried out for 15 hours, but the product yields were lower than the previous system. Additionally, attempted reuse of the catalyst following precipitation reduced the product yield still further to only 22 %, with the *ee* falling to 36 %. The fall in activity and selectivity was attributed to the co-precipitation of inseparable zinc and titanium contaminants, which reduced the solubility of the catalyst in subsequent catalytic runs.

Chan *et al.* have synthesised bis- and tetra-perfluoroalkylated BINOL derivatives for use as ligands in the addition of diethylzinc to benzaldehyde.<sup>21</sup> Here, the reaction was carried out under fluoruous biphasic conditions using hexane and perfluoromethyldecalin as solvents to allow the fluoruous BINOL ligands to be recycled by decantation and reuse of the fluoruous phase in further catalysis. Three of the ligands used are shown in Figure 4.12, along with their partition coefficients in hexane/perfluoromethyldecalin.

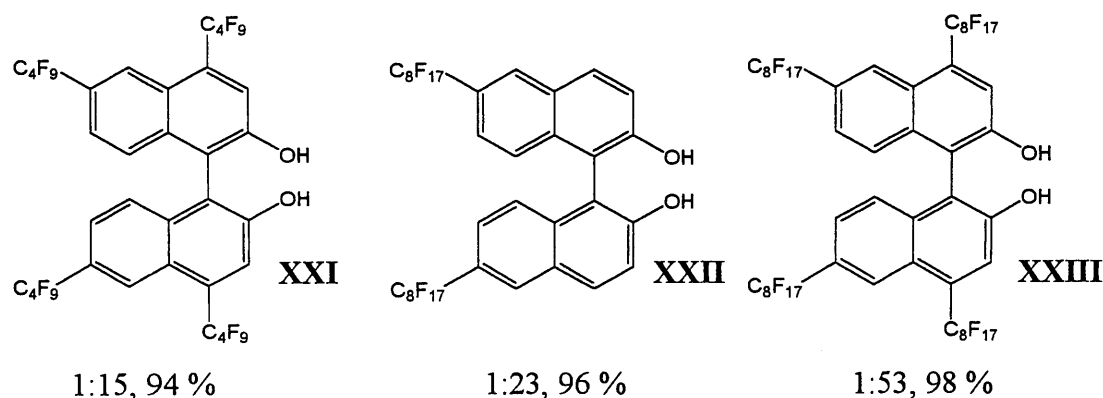


Figure 4.12. Fluoruous BINOL ligands and their partition coefficients (Hexane:perfluoromethyldecalin, percentage in fluoruous phase)

The BINOL ligand was dissolved in the perfluorocarbon solvent and a hexane solution of  $Ti(O^iPr)_4$  added to form a biphasic system at room temperature. This was heated to 45 °C, whereupon the mixture became homogeneous. After the addition of benzaldehyde and diethylzinc, the reaction mixture was stirred for 30 minutes before being cooled to 0 °C to reform the biphasic system. The organic layer was separated and the fluoruous phase was then recycled with the addition of more  $Ti(O^iPr)_4$  and reactants.

Of the ligands used, Ligands **XXI**, **XXII**, and **XXIII**, could be recycled the greatest number of times using this method. Ligand **XXI** was reused 3 times, but the product *ee* fell steadily after each recycle and fell drastically after the third cycle. Ligand **XXII** fared similarly, but the product *ee*'s were lower after each recycle than for ligand **XXI**. However, ligand **XXIII** could be used 9 times without significant loss of product yield or enantiomeric excess. The authors do not comment upon the loss of ligand due to leaching into the organic phase, but the differences in preferential perfluorocarbon solubility of the ligands are likely to be responsible for the differing ease of recycling of the ligands and the falls in conversion and enantiomeric excesses.

Whilst these results show promise, the authors achieved 100 % conversion and 88 % product *ee* when using non-fluorous BINOL,<sup>5</sup> which is much better than the maximum 80 % conversion and 60 % *ee* achieved using ligand **XXIII**. In addition, it is likely that contamination of the organic product with fluorous BINOL ligands occurs. Finally, an active catalyst cannot be recovered, with additional titanium tetrakisopropoxide required for each subsequent catalytic run.

Nakamura *et al.* have reported a similar system which uses a fluorous biphasic system and FRP silica gel to recycle the BINOL ligand.<sup>22</sup> A six-tailed BINOL derivative is used (Figure 4.13) and the reaction carried out in a hexane/toluene/FC-72 biphasic system.

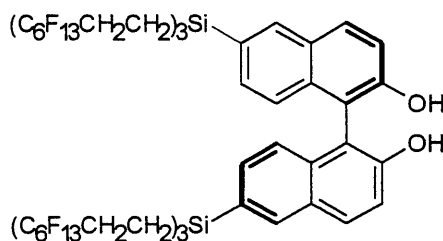


Figure 4.13. A six-tailed BINOL derivative

After reaction, the FC-72 phase was separated and the organic phase washed with aqueous hydrochloric acid and passed down a column of FRP silica gel. The organic product was eluted with acetonitrile and the BINOL ligand then eluted with FC-72 and combined with the first FC-72 phase for reuse. The fluorous fractions, after recombination, could be recycled 5 times with no loss of activity and product *ee*'s were maintained at around 80 %.

The amount of BINOL ligand recovered from the organic phase after FRP silica gel separation was around 10 %, showing that the ligand was not exclusively soluble in the perfluorocarbon solvent. It was shown that the fluorous layer was required to achieve high product enantiomeric excess and that the reaction did not just occur in the organic phase.

Not only does this system require the use of expensive perfluorocarbon solvents, it also requires the use of FRP silica gel to fully recover the ligand and, effectively, two processing stages, making this recovery process prohibitively expensive.

The allylation of aldehydes has also been studied using fluorinated-BINOL ligands (see Figure 4.3).<sup>23</sup> Again, a fluorinated biphasic system was used to recycle the BINOL ligand, either 6,6'-bis(1*H*,1*H*,2*H*,2*H*-perfluoro-*n*-octyl)-1,1'-bi-2-naphthol or 6,6'-bis(1*H*,1*H*,2*H*,2*H*-perfluoro-*n*-decyl)-1,1'-bi-2-naphthol. Under homogeneous conditions in hexane using C<sub>6</sub>F<sub>13</sub>-BINOL, the allylation of benzaldehyde using allyltri-*n*-butyltin could be achieved in 75 % yield and 83 % product *ee*. These results were slightly better than those obtained using non-fluorinated BINOL, where a yield of 74 % and an *ee* of 78 % were obtained. Under biphasic conditions using hexane/FC-72, the use of C<sub>6</sub>F<sub>13</sub>-BINOL led to product yields and *ee*'s of 85 % and 90 % respectively, whereas the use of C<sub>8</sub>F<sub>17</sub>-BINOL gave product in 83 % yield and 90 % *ee*. However, there was significant leaching of the ligands into the organic phase and no mention of the phase in which the reaction occurs was made. In addition, no attempt was made to reuse the fluorinated phases in further catalysis, the ligands being recovered by removal of the fluorinated solvent instead. The reason for recovering the ligand in this way was not given and, in the C<sub>6</sub>F<sub>13</sub>-BINOL case, only 49 % of the ligand could be recovered from the perfluorocarbon solvent; 24 % was recovered from the organic phase whilst the other 27 % was lost. It is clear that these fluorinated analogues of BINOL are not appropriate for biphasic catalysis, which, considering their percentage fluorine content by weight, is not surprising.

Finally, Fan *et al.* have used dendritic BINOL ligands in the asymmetric catalytic addition of diethylzinc to benzaldehyde using titanium tetrakisopropoxide (Figure 4.14).<sup>24</sup>

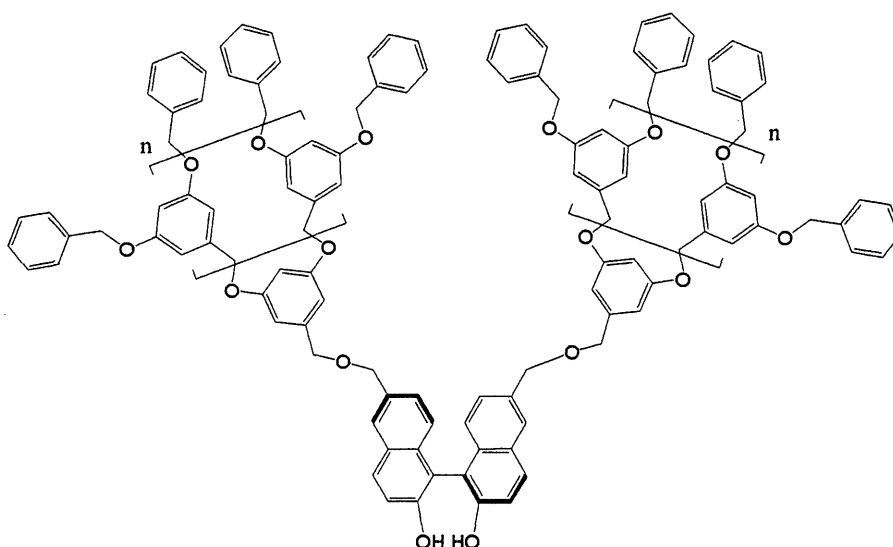


Figure 4.14. Dendritic BINOL

Dendrimers can be recovered after reaction by precipitation from the reaction mixture and filtration. The dendrimers shown above (where  $n = 1, 2$  or  $3$ ) were used in catalytic runs and product conversion was greater than 99 % in all cases. Additionally, product *ee*'s were greater than 80 %, and when the dendrimer with  $n = 3$  was used in a second run after re-isolation, the product conversion remained greater than 99 % and the product *ee* was 86 %; the same product enantiopurity that was observed in the first run. However, no further recycles were attempted.

These examples of reusable BINOL are interesting, but often they require extensive functionalisation of the binaphthyl backbone before separation is achievable. In addition, in many cases, the activity and selectivity of the modified BINOL catalysts are reduced in comparison to unmodified BINOL systems, making the techniques employed for catalyst recovery detrimental to the overall catalytic process. It seemed, therefore, that the light fluororous approach to BINOL ligand/catalyst recovery might be able to succeed where other methods of catalyst/ligand recovery had failed; namely the ability to both catalyse an asymmetric reaction in high conversion and enantioselectivity and to allow recovery and reuse of the ligand/catalyst without reduction in either activity or specificity.

## 4.2 Results and Discussion

Following the synthesis of a range of perfluoroalkylated BINOL compounds as intermediates in the synthesis of BINAP and MonoPhos (see chapters Two and Three) and in view of the conclusion that stable catalysts are needed in order for the light fluororous approach to catalyst recovery to be successful, the stable fluororous and non-fluororous BINOL compounds were investigated in two titanium-catalysed reactions. However, as the studies of BINAP and MonoPhos have shown, the addition of  $C_2H_2$  or  $C_2H_4$  spacer groups has little effect on the donor atom properties and so studies were limited to the (*R*)- and (*S*)-enantiomers of BINOL and Rf-BINOL (Figure 4.15).

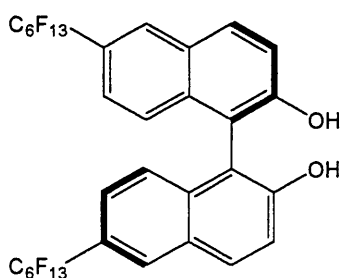


Figure 4.15. (*R*)-Rf-BINOL

### 4.2.1 The Addition of Diethylzinc

Since most of the work in the literature has focussed on the asymmetric addition of diethylzinc to benzaldehyde (Figure 4.16), this system was examined first.

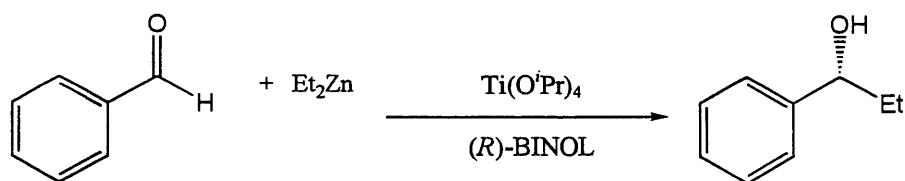


Figure 4.16. The addition of diethylzinc to benzaldehyde

The methodology of Chan *et al.* was taken and adapted for the light fluoros approach.<sup>5</sup> It was shown by Chan that the use of dichloromethane as solvent at 0 °C gave the best product conversions and enantioselectivities. An excess of titanium tetraisopropoxide and diethylzinc was also required to ensure high conversion and enantiopurity values. The BINOL:Ti ratio was also found to be important. It was shown that, in a 1:1.4 ratio, the reaction gave low conversion but relatively high product enantiomeric excess. However, at lower concentrations of BINOL, higher conversions and *ee*'s could be obtained, with a ratio of 1:7 giving the best product conversion and *ee*. It was suggested that this observation was caused by the need for free  $\text{Ti}(\text{O}^i\text{Pr})_4$  which may act as a co-catalyst during reaction. This was in agreement with the observations made by Walsh *et al.*<sup>16</sup> (see section 4.2.1).

To begin with, catalytic studies using (*R*)-BINOL as ligand were carried out. The ligand and titanium tetraisopropoxide in a 1:7 ratio were stirred together for one hour in dichloromethane under nitrogen and then benzaldehyde added *via* syringe and the mixture cooled to -20 °C. After ten minutes of stirring, diethylzinc was added and the reaction was then left to stir for 18 hours before being quenched with hydrochloric acid solution. The resulting organic layer was dried, the solvent removed under reduced pressure and a crude NMR spectrum obtained to determine product conversion. Chiral GC was then used to determine the product *ee*. The reaction was carried out three times to make sure the results were consistent, and the results are given in Table 4.1. The product yields and *ee*'s obtained for the addition of diethylzinc to benzaldehyde using this system are highly reproducible and comparable to the 100% conversion and 92 % *ee* achieved by Chan *et al.*<sup>5</sup>

Run <sup>a</sup>	Conversion (%) <sup>b</sup>	ee (%) <sup>c</sup>
1	90	86
2	85	90
3	90	90

<sup>a</sup> Ligand = (*R*)-BINOL, t = 18 h, DCM, BINOL:Ti = 1:7 <sup>b</sup> By <sup>1</sup>H NMR spectroscopy <sup>c</sup> By chiral GC

Table 4.1. Results of addition of diethylzinc to benzaldehyde using (*R*)-BINOL as ligand

Next, the addition reaction was tried using (*R*)-Rf-BINOL as ligand. Again, a BINOL:Ti ratio of 1:7 was used and the reaction carried out in dichloromethane under nitrogen for 18 hours. At the end of the reaction, aqueous hydrochloric acid was added to quench the excess diethylzinc, the organic layer separated and dried and the solvent removed to yield the crude product. Again, <sup>1</sup>H NMR spectroscopic analysis was then used to determine the percentage conversion to product and chiral GC was used to determine the product *ee*. The reaction using (*R*)-Rf-BINOL as ligand was also carried out three times to test the reproducibility of the system. The results for the three runs are given in Table 4.2.

Run <sup>a</sup>	Conversion (%) <sup>b</sup>	ee (%) <sup>c</sup>
1	90	77
2	86	70
3	88	75

<sup>a</sup> Ligand = (*R*)-Rf-BINOL, t = 18 h, DCM, Rf-BINOL:Ti = 1:7 <sup>b</sup> By <sup>1</sup>H NMR spectroscopy <sup>c</sup> By chiral GC

Table 4.2. Results of addition of diethylzinc to benzaldehyde using (*R*)-Rf-BINOL as ligand

It was pleasing to note that, when either (*R*)-BINOL or (*R*)-Rf-BINOL was used as ligand, the results from both systems proved to be highly reproducible and similar product yields could be obtained using either ligand, although the observed product *ee*'s were slightly lower when (*R*)-Rf-BINOL was used in place of (*R*)-BINOL. However, the fall in enantiopurity of the product was not dramatic and may be due to the ligand not being 100 % enantiomerically pure or the presence of some negative non-linear effects in the system; previous analysis of synthesised Rf-BINOL ligands (see Chapter 3) suggested that they were around 95 % enantiomerically pure, which does not completely explain the fall in product *ee*'s observed here. In comparison to previous work where the analogous 6,6'-bis(perfluoro-*n*-octyl)-1,1'-bi-2-naphthol was used under fluoruous biphasic conditions,<sup>21</sup> the results obtained here show lower conversions at 88 % *versus* 99 %, but the *ee*

achieved here is higher at 75 % *versus* 64 %. This difference in product *ee* is most likely due to the use of a highly non-polar solvent in the previous work and the requirement of a relatively high temperature of 45 °C to achieve a homogeneous reaction mixture.

Enhancement of the Rf-BINOL ligand *ee* synthesised here could have been achieved by the separation of synthesised Rf-BINOL/camphor-based diastereomers by column chromatography, but since the focus of the work was separation, recovery and reuse of the catalyst, non-optimised enantioselectivities were not considered to be a significant issue.

#### 4.2.2 Separation Studies

Once it had been shown that Rf-BINOL ligands were effective in the addition of diethylzinc to benzaldehyde, the separation and recovery of the BINOL ligands post-reaction was investigated. In this system, it was not possible to re-isolate an active catalyst, as the acid work-up of the crude reaction mixture, which quenches the excess diethylzinc present, breaks down the sensitive Ti-BINOL complex.

To begin with, the separation and recovery of non-derivatised BINOL was investigated. A standard addition reaction was carried out using (*R*)-BINOL as ligand and, at the end of the reaction, the mixture was hydrolysed with aqueous hydrochloric acid. The organic layer was dried and concentrated *in vacuo* and then added to the top of a short column of silica gel around 3 cm in length. Due to the robust nature of BINOL, it was not necessary to carry out the recovery attempt under nitrogen. Acetonitrile was used as the elutant and a portion of the solvent added to the column and passed through under pressure using a hand pump. The product was eluted, but the ligand was also washed off the column and was clearly visible as a contaminant by <sup>1</sup>H NMR spectroscopic analysis.

Hexane and petroleum spirit were also tried as eluting solvents but once more, even though pure BINOL is not soluble in hexane or petroleum spirit, the ligand was washed off the column with the product. It was proposed that the reason for this observation was that the BINOL ligand had a high solubility in the liquid product and so remained soluble even with the addition of highly non-polar solvents and was eluted. The use of alternative solvents was not possible, as the ligand was soluble in other common organic solvents and, therefore, would not be selectively retained on the silica. With the use of a long column of silica, it was possible to isolate the product free of ligand contamination, but column chromatography is not a desirable ligand isolation method due to the large volumes of solvent required and the inability to reliably scale up the process.

Next, a standard addition reaction was carried out using (*R*)-Rf-BINOL as ligand. At the end of the reaction, the mixture was hydrolysed with aqueous hydrochloric acid and then the organic layer dried and concentrated *in vacuo*. The reduced-volume crude mixture was added to the top of a

short column of FRP silica gel around 3 cm in length and then, using acetonitrile as elutant once again, recovery of pure product was attempted. However, once more, the ligand was eluted along with the product and was clearly visible by  $^1\text{H}$  and  $^{19}\text{F}$  NMR spectroscopic analysis of the isolated material. It was not necessary to test hexane as elutant for the (*R*)-Rf-BINOL system; (*R*)-BINOL was eluted from the column previously and this ligand was not soluble in hexane, while (*R*)-Rf-BINOL is soluble and would, therefore, be washed off the column with the product.

Once again, it was possible to isolate the product free of ligand contamination using column chromatography, but the addition of fluororous ponytails is unnecessary if this method of product purification is to be employed. Unfortunately, this method of ligand isolation and recovery using lightly fluorinated BINOL is no better than the fluororous biphasic methodology employed previously,<sup>21</sup> where the product was also contaminated with fluorinated BINOL ligand. It was decided that, to prove the FRP silica gel separation methodology, an alternative system was needed in which the product formed was not a good solvent for BINOL.

#### 4.2.3 The Addition of Diethylzinc Using Rf<sub>4</sub>-BINOL

Since the solubility of (*R*)-4,4'-6,6'-tetra(perfluoro-*n*-hexyl)-1,1'-bi-2-naphthol ((*R*)-Rf<sub>4</sub>-BINOL) was very different to Rf-BINOL, its ability as a ligand in the addition of diethylzinc to benzaldehyde was also investigated. It was hoped that, with the correct choice of solvents, it may be possible to use the ligand in the addition reaction and then achieve successful recovery using FRP silica gel after the acid wash. This study would also be comparable to previous work by Chan<sup>21</sup> and Nakamura *et al.*<sup>22</sup> who used a tetra-substituted BINOL and six-tailed disubstituted BINOL with a silicon spacer respectively under fluororous biphasic conditions (see Section 4.1.3).

A catalytic run was, therefore, carried out using (*R*)-Rf<sub>4</sub>-BINOL in place of (*R*)-Rf-BINOL in ethyl acetate rather than toluene. The solvent switch was required as Rf<sub>4</sub>-BINOL is not soluble in toluene. The reaction mixture was worked up in the same way. The organic layer was dried, filtered, concentrated *in vacuo* and then placed onto a short column of FRP silica gel and the product eluted with acetonitrile. Analysis of the isolated material by  $^1\text{H}$  and  $^{19}\text{F}$  NMR spectroscopy and GC showed that the product had been formed in 65 % overall conversion but with just 33 % *ee*. These results show that the ligand is not as active or selective as (*R*)-Rf-BINOL under these conditions or the conditions used for the closely related XXIII under fluororous biphasic conditions.<sup>21</sup> In addition, a significant amount of ligand had still leached off the column along with the product, even though (*R*)-Rf<sub>4</sub>-BINOL has no apparent solubility in pure acetonitrile. It was determined by  $^1\text{H}$  NMR spectroscopy that 20 % ligand loss into the product had occurred after the first separation. This is much worse than in the Nakamura *et al.* system,<sup>22</sup> where no ligand leaching into the product was observed. However, as Nakamura used fluororous biphasic catalysis followed by phase separation,

only the organic phase was passed through FRP silica gel, which contained around only 10 % of the ligand present in the reaction. Here, all of the ligand present in the reaction was passed through FRP silica gel along with the product, possibly explaining why ligand leaching was observed.

The ligand retained on the FRP silica gel column was recovered by elution with ethyl acetate and its chemical and optical purity determined. NMR spectroscopic analysis showed that the ligand had not been degraded during reaction or separation and optical rotation measurements confirmed the ligand had not been racemised. The recovered (*R*)-Rf<sub>4</sub>-BINOL was used in one subsequent reaction, with the amounts of reactants adjusted accordingly, and separated again using FRP silica gel and acetonitrile. Once more by <sup>1</sup>H NMR spectroscopic analysis, the ligand was observed in the product and only 50 % of the ligand originally added was recovered from the column. The product was obtained in 60 % conversion and 28 % *ee*, again much lower than the values obtained after the second catalytic runs in previous work.<sup>21,22</sup> Due to the highly expensive nature of the ligand and the fact that leaching from the column was still observed in this system, further reuse of the ligand in catalysis as well as optimisation of conditions was abandoned.

#### 4.2.4 The Addition of Allyltri-*n*-butyltin

Although the addition of allyltri-*n*-butyltin to aldehydes is not as commonly studied as the addition of diethylzinc, the reaction has still been shown to give high conversion to products with high *ee*'s.<sup>7,24</sup> Allyltri-*n*-butyltin is a common reagent for the addition of allyl groups to organic substrates<sup>16,17</sup> and is cheap and easily obtained. However, the requirement to avoid traces of highly toxic tin and tin species in pharmaceutical and fine chemical products has, probably, contributed to the relative intensity of investigations into this reaction.

The addition of allyltri-*n*-butyltin to benzaldehyde (see Figure 4.3) using perfluoroalkylated ligands has been studied by Zhao *et al.* and shown to give good product conversion and *ee*.<sup>20</sup> It was decided, therefore, that this addition would be attempted employing (*R*)-BINOL and (*R*)-Rf-BINOL as ligands and then the efficacy of ligand recovery investigated.

The conditions used by Zhao were taken and used with only slight modification. A ligand:titanium ratio of 1:2 was used by Zhao and hexane used as the reaction solvent. However, when (*R*)-BINOL was used as ligand, hexane could not be used as the solvent, as the ligand itself was not highly soluble and the titanium complex was apparently completely insoluble. Therefore, to begin with, dichloromethane was used for the non-fluorous reactions and hexane used as solvent for the fluorous systems to allow comparison with the work by Zhao.

The addition reaction was carried out three times for each ligand at 0 °C and the products isolated by hydrolysis of the reaction mixture followed by column chromatography. The purified products were then analysed by <sup>1</sup>H NMR spectroscopy, checked for fluorous ligand contamination

by  $^1\text{H}$  and  $^{19}\text{F}$  NMR spectroscopic analysis (when (*R*)-Rf-BINOL had been used) and their *ee*'s determined by conversion into the Mosher's acid ester (Figure 4.17) followed by GC analysis. The results of the catalytic runs are given in Table 4.3.

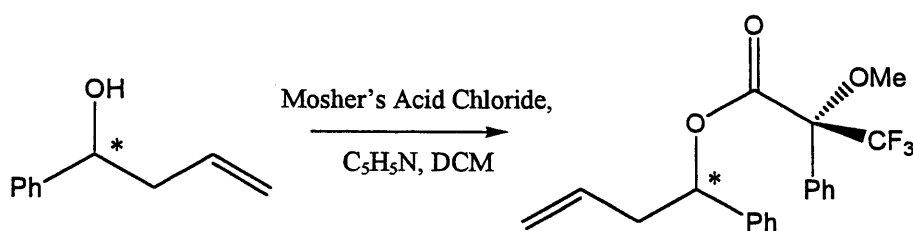


Figure 4.17. Mosher's acid ester of 4-phenyl-1-buten-4-ol

Ligand	Conversion (%) <sup>a</sup>	<i>ee</i> (%) <sup>b</sup>
( <i>R</i> )-BINOL <sup>c</sup>	90	82
( <i>R</i> )-BINOL <sup>c</sup>	90	78
( <i>R</i> )-BINOL <sup>c</sup>	88	78
( <i>R</i> )-Rf-BINOL <sup>d</sup>	86	74
( <i>R</i> )-Rf-BINOL <sup>d</sup>	90	78
( <i>R</i> )-Rf-BINOL <sup>d</sup>	88	74

<sup>a</sup> By  $^1\text{H}$  NMR spectroscopy <sup>b</sup> By GC of Mosher's acid ester <sup>c</sup> In DCM, 0 °C, t = 6 h <sup>d</sup> In hexane, 0 °C, t = 6 h

Table 4.3. Catalytic asymmetric addition results

It is pleasing to note that both (*R*)-BINOL and (*R*)-Rf-BINOL give very similar product conversions and *ee*'s, indicating that the perfluoroalkyl chains have no detrimental effect on the abilities of the modifying ligand. In addition, the catalytic reaction is highly reproducible, with similar product conversions and enantiopurities observed after three separate runs. The fact that the non-fluorous reaction was carried out in dichloromethane and the fluorous reaction carried out using hexane as solvent made no difference to the product yields or *ee*'s obtained. This was surprising, as changing the solvent can often have a dramatic effect on product *ee*'s. The effect of the solvent was, therefore, probed during comparison between the ability to isolate and reuse the fluorous and non-fluorous ligands after catalysis.

#### 4.2.5 Separation Studies

Once the effectiveness of the ligands in the asymmetric addition reaction had been assessed, the separation of the ligand/catalyst from the product and the reuse of the isolated material in further catalysis were investigated. Both the fluorous and non-fluorous catalytic tests were now carried out in dichloromethane to allow direct comparison.

Unlike for the diethylzinc system, it was not necessary to carry out an acid wash before attempting the catalyst isolation, as the allyltri-*n*-butyltin was added in a stoichiometric amount. Therefore, a standard catalytic addition reaction was carried out using (*R*)-BINOL and the mixture concentrated *in vacuo* post-reaction. The crude product was then added to the top of a short column of silica gel three centimetres long and elution with acetonitrile carried out. A dark orange band stayed at the top of the column while a lighter orange solution passed through the silica and was collected. Analysis, by  $^1\text{H}$  NMR spectroscopy, of the material collected showed it to be a mixture of the product, an (*R*)-BINOL-containing species and a species that gave rise to butyl peaks. The dark band of material that remained adhered to the silica column was very difficult to elute and was finally partially collected using methanol as eluant, with some dark orange material remaining stuck to the column. This material was shown, by  $^1\text{H}$  NMR spectroscopy, to contain an (*R*)-BINOL-containing species that also gave rise to butyl peaks.

Due to leaching of the (*R*)-BINOL from the column using acetonitrile as elutant, the separation was attempted again using a longer column of silica gel. A standard reaction was carried out again using (*R*)-BINOL and, after concentration *in vacuo*, the bright orange material was placed on one side while the column was prepared. During this short period of time, large crystals suitable for X-ray analysis formed in the residue. The structures are given in Figure 4.18 and 4.19 below.

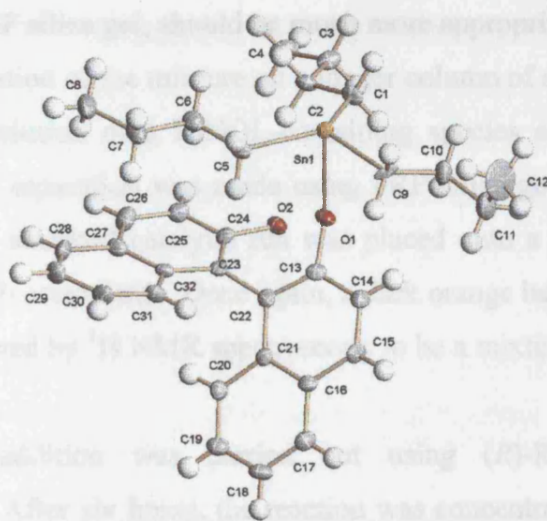


Figure 4.18. The monomer unit of the Sn-BINOL polymer showing 50 % displacement ellipsoids

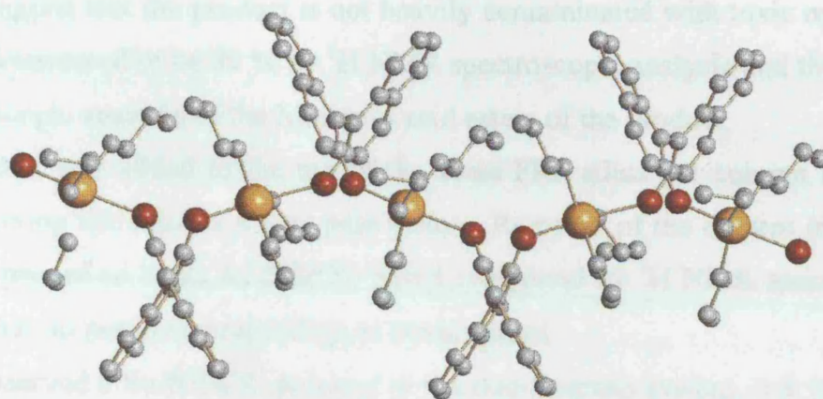


Figure 4.19. Solid-state structure of the Sn-BINOL polymer bridging through BINOL oxygens

The structure shows that, after addition of the allyl group to benzaldehyde, some of the tin-containing residue binds to the oxygen atoms of BINOL and forms a polymeric chain containing tributyltin and BINOL units.  $^1\text{H}$  NMR spectroscopic analysis of the crystals was in agreement with the crystal structure, although satisfactory elemental analysis data could not be obtained. This structure is very interesting because it suggests that the material to be isolated at the end of reaction and reused may not be a titanium-containing species at all. The formation of this Sn-BINOL polymer clearly changes the separation dynamics of the mixture, suggesting that a non-polar solid separation media, such as FRP silica gel, should be much more appropriate for ligand retention.

Attempting the separation of the mixture on a longer column of silica gel did not prove to be any more successful, with elution of a BINOL-containing species along with the product still observed. A final attempt at separation was made using FRP silica gel in place of silica gel. The concentrated residue from a standard catalytic run was placed onto a three-centimetre column of FRP silica gel and eluted with acetonitrile. Once again, a dark orange band passed down the column and the isolated material proved by  $^1\text{H}$  NMR spectroscopy to be a mixture of product and a BINOL-containing species.

Next, a catalytic addition was carried out using (*R*)-Rf-BINOL as ligand and dichloromethane as solvent. After six hours, the reaction was concentrated *in vacuo* and the crude mix added to the top of a short column of FRP silica gel. Again, acetonitrile was used as elutant, and an orange band remained at the top of the column while a pale yellow band was eluted. The solvent was removed *in vacuo* to yield a yellow oil which was shown to be 4-phenyl-1-buten-4-ol product by  $^1\text{H}$  NMR spectroscopic analysis containing no (*R*)-Rf-BINOL contamination, but butyl peaks corresponding to a small amount of contamination possibly by a tin-based species. ICP analysis of an acid wash of the product showed a tin contamination of 1.24 ppm (0.02 % of original tin added) and a titanium contamination of 2.21 ppm (0.88 % of titanium added). These values are

very small and suggest that the product is not heavily contaminated with toxic metals. The product conversion was determined to be 89 % by  $^1\text{H}$  NMR spectroscopic analysis and the *ee* to be 70 % by  $^1\text{H}$  NMR spectroscopic analysis of the Mosher's acid esters of the product.

Diethyl ether was added to the top of the same FRP silica gel column and a dark orange species eluted, leaving the column a very pale yellow. Removal of the solvent *in vacuo* yielded an orange oil which proved to be an Rf-BINOL-based compound by  $^1\text{H}$  NMR spectroscopic analysis, with butyl peaks but no peaks corresponding to *iso*-propanol.

Having observed a Sn-BINOL polymer in the non-fluorous system, it is likely that a similar species is formed in the light fluoruous BINOL system, containing bridging tri-*n*-butyltin groups. However, due to the bulky nature of the perfluoroalkyl chains and their tendency to retain solvents, crystals of the material suitable for X-ray analysis could not be obtained. However,  $^{119}\text{Sn}\{^1\text{H}\}$  NMR spectroscopy was obtained of both the fluoruous and non-fluorous material and two peaks in a 2:1 ratio observed in both spectra. For the non-fluorous system, peaks were observed in the  $^{119}\text{Sn}\{^1\text{H}\}$  spectrum at 105.47 and 115.63 ppm (2:1) corresponding to two different tin environments in the compound. For the fluoruous system, two peaks were observed at 106.20 and 123.05 ppm (2:1). The spectra suggest that the materials are very similar in structure, with higher chemical shift values in the fluoruous system due to the electron-withdrawing effect of the fluoruous ponytails. Samples of both materials were submitted for elemental analysis, but satisfactory values could not be obtained. The NMR spectroscopy data also suggests the material does exist as an oligomer or other species in solution, as the presence of two species is not accounted for in the crystal structure.

This isolated material was taken, dried and used in a second standard catalytic run without further modification. At the end of the reaction, a second recovery was attempted and a dark yellow oil collected which proved to be unreacted starting material by  $^1\text{H}$  NMR spectroscopy with no BINOL contamination, showing the isolated Rf-BINOL-containing species was not active in further catalysis. This supports the theory that the isolated material is a Sn-Rf-BINOL polymer or similar inactive species, which is not broken down by the addition of titanium tetraisopropoxide to form an active catalyst species.

A standard catalytic addition reaction in dichloromethane at 0 °C was carried out once more and the separation of the product from the Rf-BINOL-containing species achieved using FRP silica gel and acetonitrile as elutant. Then, again using diethyl ether, an orange solution was collected which, after removal of the solvent *in vacuo*, proved by  $^1\text{H}$  NMR spectroscopic analysis to be an Rf-BINOL-containing species, with peaks corresponding to butyl groups also present.

The isolated orange oil was redissolved in hexane and washed with 4M hydrochloric acid, whereupon the solution turned dark red and then yellow. Separation of the organic layer followed

by drying and removal of the solvent yielded (*R*)-Rf-BINOL with no racemisation observed by optical rotation analysis.

It can be envisaged that retention of the material on the column of FRP silica gel is due to the moiety's highly hydrophobic nature and subsequent favourable fluororous and non-polar Van der Waals interactions with the solid support. This allows the relatively polar acetonitrile solvent to wash off the product from the column while leaving behind the non-polar Rf-BINOL-containing species and any free Rf-BINOL. Diethyl ether, which is a very fluorophilic solvent, can then be used to recover the Rf-BINOL species and free (*R*)-Rf-BINOL can be recovered by simple acid hydrolysis. The recovered (*R*)-Rf-BINOL ligand was reused in three further catalytic runs using the same catalysis, separation and recovery methodology. The results for these runs are given in Table 4.4.

Run	Conversion (%) <sup>a</sup>	<i>ee</i> (%) <sup>b</sup>	Sn content (ppm) <sup>c</sup>	Ti content (ppm) <sup>d</sup>
1	85	66	1.24, (0.02 %)	2.21, (0.88 %)
2 <sup>e</sup>	85	63	0.75, (0.01 %)	1.99, (0.83 %)
3 <sup>e</sup>	82	58	2.73, (0.04 %)	2.86, (1.19 %)
4 <sup>e</sup>	78	58	4.40, (0.07 %)	4.65, (1.93 %)

<sup>a</sup> By <sup>1</sup>H NMR spectroscopy <sup>b</sup> By GC of Mosher's acid ester <sup>c</sup> Of product by ICP spectroscopic analysis, overall percentage shown in brackets  
<sup>d</sup> Of product by ICP spectroscopic analysis, overall percentage shown in brackets <sup>e</sup> Using ligand from previous run

Table 4.4. Catalytic addition results obtained using recovered (*R*)-Rf-BINOL

The data shows that similar product conversions are achieved after each run, with a slight fall after the third ligand reuse. This is most likely due to mechanical losses of the ligand after each recycle rather than any deterioration of the ligand itself, as the BINOL ligands are very stable. Using the experimental procedure employed here, small losses of material were inevitable. The fall in product *ee* is also slight, and is probably due to a small amount of ligand racemisation. Optical rotation measurements of the (*R*)-Rf-BINOL ligand recovered after the third recycle showed the ligand had racemised slightly, with an increase in the value observed from  $-17.2^\circ$  to  $-16.4^\circ$ . The conversions to product using this methodology are better than those observed previously,<sup>23</sup> but the product *ee*'s are lower. This is very interesting, as the *ee*'s obtained using dichloromethane as solvent in the fluororous system have fallen in comparison to the *ee*'s obtained using BINOL as ligand in dichloromethane and Rf-BINOL as ligand in hexane. This suggests that solvent effects are present in this addition reaction. The amounts of tin and titanium in the product were very small and could be removed to below detectable levels by passing the sample through a short column of silica using acetonitrile as elutant. This would make the system useful for the synthesis of compounds

where metal contamination is unacceptable. Finally, unlike previously, the data shows that the ligand can be successfully recovered and reused after use in catalysis.

Reactions carried out using hexane as solvent showed the (*R*)-Rf-BINOL ligand could be used to effect high product *ee*'s. However, as the separation procedure had been carried out on material obtained after reaction in dichloromethane, it was necessary to check that ligand isolation was still possible after reaction in hexane. Therefore, a catalytic reaction was carried out using (*R*)-Rf-BINOL as ligand in hexane at 0 °C. After reaction, the reaction mixture was concentrated *in vacuo* and placed on a 3 cm-long column of FRP silica gel. Acetonitrile was then used as elutant, and a dark orange band remained at the top of the column while a pale yellow solution was collected. Removal of the acetonitrile *in vacuo* and analysis of the yellow oil obtained, by <sup>1</sup>H NMR spectroscopy and ICP atomic emission spectroscopy, showed the oil to be product which was free of ligand contamination and had a tin content of 1.18 ppm and a titanium content of 2.11 ppm; values comparable to those obtained when dichloromethane was used as reaction solvent. Most importantly, determination of the product *ee* by conversion of a sample of the alcohol into the Mosher's acid ester followed by GC analysis showed the product had been obtained in 78 % *ee*; the same value as obtained previously when hexane was used as solvent. Diethyl ether was then used to wash off the (*R*)-Rf-BINOL-containing species as before, the solution washed with 4M HCl, dried, concentrated *in vacuo* and the material analysed. <sup>1</sup>H and <sup>19</sup>F NMR spectroscopic analyses both showed the ligand had been recovered without degradation and optical rotation analysis of a sample of the recovered ligand showed no ligand racemisation had occurred. This final test shows the light fluororous approach can be successfully used in the allylation of benzaldehyde to yield product in high conversion and enantiopurity while allowing the ligand to be isolated, recovered and reused without loss of activity or selectivity.

#### 4.2.6 Alternative Solid Supports

To validate the requirement of FRP silica gel for the separation and recovery of (*R*)-Rf-BINOL and to investigate the method of retention, other separation media were investigated for recovery of the light fluororous ligand. Silica gel was employed along with a highly non-polar C<sub>8</sub> reverse phase silica gel, which has surface hydroxyl groups capped with C<sub>8</sub>H<sub>17</sub> hydrocarbon chains. Finally, powdered poly(tetrafluoroethylene) (PTFE) was used as a highly non-polar and fluororous solid phase. The observed retaining characteristics of each of the solid phases are detailed in Table 4.5.

Separation media	Elution with acetonitrile	Elution with diethyl ether
Powdered PTFE	Ligand/catalyst is <b>not</b> retained, no retention observed	Not required
FRP silica gel	Ligand/catalysts is retained on column, very slow orange colour movement	Ligand species is washed off column
C <sub>8</sub> reverse phase silica gel	Ligand/catalyst is <b>partially</b> retained, orange material leaching observed	Not required
Silica gel	Ligand/catalyst is <b>partially</b> retained, orange material leaching observed	Retained species only recovered using DCM/MeOH

Table 4.5. Separation of (*R*)-Rf-BINOL species post-reaction using different solid supports

The data shows that FRP silica gel is required for successful separation and recovery of the (*R*)-Rf-BINOL ligand. If C<sub>8</sub> reverse phase silica gel is used instead, the ligand-containing species is not completely retained on the column, and peaks corresponding to the binaphthyl backbone can be observed in the <sup>1</sup>H NMR spectrum of the product indicating leaching. Powdered PTFE showed almost no retention of the ligand-containing species, possibly due to the low surface area of the solid phase and only single fluorine atoms to supply the fluorophilic affinity, rather than long chain perfluoroalkyl groups in the case of FRP silica gel. Leaching of a ligand-containing species was also observed in the case of silica gel using acetonitrile as elutant, but elution with diethyl ether failed to wash off the remaining species from the column. As for the non-fluorophilic system, methanol could be used to recover the material, which was shown to contain Rf-BINOL and butyl groups by <sup>1</sup>H NMR spectroscopy. It was suggested that the reason for the retention of some of the ligand on the silica was that the species involved had a strong interaction with the surface hydroxyl groups, strongly binding the material to the silica. By using methanol as elutant, the interaction could be overcome and the species eluted. This is of little value, however, as over half of the ligand is lost in both the BINOL and Rf-BINOL cases by co-elution with the product using acetonitrile, making the use of silica gel for ligand recovery unfeasible.

#### 4.2.7 Partition Coefficients

Although the BINOL ligands used here were not synthesised for use in fluorophilic biphasic catalysis, the partition coefficients of the ligands in a PP3/toluene biphasic system were determined to allow comparison to other systems. Around sixty milligrams of the (*R*)-enantiomers of each of the BINOL ligands were stirred in the toluene/PP3 biphasic system, allowed to separate and then aliquots of each phase taken, the solvent removed under reduced pressure and the residue analysed gravimetrically. The data obtained is outlined in Table 4.6.

Ligand <sup>a</sup>	Observation	Undissolved Ligand (mg)	Ligand in Toluene (mg)	Ligand in PP3 (mg)	Partition Coefficient <sup>c</sup>
( <i>R</i> )-BINOL	Ligand not fully dissolved <sup>b</sup>	25	46	0	100 %
( <i>R</i> )-Rf-BINOL	Ligand dissolved fully	/	44	16	73 %

<sup>a</sup> Conditions: 2.0 ml PP3, 2.0 ml toluene, rt, stir = 20 mins, settle = 20 mins, 1.0 ml of each layer analysed <sup>b</sup> Ligand at interface <sup>c</sup> % in toluene phase

Table 4.6. Partition coefficient data for BINOL ligands in a toluene/PP3 biphasic system

As expected, neither ligand was preferentially soluble in the fluorous phase, with both ligands being partitioned selectively in the toluene phase.

### 4.3 Conclusions

It is clear from the data obtained that (*R*)-Rf-BINOL is a successful ligand in Lewis acid-catalysed addition reactions and gives similar product conversions and *ee*'s to (*R*)-BINOL. Due to the requirement of an acid wash to quench the reaction after the alkylation of benzaldehyde using diethylzinc, successful ligand and product separation could not be achieved when either (*R*)-BINOL or (*R*)-Rf-BINOL was used as ligand in this reaction. However, for the addition of an allyl group to benzaldehyde using allyltri-*n*-butyltin, an acid wash is not essential after reaction and so solid phase extraction can be used directly. For the non-fluorous system, elution of the product using acetonitrile from a silica gel solid phase support occurs with the elution of a BINOL-containing species and product contamination. To recover the ligand successfully, an alternative separation technique would, therefore, also need to be employed, such as distillation or column chromatography. The same outcome is observed if FRP silica gel is used as the solid phase. For the Rf-BINOL system, however, when dichloromethane is used as reaction solvent, the use of acetonitrile as elutant during solid-phase separation allows the ligand and product to be successfully separated using FRP silica gel. Then, with elution using diethyl ether followed by an acid wash, free (*R*)-Rf-BINOL can be recovered and reused in further catalysis without loss of activity or selectivity. This same outcome cannot be achieved if silica gel, C<sub>8</sub>-reverse phase silica gel or powdered PTFE are used as solid supports, with leaching of the ligand-based species and contamination of the product occurring in all cases. Switching the reaction solvent to hexane still allows ligand and product separation to be achieved, but the product *ee*'s are increased to levels comparable to those obtained in the non-fluorous system.

A schematic representation of the process used to isolate pure product and ligand that can be reused in catalysis is given in Figure 4.20.

Finally, partition coefficient data shows both the fluoros and non-fluorous ligands are preferentially soluble in the organic phase, which makes them incompatible with liquid-liquid extraction and fluoros biphasic catalysis methodologies for ligand recycle.

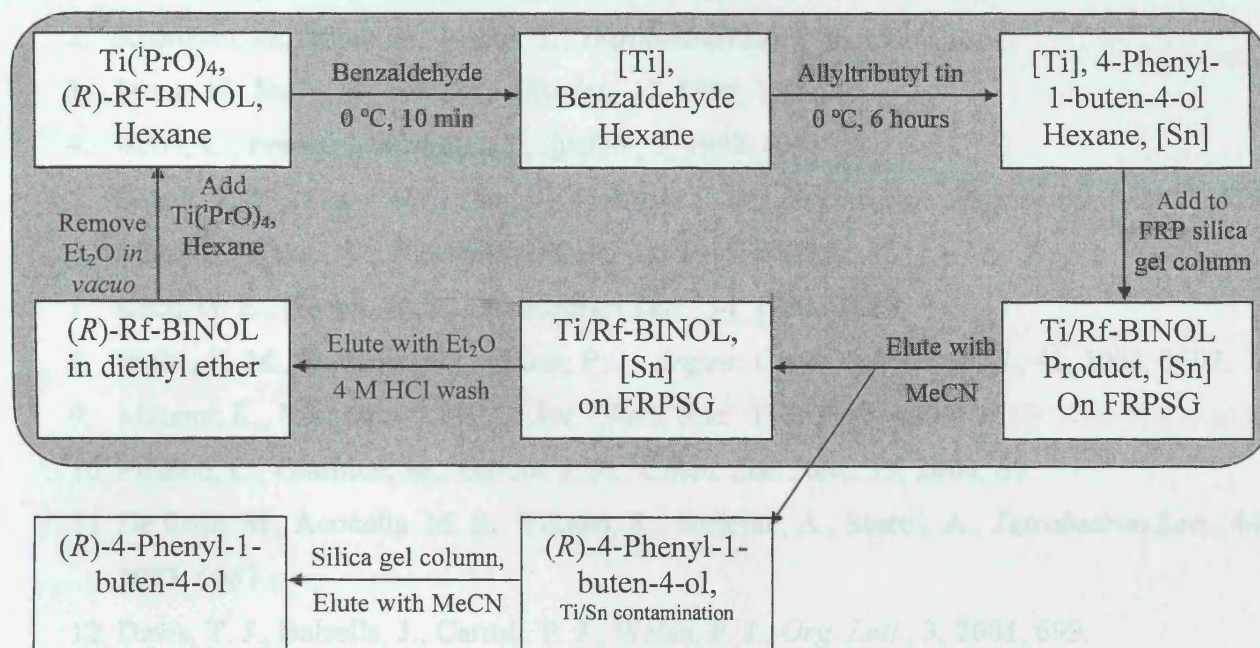


Figure 4.20

#### 4.4 References for Chapter Four

1. Corma, A., Garcia, H., *Chem. Rev.*, 103, **2003**, 4307
2. Kitamoto, D., Imma, H., Nakai, T., *Tetrahedron Lett.*, 36, **1995**, 1861.
3. Imma, H., Mori, M., Nakai, T., *Synlett*, 12, **1996**, 1229.
4. Bolm, C., Felder, M., Müller, J., *Synlett.*, 5, **1992**, 439.
5. Zhang, F.-Y., Yip, C.-W., Cao, R., Chan, A. S. C., *Tetrahedron: Asymmetry*, 8, **1997**, 585.
6. Mori, M., Nakai, T., *Tetrahedron Lett.*, 38, **1997**, 6233.
7. Keck, G. E., Geraci, L. S., *Tetrahedron Lett.*, 34, **1993**, 7827.
8. Waltz, K. M., Gavenonis J., Walsh, P. J., *Angew. Chem. Int. Ed. Engl.*, 41, **2002**, 3697.
9. Mikami, K., Matsukawa, M., *J. Am. Chem. Soc.*, 116, **1994**, 4077.
10. Palomo, C., Oiarbide, M., Garcia, J. M., *Chem. Soc. Rev.*, 33, **2004**, 65.
11. De Rosa, M., Acocella, M. R., Villano, R., Soriente, A., Scettri, A., *Tetrahedron Lett.*, 44, **2003**, 6087.
12. Davis, T. J., Balsells, J., Carroll, P. J., Walsh, P. J., *Org. Lett.*, 3, **2001**, 699.
13. Mikami, K., Terada, M., *Tetrahedron*, 48, **1992**, 5671.
14. Mori, M., Imma, H., Nakai, T., *Tetrahedron Lett.*, 38, **1997**, 6229.
15. Guo, H., Wang, X., Ding, K., *Tetrahedron Lett.*, 45, **2004**, 2009.
16. Balsells, J., Davis, T. J., Carroll, P., Walsh, P. J., *J. Am. Chem. Soc.*, 124, **2002**, 10336.
17. Girard, C., Kagan, H. B., *Angew. Chem. Int. Ed.*, 37, **1998**, 2922.
18. Boyle, T. J., Barnes, D. L., Heppert, J. A., Morales, L., Takusagawa, F., Connolly, J. C., *Organometallics*, 11, **1992**, 1112.
19. Ikegami, S., Ichinohe, M., Takahashi, H., Yamada, Y., *Tetrahedron Lett.*, 43, **2002**, 3431.
20. Jayaprakash, D., Sasai, H., *Tetrahedron Asymmetry*, 12, **2001**, 2589.
21. Tian, Y., Yang, Q. C., Mak, T. C. W., Chan, K. S., *Tetrahedron*, 58, **2002**, 3951.
22. Nakamura, Y., Takeuchi, S., Ohgo, Y., Curran, D. P., *Tetrahedron Lett.*, 41, **2000**, 57.
23. Yin, Y.-Y., Zhao, G., Qian, Z.-S., Yin, W.-X., *J. Fluorine Chem.*, 120, **2003**, 117.
24. Liu, G. H., Tang, W. J., Fan, Q. H., *Tetrahedron*, 59, **2003**, 8603.

## Investigation of Palladium-BINAP Chemistry

### 5.1 Introduction

#### 5.1.1 Pd/BINAP Chemistry

As was explained in Chapter 2, BINAP is an exceptional ligand in a wide range of asymmetric catalyses but, due to its sensitivity to oxidation, it is largely used by industry for the manufacture of high-cost products, where loss of the expensive ligand can be tolerated. In an attempt to address the problem of ligand loss post-reaction, the investigation of the synthesis, catalysis and recovery of light fluorescent analogues of Pd-BINAP catalysts for use in asymmetric hydrogenation reactions was carried out. However, due to the highly reactive and unstable nature of the catalytically active species, it was not possible to recover an active catalyst, and only the ligand could be recovered and reused.

Clearly, to achieve this, the catalyst must have a stable resting state and be stable to oxygen and oxygen. Study of the literature for a system employing BINAP that may use such a species uncovered a hydrogenation catalyst that employed BINAP to impart the chiral influence (Figure 1.1).

## Chapter Five



“We must believe in luck. For how else can we explain the success of those we don't like?”  
- Jean Cocteau

Figure 5.1 Palladium(II) diacyl catalyst (XXIV)

It was clear that the catalyst would have no water sensitivity and, with a strongly coordinating BINAP ligand, there would be very little opportunity for ligand oxidation. In the system described, the catalyst was used in the enantioselective addition of enol allyl ethers to imines (Figure 4.2).



Figure 4.2. Michael-type addition catalyzed by a palladium(II)-BINAP catalyst (XXIV)

## 5 Investigation of Palladium BINAP Chemistry

### 5.1 Introduction

#### 5.1.1 Pd/BINAP Chemistry

As was explained in Chapter 2, BINAP is an exceptional ligand in a wide range of asymmetric catalyses but, due to its sensitivity to oxidation, it is largely used by industry for the manufacture of high-cost products, where loss of the expensive ligand can be tolerated. In an attempt to overcome the problem of ligand loss post-reaction, the investigation of the synthesis, catalysis and recovery of light fluororous analogues of Ru-BINAP catalysts for use in asymmetric hydrogenation reactions was carried out. However, due to the highly reactive and unstable nature of the catalytically active species, it was not possible to recover an active catalyst, and only the ligand could be recovered and reused.

Clearly, to achieve the recovery of an active catalyst species, the catalyst must have a stable resting state and be stable to moisture and oxygen. Study of the literature for a system employing BINAP that may use such a species uncovered a palladium-diaqua catalyst that employed BINAP to impart the chiral information (Figure 5.1).<sup>1</sup>

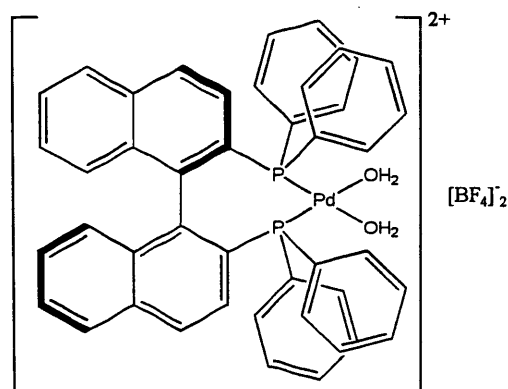


Figure 5.1. Palladium (II) diaqua catalyst (XXIV)<sup>1</sup>

It was clear that the catalyst would have no water sensitivity and, with a strongly coordinating BINAP ligand, there would be very little opportunity for ligand oxidation. In the system described,<sup>1</sup> the catalyst was used in the enantioselective addition of enol silyl ethers to imines (Figure 4.2).

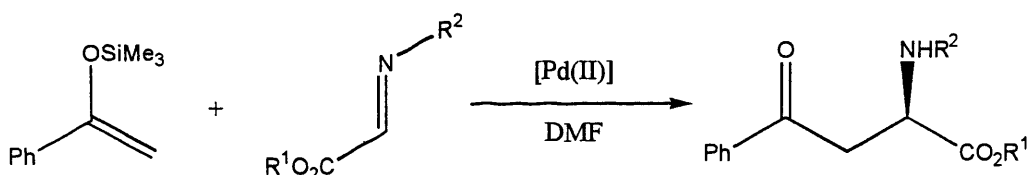


Figure 4.2. Mannich-type addition catalysed by a palladium(II)-BINAP catalyst (XXIV)

When  $R^1$  equalled *iso*-propyl and  $R^2$  equalled *para*-methoxyphenyl, the product could be obtained in 85 % yield and 67 % *ee*. Interestingly, when the temperature was decreased from 65 °C to 25 °C, the yield of product remained the same, but the *ee* fell to only 3 %. The reaction was very sensitive to other changes in reaction conditions. Adding the imine in high concentration caused a dramatic fall in the enantioselectivity, as did changing the solvent from DMF to DCM or benzotrifluoride. Preincubation of the palladium catalyst with the enol silyl ether was also required to achieve high product *ee*'s. The authors ascribed this sensitivity to a competing undesired proton-catalysed reaction which led to the racemic product.

A similar catalyst has been used in the enantioselective fluorination of various  $\beta$ -ketoesters.<sup>2</sup> For the starting material shown in Figure 5.3, a yield of product of 72 % could be achieved with an enantiomeric excess of 79 % at only 5 mol % catalyst loading. The catalyst counter-ions in this system were triflate anions rather than tetrafluoroborate anions.

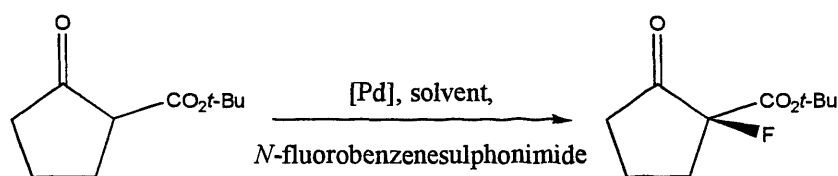


Figure 5.3. Enantioselective fluorination using a palladium(II)-BINAP catalyst

Changing the BINAP ligand to 2,2'-bis(3,5-dimethylphenylphosphino)-1,1'-binaphthyl (DM-BINAP) increased the yield to 99 % and the product *ee* to 88 %. Changing the catalyst to the similar species (XXV) (Figure 5.4) allowed a smaller catalyst loading of 2.5 mol % to be used, while the product yield and *ee* was maintained. The reaction could also be carried out at a higher temperature of 10 °C rather than -20 °C.

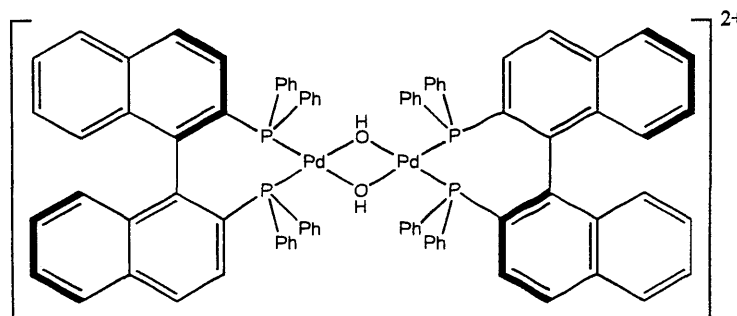


Figure 5.4. Dinuclear Palladium(II)-BINAP catalyst (XXV)

Enantioselective Michael additions using a range of enones and ketoesters have also been carried out by Sodeoka *et al.* (Figure 5.5).<sup>3</sup>

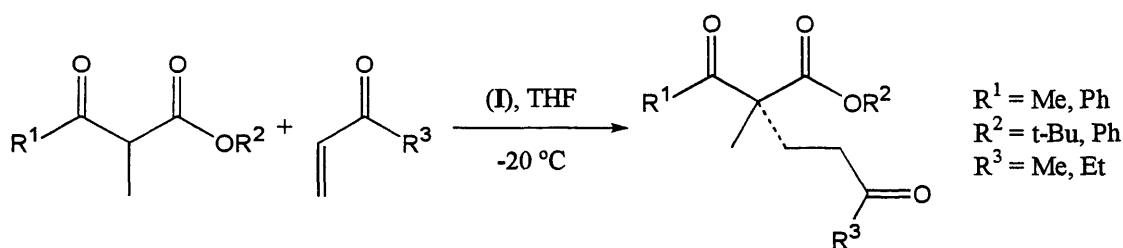


Figure 5.5. Michael addition using palladium diaqua catalyst (XXIV)

Using the palladium diaqua catalyst (XXIV) with triflate anions in place of tetrafluoroborate anions, yields of up to 93 % could be achieved with product *ee*'s of up to 92 %, depending on the ketoester and enone used. It was noted that bulky  $R^3$  groups were required to induce good enantioselectivity, which was attributed to a steric interaction of the group with the phenyl rings on the BINAP ligand, causing attack of the enolate to occur from one face of the ketoester only.

Strukul *et al.* have used palladium and platinum catalysts based on (XXV) with a range of bisphosphines, including (*R*)-BINAP, as catalysts in the addition of (*R*)-1,2-propanediol to benzaldehyde. In this reaction, two diastereomers can be formed (Figure 5.6).<sup>4</sup>

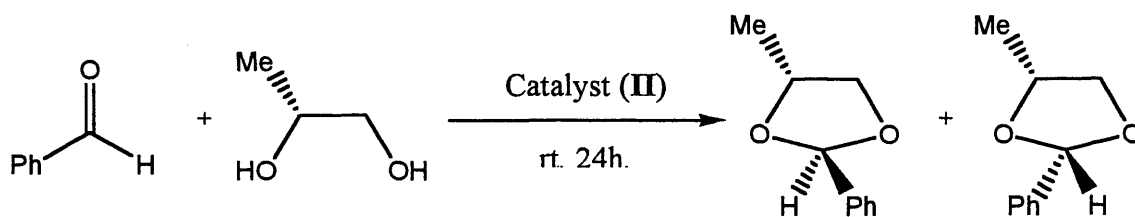


Figure 5.6. Reaction of benzaldehyde with 1,2-propanediol

Both diastereomers were formed when dppe and (*R*)-BINAP were used with a palladium metal centre. When dppe was used, conversion was 62 %, and the diastereomeric excess was 60 %. When (*R*)-BINAP was used however, the diastereomeric excess did not increase (60 %) and the conversion fell to 45 %. The results indicated the stereochemistry of the reaction was controlled mainly by the stereocentre in the 1,2-propanediol.

These examples are, to our knowledge, the only examples of the use of such catalysts in the literature. López *et al.* have studied the formation of two palladium(II) diaqua species with triphenylphosphine and triphenylarsine<sup>5</sup> and a range of crystal structures of other asymmetric palladium(II) diaqua species have been published.<sup>6,7</sup> Asymmetric palladium(II) diaqua catalysts bearing 1,2-bis(*N*-indolinyl)ethane ligands have also been used for the polymerisation of norbornene with very high activity and conversion to poly(2,3-bicyclo[2.2.1]hept-2-ene).<sup>8</sup> Methoxycarbonylation using a palladium diaqua catalyst with 1,1'-bis(diphenylphosphino)-

ferrocene (dppf) and 1,1'-bis(diphenylphosphino)octamethylferrocene (dppomf) ligands has also been studied (Figure 5.7).<sup>9</sup>

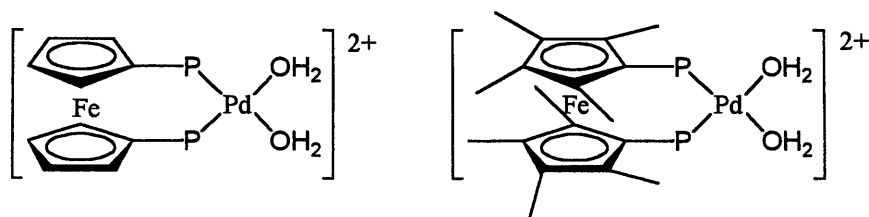


Figure 5.7. Dppf and dppomf palladium diaqua catalysts

When dppomf was used, methyl propanoate was the only product formed, but when dppf was used, a range of similar products were obtained. This reactivity was found to be due to the formation of an Fe-Pd bond in the catalyst with dppomf ligands which forced the phosphorus atoms to adopt a *trans*-orientation around the metal centre. A species that did not react with ethene in methanol was thus formed which led to the production of methyl propanoate only. However, these are not examples of asymmetric catalysis and, discounting the BINAP-based systems, there are no other examples where asymmetric catalysis has been achieved. With such a dearth of literature on these apparently active and selective BINAP-based catalysts, a study of the synthesis and use of a light fluororous analogue of the catalyst seemed novel and worthwhile.

### 5.1.2 Recyclable Pd(II)-Diaqua Catalysts

Despite the lack of literature on the system, one example of the recovery and recycle of palladium-diaqua catalysts after an aldol-type addition reaction has been investigated.<sup>10</sup> Here, a polystyrene-supported  $[\text{Pd}(\text{H}_2\text{O})_2((R)\text{-BINAP})][\text{BF}_4]_2$  catalyst bound by a hydrocarbon chain attached to the 6-position on one of the naphthyl rings was used in the asymmetric addition of 1-phenyl-1-trimethylsilyloxyethane to benzaldehyde (Figure 5.8).

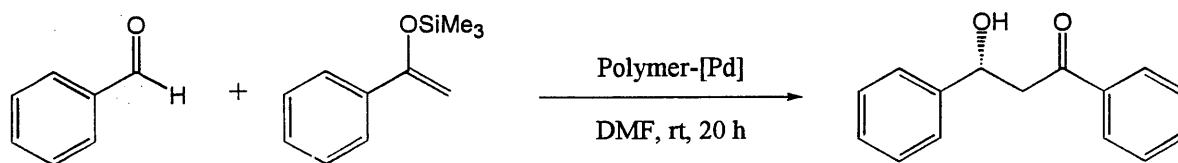


Figure 5.8. Aldol-type addition using polymer-supported palladium(II) catalyst

Using 5 mol % of the supported catalyst in the reaction led to 94 % conversion to product with 74 % *ee* after 20 hours at room temperature. Recovery of the catalyst was easily achieved by filtration of the mixture and reuse of the isolated supported catalyst in a second run led to the

formation of product in 81 % yield and 71 % *ee*. However, it was necessary to double the reaction time in order to achieve this conversion and *ee*, indicating the loss of catalyst activity after recycling. It was also noted that the addition of 0.2 equivalents of water was required in order for the catalyst to be highly active. Running the reaction without the addition of water led to a conversion of only 35 % to product after 35 hours, although the product *ee* was very similar.

It is clear from this system that the catalyst can be recovered without destruction of the catalyst species and reused in further catalysis. However, only one recycle attempt was reported and a loss of activity of 50 % was recorded. Although the authors state optimisation is required, it would seem that the loss of activity is a factor of the use of a polymer support and the formation of inactive species.

As stated previously, the use of polymer-supported catalysts is often disadvantageous even though catalyst recovery is facile, as a reduction in catalyst activity and selectivity is often observed. Use of a light fluoruous analogue of this catalyst may overcome these problems as the species would be homogeneous during reaction whilst containing a 'handle' which could be used for recovery post-reaction. Faced with this recovery data and the relative ease of synthesis of the catalyst, light fluoruous analogues containing (*R*)-Rf-BINAP were investigated.

## 5.2 The Synthesis of Non-Fluorous and Light Fluorous Palladium(II)-Diaqua Catalysts

The synthesis of non-fluorous analogues of the catalyst had been reported previously<sup>11</sup> and this synthetic strategy was adopted for the preparation of light fluoruous analogues of the catalyst (Figure 5.9).

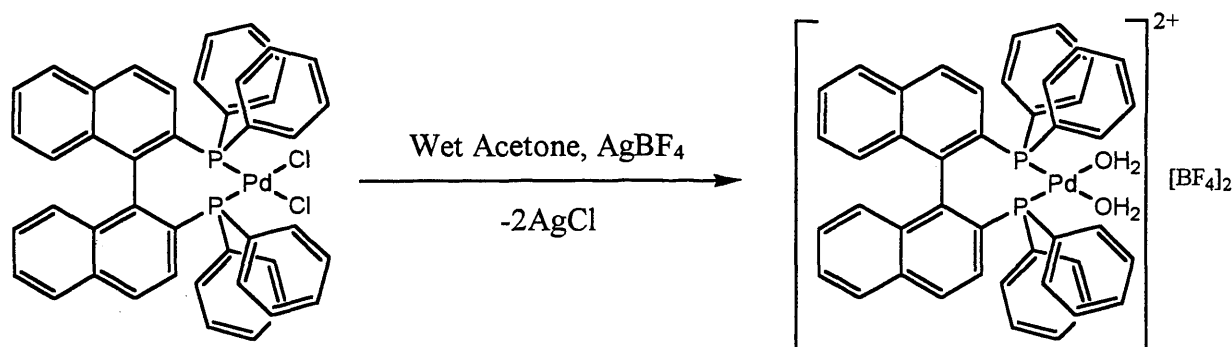


Figure 5.9. Preparation of Palladium(II) catalyst

[PdCl<sub>2</sub>((*R*)-BINAP)] or [PdCl<sub>2</sub>((*R*)-Rf-BINAP)] was treated with silver tetrafluoroborate in acetone with 5 mol% water added and stirred in sunlight for 1 hour. Black silver chloride was precipitated and the reaction mixture was filtered through celite to remove this. The yellow-green solution was then passed through a short plug of silica to remove any fine particles of silver chloride and the solvent removed under reduced pressure to yield the catalysts as yellow-green

solids, which showed broad singlets in their  $^1\text{H}$  NMR spectra indicative of bound water molecules and tetrafluoroborate peaks in their  $^{19}\text{F}$  NMR spectra. A down-field shift in the peak position indicative of phosphine was also observed in the  $^{31}\text{P}$  NMR spectra, consistent with the data reported previously.<sup>4,11</sup>

It was noted that, after storage in sunlight, the compounds turned black. Re-dissolving the catalysts in acetone and passing once more through silica gel removed the black material, and removal of the solvent under reduced pressure yielded yellow solids. A concern was raised that the catalysts may be decomposing to form palladium black, but exposure of the catalyst material to sunlight after the second filtration through silica did not produce any further black material. It was, therefore, hypothesised that additional silver chloride must have been present in the catalysts that reacted with sunlight upon storage of the catalysts. It is necessary therefore to leave the catalysts in sunlight for two days before use to show that all of the silver chloride has been removed. If not, silver salts may persist which could have a detrimental effect on subsequent catalysis.

### 5.3 Catalytic Testing and Recovery of Palladium(II)-Diaqua Catalysts

Before testing of the light fluorous analogues was attempted, it was decided that, for fair comparison, the work by Sodeoka *et al.* would be repeated with the non-fluorous catalyst synthesised here. The method of catalysis was, therefore, taken from the previous work<sup>10</sup> and followed without deviation.

Due to the high boiling point of the DMF, traces of the solvent remained after removal by distillation and were difficult to remove. It was decided that the reaction residue would be redissolved in diethyl ether and washed with water to remove the DMF solvent traces. However, upon addition of the diethyl ether solvent, a yellow-green solid precipitated out of the mixture. The solid was recovered by filtration and analysed by NMR spectroscopy and mass spectrometry and determined to be the diaqua catalyst prepared initially.

Clearly, this observation was very interesting. Although previous work on anchoring the BINAP ligand to a polymer support to allow recovery of the catalyst had been carried out, it was apparent that, for this catalytic reaction, such modifications were unnecessary. In a much more straightforward manner, the catalyst could be simply and easily recovered by precipitation.

The recovered catalyst was dried and reused in two further catalytic runs. At the end of each run, the majority of the DMF solvent was removed by distillation and diethyl ether added to precipitate the catalyst, which was recovered by filtration. The filtrate was concentrated *in vacuo* and analysed by  $^1\text{H}$  NMR spectroscopy. To determine the product *ee*, a sample was reacted with Mosher's acid chloride to form ester diastereomers, which were then analysed by  $^1\text{H}$  NMR spectroscopy (Figure 5.10). The results of the catalytic runs are given in Table 5.1.

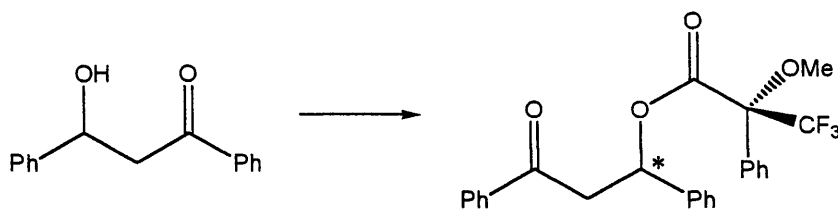


Figure 5.10. The formation of Mosher's acid ester diastereomers

Run	Conversion (%) <sup>a</sup>	<i>ee</i> (%) <sup>b</sup>	Pd Leaching (ppm (%)) <sup>c</sup>
1	> 95	50	1.09 (0.06)
2 <sup>d</sup>	90	22	0.48 (0.03)
3 <sup>d</sup>	88	0	n.d.

<sup>a</sup> Determined by <sup>1</sup>H NMR analysis <sup>b</sup> Determined by <sup>1</sup>H NMR analysis of Mosher's acid ester

<sup>c</sup> Percentage of original Pd added by weight determined by ICP spectroscopic analysis <sup>d</sup> Using catalyst isolated from previous run

Table 5.1. Asymmetric aldol condensation results

The product *ee* obtained after the first run is not as high as in previous work,<sup>10</sup> where a value of 74 % was achieved, with an isolated yield of 65 %. As the data shows, the recovered catalyst shows similar activity in subsequent reactions to the starting catalyst precursor, but the selectivity fell to zero after being recycled twice, showing the ligand was undergoing racemisation. As the starting catalyst did show selectivity, it was assumed that the ligand was being racemised during the distillation of the DMF solvent under reduced pressure and increased temperature. It was shown previously (see Chapter 2) that heating the BINAP ligands led to racemisation and loss of selectivity in further catalytic runs, and the results obtained here indicate the same process occurs for this system. To see if this was the case, a known amount of catalyst was dissolved in DMF, stirred for 20 minutes and then the solvent removed by distillation under reduced pressure. The residue was then analysed by optical rotation and compared to the optical rotation value obtained using fresh catalyst dissolved in DMF. The latter gave an optical rotation value of 432 °, while the former gave a value of just 120 °, indicating the catalyst does racemise under the distillation conditions. It was very pleasing to note, however, that palladium leaching levels into the product were exceptionally low, with less than 0.1 % detected in the products after the first and second catalytic runs.

These results are however, needless to say, disappointing. When such an easy catalyst recovery is possible, it is frustrating that the ligand undergoes racemisation and is of no further use in catalysis. It was hoped, however, that the light fluorinated BINAP ligand might be more stable to racemisation, with the extra bulk of the fluorinated ponytails. Therefore, the catalytic testing and recovery of the light fluorinated analogue of the catalyst was still investigated.

A standard asymmetric addition reaction was carried out using the light fluororous palladium diaqua catalyst and, at the end of the reaction, the DMF was removed by distillation. However, due to the highly fluorophilic nature of diethyl ether, when the solvent was added to the residue, the catalyst was not precipitated. The organic solvent was washed with water, dried and concentrated *in vacuo*. The residue was then placed onto a three-centimetre column of FRP silica gel and the product eluted with toluene. Analysis of the isolated material by  $^1\text{H}$  NMR spectroscopy showed no visible leaching of the catalyst species into the product, which had been obtained in > 95 % conversion and 48 % *ee*. Again, the product *ee* was lower than that reported previously.<sup>10</sup>

Re-isolation of the catalyst species was then attempted by elution with acetone. Analysis of the recovered material by  $^1\text{H}$ ,  $^{19}\text{F}$  and  $^{31}\text{P}$  NMR spectroscopy showed the catalyst precursor had been recovered in 90 % yield. This material was used without further purification in a second catalyst run. At the end of the reaction, the product was recovered, once more free of catalyst contamination by  $^1\text{H}$  NMR spectroscopic analysis, using FRP silica gel. The catalyst precursor was again eluted with acetone and recovered by removal of the solvent *in vacuo*. One further catalytic run was carried out using the recovered material and the results are given in Table 5.2.

Run	Conversion (%) <sup>a</sup>	<i>ee</i> (%) <sup>b</sup>	Pd Leaching (ppm (%)) <sup>c</sup>
1	> 95 %	48	1.07 (0.06)
2 <sup>d</sup>	90 %	56	0.50 (0.03)
3 <sup>d</sup>	90 %	54	0.22 (0.02)

<sup>a</sup> Determined by  $^1\text{H}$  NMR analysis <sup>b</sup> Determined by  $^1\text{H}$  NMR analysis of Mosher's acid ester

<sup>c</sup> Percentage of original Pd added by weight determined by ICP spectroscopic analysis <sup>d</sup> Using catalyst isolated from previous run

Table 5.2. Asymmetric aldol condensation results using light fluororous catalyst.

As can be seen from Table 5.2, the activity of the light fluororous analogue of the palladium(II)-diaqua catalyst compares favourably to the non-fluororous analogue, with similar conversions observed in both cases. Of greater significance, for the light fluororous system, the recovered catalyst retains its selectivity after it has been recovered and can be used in two further catalytic runs to give the product in similar *ee*. This observation is excellent, as it implies that the light fluororous analogue of the catalyst could be used in a wide range of reactions and selectively retained, recovered and reused in further catalysis using solid phase extraction with no loss of activity or selectivity. Added to this fact, the palladium leaching levels into the product are once again exceptionally low, with the total palladium leaching level at only 0.11 % by weight of the original palladium added in the catalyst. With optimisation of the conditions, it is likely that increased product enantioselectivity could be achieved, making this system highly desirable. In comparison to the previous system,<sup>10</sup> only one catalyst recycle was attempted and, to achieve

similar product yields and *ee*'s to the first run, the reaction time had to be doubled. Additionally, the isolated product yields fell from 94 % to 81 %, while a similar drop in conversion is not observed in this study. Finally, Sodeoka *et al.* do not report the palladium content of the product so a comparison of metal contamination cannot be made.

#### 5.4 Palladium Diaqua Catalysts Based on MonoPhos

Although the BINAP-based palladium diaqua catalysts proved to be successful in the asymmetric catalytic aldol reaction, it was decided that the synthesis of analogous MonoPhos-based catalysts may be possible and potentially useful. Also, as the synthesis had not been attempted previously, it was decided that a study of the synthesis may be interesting. The synthesis of MonoPhos ligands is much more facile than the synthesis of BINAP ligands and the ligand itself is more stable than BINAP (see Chapter Three). It was thought, therefore, that if a MonoPhos-based catalyst proved to be active and selective for the above aldol condensation, it may actually be a better choice than the BINAP-based catalyst.

The synthesis of a MonoPhos-based palladium(II) diaqua species was easily achieved by reaction of  $[\text{PdCl}_2((R)\text{-MonoPhos})_2]$  with silver tetrafluoroborate in wet acetone (Figure 5.11).

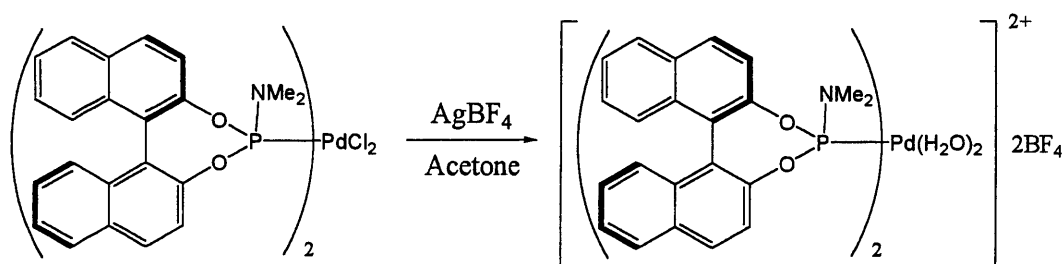


Figure 5.11. MonoPhos-based palladium(II) diaqua species

As *trans*- $[\text{PdCl}_2((R)\text{-MonoPhos})_2]$  was used as the starting material, it was assumed that the *trans*-isomer of the palladium(II) diaqua catalyst would be synthesised. The material collected was fully analysed by NMR spectroscopy and mass spectrometry and the *trans*-configuration confirmed by IR spectroscopic analysis, although satisfactory elemental analysis could not be obtained. Once more, leaving the material in sunlight caused the formation of a black material that was removed by passing an acetone solution of the catalyst precursor through a short plug of silica gel. The material was recovered by removal of the solvent *in vacuo* to yield a yellow powder.

The material was used in the catalytic asymmetric aldol condensation that had been used previously to test the BINAP-based catalysts. The reaction was carried out using the same conditions and the palladium species isolated at the end of reaction by precipitation with diethyl ether. However, analysis of the material dissolved in the organic solvent showed that no reaction

had occurred and the residue contained only peaks associated with the enol starting material and benzaldehyde. It is assumed that the reason for the non-catalytic behaviour of the moiety was because a *trans*-phosphorus species would be present during the reaction, which would not allow an interaction between bound benzaldehyde and enol silyl ether starting materials as they would also be *trans* to one another. As a result, no product would be formed and the starting materials would be re-isolated at the end of the reaction as was observed. Analysis of the recovered material showed no sign of decomposition, also indicating that the material was not catalytically active in the system, rather than not being active due to degradation.

### 5.5 Palladium Diaqua Catalysts – Conclusions

As the area of palladium diaqua catalysts is very small, there seems to be a vast area of research which could be investigated. Many organic conversions employ palladium-based catalysts, such as Heck,<sup>12</sup> Suzuki<sup>13</sup> and Stille<sup>14</sup> reactions, which often suffer from catalyst degradation and the formation of palladium black. The use of a more stable catalyst could overcome this problem whilst also adding the benefits of high reactivity and selectivity.

For the reaction studied here, the catalyst is highly active and moderately selective. When a non-fluorous catalyst is used, the catalyst, in its resting state, can be recovered by simple precipitation from the crude reaction mixture by addition of diethyl ether followed by filtration. The recovered catalyst retained its activity over three runs and there was no sign of palladium black formation, but the selectivity of the catalyst was reduced to zero after two recycles, most likely because of racemisation caused by the distillation step required to remove the DMF reaction solvent.

When the light fluorine catalyst was used in the reaction, product yields and enantiopurities similar to the non-fluorous system could be obtained. Although the catalyst could not be recovered by precipitation with diethyl ether, it could be selectively retained on a column of FRP silica gel using toluene as eluant. As the catalyst was not air or moisture sensitive, the separation could be carried out in air and the product obtained free of catalyst contamination, with less than 0.1 % palladium leaching. The catalyst in its resting state could then be removed from the column using acetone, the solvent removed under reduced pressure and the resulting solid reused in further catalysis. The catalyst material was used in three catalytic runs with no loss of activity or selectivity.

Clearly, as the light fluorine and non-fluorous catalysts were highly active and the light fluorine catalyst was recyclable, the system is ideal for exploitation in a wide range of catalyses. For systems where the recovery of an active catalyst is not required, a non-fluorous catalyst can be used and removed from the system after reaction by simple precipitation with diethyl ether, leaving

the product uncontaminated. For other systems where recovery of an active catalyst is desirable or the products are not soluble in diethyl ether, the light fluororous analogue of the catalyst could be used to yield a product potentially with the same yield and enantiopurity as could be obtained with the non-fluororous catalyst. In addition, the catalyst could then be used in further catalytic reactions and the product would again have no catalyst contamination. Other investigations of systems using this type of catalyst could prove to be very rewarding.

Finally, a MonoPhos-based example of the catalyst proved to be inactive in the catalytic reaction. The most likely reason for this observation is the orientations adapted by the modifying ligands. BINAP adopts a *cis*-conformation due to the rigidity of its structure. The MonoPhos ligands are likely to adopt a *trans*-conformation, which blocks the catalytic reaction pathway and so the palladium species is inactive in catalysis. This problem is likely to persist in any such catalytic reaction, making MonoPhos-based materials with two ligands inappropriate for such systems.

## 5.6 References

1. Fujii, A., Hagiwara, E., Sodeoka, M., *J. Am. Chem. Soc.*, 121, **1999**, 5450.
2. Hamashima, Y., Yagi, K., Takano, H., Tamás, L., Sodeoka, M., *J. Am. Chem. Soc.*, 124, **2002**, 14530.
3. Hamashima, Y., Hotta, D., Sodeoka, M., *J. Am. Chem. Soc.*, 124, **2002**, 11240.
4. Cataldo, M., Nieddu, E., Gavagnin, R., Pinna, F., Strukul, G., *J. Mol. Catal. A.: Chemical*, 142, **1999**, 305.
5. Ruiz, J., Florenciano, F., Vicente, C., Ramírez de Arellano, M. C., López, G., *Inorg. Chem. Commun.*, 3, **2000**, 73.
6. Stang, P. J., Cao, D. H., Poulter, G. T., Arif, A. M., *Organometallics*, 4, **1995**, 1110.
7. Vicente, J., Arcas, A., Blasco, M. A., Lozano, J., Ramírez de Arellano, M. C., *Organometallics*, 17, **1998**, 5374
8. Abu-Surrah, A.S., Rieger, B., *J. Mol. Catal. A.*, 128, **1998**, 239.
9. Bianchini, C., Meli, A., Oberhauser, W., van Leeuwen, P. W. N. M., Zuideveld, M. A., Freixa, Z., Kamer, P. C. J., Spek, A. L., Gusev, O. V., Kal'sin, A. M., *Organometallics*, 22, **2003**, 2409.
10. Fujii, A., Sodeoka, M., *Tetrahedron Lett.*, 40, **1999**, 8011.
11. Hagiwara, E., Miyazaki, F., Shibasaki, M., Sodeoka, M., Tokunoh, R., *Synlett.*, **1997**, 463.
12. Nakamura, I., Yamamoto, Y., *Chem. Rev.*, 104, **2004**, 2127.
13. Miyaura, N., Suzuki, A., *Chem. Rev.*, 95, **1995**, 2457.
14. Ricci, A., Lo Sterzo, C., *J. Organomet. Chem.*, 653, **2002**, 177.

# Chapter Six



**"I can take any amount of criticism, so long as it is unqualified praise."**

**- Noel Coward**

## 6 Experimental Details

### 6.1 General Procedures

#### 6.1.1 Nuclear Magnetic Resonance Spectroscopy

The  $^1\text{H}$ ,  $^{19}\text{F}$ ,  $^{31}\text{P}$  and  $^{13}\text{C}$  NMR spectra were recorded on a Bruker AM 300 at 300.14, 282.41, 121.50 and 62.90 MHz respectively or a Bruker ARX 250 spectrometer at 250.13, 235.34, 101.26 and 75.47 MHz respectively. All chemical shifts are quoted in ppm and referenced to external  $\text{SiMe}_4$  ( $^1\text{H}$ ),  $\text{CFCl}_3$  ( $^{19}\text{F}$ ), and  $\text{H}_3\text{PO}_4$  ( $^{31}\text{P}$ ) using the high frequency positive convention. Deuterated chloroform was used as a solvent unless otherwise quoted. Perfluoroalkyl chain carbon atoms were not visible in the  $^{13}\text{C}$  NMR spectra due to extensive coupling to fluorine and so are not reported.

#### 6.1.2 Mass Spectrometry

Electron impact (EI) and fast atom bombardment (FAB) mass spectra were recorded on a Kratos concept 1 H, double focussing, forward geometry mass spectrometer. 3-Nitrobenzyl alcohol was used as the matrix for the FAB spectra. Electrospray mass spectra were obtained on a Micromass Quatro LC.

#### 6.1.3 Elemental Analysis

Elemental analyses were performed by the University of North London.

#### 6.1.4 Optical Rotation

Optical rotation analyses were carried out using a Perkin Elmer 341 Polarimeter at 589 nm using a sodium/halogen lamp. Samples were dissolved in the solvent indicated.

#### 6.1.5 Enantiomeric Purity Determination

Product *ee*'s were determined either by  $^1\text{H}$  NMR of formed diastereomers or chiral HPLC and Chiral GC. Chiral HPLC was performed at the University of Nottingham using a Diacel Chiralcel OD-H column, a sample loop size of 6  $\mu\text{l}$ , 8 % IPA in hexane mobile phase at 1  $\text{ml min}^{-1}$  and a 220 nm detector. Chiral GC was either performed at the University of Nottingham using a Shimadzu GC-17A gas chromatogram fitted with a Supelco Beta Dex 225 column or at the University of Leicester using a Perkin Elmer Clarus 500 GC fitted with an SGE CYDEX-B column. Peak identities were determined by comparison to traces obtained of commercial samples.

### 6.1.6 IR Analyses

IR data was obtained using a Perkin Elmer Spectrum One FT-IR. Samples were made into a Nujol mull and pressed between polypropylene discs for analysis.

### 6.1.7 X-Ray Crystallography

X-ray crystallography data were collected on a Bruker Apex SMART 2000 diffractometer. Crystal data and structure refinement can be found in the appendix.

### 6.1.8 ICP Spectroscopy

Samples were analysed for metal content on a JY Horiba Ultima 2 sequential ICP-AES with generator power and flow rates optimised for sensitivity.

### 6.1.9 Starting Materials

Compounds were used as supplied from Sigma-Aldrich, Apollo, Lancaster or Fluorochem, whilst solvents were dried according to literature methods; PP3, ethyl acetate and dichloromethane were dried over calcium hydride whilst sodium wire was employed to dry THF, hexane, toluene and diethyl ether using a benzophenone indicator. Methanol was dried by distilling from magnesium sulphate. DMF was purchased dry from Aldrich. All solvents were stored in sealed ampoules under an atmosphere of dry nitrogen over 4Å molecular sieves. Where necessary, solvents were freeze-pump-thaw degassed at least three times prior to use. Diphenylphosphine was transferred and stored under nitrogen in an ampoule. Pyridine and triethylamine were dried over calcium hydride and distilled into dried ampoules under nitrogen. The bases were then stored under nitrogen. Trifluoromethanesulphonic anhydride was transferred under nitrogen into a dry ampoule which was sealed and stored in the refrigerator.  $[\text{PtCl}_2(\text{MeCN})_2]$ ,<sup>1</sup>  $[\text{PdCl}_2(\text{MeCN})_2]$ <sup>2</sup> and  $[\text{NiCl}_2(\text{dppe})]$ <sup>3</sup> were prepared by literature methods.

## 6.2 Experimental Details for Chapter Two

### 6.2.1 Synthesis of BINAP-based Molecules

#### Preparation of (*R*)-6,6'-Dibromo-1,1'-bi-2-naphthol ((*R*)-2.1)

(*R*)-1,1'-bi-2-naphthol (5.04 g, 17.5 mmol) was dissolved in dichloromethane (50 ml) and cooled to -78 °C with constant stirring. To this solution, bromine (2.5 ml, 48.3 mmol) in dichloromethane (10 ml) was added dropwise over ten minutes and then, with constant stirring, the solution was allowed to warm to room temperature and stirred overnight.

The excess bromine was quenched with sodium bisulphite solution (10 % solution, 50 ml) and the solid product filtered directly from the mixture (7.23 g, 93 %). M.p. 198 – 200 °C. *m/z* (ES<sup>+</sup>)

443 [M]<sup>-</sup> (100 %), 363 [M-Br]<sup>-</sup> (38 %), 285 [M-2Br]<sup>-</sup> (8 %). [ $\alpha$ ]<sub>D</sub> (CHCl<sub>3</sub>) -124 ° (*c* = 1.2).  $\delta$ <sub>H</sub> 7.25 (2H, d, <sup>3</sup>*J*<sub>HH</sub> 9.0 Hz, ArH), 7.65 (2H, dd, <sup>3</sup>*J*<sub>HH</sub> 9.0 Hz, <sup>4</sup>*J*<sub>HH</sub> 2.1 Hz, ArH), 7.68 (2H, d, <sup>3</sup>*J*<sub>HH</sub> 9.0 Hz, ArH), 8.16 (2H, d, <sup>3</sup>*J*<sub>HH</sub> 8.9 Hz, ArH), 8.33 (2H, d, <sup>4</sup>*J*<sub>HH</sub> 1.8 Hz, ArH), 8.35 (2H, s, ArOH).  $\delta$ <sub>C</sub> 111.11 (C), 118.41 (C), 119.39 (CH), 126.29 (CH), 130.85 (CH), 130.99 (CH), 131.07 (CH), 131.26 (C), 132.31 (C), 153.39 (C-O).

### Preparation of (*S*)-6,6'-Dibromo-1,1'-bi-2-naphthol ((*S*)-2.1)

The title compound was prepared employing the same method as outlined for compound (*R*)-2.1 above using (*S*)-1,1'-bi-2-naphthol (5.02 g, 17.5 mmol). The product was obtained as an off-white powder (6.98 g, 90 %). M.p. 198 – 200 °C *m/z* (ES<sup>-</sup>) 443 [M]<sup>-</sup> (100 %), 363 [M-Br]<sup>-</sup> (44 %), 285 [M-2Br]<sup>-</sup> (12 %). [ $\alpha$ ]<sub>D</sub> (CHCl<sub>3</sub>) +127 ° (*c* = 2.2).  $\delta$ <sub>H</sub> 7.22 (2H, d, <sup>3</sup>*J*<sub>HH</sub> 9.0 Hz, ArH), 7.64 (2H, dd, <sup>3</sup>*J*<sub>HH</sub> 9.0 Hz, <sup>4</sup>*J*<sub>HH</sub> 2.1 Hz, ArH), 7.66 (2H, d, <sup>3</sup>*J*<sub>HH</sub> 9.0 Hz, ArH), 8.17 (2H, d, <sup>3</sup>*J*<sub>HH</sub> 8.9 Hz, ArH), 8.31 (2H, d, <sup>4</sup>*J*<sub>HH</sub> 1.8 Hz, ArH), 8.35 (2H, s, ArOH).  $\delta$ <sub>C</sub> 111.20 (C), 118.42 (C), 119.39 (CH), 126.31 (CH), 130.84 (CH), 130.96 (CH), 131.02 (CH), 131.26 (C), 132.33 (C), 153.35 (C-O).

### Preparation of (*R*)-6,6'-Dibromo-2,2'-diacetoxy-1,1'-binaphthyl ((*R*)-2.2)

Acetic anhydride (1.39 g, 13.6 mmol) was added dropwise to a stirring dichloromethane solution of 6,6'-dibromo-1,1'-bi-2-naphthol, (3.04 g, 6.8 mmol in 50 ml solvent), triethylamine (4.19 g, 40.8 mmol) and DMAP (0.01 g, 0.08 mmol). The solution was refluxed for one hour. After cooling to room temperature, the solution was washed with 1M hydrochloric acid (50 ml), 5 % w/w sodium carbonate solution (50 ml) and water (50 ml), dried (MgSO<sub>4</sub>), filtered and the solvent evaporated under reduced pressure. The residue was washed with hexane to yield the title compound as an off-white solid, which was recrystallised from ethanol (2.52 g, 70 %). M.p. 173 – 174 °C. *m/z* (FAB) 529 [MH]<sup>+</sup> (14 %), 486 [MH-COCH<sub>3</sub>]<sup>+</sup> (14 %). [ $\alpha$ ]<sub>D</sub> (CHCl<sub>3</sub>) -33.7 ° (*c* = 6.4). Elemental analysis (expected (found)) C 54.55 (54.71), H 3.03 (2.89).  $\delta$ <sub>H</sub> 1.84 (6H, s, COCH<sub>3</sub>), 7.05 (2H, d, <sup>3</sup>*J*<sub>HH</sub> 9.0 Hz, ArH), 7.49 (2H, dd, <sup>3</sup>*J*<sub>HH</sub> 9.0 Hz, <sup>4</sup>*J*<sub>HH</sub> 1.8 Hz, ArH), 7.64 (2H, d, <sup>3</sup>*J*<sub>HH</sub> 9.0 Hz, ArH), 8.14 (2H, d, <sup>3</sup>*J*<sub>HH</sub> 9.0 Hz, ArH), 8.32 (2H, d, <sup>4</sup>*J*<sub>HH</sub> 1.8 Hz, ArH).  $\delta$ <sub>C</sub> 20.91 (CH<sub>3</sub>), 120.48 (C), 123.50 (CH), 123.62 (C), 128.15 (C), 129.24 (CH), 130.50 (CH), 130.69 (CH), 132.11 (C), 133.01 (C), 147.44 (C), 169.53 (C-O).

### Preparation of (*S*)-6,6'-Dibromo-2,2'-diacetoxy-1,1'-binaphthyl ((*S*)-2.2)

The title compound was prepared in a similar manner to compound (*R*)-2.2 above using (*S*)-6,6'-dibromo-1,1'-binaphthol (3.12 g, 7 mmol). The product was isolated after recrystallisation from ethanol as a white powder (2.81 g, 77 %). M.p. 171 – 172 °C. *m/z* (ES<sup>+</sup>) 528 [M]<sup>+</sup> (33 %), 485 [M-C(O)CH<sub>3</sub>]<sup>+</sup> (29 %). [ $\alpha$ ]<sub>D</sub> (CHCl<sub>3</sub>) 69.2 ° (*c* = 1.4). Elemental analysis (expected (found)) C

54.55 (54.62), H 3.03 (2.90).  $\delta_{\text{H}}$  1.83 (6H, s, COCH<sub>3</sub>), 7.04 (2H, d,  $^3J_{\text{HH}}$  9.2 Hz, ArH), 7.49 (2H, dd,  $^3J_{\text{HH}}$  9.0 Hz,  $^4J_{\text{HH}}$  2.1 Hz, ArH), 7.64 (2H, d,  $^3J_{\text{HH}}$  9.0 Hz, ArH), 8.15 (2H, d,  $^3J_{\text{HH}}$  8.7 Hz, ArH), 8.30 (2H, d,  $^4J_{\text{HH}}$  1.8 Hz, ArH).  $\delta_{\text{C}}$  20.93 (CH<sub>3</sub>), 120.45 (C), 123.46 (CH), 123.59 (C), 128.17 (C), 129.26 (CH), 130.54 (CH), 130.66 (CH), 132.13 (C), 133.04 (C), 147.43 (C), 169.53 (C-O).

### Preparation of (*R*)-6,6'-Bis-(perfluoro-*n*-hexyl)-2,2'-diacetoxy-1,1'-binaphthyl ((*R*)-2.3)

A mixture of (*R*)-6,6'-dibromo-2,2'-diacetoxy-1,1'-binaphthyl (2.02 g, 3.83 mmol), perfluoro-*n*-hexyl iodide (5.02 g, 11.3 mmol), copper powder (2.52 g, 39.7 mmol), 2,2'-bipyridine (0.24 g, 1.5 mmol), fluorobenzene (50 ml) and DMSO (50 ml) was stirred for 72 h at 80 °C. After cooling to room temperature, the reaction mixture was diluted with water (150 ml) and diethyl ether (150 ml) and filtered. The organic layer was separated, washed with 1M HCl (3 x 100 ml) and water (3 x 100 ml), dried (MgSO<sub>4</sub>), filtered and the solvent removed under reduced pressure to yield a yellow oil. The oil was purified by column chromatography (silica gel, ethyl acetate:hexane = 1:9) and the resulting yellow oil solidified by prolonged drying under vacuum. The product was recrystallised from hexane to yield an off-white powder (3.49 g, 68 %). M.p. 98 - 100 °C. *m/z* (FAB) 1007 [MH]<sup>+</sup> (8 %).  $[\alpha]_{\text{D}}$  (CHCl<sub>3</sub>) -2.7 ° (*c* = 5.7). Elemental analysis (expected (found)) C 42.94 (42.84), H 1.59 (1.75).  $\delta_{\text{H}}$  1.81 (6H, s, COCH<sub>3</sub>), 6.93 (2H, d,  $^3J_{\text{HH}}$  9.0 Hz, ArH), 7.24 (2H, d,  $^3J_{\text{HH}}$  9.0 Hz, ArH), 7.41 (2H, d,  $^3J_{\text{HH}}$  9.0 Hz, ArH), 7.85 (2H, d,  $^3J_{\text{HH}}$  9.0 Hz, ArH), 8.08 (2H, s, ArH).  $\delta_{\text{F}}$  -81.31 (6F, t,  $^4J_{\text{FF}}$  10.61 Hz, CF<sub>3</sub>), -110.70 (4F, tm,  $^4J_{\text{FF}}$  14.1 Hz,  $\alpha$ -CF<sub>2</sub>), -121.89 (4F, um,  $\alpha$ -CF<sub>2</sub>), -121.95 (4F, um, CF<sub>2</sub>), -123.17 (4F, um, CF<sub>2</sub>), -126.52 (4F, um, CF<sub>2</sub>).  $\delta_{\text{C}}$  20.85 (CH<sub>3</sub>), 123.36 (C), 123.92 (CH), 123.95 (t,  $^3J_{\text{CF}}$  6.3 Hz, CH), 126.79 (t,  $^2J_{\text{CF}}$  25.2 Hz, C-CF<sub>2</sub>), 127.10 (CH), 128.43 (t,  $^3J_{\text{CF}}$  7.1 Hz, CH), 130.79 (C), 131.24 (CH), 135.03 (C), 149.11 (C), 169.39 (C-O).

### Preparation of (*S*)-6,6'-Bis-(perfluoro-*n*-hexyl)-2,2'-diacetoxy-1,1'-binaphthyl ((*S*)-2.3)

The title compound was prepared similarly to compound (*R*)-2.3 above using a mixture of (*S*)-6,6'-dibromo-2,2'-diacetoxy-1,1'-binaphthyl (2.04 g, 3.83 mmol), perfluoro-*n*-hexyl iodide (5.07 g, 11.3 mmol), copper powder (2.50 g, 39.7 mmol), 2,2'-bipyridine (0.24 g, 1.5 mmol), fluorobenzene (50 ml) and DMSO (50 ml). A yellow oil was obtained which was purified by column chromatography (silica gel, ethyl acetate:hexane = 1:9) to yield a yellow oil which did not solidify even after prolonged drying (2.23 g, 58 %). *m/z* (FAB) 1007 [MH]<sup>+</sup> (14 %).  $[\alpha]_{\text{D}}$  (CHCl<sub>3</sub>) 4.1 ° (*c* = 1.2). Elemental analysis (expected (found)) C 42.94 (42.72), H 1.59 (1.50).  $\delta_{\text{H}}$  1.83 (6H, s, COCH<sub>3</sub>), 7.45 (2H, d,  $^3J_{\text{HH}}$  9.0 Hz, ArH), 7.74 (2H, d,  $^3J_{\text{HH}}$  9.0 Hz, ArH), 7.89 (2H, d,  $^3J_{\text{HH}}$  9.0 Hz, ArH), 8.51 (2H, d,  $^3J_{\text{HH}}$  9.0 Hz, ArH), 8.61 (2H, s, ArH).  $\delta_{\text{F}}$  -81.17 (6F, t,  $^4J_{\text{FF}}$  10.61 Hz, CF<sub>3</sub>), -110.70 (4F, tm,  $^4J_{\text{FF}}$  14.2 Hz,  $\alpha$ -CF<sub>2</sub>), -121.86 (8F, um, CF<sub>2</sub>), -123.17 (4F, um, CF<sub>2</sub>), -126.52 (4F, um, CF<sub>2</sub>).  $\delta_{\text{C}}$  20.82 (CH<sub>3</sub>), 123.46 (C), 123.92 (CH), 123.95 (t,  $^3J_{\text{CF}}$  6.3 Hz, CH), 126.72 (t,  $^2J_{\text{CF}}$

25.2 Hz, C-CF<sub>2</sub>), 127.16 (CH), 128.47 (t, <sup>3</sup>J<sub>CF</sub> 7.1 Hz, CH), 130.76 (C), 131.28 (CH), 135.08 (C), 149.18 (C), 169.49 (C-O).

#### Preparation of (*R*)-6,6'-Bis-(perfluoro-*n*-hexyl)-1,1'-bi-2-naphthol ((*R*)-2.4)

Sodium ethoxide (0.50 g, 7.4 mmol) was added to a stirred solution of 6,6'-bis-(perfluoro-*n*-hexyl)-2,2'-diacetoxy-1,1'-binaphthyl (2.00 g, 1.9 mmol) in methanol (25 ml). After five minutes, the reaction was quenched with 2M hydrochloric acid (40 ml). The solution was extracted with dichloromethane (2 x 50 ml), the organic extracts dried over MgSO<sub>4</sub> and filtered. The solvent was removed under reduced pressure to obtain the product as an off-white solid. The pure product was obtained by recrystallisation from dichloromethane/hexane (1.79 g, 98 %). M.p. 77 – 79 °C. m/z (ES<sup>-</sup>) 922 [M]<sup>-</sup> (33 %), 921 [M-H]<sup>-</sup> (100 %). [α]<sub>D</sub> (CHCl<sub>3</sub>) -17.2 ° (c = 1.5). Elemental analysis (expected (found)) C 41.65 (41.72) H 1.30 (1.27) δ<sub>H</sub> 5.21 (2H, s, OH), 7.18 (2H, d, <sup>3</sup>J<sub>HH</sub> 9.0 Hz, ArH), 7.37 (2H, d, <sup>3</sup>J<sub>HH</sub> 9.2 Hz, ArH), 7.44 (2H, d, <sup>3</sup>J<sub>HH</sub> 9.0 Hz, ArH), 8.11 (2H, d, <sup>3</sup>J<sub>HH</sub> 9.0 Hz, ArH), 8.24 (2H, s, ArH). δ<sub>F</sub> -81.22 (6F, t, <sup>4</sup>J<sub>FF</sub> 10.7 Hz, CF<sub>3</sub>), -110.98 (4F, tm, <sup>4</sup>J<sub>FF</sub> 14.2 Hz, α-CF<sub>2</sub>), -121.88 (8F, um, CF<sub>2</sub>), -123.21 (4F, um, CF<sub>2</sub>), -126.59 (4F, um, CF<sub>2</sub>). δ<sub>C</sub> 110.96 (CH), 119.69 (C), 124.72 (t, <sup>3</sup>J<sub>CF</sub> 6.3 Hz, CH), 124.92 (C), 125.15 (t, <sup>2</sup>J<sub>CF</sub> 25.2 Hz, C-CF<sub>2</sub>), 128.64 (CH), 128.74 (t, <sup>3</sup>J<sub>CF</sub> 7.2 Hz, CH), 133.10 (C), 135.41 (CH), 155.13 (CH).

#### Preparation of (*S*)-6,6'-Bis-(perfluoro-*n*-hexyl)-1,1'-bi-2-naphthol ((*S*)-2.4)

The title compound was prepared in the same manner as for (*R*)-2.4 using (*S*)-6,6'-bis-(perfluoro-*n*-hexyl)-2,2'-diacetoxy-1,1'-binaphthyl (2.03 g 1.9 mmol). (1.76 g, 98 %). M.p. 81 – 83 °C. m/z (ES<sup>-</sup>) 922 [M]<sup>-</sup> (33 %), 921 [M-H]<sup>-</sup> (100 %). [α]<sub>D</sub> (CHCl<sub>3</sub>) 17.4 ° (c = 1.5). Elemental analysis (expected (found)) C 41.65 (41.73), H 1.30 (1.31). δ<sub>H</sub> 5.21 (2H, s, OH), 7.18 (2H, d, <sup>3</sup>J<sub>HH</sub> 9.0 Hz, ArH), 7.36 (2H, d, <sup>3</sup>J<sub>HH</sub> 9.2 Hz, ArH), 7.46 (2H, d, <sup>3</sup>J<sub>HH</sub> 9.0 Hz, ArH), 8.12 (2H, d, <sup>3</sup>J<sub>HH</sub> 9.0 Hz, ArH), 8.23 (2H, s, ArH). δ<sub>F</sub> -81.22 (6F, t, <sup>4</sup>J<sub>FF</sub> 10.66 Hz, CF<sub>3</sub>), -110.45 (4F, tm, <sup>4</sup>J<sub>FF</sub> 14.2 Hz, α-CF<sub>2</sub>), -121.86 (4F, um, CF<sub>2</sub>), -121.87 (4F, um, CF<sub>2</sub>), -123.18 (4F, um, CF<sub>2</sub>), -126.54 (4F, um, CF<sub>2</sub>). δ<sub>C</sub> 110.90 (CH), 119.66 (C), 124.76 (t, <sup>3</sup>J<sub>CF</sub> 6.3 Hz, CH), 124.94 (C), 125.13 (t, <sup>2</sup>J<sub>CF</sub> 25.2 Hz, C-CF<sub>2</sub>), 128.59 (CH), 128.75 (t, <sup>3</sup>J<sub>CF</sub> 7.2 Hz, CH), 133.19 (C), 135.40 (CH), 155.12 (CH).

#### Preparation of (*R*)-6,6'-Bis-(perfluoro-*n*-hexyl)-2,2'-di-(trifluoromethane-sulphonyloxy)-1,1'-binaphthyl ((*R*)-2.5)

Triflic anhydride (0.73 g, 2.58 mmol) was added dropwise to a solution of 6,6'-bis-(perfluoro-*n*-hexyl)-1,1'-bi-2-naphthol (1.0 g, 1.1 mmol in 50 ml solvent) and pyridine (0.15 g, 3.21 mmol) at 0 °C in dry dichloromethane and the mixture stirred for four hours. The solvent was removed under reduced pressure and the product extracted into ethyl acetate (50 ml). This solution

was then washed with 5 % hydrochloric acid (100 ml), saturated NaHCO<sub>3</sub> (100 ml), 10 % NaCl solution (100 ml) and water (100 ml). The organic phase was dried over magnesium sulphate, filtered and the solvent removed under reduced pressure. The crude product was recrystallised from hexane (1.02 g, 83 %). M.p. 120 - 122 °C. m/z (FAB) 1186 [M]<sup>+</sup> (82 %). [α]<sub>D</sub> (CHCl<sub>3</sub>) - 48.4 ° (c = 2.3). Elemental analysis (Expected (Found)) C 34.40 (34.39), H 0.84 (0.80). δ<sub>H</sub> 7.29 (2H, d, <sup>3</sup>J<sub>HH</sub> 9.0 Hz, ArH), 7.51 (2H, d, <sup>3</sup>J<sub>HH</sub> 9.2 Hz, ArH), 7.70 (2H, d, <sup>3</sup>J<sub>HH</sub> 9.2 Hz, ArH), 8.24 (2H, d, <sup>3</sup>J<sub>HH</sub> 9.0 Hz, ArH), 8.26 (2H, s, ArH). δ<sub>F</sub> -74.92 (6F, s, OSO<sub>2</sub>CF<sub>3</sub>), -81.24 (6F, t, <sup>4</sup>J<sub>FF</sub> 10.7 Hz, CF<sub>3</sub>), -111.00 (4F, tm, <sup>4</sup>J<sub>FF</sub> 13.8 Hz, α-CF<sub>2</sub>), -121.88 (8F, um, CF<sub>2</sub>), -123.18 (4F, um, CF<sub>2</sub>), -126.54 (4F, um, CF<sub>2</sub>). δ<sub>C</sub> 114.58 (C), 119.92 (CH), 122.03 (C), 124.09 (t, <sup>3</sup>J<sub>CF</sub> 6.3 Hz, CH), 126.29 (t, <sup>2</sup>J<sub>CF</sub> 25.2 Hz, C-CF<sub>2</sub>), 127.41 (CH), 130.35 (CH), 132.46 (t, <sup>3</sup>J<sub>CF</sub> 7.2 Hz, CH), 133.68 (C), 146.02 (C).

#### Preparation of (*S*)-6,6'-Bis-(perfluoro-*n*-hexyl)-2,2'-di-(trifluoromethane-sulphonyloxy)-1,1'-binaphthyl ((*S*)-2.5)

The title compound was prepared as for compound (*R*)-2.5 above using (*S*)-6,6'-bis-(perfluoro-*n*-hexyl)-1,1'-bi-2-naphthol (1.04 g, 1.1 mmol) and isolated as a yellow oil which solidified after prolonged drying under high vacuum (1.16 g, 95 %). M.p. 121 - 122 °C. m/z (FAB) 1186 [M]<sup>+</sup> (93 %). [α]<sub>D</sub> (CHCl<sub>3</sub>) 51.9 ° (c = 2.6). Elemental analysis (Expected (Found)) C 34.40 (34.36) H 0.84 (0.88). δ<sub>H</sub> 7.32 (2H, d, <sup>3</sup>J<sub>HH</sub> 9.0 Hz, ArH), 7.51 (2H, d, <sup>3</sup>J<sub>HH</sub> 9.2 Hz, ArH), 7.70 (2H, d, <sup>3</sup>J<sub>HH</sub> 9.2 Hz, ArH), 8.23 (2H, d, <sup>3</sup>J<sub>HH</sub> 9.0 Hz, ArH), 8.25 (2H, s, ArH). δ<sub>F</sub> -74.86 (6F, s, OSO<sub>2</sub>CF<sub>3</sub>), -81.24 (6F, t, <sup>4</sup>J<sub>FF</sub> 10.7 Hz, CF<sub>3</sub>), -111.00 (4F, tm, <sup>4</sup>J<sub>FF</sub> 13.9 Hz, α-CF<sub>2</sub>), -121.88 (4F, um, CF<sub>2</sub>), -121.93 (4F, um, CF<sub>2</sub>), -123.18 (4F, um, CF<sub>2</sub>), -126.54 (4F, um, CF<sub>2</sub>). δ<sub>C</sub> 114.67 (C), 119.96 (CH), 122.08 (C), 124.02 (t, <sup>3</sup>J<sub>CF</sub> 6.3 Hz, CH), 126.31 (t, <sup>2</sup>J<sub>CF</sub> 25.2 Hz, C-CF<sub>2</sub>), 127.45 (CH), 130.29 (CH), 132.41 (t, <sup>3</sup>J<sub>CF</sub> 7.2 Hz, CH), 133.41 (C), 145.97 (C).

#### Preparation of (*R*)-6,6'-Bis-(perfluoro-*n*-hexyl)-2,2'-bis-(diphenylphosphino)-1,1'-binaphthyl ((*R*)-2.6)

To a dry and degassed DMF solution of NiCl<sub>2</sub>(dppe) (0.044 g, 8.3 x 10<sup>-5</sup> mol in 50 ml) was added diphenylphosphine (0.19 g, 1.05 mmol, 0.12 ml). The solution was then heated to 150 °C for thirty minutes. A DMF solution of (*R*)-6,6'-bis(perfluoro-*n*-hexyl)-2,2'-di-trifluoromethane sulphonyl-oxy-1,1'-binaphthyl (1.02 g, 8.6 x 10<sup>-4</sup> mol) was then added. DABCO (0.38 g, 3.33 mmol) was also added at this stage. The resulting green solution was stirred at 110 °C for a further 4 h. An additional portion of diphenylphosphine (0.19 g, 1.05 mmol, 0.12 ml) was then added via a syringe. Heating and stirring was continued for 72 h.

The reaction was allowed to cool to room temperature and the DMF distilled from the reaction mixture. The resulting brown solid was stirred for thirty minutes in MeOH (50 ml) and

filtered to yield an off-white solid. The crude product was washed with methanol and dried *in vacuo*. A pure product was obtained by recrystallisation from dichloromethane/methanol. (0.32 g, 30 %). M.p. 249 – 253 °C (dec).  $m/z$  ( $ES^+$ ) 1259  $[MH]^+$  (5 %).  $[\alpha]_D$  ( $C_6H_6$ ) 104.2 ° ( $c = 1.0$ ). Elemental analysis (expected (found)) C 53.42 (53.34), H 2.39 (2.29).  $\delta_H$  6.84 – 7.36 (20H, um, Ph), 6.78 (2H, d,  $^3J_{HH}$  9.4 Hz, ArH), 7.38 (2H, d,  $^3J_{HH}$  8.5 Hz, ArH), 7.50 (2H, d,  $^3J_{HH}$  8.0 Hz, ArH), 7.93 (2H, d,  $^3J_{HH}$  8.5 Hz, ArH), 8.06 (2H, s, ArH).  $\delta_F$  -81.21 (6F, t,  $^4J_{FF}$  10.6 Hz,  $CF_3$ ), -110.75 (4F, tm,  $^4J_{FF}$  14.1 Hz,  $\alpha$ - $CF_2$ ), -121.82 (4F, um,  $CF_2$ ), -121.82 (4F, um,  $CF_2$ ), -123.16 (4F, um,  $CF_2$ ), -126.51 (4F, um,  $CF_2$ ).  $\delta_P$  -13.78 (s).  $\delta_C$  126.22 – 138.51 (Complex aromatic region).

### Preparation of (*S*)-6,6'-Bis-(perfluoro-*n*-hexyl)-2,2'-bis-(diphenylphosphino)-1,1'-binaphthyl ((*S*)-2.6)

The title compound was prepared in a similar manner to compound (*R*)-2.6 above using (*S*)-6,6'-bis(perfluoro-*n*-hexyl)-2,2'-di-trifluoromethanesulphonyloxy-1,1'-binaphthyl (0.98 g,  $8.3 \times 10^{-4}$  mol). The crude product was isolated as an off-white solid, which was recrystallised from dichloromethane/methanol to yield a white solid. (0.46 g, 44 %). M.p. 257 – 260 °C (dec).  $m/z$  ( $ES^+$ ) 1259  $[MH]^+$  (3 %).  $[\alpha]_D$  ( $CHCl_3$ ) -96.4 ° ( $c = 1.3$ ).  $\delta_H$  6.84 – 7.36 (20H, um, Ph), 6.78 (2H, d,  $^3J_{HH}$  9.4 Hz, ArH), 7.38 (2H, d,  $^3J_{HH}$  8.5 Hz, ArH), 7.50 (2H, d,  $^3J_{HH}$  8.0 Hz, ArH), 7.93 (2H, d,  $^3J_{HH}$  8.5 Hz, ArH), 8.06 (2H, s, ArH).  $\delta_F$  -81.23 (6F, t,  $^4J_{FF}$  10.6 Hz,  $CF_3$ ), -110.74 (4F, tm,  $^4J_{FF}$  14.1 Hz,  $\alpha$ - $CF_2$ ), -121.80 (8F, um,  $CF_2$ ), -123.16 (4F, um,  $CF_2$ ), -126.51 (4F, um,  $CF_2$ ).  $\delta_P$  -13.52 (s).  $\delta_C$  126.22 – 138.53 (Complex aromatic region).

### Preparation of (*R*)-6,6'-Bis-(1*H*,2*H*-perfluoro-*n*-1-octenyl)-1,1'-bi-2-naphthol ((*R*)-2.7)

A solution of (*R*)-6,6'-dibromo-1,1'-bi-2-naphthyl (2 g, 4.5 mmol), 1*H*,1*H*,2*H*-perfluoro-*n*-1-octene (6.23 g, 18.0 mmol), Herrmann's Catalyst (100 mg,  $1 \times 10^{-4}$  mol) and NaOAc (1.02 g, 0.013 mol) in wet DMF (2 ml of water in 40 ml of DMF) was stirred under nitrogen at 120 °C for 72 hours. After cooling, the solvent was removed under reduced pressure and the residue partitioned between ethyl acetate (40 ml) and water (40 ml). The organic layer was separated, washed with water (40 ml) and brine (40 ml), dried ( $MgSO_4$ ), filtered and the solvent removed under reduced pressure to yield a yellow-brown solid, which was recrystallised from hexane (2.78 g, 63 %). M.p. 85 – 88 °C.  $m/z$  ( $ES^-$ ) 974  $[M]^-$  (48 %), 973  $[M-H]^-$  (83 %).  $[\alpha]_D$  ( $CHCl_3$ ) -89.9 ° ( $c = 1.2$ ). Elemental analysis (expected (found)) C 44.35 (44.49), H 1.64 (1.58).  $\delta_H$  5.40 (2H, bs, OH), 6.14 (2H, um, =CH), 6.91 (2H, d,  $^3J_{HH}$  8.7 Hz, ArH), 7.14 (2H, um, =CH), 7.32 (2H, um, ArH), 7.35 (2H, d,  $^3J_{HH}$  9.0 Hz, ArH), 7.86 (2H, d,  $^3J_{HH}$  9.0 Hz, ArH), 8.04 (2H, s, ArH).  $\delta_F$   $\{^1H\}$  -81.20 (6F, t,  $^4J_{FF}$  10.2 Hz,  $CF_3$ ), -111.24 (4F, tm,  $^4J_{FF}$  13.8 Hz,  $\alpha$ - $CF_2$ ), -121.95 (4F, um,  $CF_2$ ), -123.24 (4F, um,  $CF_2$ ), -123.55 (4F, um,  $CF_2$ ), -126.53 (4F, um,  $CF_2$ ).  $\delta_C$  113.10 (=CH), 117.82 (CH),

118.00 (C), 124.03 (CH), 128.41 (C), 128.56 (CH), 129.42 (CH), 131.02 (CH), 131.53 (C), 132.69 (C), 138.35 (=CH), 152.91 (C).

#### Preparation of (*S*)-6,6'-Bis-(1*H*,2*H*-perfluoro-*n*-1-octenyl)-1,1'-bi-2-naphthol ((*S*)-2.7)

The title compound was prepared similarly to compound (*R*)-2.7 above using (*S*)-6,6'-dibromo-1,1'-bi-2-naphthyl (2.02 g, 4.5 mmol). The product was obtained as a yellow solid (2.98 g, 68 %). M.p. 83 – 86 °C. *m/z* (ES-) 974 [M]<sup>-</sup> (48 %), 973 [M-H]<sup>-</sup> (83 %). Elemental analysis (expected (found)) C 44.35 (44.22), H 1.64 (1.58). [α]<sub>D</sub> (CHCl<sub>3</sub>) 78.4 ° (c = 1.4). δ<sub>H</sub> 4.85 (2H, bs, OH), 6.14 (2H, um, =CH), 6.86 (2H, d, <sup>3</sup>J<sub>HH</sub> 8.8 Hz, ArH), 7.05 (2H, um, =CH), 7.32 (2H, um, ArH), 7.35 (2H, d, <sup>3</sup>J<sub>HH</sub> 9.0 Hz, ArH), 7.86 (2H, d, <sup>3</sup>J<sub>HH</sub> 9.0 Hz, ArH), 8.04 (2H, s, ArH). δ<sub>F</sub>{<sup>1</sup>H} – 81.20 (6F, t, <sup>4</sup>J<sub>FF</sub> 10.2 Hz, CF<sub>3</sub>), -111.24 (4F, tm, <sup>4</sup>J<sub>FF</sub> 13.8 Hz, α-CF<sub>2</sub>), -121.95 (4F, um, CF<sub>2</sub>), -123.24 (4F, um, CF<sub>2</sub>), -123.55 (4F, um, CF<sub>2</sub>), -126.53 (4F, um, CF<sub>2</sub>). δ<sub>C</sub> 114.11 (=CH), 118.82 (CH), 119.00 (C), 125.08 (CH), 129.24 (C), 129.44 (CH), 129.61 (CH), 132.16 (CH), 132.53 (C), 132.69 (C), 139.35 (=CH), 153.91 (C).

#### Preparation of (*R*)-6,6'-Bis-(1*H*,2*H*-perfluoro-*n*-1-octenyl)-2,2'-di-(trifluoromethanesulphonyloxy)-1,1'-binaphthyl ((*R*)-2.8)

(*R*)-6,6'-Bis-(1*H*,2*H*-perfluoro-*n*-1-octenyl)-1,1'-bi-2-naphthol (1.02 g, 1.0 mmol) was dissolved in dry dichloromethane (50 ml) and dry pyridine (0.49 g, 6.2 mmol) added. The solution was cooled to 0 °C and trifluoromethanesulphonic anhydride (1.46 g, 5.16 mmol) added dropwise. The solution was then stirred over night.

Hydrochloric acid (5 % solution, 50 ml) was added to quench the reaction and the organic layer separated. This was washed with saturated sodium carbonate solution (50 ml), brine (50 ml) and water (50 ml), dried (MgSO<sub>4</sub>), filtered and the solvent removed to yield the crude product as a thick brown oil. This oil was washed with hexane and the solvent residues removed under vacuum to yield a yellow-brown solid. (0.88 g, 74 %). M.p. 42 – 45 °C. *m/z* (FAB) 1238 [M]<sup>+</sup> (5 %). [α]<sub>D</sub> (CHCl<sub>3</sub>) –100.8 ° (c = 1.7). Elemental analysis (expected (found)) C 36.83 (37.11), H 1.13 (1.17). δ<sub>H</sub> 6.23 (2H, um, =CH), 7.18 (2H, d, <sup>3</sup>J<sub>HH</sub> 8.7 Hz, ArH), 7.26 (2H, um, =CH), 7.47 (2H, dd, <sup>3</sup>J<sub>HH</sub> 8.97 Hz, <sup>4</sup>J<sub>HH</sub> 1.61 Hz, ArH), 7.59 (2H, d, <sup>3</sup>J<sub>HH</sub> 9.1 Hz, ArH), 7.98 (2H, s, ArH), 8.10 (2H, d, <sup>3</sup>J<sub>HH</sub> 9.1, ArH). δ<sub>F</sub>{<sup>1</sup>H} –74.84 (3F, s, SO<sub>2</sub>CF<sub>3</sub>), –81.27 (6F, t, <sup>4</sup>J<sub>FF</sub> 10.2 Hz, CF<sub>3</sub>), -111.69 (4F, tm, <sup>4</sup>J<sub>FF</sub> 13.9 Hz, α-CF<sub>2</sub>), -121.98 (4F, um, CF<sub>2</sub>), -123.28 (4F, um, CF<sub>2</sub>), -123.48 (4F, um, CF<sub>2</sub>), -126.58 (4F, um, CF<sub>2</sub>). δ<sub>C</sub> 114.62 (C), 119.52 (CH), 122.40 (C), 124.57 (CH), 126.47 (CH), 128.22 (CH), 130.85 (C), 131.34 (CH), 131.53 (=CH), 132.69 (C), 137.75 (=CH), 145.11 (C).

**Preparation of (*S*)-6,6'-Bis-(1*H*,2*H*-perfluoro-*n*-1-octenyl)-2,2'-di-(trifluoromethane sulphonyloxy)-1,1'-binaphthyl ((*S*)-2.8)**

The title compound was prepared similarly to the (*R*)-analogue above using (*S*)-6,6'-bis-(1*H*,2*H*-perfluoro-*n*-1-octenyl)-1,1'-bi-2-naphthol (2.02 g, 2.1 mmol). The product was obtained as a yellow crystalline solid. (1.66 g, 65 %). M.p. 47 – 50 °C. *m/z* (FAB) 1238 [M]<sup>+</sup> (3 %). [α]<sub>D</sub> (CHCl<sub>3</sub>) 110.9 ° (c = 1.9). Elemental analysis (expected (found)) C 36.83 (36.99), H 1.13 (1.22). δ<sub>H</sub> 6.23 (2H, um, =CH), 7.18 (2H, d, <sup>3</sup>J<sub>HH</sub> 8.7 Hz, ArH), 7.26 (2H, um, =CH), 7.47 (2H, dd, <sup>3</sup>J<sub>HH</sub> 9.0 Hz, <sup>4</sup>J<sub>HH</sub> 1.6 Hz, ArH), 7.59 (2H, d, <sup>3</sup>J<sub>HH</sub> 9.1 Hz, ArH), 7.98 (2H, s, ArH), 8.10 (2H, d, <sup>3</sup>J<sub>HH</sub> 8.9, ArH). δ<sub>F</sub>{<sup>1</sup>H} -74.91 (6F, um, CF<sub>3</sub>), -81.22 (6F, t, <sup>4</sup>J<sub>FF</sub> 10.1 Hz, CF<sub>3</sub>), -111.67 (4F, tm, <sup>4</sup>J<sub>FF</sub> 13.9 Hz, α-CF<sub>2</sub>), -121.95 (4F, um, CF<sub>2</sub>), -123.26 (4F, um, CF<sub>2</sub>), -123.48 (4F, um, CF<sub>2</sub>), -126.55 (4F, um, CF<sub>2</sub>). δ<sub>C</sub> 115.42 (C), 119.57 (CH), 122.42 (C), 124.60 (CH), 126.47 (CH), 128.22 (CH), 130.58 (C), 131.35 (CH), 131.67 (=CH), 132.71 (C), 137.67 (=CH), 145.13 (C).

**Preparation of (*R*)-6,6'-Bis-(1*H*,2*H*-perfluoro-*n*-1-octenyl)-2,2'-diphenylphosphino-1,1'-binaphthyl ((*R*)-2.9)**

To a dry DMF solution of [NiCl<sub>2</sub>(dppe)] (0.044 g, 8.3 x 10<sup>-5</sup> mol in 50 ml) was added diphenylphosphine (1.57 mmol, 0.18 ml). The solution was then heated to 150 °C for thirty minutes. A DMF solution of (*R*)-6,6'-bis-(1*H*,2*H*-perfluoro-*n*-1-octenyl)-2,2'-di-(trifluoromethane-sulphonyloxy)-1,1'-binaphthyl (1.50 g, 1.2 mmol in 40 ml) was then added. DABCO (0.38 g, 3.33 mmol) was also added at this stage. The resulting green solution was stirred at 110 °C for a further 4 h. An additional portion of diphenylphosphine (1.57 mmol, 0.18 ml) was then added via a syringe. Heating and stirring was continued for 72 h.

The reaction was allowed to cool to room temperature and the DMF distilled from the reaction mixture. The resulting brown solid was stirred for thirty minutes in MeOH (80 ml) and filtered. The crude product was washed with methanol and dried *in vacuo*. A pure product was obtained by recrystallisation from dichloromethane/MeOH. (0.32 g, 21 %). M.p. 165 – 167 °C. *m/z* (FAB) 1310 [M]<sup>+</sup> (3 %), 1125 [M-PPH<sub>2</sub>]<sup>+</sup> (69 %). [α]<sub>D</sub> (CHCl<sub>3</sub>) 18.9 ° (c = 1.7). δ<sub>H</sub> 6.05 (2H, um, =CH), 6.62 (2H, d, <sup>3</sup>J<sub>HH</sub> 8.7 Hz, ArH), 6.81 (2H, um, =CH), 6.87 – 7.16 (22H, complex aromatic region, Ph and ArH), 7.40 (2H, d, <sup>3</sup>J<sub>HH</sub> 8.1 Hz, ArH), 7.79 (2H, s, ArH), 7.84 (2H, d, <sup>3</sup>J<sub>HH</sub> 8.5 Hz, ArH). δ<sub>F</sub>{<sup>1</sup>H} -81.22 (6F, t, <sup>4</sup>J<sub>FF</sub> 10.0 Hz, CF<sub>3</sub>), -111.43 (4F, tm, <sup>4</sup>J<sub>FF</sub> 14.0 Hz, α-CF<sub>2</sub>), -121.94 (4F, um, CF<sub>2</sub>), -123.26 (4F, um, CF<sub>2</sub>), -123.64 (4F, um, CF<sub>2</sub>), -126.52 (4F, um, CF<sub>2</sub>). δ<sub>P</sub> -14.48 (s).

**Preparation of (*S*)-6,6'-Bis-(1*H*,2*H*-perfluoro-*n*-1-octenyl)-2,2'-diphenylphosphino-1,1'-binaphthyl ((*S*)-2.9)**

The title compound was prepared in a similar manner to compound (*R*)-2.9 above using (*S*)-6,6'-bis-(1*H*,2*H*-perfluoro-*n*-1-octenyl)-2,2'-di-(trifluoromethanesulphonyloxy)-1,1'-binaphthyl (1.48 g, 1.2 mmol). The crude product was collected as a pink-white solid, which was recrystallised from dichloromethane/methanol to yield the pure product. (0.31 g, 19 %). M.p. 164 – 166 °C. *m/z* (ES<sup>+</sup>) 1311 [MH]<sup>+</sup> (26 %). [α]<sub>D</sub> (CHCl<sub>3</sub>) –13.3 ° (c = 1.5). δ<sub>H</sub> 6.05 (2H, um, =CH), 6.60 (2H, d, <sup>3</sup>J<sub>HH</sub> 8.8 Hz, ArH), 6.82 (2H, um, =CH), 6.86 – 7.17 (22H, complex aromatic region, Ph and ArH), 7.40 (2H, d, <sup>3</sup>J<sub>HH</sub> 8.2 Hz, ArH), 7.79 (2H, s, ArH), 7.83 (2H, d, <sup>3</sup>J<sub>HH</sub> 8.5 Hz, ArH). δ<sub>F</sub>{<sup>1</sup>H} –81.19 (6F, t, <sup>4</sup>J<sub>FF</sub> 10.2 Hz, CF<sub>3</sub>), –111.41 (4F, tm, <sup>4</sup>J<sub>FF</sub> 14.1 Hz, α-CF<sub>2</sub>), –121.92 (4F, um, CF<sub>2</sub>), –123.22 (4F, um, CF<sub>2</sub>), –123.58 (4F, um, CF<sub>2</sub>), –126.52 (4F, um, CF<sub>2</sub>). δ<sub>P</sub> –14.47 (s).

**Preparation of (*R*)-6,6'-Bis-(1*H*,1*H*,2*H*,2*H*-perfluoro-*n*-octyl)-1,1'-bi-2-naphthol ((*R*)-2.10)**

(*R*)-6,6'-Bis-(1*H*,2*H*-perfluoro-*n*-1-octenyl)-1,1'-bi-2-naphthol (3.12 g, 3.2 mmol) was dissolved in dichloromethane (15 ml) and 10 % palladium on charcoal added (100 % by weight, 3.08 g). The mixture was added to a 50 ml autoclave and placed under a dynamic atmosphere of hydrogen (90 bar) for 18 hours.

The gas was carefully vented and the reaction mixture removed from the autoclave. The solution was passed through celite and the solvent removed under reduced pressure to yield the product as a white solid (2.89 g, 92 %). M.p. 144 - 146 °C. *m/z* (ES<sup>-</sup>) 978 [M]<sup>-</sup> (28 %). [α]<sub>D</sub> (CHCl<sub>3</sub>) –14.9 ° (c = 2.1). Elemental analysis (expected (found)) C 44.17 (44.12), H 2.05 (2.15). δ<sub>H</sub> 2.37 (4H, um, CH<sub>2</sub>), 2.98 (4H, um, CH<sub>2</sub>), 4.98 (2H, bs, OH), 7.04 (2H, d, <sup>3</sup>J<sub>HH</sub> 8.5 Hz, ArH), 7.11 (2H, dd, <sup>3</sup>J<sub>HH</sub> 8.7 Hz, <sup>4</sup>J<sub>HH</sub> 1.38 Hz, ArH), 7.33 (2H, d, <sup>3</sup>J<sub>HH</sub> 8.7 Hz, ArH), 7.67 (2H, s, ArH), 7.88 (2H, d, <sup>3</sup>J<sub>HH</sub> 9.0 Hz, ArH). δ<sub>F</sub>{<sup>1</sup>H} –81.22 (6F, t, <sup>4</sup>J<sub>FF</sub> 10.2 Hz, CF<sub>3</sub>), –114.92 (4F, tm, <sup>4</sup>J<sub>FF</sub> 14.1 Hz, α-CF<sub>2</sub>), –122.26 (4F, um, CF<sub>2</sub>), –123.26 (4F, um, CF<sub>2</sub>), –123.89 (4F, um, CF<sub>2</sub>), –126.51 (4F, um, CF<sub>2</sub>). δ<sub>C</sub> 26.29 (CH<sub>2</sub>), 32.93 (t, <sup>2</sup>J<sub>CF</sub> 21.1 Hz, CH<sub>2</sub>), 110.89 (C), 118.22 (CH), 124.83 (CH), 127.27 (CH), 128.24 (CH), 129.60 (C), 130.95 (CH), 132.25 (C), 134.78 (C), 152.62 (C).

**Preparation of (*S*)-6,6'-Bis-(1*H*,1*H*,2*H*,2*H*-perfluoro-*n*-octyl)-1,1'-bi-2-naphthol ((*S*)-2.10)**

The title compound was prepared as for compound (*R*)-2.10 above using (*S*)-6,6'-bis-(1*H*,2*H*-perfluoro-*n*-1-octenyl)-1,1'-bi-2-naphthol (2.02 g, 2.1 mmol) and 10 % palladium on charcoal (100 % by weight, 2.04 g). The product was obtained as a white solid (1.96 g, 98 %). M.p. 143 - 145 °C. *m/z* (ES<sup>-</sup>) 978 [M]<sup>-</sup> (45 %), 977 [M-H]<sup>-</sup> (68 %). [α]<sub>D</sub> (CHCl<sub>3</sub>) 19.79 ° (c = 2.2). Elemental analysis (expected (found)) C 44.17 (44.16) H 2.05 (2.13). δ<sub>H</sub> 2.35 (4H, um, CH<sub>2</sub>), 2.97 (4H, um, CH<sub>2</sub>), 4.95 (2H, bs, OH), 7.04 (2H, d, <sup>3</sup>J<sub>HH</sub> 8.5 Hz, ArH), 7.11 (2H, dd, <sup>3</sup>J<sub>HH</sub> 8.7 Hz, <sup>4</sup>J<sub>HH</sub>

1.38 Hz, ArH), 7.33 (2H, d,  $^3J_{\text{HH}}$  8.7 Hz, ArH), 7.67 (2H, s, ArH), 7.88 (2H, d,  $^3J_{\text{HH}}$  9.0 Hz, ArH).  $\delta_{\text{F}}\{^1\text{H}\}$  -81.22 (6F, t,  $^4J_{\text{FF}}$  10.2 Hz, CF<sub>3</sub>), -114.92 (4F, tm,  $^4J_{\text{FF}}$  14.2 Hz,  $\alpha$ -CF<sub>2</sub>), -122.26 (4F, um, CF<sub>2</sub>), -123.26 (4F, um, CF<sub>2</sub>), -123.89 (4F, um, CF<sub>2</sub>), -126.51 (4F, um, CF<sub>2</sub>).  $\delta_{\text{C}}$  25.27 (CH<sub>2</sub>), 31.90 (t,  $^2J_{\text{CF}}$  21.9 Hz, CH<sub>2</sub>), 109.92 (C), 117.21 (CH), 123.84 (CH), 126.25 (CH), 127.21 (CH), 128.58 (C), 129.90 (CH), 131.26 (C), 133.75 (C), 151.61 (C).

**Preparation of (*R*)-6,6'-Bis-(1*H*,1*H*,2*H*,2*H*-perfluoro-*n*-octyl)-2,2'-di-(trifluoromethanesulphonyloxy)-1,1'-binaphthyl ((*R*)-2.11)**

Triflic anhydride (0.73 g, 2.58 mmol) was added dropwise to a solution of (*R*)-6,6'-bis-(1*H*,1*H*,2*H*,2*H*-perfluoro-*n*-octyl)-1,1'-bi-2-naphthyl (1.02 g, 1.0 mmol) and dry pyridine (0.15 g, 3.21 mmol) at 0 °C in dry dichloromethane and the mixture stirred for four hours. The solvent was removed under reduced pressure and the product extracted into ethyl acetate (50 ml). This solution was then washed with 5 % hydrochloric acid (100 ml), saturated NaHCO<sub>3</sub> (100 ml), 10 % NaCl solution (100 ml) and water (100 ml). The organic phase was dried over sodium sulphate, filtered and the solvent removed under reduced pressure. The crude product was recrystallised from hexane to yield an off-white solid (1.64 g, 75 %). M.p. 74 – 76 °C. *m/z* (FAB) 1242 [M]<sup>+</sup> (3 %).  $[\alpha]_{\text{D}}$  (CHCl<sub>3</sub>) -32.4 ° (c = 0.6). Elemental analysis (expected (found)) C 36.71 (36.81), H 1.45 (1.36).  $\delta_{\text{H}}$  2.39 (4H, um, CH<sub>2</sub>), 3.01 (4H, um, CH<sub>2</sub>), 7.12 (2H, d,  $^3J_{\text{HH}}$  8.5 Hz, ArH), 7.17 (2H, d,  $^3J_{\text{HH}}$  8.7 Hz, ArH), 7.53 (2H, d,  $^3J_{\text{HH}}$  8.9 Hz, ArH), 7.74 (2H, s, ArH), 7.91 (2H, d,  $^3J_{\text{HH}}$  9.0 Hz, ArH).  $\delta_{\text{F}}\{^1\text{H}\}$  -74.99 (6F, s, SO<sub>2</sub>CF<sub>3</sub>), -81.28 (6F, t,  $^4J_{\text{FF}}$  10.1 Hz, CF<sub>3</sub>), -114.90 (4F, tm,  $^4J_{\text{FF}}$  13.9 Hz,  $\alpha$ -CF<sub>2</sub>), -122.29 (4F, um, CF<sub>2</sub>), -123.30 (4F, um, CF<sub>2</sub>), -123.85 (4F, um, CF<sub>2</sub>), -126.58 (4F, um, CF<sub>2</sub>).  $\delta_{\text{C}}$  25.42 (CH<sub>2</sub>), 31.48 (CH<sub>2</sub>), 118.83 (CH), 122.43 (C), 126.13 (CH), 126.35 (CH), 127.83 (CH), 130.58 (CH), 131.03 (C), 131.63 (C), 137.36 (C), 144.29 (C).

**Preparation of (*S*)-6,6'-Bis-(1*H*,1*H*,2*H*,2*H*-perfluoro-*n*-octyl)-2,2'-di-(trifluoromethanesulphonyloxy)-1,1'-binaphthyl ((*S*)-2.11)**

The title compound was prepared similarly to (*R*)-2.11 above using (*S*)-6,6'-bis-(1*H*,1*H*,2*H*,2*H*-perfluoro-*n*-octyl)-1,1'-bi-2-naphthyl (1.0 g, 1.0 mmol). The crude product was recrystallised from hexane to yield an off-white solid (0.96 g, 77 %). *m/z* (FAB) 1242 [M]<sup>+</sup> (29 %).  $[\alpha]_{\text{D}}$  (CHCl<sub>3</sub>) 49.51 ° (c = 1.6). Elemental analysis (expected (found)) C 36.71 (36.82), H 1.45 (1.30).  $\delta_{\text{H}}$  2.37 (4H, um, CH<sub>2</sub>), 3.01 (4H, um, CH<sub>2</sub>), 7.06 (2H, d,  $^3J_{\text{HH}}$  8.5 Hz, ArH), 7.15 (2H, dd,  $^3J_{\text{HH}}$  8.7 Hz,  $^4J_{\text{HH}}$  1.38 Hz, ArH), 7.53 (2H, d,  $^3J_{\text{HH}}$  8.7 Hz, ArH), 7.69 (2H, s, ArH), 7.86 (2H, d,  $^3J_{\text{HH}}$  9.0 Hz, ArH).  $\delta_{\text{F}}\{^1\text{H}\}$  -74.93 (6F, s, SO<sub>2</sub>CF<sub>3</sub>), -81.22 (6F, t,  $^4J_{\text{FF}}$  10.2 Hz, CF<sub>3</sub>), -114.92 (4F, tm,  $^4J_{\text{FF}}$  14.0 Hz,  $\alpha$ -CF<sub>2</sub>), -122.26 (4F, um, CF<sub>2</sub>), -123.26 (4F, um, CF<sub>2</sub>), -123.89 (4F, um, CF<sub>2</sub>), -126.51 (4F, um, CF<sub>2</sub>).  $\delta_{\text{C}}$  26.42 (CH<sub>2</sub>), 32.45 (t,  $^2J_{\text{CF}}$  22.6 Hz, CH<sub>2</sub>), 119.81 (CH), 123.39 (C),

127.11 (CH), 127.32 (CH), 128.82 (CH), 131.56 (CH), 131.98 (C), 132.58 (C), 133.32 (C), 145.24 (C).

**Preparation of (*R*)-6,6'-Bis-(1*H*,1*H*,2*H*,2*H*-perfluoro-*n*-octyl)-2,2'-bis-(diphenylphosphino)-1,1'-binaphthyl ((*R*)-2.12)**

To a dry DMF solution of NiCl<sub>2</sub>(dppe) (0.088 g, 1.7 × 10<sup>-4</sup> mol in 50 ml) was added diphenylphosphine *via* syringe (0.38 g, 2.1 mmol, 0.24 ml). The solution was then heated to 150 °C for thirty minutes. A DMF solution of (*R*)-6,6'-Bis-(1*H*,1*H*,2*H*,2*H*-perfluoro-*n*-octyl)-2,2'-di-(trifluoromethane-sulphonyloxy)-1,1'-bi-2-naphthyl (2.01 g, 1.6 mmol) was then added. DABCO (0.76 g, 3.33 mmol) was also added at this stage. The resulting green solution was stirred at 110 °C for a further 4 h. An additional portion of diphenylphosphine (0.38 g, 1.05 mmol, 0.24 ml) was then added *via* a syringe. Heating and stirring was continued for 72 h.

The reaction was allowed to cool to room temperature and the DMF distilled from the reaction mixture. The resulting brown solid was stirred for thirty minutes in MeOH (50 ml) and filtered. The crude product was washed with methanol and dried *in vacuo*. A pure product was obtained by recrystallisation from 1:10 dichloromethane/methanol (1.22 g, 58 %). M.p. 205 – 207 °C. *m/z* (ES<sup>+</sup>) 1314 [M]<sup>+</sup> (8 %). [α]<sub>D</sub> (CHCl<sub>3</sub>) 64.6 ° (c = 0.9). Elemental analysis (Expected (Found)) C 54.79 (54.82), H 2.89 (2.89). δ<sub>H</sub> 2.36 (4H, um, CH<sub>2</sub>CF<sub>2</sub>), 2.88 (4H, um, CH<sub>2</sub>Ar), 6.60 (2H, d, <sup>3</sup>J<sub>HH</sub> 8.5 Hz, ArH), 6.66 (2H, d, <sup>3</sup>J<sub>HH</sub> 8.8 Hz, ArH), 6.85 – 7.25 (20H, um, PhH), 7.38 (2H, d, <sup>3</sup>J<sub>HH</sub> 9.0 Hz, ArH), 7.59 (2H, s, ArH), 7.73 (2H, d, <sup>3</sup>J<sub>HH</sub> 8.5 Hz, ArH). δ<sub>F</sub>{<sup>1</sup>H} –81.21 (6F, t, <sup>4</sup>J<sub>FF</sub> 10.2 Hz, CF<sub>3</sub>), –114.98 (4F, tm, <sup>4</sup>J<sub>FF</sub> 14.2 Hz, α-CF<sub>2</sub>), –122.21 (4F, um, CF<sub>2</sub>), –123.24 (4F, um, CF<sub>2</sub>), –123.93 (4F, um, CF<sub>2</sub>), –126.54 (4F, um, CF<sub>2</sub>). δ<sub>P</sub> –15.56 (s). δ<sub>C</sub> 25.41 (CH<sub>2</sub>), 31.80 (CH<sub>2</sub>), 125.25 – 136.19 (complex aromatic region), 161.51 (C).

**Preparation of (*S*)-6,6'-Bis-(1*H*,1*H*,2*H*,2*H*-perfluoro-*n*-octyl)-2,2'-bis-(diphenylphosphino)-1,1'-binaphthyl ((*S*)-2.12)**

The title compound was prepared as for compound (*R*)-2.12 above, using (*S*)-6,6'-Bis-(1*H*,1*H*,2*H*,2*H*-perfluoro-*n*-octyl)-2,2'-di-(trifluoromethane-sulphonyloxy)-1,1'-binaphthyl (1.03 g, 0.83 mmol). (0.25 g, 23 %). M.p. 203 – 205 °C. *m/z* (ES<sup>+</sup>) 1315 [MH]<sup>+</sup> (35 %). [α]<sub>D</sub> (CHCl<sub>3</sub>) –58.5 ° (c = 0.7). δ<sub>H</sub> 2.26 (4H, um, CH<sub>2</sub>CF<sub>2</sub>), 2.88 (4H, um, CH<sub>2</sub>Ar), 6.60 (2H, d, <sup>3</sup>J<sub>HH</sub> 8.5 Hz, ArH), 6.65 (2H, d, <sup>3</sup>J<sub>HH</sub> 8.8 Hz, ArH), 6.90 – 7.21 (20H, um, PhH), 7.35 (2H, d, <sup>3</sup>J<sub>HH</sub> 9.0 Hz, ArH), 7.57 (2H, s, ArH), 7.76 (2H, d, <sup>3</sup>J<sub>HH</sub> 8.5 Hz, ArH). δ<sub>F</sub>{<sup>1</sup>H} –81.23 (6F, t, <sup>4</sup>J<sub>FF</sub> 10.2 Hz, CF<sub>3</sub>), –114.94 (4F, tm, <sup>4</sup>J<sub>FF</sub> 14.2 Hz, α-CF<sub>2</sub>), –122.22 (4F, um, CF<sub>2</sub>), –123.24 (4F, um, CF<sub>2</sub>), –123.91 (4F, um, CF<sub>2</sub>), –126.53 (4F, um, CF<sub>2</sub>). δ<sub>P</sub> –15.56 (s). δ<sub>C</sub> 25.43 (CH<sub>2</sub>), 31.84 (CH<sub>2</sub>), 125.20 – 136.22 (complex aromatic region), 161.54 (C).

### Preparation of (*R*)-2,2'-di-(trifluoromethane-sulphonyloxy)-1,1'-binaphthyl ((*R*)-2.13)

The title compound was prepared in the same manner as for compound 2.12 above using (*R*)-1,1'-bi-2-naphthol (3.00 g, 10.5 mmol) (2.98 g, 53 %). M.p. 80 – 82 °C. *m/z* (FAB) 550 [M]<sup>+</sup> (69 %). [α]<sub>D</sub> (CHCl<sub>3</sub>) –145.2 ° (c = 0.6). δ<sub>H</sub> 7.19 (2H, d, <sup>3</sup>J<sub>HH</sub> 8.49, ArH), 7.38 (2H, dt, <sup>3</sup>J<sub>HH</sub> 8.49, <sup>4</sup>J<sub>HH</sub> 1.2 Hz, ArH), 7.54 (2H, dt, <sup>3</sup>J<sub>HH</sub> 8.0 Hz, <sup>4</sup>J<sub>HH</sub> 1.2 Hz, ArH), 7.60 (2H, d, <sup>3</sup>J<sub>HH</sub> 9.2 Hz, ArH), 7.94 (2H, d, <sup>3</sup>J<sub>HH</sub> 8.0 Hz, ArH), 8.13 (2H, d, <sup>3</sup>J<sub>HH</sub> 9.0 Hz, ArH). δ<sub>F</sub> –75.00 (6F, s, CF<sub>3</sub>). δ<sub>C</sub> 119.31 (CH), 123.43 (C), 126.74 (CH), 127.30 (CH), 127.96 (CH), 128.33 (CH), 131.97 (CH), 132.33 (C), 133.13 (C), 145.37 (C).

### Preparation of (*S*)-2,2'-di-(trifluoromethane-sulphonyloxy)-1,1'-binaphthyl ((*S*)-2.13)

The title compound was prepared in the same manner as for compound (*R*)-2.13 above using (*S*)-1,1'-bi-2-naphthol (2.98 g, 10.5 mmol). The product was collected as a white powder (4.26 g, 77 %). M.p. 83 – 85 °C. *m/z* (FAB) 550 [M]<sup>+</sup> (57 %). [α]<sub>D</sub> (CHCl<sub>3</sub>) 142.4 ° (c = 1.0). δ<sub>H</sub> 7.17 (2H, d, <sup>3</sup>J<sub>HH</sub> 8.49, ArH), 7.39 (2H, dt, <sup>3</sup>J<sub>HH</sub> 8.49, <sup>4</sup>J<sub>HH</sub> 1.2 Hz, ArH), 7.54 (2H, dt, <sup>3</sup>J<sub>HH</sub> 8.0 Hz, <sup>4</sup>J<sub>HH</sub> 1.2 Hz, ArH), 7.61 (2H, d, <sup>3</sup>J<sub>HH</sub> 9.2 Hz, ArH), 7.91 (2H, d, <sup>3</sup>J<sub>HH</sub> 8.0 Hz, ArH), 8.13 (2H, d, <sup>3</sup>J<sub>HH</sub> 9.0 Hz, ArH). δ<sub>F</sub> –74.54 (6F, s, CF<sub>3</sub>). δ<sub>C</sub> 119.33 (CH), 123.46 (C), 126.76 (CH), 127.33 (CH), 127.99 (CH), 128.36 (CH), 132.01 (CH), 132.36 (C), 133.16 (C), 145.41 (C).

### Preparation of (*R*)-2,2'-bis-(diphenylphosphino)-1,1'-binaphthyl ((*R*)-BINAP) ((*R*)-2.14)

(*R*)-BINAP was prepared following the same procedure as for compound 2.12 above using (*R*)-2,2'-di-(trifluoromethane-sulphonyloxy)-1,1'-binaphthyl (2.04 g, 3.6 mmol). (1.42 g, 62 %). M.p. 240 – 242 °C. *m/z* (FAB) 623 [MH]<sup>+</sup> (8 %). [α]<sub>D</sub> (CHCl<sub>3</sub>) 224 ° (c = 1.2). δ<sub>H</sub> 6.73 – 7.83 (complex aromatic region, 32 H, binaphthyl backbone and PPh<sub>2</sub> groups). δ<sub>P</sub> –15.54 (s).

### Preparation of (*S*)-2,2'-bis-(diphenylphosphino)-1,1'-binaphthyl ((*S*)-BINAP) ((*S*)-2.14)

(*S*)-BINAP was prepared following the same procedure as for compound (*R*)-2.14 above using (*S*)-2,2'-di-(trifluoromethane-sulphonyloxy)-1,1'-binaphthyl (1.97 g, 3.6 mmol). (1.82 g, 81 %). M.p. 239 – 241 °C. *m/z* (ES<sup>+</sup>) 623 [MH]<sup>+</sup> (11 %). [α]<sub>D</sub> (CHCl<sub>3</sub>) –229 ° (c = 1.0). δ<sub>H</sub> 6.73 – 7.83 (complex aromatic region, 32 H, binaphthyl backbone and PPh<sub>2</sub> groups). δ<sub>P</sub> –15.12 (s).

## 6.2.2 General Procedure for the Determination of BINAP Partition Coefficients

A known quantity of ligand was stirred for 20 minutes in dry and degassed toluene (2.0 ml) and PP3 (2.0 ml) at room temperature. The mixtures was then allowed to stand for 20 minutes before 1.0 ml of each layer was collected *via* syringe and dried to constant mass under vacuum. The

partition coefficient was determined by comparison of the amount of ligand by weight in each fraction and repeated three times to ensure accuracy.

#### Determination of (*R*)-BINAP Partition Coefficient

(*R*)-BINAP (60 mg) was used. 28 mg of ligand was found in the 1.0 ml of toluene phase. The PP3 sample contained no ligand. Partition coefficient: 100 % in toluene phase.

#### Determination of (*R*)-Rf-BINAP Partition Coefficient

(*R*)-Rf-BINAP (63 mg) was used. 19 mg of ligand was found in the 1.0 ml of toluene phase. 1 mg was found in the PP3 phase. The ligand was not completely soluble in either phase. Partition coefficient: 95 % in toluene phase, 63 % dissolved.

#### Determination of (*R*)-Rf-C<sub>2</sub>H<sub>2</sub>-BINAP Partition Coefficient

(*R*)-Rf-C<sub>2</sub>H<sub>2</sub>-BINAP (58 mg) was used. 24 mg of ligand was found in the 1.0 ml of toluene phase. 1 mg was found in the PP3 phase. The ligand was not completely soluble in either phase. Partition coefficient: 95 % in toluene phase, 72 % dissolved.

#### Determination of (*R*)-Rf-C<sub>2</sub>H<sub>4</sub>-BINAP Partition Coefficient

(*R*)-Rf-C<sub>2</sub>H<sub>4</sub>-BINAP (60 mg) was used. 19 mg of ligand was found in the 1.0 ml of toluene phase. 2 mg was found in the PP3 phase. The ligand was not completely soluble in either phase. Partition coefficient: 95 % in toluene phase, 67 % dissolved.

### 6.2.3 Preparation of Coordination Complexes and Selenides

#### Preparation of [PtCl<sub>2</sub>((*R*)-Rf-BINAP)] ((*R*)-2.15)

*Cis*-[PtCl<sub>2</sub>(MeCN)<sub>2</sub>] (0.03 g, 9.5 × 10<sup>-5</sup> mol) and (*R*)-Rf-BINAP (0.12 g, 9.5 × 10<sup>-5</sup> mol) were dissolved in dry and degassed dichloromethane (35 ml) and the mixture heated to reflux under nitrogen for three hours. Upon cooling, approximately 30 ml of the solvent was removed under reduced pressure and the product precipitated from the solution by the addition of petroleum ether (b. p. 40 – 60 °C, 10 ml). The off-white solid was collected by filtration and dried *in vacuo* (98 mg, 68 %). M.p. 186 – 188 °C. *m/z* (FAB) 1489 [M-Cl]<sup>+</sup> (97 %), 1453 [M-Cl-HCl]<sup>+</sup> (100 %). [α]<sub>D</sub> (CHCl<sub>3</sub>) 264.6 ° (c = 1.6). Elemental analysis (expected (found)) C 44.09 (43.89), H 1.97 (1.91). δ<sub>H</sub> 6.62 (6H, um, PhH), 6.75 (4H, um, ArH), 7.22 (2H, d, <sup>3</sup>J<sub>HH</sub> 9.0 Hz, ArH), 7.37 – 7.51 (10H, um, PhH), 7.62 (2H, d, <sup>3</sup>J<sub>HH</sub> 8.4 Hz, ArH), 7.74 (4H, um, PhH), 7.82 (2H, s, ArH). δ<sub>F</sub> -81.12 (6F, t, <sup>4</sup>J<sub>FF</sub> 10.4 Hz, CF<sub>3</sub>), -111.11 (4F, um, α-CF<sub>2</sub>), -121.32 (2F, um, CF<sub>2</sub>), -122.69 (2F, um, CF<sub>2</sub>), -123.18 (2F, um, CF<sub>2</sub>), -126.49 (2F, um, CF<sub>2</sub>). δ<sub>P</sub> 10.79 (ss, <sup>1</sup>J<sub>Pt-P</sub> 3636 Hz).

### Preparation of [PtCl<sub>2</sub>((*S*)-Rf-BINAP)] ((*S*)-2.15)

The title compound was prepared similarly to compound (*R*)-2.15 using (*S*)-Rf-BINAP (0.12 g,  $9.5 \times 10^{-5}$  mol) and *cis*-[PtCl<sub>2</sub>(MeCN)<sub>2</sub>] (0.03 g,  $9.5 \times 10^{-5}$  mol). The product was collected as an off-white powder (89 mg, 62 %). M.p. 184 – 186 °C. *m/z* (FAB) 1489 [M-Cl]<sup>+</sup> (86 %), 1452 [M-Cl-HCl]<sup>+</sup> (59 %). [α]<sub>D</sub> (CHCl<sub>3</sub>) -271.2 ° (c = 1.6). Elemental analysis (expected(found)) C 44.09 (44.13), H 1.97 (1.82). δ<sub>H</sub> 6.62 (6H, um, PhH), 6.75 (4H, um, ArH), 7.22 (2H, d, <sup>3</sup>J<sub>HH</sub> 8.7 Hz, ArH), 7.38 – 7.51 (10H, um, PhH), 7.61 (2H, d, <sup>3</sup>J<sub>HH</sub> 9.0 Hz, ArH), 7.74 (4H, um, PhH), 7.82 (2H, s, ArH). δ<sub>F</sub> -80.67 (6F, t, <sup>4</sup>J<sub>FF</sub> 10.6 Hz, CF<sub>3</sub>), -110.63 (4F, um, α-CF<sub>2</sub>), -120.92 (4F, um, CF<sub>2</sub>), -121.33 (4F, um, CF<sub>2</sub>), -122.73 (4F, um, CF<sub>2</sub>), -126.09 (4F, um, CF<sub>2</sub>). δ<sub>P</sub> 10.78 (ss, <sup>1</sup>J<sub>Pt-P</sub> 3638 Hz).

### Preparation of [PtCl<sub>2</sub>((*R*)-Rf-C<sub>2</sub>H<sub>2</sub>-BINAP)] ((*R*)-2.16)

*Cis*-[PtCl<sub>2</sub>(MeCN)<sub>2</sub>] (31 mg,  $8.8 \times 10^{-5}$  mol) and (*R*)-Rf-C<sub>2</sub>H<sub>2</sub>-BINAP (113 mg,  $8.8 \times 10^{-5}$  mol) were dissolved in dry and degassed dichloromethane (15 ml) and the mixture heated to reflux for 3 hours under nitrogen. Upon cooling, the solvent was removed under reduced pressure and the resulting yellow crude product recrystallised from 1:10 dichloromethane/hexane to yield an off-white solid. (94 mg, 69 %). M.p. 189 – 191 °C. *m/z* (FAB) 1541 [M-Cl]<sup>+</sup> (35 %), 1505 [M-Cl-HCl]<sup>+</sup> (31 %). [α]<sub>D</sub> (CHCl<sub>3</sub>) 153.13 ° (c = 0.8). Elemental analysis (expected(found)) C 45.69 (45.53), H 2.16 (2.06). δ<sub>H</sub> 6.17 (2H, um, =CH), 6.65 (2H, d, <sup>3</sup>J<sub>HH</sub> 9.0 Hz, ArH), 6.77 (2H, um, =CH), 7.16 – 7.76 (22H, complex aromatic region, Ph and ArH), 7.50 (2H, d, <sup>3</sup>J<sub>HH</sub> 8.8 Hz, ArH), 7.58 (2H, s, ArH), 7.71 (2H, d, <sup>3</sup>J<sub>HH</sub> 8.6 Hz, ArH). δ<sub>F</sub> -80.71 (6F, t, <sup>4</sup>J<sub>FF</sub> 9.6 Hz, CF<sub>3</sub>), -111.20 (4F, um, α-CF<sub>2</sub>), -121.50 (4F, um, CF<sub>2</sub>), -122.78 (4F, um, CF<sub>2</sub>), -123.04 (4F, um, CF<sub>2</sub>), -126.05 (4F, um, CF<sub>2</sub>). δ<sub>P</sub> -10.30 (ss, <sup>1</sup>J<sub>Pt-P</sub> 3647 Hz).

### Preparation of [PtCl<sub>2</sub>((*S*)-Rf-C<sub>2</sub>H<sub>2</sub>-BINAP)] ((*S*)-2.16)

The title compound was prepared similarly to (*R*)-2.16 above using (*S*)-Rf-C<sub>2</sub>H<sub>2</sub>-BINAP (115 mg,  $8.8 \times 10^{-5}$  mol). The crude product was recrystallised from 1:10 dichloromethane/hexane to yield an off-white solid. (98 mg, 71 %). M.p. 190 – 192 °C. *m/z* (FAB) 1541 [M-Cl]<sup>+</sup> (35 %), 1505 [M-Cl-HCl]<sup>+</sup> (27 %). [α]<sub>D</sub> (CHCl<sub>3</sub>) -142.11 ° (c = 1.0). Elemental analysis (expected(found)) C 45.69 (45.59), H 2.16 (2.05). δ<sub>H</sub> 6.21 (2H, um, =CH), 6.64 (2H, d, <sup>3</sup>J<sub>HH</sub> 9.0 Hz, ArH), 6.77 (2H, um, =CH), 6.92 – 7.75 (22H, complex aromatic region, Ph and ArH), 7.52 (2H, d, <sup>3</sup>J<sub>HH</sub> 8.3 Hz, ArH), 7.70 (2H, s, ArH), 7.74 (2H, d, <sup>3</sup>J<sub>HH</sub> 8.4 Hz, ArH). δ<sub>F</sub> -81.19 (6F, t, <sup>4</sup>J<sub>FF</sub> 10.4 Hz, CF<sub>3</sub>), -111.38 (4F, um, α-CF<sub>2</sub>), -121.95 (4F, um, CF<sub>2</sub>), -123.25 (4F, um, CF<sub>2</sub>), -123.44 (4F, um, CF<sub>2</sub>), -126.50 (4F, um, CF<sub>2</sub>). δ<sub>P</sub> -10.29 (ss, <sup>1</sup>J<sub>Pt-P</sub> 3644 Hz).

**Preparation of [PtCl<sub>2</sub>((*R*)-Rf-C<sub>2</sub>H<sub>4</sub>-BINAP)] ((*R*)-2.17)**

*Cis*-[PtCl<sub>2</sub>(MeCN)<sub>2</sub>] (26 mg, 7.6 x 10<sup>-5</sup> mol) and (*R*)-Rf-C<sub>2</sub>H<sub>4</sub>-BINAP (100 mg, 7.6 x 10<sup>-5</sup> mol) were dissolved in dry and degassed dichloromethane (15 ml) and the mixture heated to reflux for 4 hours. Upon cooling, the solvent was removed under reduced pressure and the resulting yellow crude product recrystallised from dichloromethane/hexane to yield an off-white solid. (67 mg, 56 %). M.p. 181 – 184 °C. *m/z* (FAB) 1545 [M-Cl]<sup>+</sup> (93 %), 1509 [M-Cl-HCl]<sup>+</sup> (74 %). [α]<sub>D</sub> (CHCl<sub>3</sub>) 198.3 ° (c = 0.7). Elemental analysis (expected (found)) C 45.57 (45.54), H 2.41 (2.35). δ<sub>H</sub> 2.35 (4H, um, CH<sub>2</sub>CF<sub>2</sub>), 2.95 (4H, um, CH<sub>2</sub>Ar), 6.61 (6H, d, <sup>3</sup>J<sub>HH</sub> 8.8 Hz, ArH and PhH), 6.75 (2H, t, <sup>3</sup>J<sub>HH</sub> 7.3 Hz, ArH), 6.92 (2H, dd, <sup>3</sup>J<sub>HH</sub> 8.8 Hz, <sup>4</sup>J<sub>HH</sub> 2.3 Hz, ArH), 7.27 – 7.42 (12H, complex aromatic region, PhH), 7.53 (4H, um, PhH), 7.72 (4H, dt, <sup>3</sup>J<sub>HH</sub> 9.9 Hz, <sup>4</sup>J<sub>HH</sub> 2.3 Hz, ArH) δ<sub>F</sub> -80.72 (6F, t, <sup>4</sup>J<sub>FF</sub> 10.4 Hz, CF<sub>3</sub>), -114.16 (4F, um, α-CF<sub>2</sub>), -121.81 (4F, um, CF<sub>2</sub>), -122.77 (4F, um, CF<sub>2</sub>), -123.31 (4F, um, CF<sub>2</sub>), -126.04 (4F, um, CF<sub>2</sub>). δ<sub>P</sub> 9.75 (ss, <sup>1</sup>J<sub>Pt-P</sub> 3665 Hz).

**Preparation of [PtCl<sub>2</sub>((*S*)-Rf-C<sub>2</sub>H<sub>4</sub>-BINAP)] ((*S*)-2.17)**

The title compound was prepared similarly to (*R*)-2.17 above using (*S*)-Rf-C<sub>2</sub>H<sub>4</sub>-BINAP (104 mg, 7.9 x 10<sup>-5</sup> mol). The pure product was obtained as an off-white solid (82 mg, 66 %). M.p. 181 – 184 °C. *m/z* (FAB) 1545 [M-Cl]<sup>+</sup> (93 %), 1509 [M-Cl-HCl]<sup>+</sup> (74 %). δ<sub>H</sub> 2.35 (4H, um, CH<sub>2</sub>CF<sub>2</sub>), 2.95 (4H, um, CH<sub>2</sub>Ar), 6.60 (6H, d, <sup>3</sup>J<sub>HH</sub> 8.7 Hz, ArH and PhH), 6.75 (2H, t, <sup>3</sup>J<sub>HH</sub> 7.3 Hz, ArH), 6.92 (2H, dd, <sup>3</sup>J<sub>HH</sub> 8.8 Hz, <sup>4</sup>J<sub>HH</sub> 2.3 Hz, ArH), 7.27 – 7.42 (12H, complex aromatic region, PhH), 7.53 (4H, um, PhH), 7.72 (4H, dt, <sup>3</sup>J<sub>HH</sub> 9.9 Hz, <sup>4</sup>J<sub>HH</sub> 2.2 Hz, ArH) δ<sub>F</sub> -80.72 (6F, t, <sup>4</sup>J<sub>FF</sub> 9.9 Hz, CF<sub>3</sub>), -114.21 (4F, um, α-CF<sub>2</sub>), -121.81 (4F, um, CF<sub>2</sub>), -122.78 (4F, um, CF<sub>2</sub>), -123.35 (4F, um, CF<sub>2</sub>), -126.04 (4F, um, CF<sub>2</sub>). δ<sub>P</sub> 9.84 (ss, <sup>1</sup>J<sub>Pt-P</sub> 3660 Hz).

**Preparation of [PtCl<sub>2</sub>((*R*)-BINAP)]<sup>4</sup> ((*R*)-2.18)**

*Cis*-[PtCl<sub>2</sub>(MeCN)<sub>2</sub>] (56 mg, 1.61 x 10<sup>-4</sup> mol) and (*R*)-BINAP (0.10 g, 1.61 x 10<sup>-4</sup> mol) were suspended in dry and degassed dichloromethane (35 ml) and the mixture heated to reflux under nitrogen for 4 hours. Upon cooling, the solvent was removed under reduced pressure and the crude product recrystallised from 1:10 dichloromethane/hexane. The product was collected as an off-white solid (0.101 g, 70 %). M.p. 201 – 204 °C. *m/z* (ES<sup>+</sup>) 888 [M]<sup>+</sup> (9 %). [α]<sub>D</sub> (CHCl<sub>3</sub>) 37.8 ° (c = 1.2). δ<sub>H</sub> 6.49 – 7.81 (32H, complex aromatic region, binaphthol backbone and PPh<sub>2</sub> groups). δ<sub>P</sub> 9.75 (ss, <sup>1</sup>J<sub>Pt-P</sub> 3665 Hz).

**Preparation of [PtCl<sub>2</sub>((*S*)-BINAP)]<sup>4</sup> ((*S*)-2.18)**

The title compound was prepared similarly to compound (*R*)-2.18 above using (*S*)-BINAP (0.10 g, 1.61 x 10<sup>-4</sup> mol) and *cis*-[PtCl<sub>2</sub>(MeCN)<sub>2</sub>] (57 mg, 1.61 x 10<sup>-4</sup>) (0.121 g, 85 %). M.p. 204 –

206 °C.  $m/z$  ( $ES^+$ ) 888  $[M]^+$  (9 %).  $[\alpha]_D$  ( $CHCl_3$ ) 37.8 ° ( $c = 1.2$ ).  $\delta_H$  6.47 – 7.84 (32H, complex aromatic region, binaphthyl backbone and  $PPh_2$  groups).  $\delta_P$  9.73 (ss,  $^1J_{Pt-P}$  3665 Hz).

#### Preparation of $[PdCl_2((R)\text{-Rf-BINAP})]$ ((*R*)-2.19)

*Cis*- $[PdCl_2(MeCN)_2]$  (0.04 g,  $1.54 \times 10^{-4}$  mol) and (*R*)-Rf-BINAP (0.190 g,  $1.5 \times 10^{-4}$  mol) were stirred in dichloromethane for 1 hour under nitrogen. The solvent was removed under reduced pressure and the crude product recrystallised from dichloromethane/hexane to yield the title compound as a deep orange solid (0.157 g, 71 %). M.p. 235 – 237 °C (dec.).  $m/z$  (FAB) 1399  $[M-Cl]^+$  (9 %).  $[\alpha]_D$  ( $CHCl_3$ ) 380.8 ° ( $c = 1.0$ ). Elemental analysis (expected (found)) C 46.83 (47.04), H 2.09 (2.14).  $\delta_H$  6.71 (2H, d,  $^3J_{HH}$  9.1 Hz, ArH), 6.88 (6H, um, ArH and PhH), 7.24 (2H, d,  $^3J_{HH}$  9.1 Hz, Ar), 7.82 (12H, um, ArH and PhH), 7.84 (6H, um, PhH), 7.89 (2H, s, ArH).  $\delta_F$  –81.14 (6F, t,  $^4J_{FF}$  10.4 Hz,  $CF_3$ ), –111.06 (4F, um,  $\alpha$ - $CF_2$ ), –121.32 (4F, um,  $CF_2$ ), –121.71 (4F, um,  $CF_2$ ), –123.13 (4F, um,  $CF_2$ ), –126.47 (4F, um,  $CF_2$ ).  $\delta_P$  33.48 (s)

#### Preparation of $[PdCl_2((S)\text{-Rf-BINAP})]$ ((*S*)-2.19)

The title compound was prepared similarly to compound (*R*)-2.19 above using  $[PdCl_2(MeCN)_2]$  (0.04 g,  $1.54 \times 10^{-4}$  mol) and (*S*)-Rf-BINAP (0.19 g,  $1.5 \times 10^{-4}$  mol) and isolated as a deep orange solid (0.157 g, 71 %). M.p. 240 – 242 °C (dec.).  $m/z$  (FAB) 1399  $[M-Cl]^+$  (7 %).  $[\alpha]_D$  ( $CHCl_3$ ) –391.7 ° ( $c = 0.4$ ). Elemental analysis (expected (found)) C 46.83 (47.01), H 2.09 (2.16).  $\delta_H$  6.75 (2H, d,  $^3J_{HH}$  9.1 Hz, ArH), 6.81 – 6.92 (2H, um, PhH), 7.26 (2H, d,  $^3J_{HH}$  8.8 Hz, ArH), 7.33 – 7.88 (22H, um, PhH and ArH), 7.90 (2H, s, ArH).  $\delta_F$  –81.14 (6F, t,  $^4J_{FF}$  10.4 Hz,  $CF_3$ ), –111.06 (4F, um,  $\alpha$ - $CF_2$ ), –121.32 (4F, um,  $CF_2$ ), –121.71 (4F, um,  $CF_2$ ), –123.13 (4F, um,  $CF_2$ ), –126.47 (4F, um,  $CF_2$ ).  $\delta_P$  33.48 (s).

#### Preparation of $[PdCl_2((R)\text{-Rf-C}_2\text{H}_2\text{-BINAP})]$ ((*R*)-2.20)

*Cis*- $[PdCl_2(MeCN)_2]$  (0.02 g,  $7.7 \times 10^{-5}$  mol) and (*R*)-Rf- $C_2H_2$ -BINAP (0.10 g,  $7.7 \times 10^{-5}$  mol) were stirred in dichloromethane for 2 hours. The solution was filtered and hexane added to the filtrate to precipitate the product as a yellow-orange solid (82 mg, 71 %). M.p. > 300 °C.  $m/z$  (FAB) 1453  $[M-Cl]^+$  (6 %).  $[\alpha]_D$  ( $CHCl_3$ ) 316.4 ° ( $c = 0.6$ ). Elemental analysis (expected (found)) C 48.42 (48.36), H 2.29 (2.19).  $\delta_H$  6.21 (2H, um, =CH), 6.63 (2H, d,  $^3J_{HH}$  9.0 Hz, ArH), 6.77 (2H, um, =CH), 6.89 – 7.70 (28H, complex aromatic region, Ph and ArH).  $\delta_F$  –80.75 (6F, t,  $^4J_{FF}$  9.0 Hz,  $CF_3$ ), –111.24 (4F, um,  $\alpha$ - $CF_2$ ), –121.51 (4F, um,  $CF_2$ ), –122.81 (4F, um,  $CF_2$ ), –122.95 (4F, um,  $CF_2$ ), –126.07 (4F, um,  $CF_2$ ).  $\delta_P$  32.69 (s)

**Preparation of [PdCl<sub>2</sub>((*S*)-Rf-C<sub>2</sub>H<sub>2</sub>-BINAP)] ((*S*)-2.20)**

The title compound was prepared similarly to (*R*)-2.20 above using (*S*)-Rf-C<sub>2</sub>H<sub>2</sub>-BINAP (0.10g,  $7.7 \times 10^{-5}$  mol) (67 mg, 58 %). M.p. > 300 °C. m/z (FAB) 1453 [M-Cl]<sup>+</sup> (6 %). [α]<sub>D</sub> (CHCl<sub>3</sub>) - 323.5 ° (c = 0.6). Elemental analysis (expected (found)) C 48.42 (48.54), H 2.29 (2.35). δ<sub>H</sub> 6.25 (2H, um, =CH), 6.65 (2H, d, <sup>3</sup>J<sub>HH</sub> 8.9 Hz, ArH), 6.77 (2H, um, =CH), 6.88 – 7.70 (28H, complex aromatic region, Ph and ArH). δ<sub>F</sub> -80.81 (6F, t, <sup>4</sup>J<sub>FF</sub> 9.6 Hz, CF<sub>3</sub>), -111.20 (4F, um, α-CF<sub>2</sub>), -121.52 (4F, um, CF<sub>2</sub>), -122.81 (4F, um, CF<sub>2</sub>), -122.95 (4F, um, CF<sub>2</sub>), -126.08 (4F, um, CF<sub>2</sub>). δ<sub>P</sub> 32.59 (s)

**Preparation of [PdCl<sub>2</sub>((*R*)-Rf-C<sub>2</sub>H<sub>4</sub>-BINAP)] ((*R*)-2.21)**

*Cis*-[PdCl<sub>2</sub>(MeCN)<sub>2</sub>] (0.08 g,  $3.1 \times 10^{-4}$  mol) and (*R*)-Rf-C<sub>2</sub>H<sub>4</sub>-BINAP (0.41 g,  $3.1 \times 10^{-4}$  mol) were stirred in dichloromethane for 2 hours. The suspension was filtered and hexane added to the filtrate to precipitate the product as a yellow-orange solid (0.25 g, 55 %). M.p. 184 – 186 °C (dec.). m/z (FAB) 1456 [M-Cl]<sup>+</sup> (9 %). [α]<sub>D</sub> (CHCl<sub>3</sub>) 327.8 ° (c = 1.1). Elemental analysis (expected (found)) C 48.29 (48.27), H 2.55 (2.50). δ<sub>H</sub> 2.71 (4H, um CH<sub>2</sub>), 3.34 (4H, um, CH<sub>2</sub>), 6.58 – 7.89 (complex aromatic region, 32H, binaphthyl backbone and PPh<sub>2</sub> groups). δ<sub>F</sub> -81.31 (6F, t, <sup>4</sup>J<sub>FF</sub> 10.1 Hz, CF<sub>3</sub>), -114.52 (4F, um, α-CF<sub>2</sub>), -122.31 (4F, um, CF<sub>2</sub>), -123.30 (4F, um, CF<sub>2</sub>), -123.77 (4F, um, CF<sub>2</sub>), -126.59 (4F, um, CF<sub>2</sub>). δ<sub>P</sub> 28.42 (s)

**Preparation of [PdCl<sub>2</sub>((*S*)-Rf-C<sub>2</sub>H<sub>4</sub>-BINAP)] ((*S*)-2.21)**

The title compound was prepared similarly to compound (*R*)-2.21 above using (*S*)-Rf-C<sub>2</sub>H<sub>4</sub>-BINAP (0.41 g,  $3.1 \times 10^{-4}$  mol). The compound was isolated as a bright orange solid. (0.27 g, 56 %). M.p. 186 – 188 °C (dec.). m/z (FAB) 1455 [M-Cl]<sup>+</sup> (7 %). [α]<sub>D</sub> (CHCl<sub>3</sub>) - 331.1 ° (c = 0.8). Elemental analysis (expected (found)) C 48.29 (48.11), H 2.55 (2.50). δ<sub>H</sub> 2.72 (4H, um CH<sub>2</sub>), 3.33 (4H, um, CH<sub>2</sub>), 6.54 – 7.87 (complex aromatic region, 32H, binaphthyl backbone and PPh<sub>2</sub> groups). δ<sub>F</sub> -81.33 (6F, t, <sup>4</sup>J<sub>FF</sub> 10.0 Hz, CF<sub>3</sub>), -114.50 (4F, um, α-CF<sub>2</sub>), -122.32 (4F, um, CF<sub>2</sub>), -123.34 (4F, um, CF<sub>2</sub>), -123.73 (4F, um, CF<sub>2</sub>), -126.58 (4F, um, CF<sub>2</sub>). δ<sub>P</sub> 28.37 (s)

**Preparation of [PdCl<sub>2</sub>((*R*)-BINAP)]<sup>4</sup> ((*R*)-2.22)**

*Cis*-[PdCl<sub>2</sub>(MeCN)<sub>2</sub>] (0.04 g,  $1.54 \times 10^{-4}$  mol) and (*R*)-BINAP (0.103 g,  $1.66 \times 10^{-4}$  mol) were stirred in dry toluene for 12 hours under nitrogen. The suspension was filtered to obtain the product as an orange solid (0.101 g, 82 %). M.p. 255 – 258 °C (dec.). m/z (FAB) 763 [M-Cl]<sup>+</sup> (10 %). [α]<sub>D</sub> (CHCl<sub>3</sub>) 682.3 ° (c = 0.5). δ<sub>H</sub> 6.54 – 7.79 (32H, complex aromatic region, binaphthyl backbone and PPh<sub>2</sub> groups). δ<sub>P</sub> 28.51 (s).

### Preparation of $[\text{PdCl}_2((S)\text{-BINAP})]^{+4}$ ((*S*)-2.22)

The title compound was prepared as for compound (*R*)-2.22 using (*S*)-BINAP (0.101 g,  $1.62 \times 10^{-4}$  mol). The product was obtained as a bright orange solid. (98 mg, 76 %). M.p. 254 – 257 °C (dec.). *m/z* (FAB) 763  $[\text{M-Cl}]^{+}$  (11 %), 727  $[\text{M-2Cl}]^{+}$  (2 %).  $[\alpha]_{\text{D}}$  ( $\text{CHCl}_3$ ) – 688.1 ° (*c* = 0.8).  $\delta_{\text{H}}$  6.57 – 7.68 (32H, complex aromatic region, binaphthyl backbone and  $\text{PPh}_2$  groups).  $\delta_{\text{P}}$  28.49 (s).

### Preparation of (*R*)-6,6'-bis(perfluoro-*n*-hexyl)-2,2'-bis(diphenylphosphino)-1,1-binaphthyl selenide ((*R*)-Rf-BINAP-Se) ((*R*)-2.23)

(*R*)-Rf-BINAP (101 mg,  $8.0 \times 10^{-5}$  mol) and selenium powder (50 mg) were refluxed in degassed chloroform for 12 hours under nitrogen. Upon cooling, the mixture was filtered through a cotton wool plug and the solvent removed under reduced pressure to yield a yellow solid (82 mg, 72 %). M.p. 125 - 127 °C. *m/z* ( $\text{ES}^{+}$ ) 1417  $[\text{MH}]^{+}$  (21 %).  $[\alpha]_{\text{D}}$  ( $\text{CHCl}_3$ ) 20.7 ° (*c* = 1.2).  $\delta_{\text{H}}$  6.59 (2H, d,  $^3J_{\text{HH}}$  10.0 Hz, ArH), 6.64 (2H, d,  $^3J_{\text{HH}}$  10.0 Hz, ArH), 7.21 – 7.35 (12H, complex aromatic region, PhH), 7.52 (2H, d,  $^3J_{\text{HH}}$  7.5 Hz, ArH), 7.54 – 7.66 (8H, complex aromatic region, PhH), 7.89 (2H, dd,  $^3J_{\text{HH}}$  10.0 Hz,  $^4J_{\text{HH}}$  2.5 Hz, ArH), 7.96 (2H, s, ArH).  $\delta_{\text{F}}$  –81.18 (6F, t,  $^4J_{\text{FF}}$  9.8 Hz,  $\text{CF}_3$ ), –110.77 (4F, um,  $\alpha\text{-CF}_2$ ), –121.48 (4F, um,  $\text{CF}_2$ ), –121.80 (4F, um,  $\text{CF}_2$ ), –123.16 (4F, um,  $\text{CF}_2$ ), –126.48 (4F, um,  $\text{CF}_2$ ).  $\delta_{\text{P}}$  32.67 (ss,  $^1J_{\text{P-Se}}$  749 Hz).

### Preparation of (*S*)-6,6'-bis(perfluoro-*n*-hexyl)-2,2'-bis(diphenylphosphino)-1,1-binaphthyl selenide ((*S*)-Rf-BINAP-Se) ((*S*)-2.23)

The title compound was prepared similarly to compound (*R*)-2.23 above using (*S*)-Rf-BINAP (71 mg,  $5.6 \times 10^{-5}$  mol) and selenium powder (50 mg). The product was obtained as a yellow solid (76 mg, 95 %). M.p. 126 - 128 °C. *m/z* ( $\text{ES}^{+}$ ) 1417  $[\text{MH}]^{+}$  (100 %).  $[\alpha]_{\text{D}}$  ( $\text{CHCl}_3$ ) – 24.7 ° (*c* = 1.1).  $\delta_{\text{H}}$  6.62 (2H, d,  $^3J_{\text{HH}}$  10.0 Hz, ArH), 6.65 (2H, d,  $^3J_{\text{HH}}$  10.0 Hz, ArH), 7.23 – 7.35 (12H, complex aromatic region, PhH), 7.53 (2H, d,  $^3J_{\text{HH}}$  7.5 Hz, ArH), 7.54 – 7.67 (8H, complex aromatic region, PhH), 7.89 (2H, dd,  $^3J_{\text{HH}}$  10.0 Hz,  $^4J_{\text{HH}}$  2.5 Hz, ArH), 7.96 (2H, s, ArH).  $\delta_{\text{F}}$  –81.29 (6F, t,  $^4J_{\text{FF}}$  9.8 Hz,  $\text{CF}_3$ ), –110.97 (4F, um,  $\alpha\text{-CF}_2$ ), –121.49 (4F, um,  $\text{CF}_2$ ), –121.81 (4F, um,  $\text{CF}_2$ ), –123.18 (4F, um,  $\text{CF}_2$ ), –126.46 (4F, um,  $\text{CF}_2$ ).  $\delta_{\text{P}}$  32.72 (ss,  $^1J_{\text{P-Se}}$  749 Hz).

### Preparation of (*R*)-6,6'-bis(1*H*,2*H*-perfluoro-*n*-1-octenyl)-2,2'-bis(diphenylphosphino)-1,1-binaphthyl selenide ((*R*)- $\text{C}_2\text{H}_2$ -Rf-BINAP-Se) ((*R*)-2.24)

(*R*)-6,6'-bis(1*H*,2*H*-perfluoro-*n*-1-octenyl)-2,2'-bis(diphenylphosphino)-1,1'-binaphthyl (52 mg,  $3.7 \times 10^{-5}$  mol) and selenium powder (50 mg) were refluxed in degassed chloroform for 12 hours. Upon cooling the solution was filtered and the solvent removed under reduced pressure to yield the product as an off-white solid. (50 mg, 92 %). M.p. 80 – 82 °C (dec.). *m/z* ( $\text{ES}^{+}$ ) 1468  $[\text{M}]^{+}$

(47 %).  $[\alpha]_D$  (CHCl<sub>3</sub>) 4.17 ° (c = 3.0).  $\delta_H$  6.04 (2H, um, =CH), 6.56 (2H, um, =CH), 7.11 – 7.81 (30H, complex aromatic region, ArH and PhH).  $\delta_F$  –80.70 (6F, t,  $^4J_{FF}$  9.5 Hz, CF<sub>3</sub>), –111.17 (4F, um,  $\alpha$ -CF<sub>2</sub>), –121.80 (4F, um, CF<sub>2</sub>), –122.78 (4F, um, CF<sub>2</sub>), –123.04 (4F, um, CF<sub>2</sub>), –126.04 (4F, um, CF<sub>2</sub>).  $\delta_p$  32.78 (ss,  $^1J_{P-Se}$  746 Hz).

**Preparation of (*S*)-6,6'-bis(1*H*,2*H*-perfluoro-*n*-1-octenyl)-2,2'-bis(diphenylphosphino)-1,1'-binaphthyl selenide ((*S*)-C<sub>2</sub>H<sub>2</sub>-Rf-BINAP-Se) ((*S*)-2.24)**

The title compound was prepared in a similar manner to (*R*)-2.24 above using (*S*)-6,6'-bis(1*H*,2*H*-perfluoro-*n*-1-octenyl)-2,2'-bis(diphenylphosphino)-1,1'-binaphthyl (47 mg, 3.6 x 10<sup>-5</sup> mol) and selenium powder (50 mg). The compound was collected as a yellow solid. (49 mg, 92 %). M.p. 81 – 84 °C (dec.). m/z (ES<sup>+</sup>) 1468 [M]<sup>+</sup> (45 %).  $[\alpha]_D$  (CHCl<sub>3</sub>) –10.3 ° (c = 1.7). Elemental analysis (expected (found)) C 49.05 (48.99), H 2.32 (2.20).  $\delta_H$  6.04 (2H, um, =CH), 6.55 (2H, um, =CH), 7.11 – 7.80 (30H, complex aromatic region, ArH and PhH).  $\delta_F$  –80.72 (6F, t,  $^4J_{FF}$  10.2 Hz, CF<sub>3</sub>), –111.16 (4F, um,  $\alpha$ -CF<sub>2</sub>), –121.45 (4F, um, CF<sub>2</sub>), –122.78 (4F, um, CF<sub>2</sub>), –123.10 (4F, um, CF<sub>2</sub>), –126.07 (4F, um, CF<sub>2</sub>).  $\delta_p$  32.76 (ss,  $^1J_{P-Se}$  746 Hz).

**Preparation of (*R*)-6,6'-bis(1*H*,1*H*,2*H*,2*H*-perfluoro-*n*-octyl)-2,2'-bis(diphenylphosphino)-1,1'-binaphthyl selenide ((*R*)-Rf-C<sub>2</sub>H<sub>4</sub>-BINAP-Se) ((*R*)-2.25)**

(*R*)-Rf-C<sub>2</sub>H<sub>4</sub>-BINAP (104 mg, 7.9 x 10<sup>-5</sup> mol) and selenium powder (50 mg) were refluxed in degassed chloroform for 12 hours. Upon cooling, the mixture was filtered through a cotton wool plug and the solvent removed under reduced pressure to yield a yellow solid (88 mg, 76 %). M.p. 127 – 131 °C. m/z (ES<sup>+</sup>) 1473 [MH]<sup>+</sup> (100 %).  $[\alpha]_D$  (CHCl<sub>3</sub>) 17.72 ° (c = 0.9). Elemental analysis (expected (found)) C 48.91 (49.14), H 2.58 (2.48).  $\delta_H$  2.25 (4H, um, CH<sub>2</sub>), 2.84 (4H, um, CH<sub>2</sub>), 6.33 (2H, dd,  $^3J_{HH}$  8.8 Hz,  $^4J_{HH}$  1.5 Hz, ArH), 6.58 (2H, d,  $^3J_{HH}$  8.7 Hz, ArH), 7.13 – 7.34 (12H, complex aromatic region, ArH and PhH), 7.40, (2H, dd,  $J_{HH}$  12.2 Hz,  $J_{HH}$  8.8 Hz, ArH), 7.50 (2H, s, ArH), 7.56 (4H, um, PhH), 7.69 (6H, um, PhH).  $\delta_F$  –80.75 (6F, t,  $^4J_{FF}$  10.4 Hz, CF<sub>3</sub>), –114.52 (4F, um,  $\alpha$ -CF<sub>2</sub>), –121.79 (4F, um, CF<sub>2</sub>), –122.80 (4F, um, CF<sub>2</sub>), –123.38 (4F, um, CF<sub>2</sub>), –126.08 (4F, um, CF<sub>2</sub>).  $\delta_p$  32.75 (ss,  $^1J_{P-Se}$  743 Hz).

**Preparation of (*S*)-6,6'-bis(1*H*,1*H*,2*H*,2*H*-perfluoro-*n*-octyl)-2,2'-bis(diphenylphosphino)-1,1'-binaphthyl selenide ((*S*)-Rf-C<sub>2</sub>H<sub>4</sub>-BINAP-Se) ((*S*)-2.25)**

The title compound was prepared as for (*R*)-2.25 using (*S*)-6,6'-bis(1*H*,1*H*,2*H*,2*H*-perfluoro-*n*-octyl)-2,2'-bis(diphenylphosphino)-1,1'-binaphthyl (111 mg, 8.4 x 10<sup>-5</sup> mol). The product was obtained as a yellow solid. (92 mg, 79 %). M.p. 127 – 130 °C. m/z (ES<sup>+</sup>) 1473 [MH]<sup>+</sup> (100 %).  $[\alpha]_D$  (CHCl<sub>3</sub>) –22.45 ° (c = 0.6). Elemental analysis (expected (found)) C 48.91 (49.14), H 2.58 (2.48).

$\delta_{\text{H}}$  2.25 (4H, um, CH<sub>2</sub>), 2.83 (4H, um, CH<sub>2</sub>), 6.34 (2H, dd,  $^3J_{\text{HH}}$  8.9 Hz,  $^4J_{\text{HH}}$  1.8 Hz, ArH), 6.58 (2H, d,  $^3J_{\text{HH}}$  8.8 Hz, ArH), 7.13 – 7.34 (12H, complex aromatic region, ArH and PhH), 7.40 (2H, um, ArH), 7.50 (2H, s, ArH), 7.57 (4H, um, PhH), 7.69 (6H, um, PhH).  $\delta_{\text{F}}$  -80.73 (6F, t,  $^4J_{\text{FF}}$  10.4 Hz, CF<sub>3</sub>), -114.53 (4F, um,  $\alpha$ -CF<sub>2</sub>), -121.79 (4F, um, CF<sub>2</sub>), -122.80 (4F, um, CF<sub>2</sub>), -123.38 (4F, um, CF<sub>2</sub>), -126.09 (4F, um, CF<sub>2</sub>).  $\delta_{\text{P}}$  32.77 (ss,  $^1J_{\text{P-Se}}$  743 Hz).

### Preparation of (*R*)-2,2'-bis(diphenylphosphino)-1,1'-binaphthyl selenide ((*R*)-BINAP-Se) ((*R*)-2.26)

(*R*)-BINAP (102 mg,  $1.6 \times 10^{-4}$  mol) and selenium powder (50 mg) were refluxed in degassed chloroform for 12 hours. Upon cooling, the mixture was filtered and the solvent removed *in vacuo* to yield an off-white solid (96 mg, 75 %). M.p. > 300 °C.  $m/z$  (ES<sup>+</sup>) 781 [MH]<sup>+</sup> (68 %).  $[\alpha]_{\text{D}}$  (CHCl<sub>3</sub>) 19.0 ° (c = 1.6).  $\delta_{\text{H}}$  6.63 (2H, um, ArH), 6.69 (2H, d,  $^3J_{\text{HH}}$  8.4 Hz, ArH), 7.09 – 7.29 (14H, um, ArH and PhH), 7.43 (2H, um, ArH), 7.53 – 7.71 (12H, complex aromatic region, ArH and PhH).  $\delta_{\text{P}}$  33.73 (ss,  $^3J_{\text{P-Se}}$  739 Hz).

### Preparation of (*S*)-2,2'-bis(diphenylphosphino)-1,1'-binaphthyl selenide ((*S*)-BINAP-Se) ((*S*)-2.26)

The title compound was prepared similarly to the (*R*)-enantiomer above using (*S*)-BINAP (106 mg,  $1.7 \times 10^{-4}$  mol) and isolated as an off-white solid (102 mg, 77 %). M.p. > 300 °C.  $m/z$  (ES<sup>+</sup>) 781 [MH]<sup>+</sup> (83 %).  $[\alpha]_{\text{D}}$  (CHCl<sub>3</sub>) -25.8 ° (c = 1.6).  $\delta_{\text{H}}$  6.63 (2H, um, ArH), 6.69 (2H, d,  $^3J_{\text{HH}}$  8.1 Hz, ArH), 7.09 – 7.29 (14H, um, ArH and PhH), 7.43 (2H, um, ArH), 7.53 – 7.71 (12H, complex aromatic region, ArH and PhH).  $\delta_{\text{P}}$  33.74 (ss,  $^3J_{\text{P-Se}}$  739 Hz).

## 6.2.4 Catalytic Testing

The following catalytic tests were all carried out using the procedure outlined below with the appropriate addition of ligand and catalyst precursor. Product *ee*'s were determined by conversion of a sample of the product into the Mosher's acid ester followed by analysis of the resulting diastereomers by <sup>1</sup>H NMR spectroscopy. The procedure for the conversion is given below. The absolute configuration of the products was determined by conversion of enantiomerically pure (*R*)- and (*S*)-methyl 3-hydroxybutyrate into the corresponding Mosher's acid esters. Comparison of the <sup>1</sup>H NMR spectra for these diastereomers to those obtained from the diastereomers of product methyl 3-hydroxybutyrate allowed determination of the *ee* and stereochemistry. Absolute configurations of products were found to favour the absolute configuration of the substituting ligand.

### **General Procedure for the Hydrogenation of Methyl Acetoacetate**

Methyl acetoacetate (10.0 g, 86 mmol) and DCM (10 ml) were placed in an autoclave under nitrogen with the required catalyst and ligand and the reactor sealed. The autoclave was then heated to 100 °C for twenty minutes with constant stirring at 700 rpm before being placed under 50 atm of hydrogen gas for one hour with continued heating and stirring. After an hour, the reactor was allowed to cool for twenty minutes with external cooling using a desk fan before the gas was carefully vented and the product collected.

### **Preparation of Mosher's Acid Ester Diastereomers**

Mosher's acid chloride ( $9.9 \times 10^{-2}$  mol dm<sup>-3</sup> solution in dry dichloromethane, 2.0 ml, 0.2 mmol) was added to a flame-dried 10 ml flask and dry pyridine (0.2 ml, 2.5 mmol) added. To this mixture, the product methyl-3-hydroxybutyrate (0.02 ml, 0.2 mmol) was added and the mixture stirred for 10 minutes.

1M HCl solution (20 ml) was added along with an additional 10 ml of DCM. The organic layer was separated and the aqueous phase extracted with DCM (10 ml). The organic layers were combined, washed with water (10 ml), dried, filtered and the solvent removed under reduced pressure to yield a colourless oil.

### **Hydrogenation using no BINAP Ligand or Ruthenium Catalyst (T1)**

The procedure was carried out as outlined above. No conversion of the starting material was observed.

### **Hydrogenation using only BINAP Ligand (T2)**

BINAP (55 mg, 88 μmol) was added to the mixture and the general procedure followed. No production of methyl 3-hydroxybutyrate was observed.

### **Hydrogenation using only [RuCl<sub>2</sub>(benzene)]<sub>2</sub> (T3)**

[RuCl<sub>2</sub>(benzene)]<sub>2</sub> (0.022 g, 44 μmol) was added to the mixture and the general procedure followed. Analysis by <sup>1</sup>H NMR showed 28 % conversion of the methyl acetoacetate to methyl 3-hydroxybutyrate. The product had no *ee*.

### **Hydrogenation using [RuCl<sub>2</sub>(benzene)]<sub>2</sub> and (*R*)-BINAP (T4)**

(*R*)-BINAP (55 mg, 88 μmol) and [RuCl<sub>2</sub>(benzene)]<sub>2</sub> (0.022 g, 44 μmol) were used in the general procedure. <sup>1</sup>H NMR analysis showed > 95 % conversion to methyl 3-hydroxybutyrate had

been achieved.  $\delta_{\text{H}}$  ( $\text{C}_6\text{D}_6$ ) 1.94 (3H, d,  $^3J_{\text{HH}}$  6 Hz,  $\text{CH}_3$ ), 3.18 (2H, d,  $^3J_{\text{HH}}$  6 Hz,  $\text{CH}_2$ ), 4.41 (3H, s,  $\text{OCH}_3$ ), 4.81 (1H, s, OH), 4.97 (1H, um, CH). *Ee*'s: Run 1: 80 %; Run 2: 74 %; Run 3: 80 %.

#### Hydrogenation using $[\text{RuCl}_2(\text{benzene})]_2$ and (*S*)-BINAP (T5)

(*S*)-BINAP (55 mg, 88  $\mu\text{mol}$ ) and  $[\text{RuCl}_2(\text{benzene})]_2$  (0.022 g, 44  $\mu\text{mol}$ ) were used in the general procedure.  $^1\text{H}$  NMR analysis showed > 95 % conversion to methyl 3-hydroxybutyrate had been achieved.  $\delta_{\text{H}}$  ( $\text{C}_6\text{D}_6$ ) 1.94 (3H, d,  $^3J_{\text{HH}}$  6 Hz,  $\text{CH}_3$ ), 3.18 (2H, d,  $^3J_{\text{HH}}$  6 Hz,  $\text{CH}_2$ ), 4.41 (3H, s,  $\text{OCH}_3$ ), 4.81 (1H, s, OH), 4.97 (1H, um, CH). *Ee*'s: Run 1: 76 %; Run 2: 72 %; Run 3: 80 %.

#### Hydrogenation using $[\text{RuCl}_2(\text{benzene})]_2$ and (*R*)-Rf-BINAP (T6)

(*R*)-Rf-BINAP (111 mg, 88  $\mu\text{mol}$ ) and  $[\text{RuCl}_2(\text{benzene})]_2$  (0.022 g, 44  $\mu\text{mol}$ ) were used in the general procedure.  $^1\text{H}$  NMR analysis showed > 95 % conversion to methyl 3-hydroxybutyrate had been achieved.  $\delta_{\text{H}}$  ( $\text{C}_6\text{D}_6$ ) 1.95 (3H, d,  $^3J_{\text{HH}}$  6 Hz,  $\text{CH}_3$ ), 3.21 (2H, d,  $^3J_{\text{HH}}$  6 Hz,  $\text{CH}_2$ ), 4.40 (3H, s,  $\text{OCH}_3$ ), 4.79 (1H, s, OH), 4.97 (1H, um, CH). *Ee*'s: Run 1: 86 %; Run 2: 70 %; Run 3: 72 %.

#### Hydrogenation using $[\text{RuCl}_2(\text{benzene})]_2$ and (*S*)-Rf-BINAP (T7)

(*S*)-Rf-BINAP (111 mg, 88  $\mu\text{mol}$ ) and  $[\text{RuCl}_2(\text{benzene})]_2$  (0.022 g, 44  $\mu\text{mol}$ ) were used in the general procedure.  $^1\text{H}$  NMR analysis showed > 95 % conversion to methyl 3-hydroxybutyrate had been achieved.  $\delta_{\text{H}}$  ( $\text{C}_6\text{D}_6$ ) 1.95 (3H, d,  $^3J_{\text{HH}}$  6 Hz,  $\text{CH}_3$ ), 3.21 (2H, d,  $^3J_{\text{HH}}$  6 Hz,  $\text{CH}_2$ ), 4.40 (3H, s,  $\text{OCH}_3$ ), 4.79 (1H, s, OH), 4.97 (1H, um, CH). *Ee*'s: Run 1: 68 %; Run 2: 76 %; Run 3: 72 %.

#### Hydrogenation using $[\text{RuCl}_2(\text{benzene})]_2$ and (*R*)- $\text{C}_2\text{H}_2$ -Rf-BINAP (T8)

(*R*)- $\text{C}_2\text{H}_2$ -Rf-BINAP (115 mg, 88  $\mu\text{mol}$ ) and  $[\text{RuCl}_2(\text{benzene})]_2$  (0.022 g, 44  $\mu\text{mol}$ ) were used in the general procedure.  $^1\text{H}$  NMR analysis showed > 95 % conversion to methyl 3-hydroxybutyrate had been achieved.  $\delta_{\text{H}}$  ( $\text{C}_6\text{D}_6$ ) 1.95 (3H, d,  $^3J_{\text{HH}}$  6 Hz,  $\text{CH}_3$ ), 3.21 (2H, d,  $^3J_{\text{HH}}$  6 Hz,  $\text{CH}_2$ ), 4.40 (3H, s,  $\text{OCH}_3$ ), 4.79 (1H, s, OH), 4.97 (1H, um, CH). *Ee*'s: Run 1: 72 %; Run 2: 80 %; Run 3: 76 %.

#### Hydrogenation using $[\text{RuCl}_2(\text{benzene})]_2$ and (*S*)- $\text{C}_2\text{H}_2$ -Rf-BINAP (T9)

(*S*)- $\text{C}_2\text{H}_2$ -Rf-BINAP (115 mg, 88  $\mu\text{mol}$ ) and  $[\text{RuCl}_2(\text{benzene})]_2$  (0.022 g, 44  $\mu\text{mol}$ ) were used in the general procedure.  $^1\text{H}$  NMR analysis showed > 95 % conversion to methyl 3-hydroxybutyrate had been achieved.  $\delta_{\text{H}}$  ( $\text{C}_6\text{D}_6$ ) 1.95 (3H, d,  $^3J_{\text{HH}}$  6 Hz,  $\text{CH}_3$ ), 3.21 (2H, d,  $^3J_{\text{HH}}$  6 Hz,  $\text{CH}_2$ ), 4.40 (3H, s,  $\text{OCH}_3$ ), 4.79 (1H, s, OH), 4.97 (1H, um, CH). *Ee*'s: Run 1: 74 %; Run 2: 74 %; Run 3: 76 %.

### Hydrogenation using [RuCl<sub>2</sub>(benzene)]<sub>2</sub> and (*R*)-C<sub>2</sub>H<sub>4</sub>-Rf-BINAP (T10)

(*R*)-C<sub>2</sub>H<sub>4</sub>-Rf-BINAP (116 mg, 88 μmol) and [RuCl<sub>2</sub>(benzene)]<sub>2</sub> (0.022 g, 44 μmol) were used in the general procedure. <sup>1</sup>H NMR analysis showed > 95 % conversion to methyl 3-hydroxybutyrate had been achieved. δ<sub>H</sub> (C<sub>6</sub>D<sub>6</sub>) 1.95 (3H, d, <sup>3</sup>J<sub>HH</sub> 6 Hz, CH<sub>3</sub>), 3.21 (2H, d, <sup>3</sup>J<sub>HH</sub> 6 Hz, CH<sub>2</sub>), 4.40 (3H, s, OCH<sub>3</sub>), 4.79 (1H, s, OH), 4.97 (1H, um, CH). *Ee*'s: Run 1: 91 %; Run 2: 68 %; Run 3: 82 %.

### Hydrogenation using [RuCl<sub>2</sub>(benzene)]<sub>2</sub> and (*S*)-C<sub>2</sub>H<sub>4</sub>-Rf-BINAP (T11)

(*S*)-C<sub>2</sub>H<sub>4</sub>-Rf-BINAP (116 mg, 88 μmol) and [RuCl<sub>2</sub>(benzene)]<sub>2</sub> (0.022 g, 44 μmol) were used in the general procedure. <sup>1</sup>H NMR analysis showed > 95 % conversion to methyl 3-hydroxybutyrate had been achieved. δ<sub>H</sub> (C<sub>6</sub>D<sub>6</sub>) 1.95 (3H, d, <sup>3</sup>J<sub>HH</sub> 6 Hz, CH<sub>3</sub>), 3.21 (2H, d, <sup>3</sup>J<sub>HH</sub> 6 Hz, CH<sub>2</sub>), 4.40 (3H, s, OCH<sub>3</sub>), 4.79 (1H, s, OH), 4.97 (1H, um, CH). *Ee*'s: Run 1: 78 %; Run 2: 80 %; Run 3: 68 %.

## 6.2.5 Hydrogenation Using Catalyst Recovered by Product Distillation

### Hydrogenation Using (*R*)-BINAP

The hydrogenation reaction was carried out as for T4 above. At the end of reaction, the catalysis mixture was removed from the autoclave by syringe using a positive flow of nitrogen and placed in an ampoule. The product was distilled under vacuum at 90 °C until a thick red-brown oil remained in the ampoule. This oil was reused in catalysis.

The distilled product was separated from the dichloromethane reaction solvent by further distillation and the percentage conversion and *ee* determined. δ<sub>H</sub> (C<sub>6</sub>D<sub>6</sub>) 1.95 (3H, d, <sup>3</sup>J<sub>HH</sub> 6 Hz, CH<sub>3</sub>), 3.21 (2H, d, <sup>3</sup>J<sub>HH</sub> 6 Hz, CH<sub>2</sub>), 4.40 (3H, s, OCH<sub>3</sub>), 4.79 (1H, s, OH), 4.97 (1H, um, CH). Run 1: > 95 % conversion, 82 % *ee*; Run 2: > 95 % conversion, 2 % *ee*; Run 3: > 95 % conversion, 0 % *ee*.

### Hydrogenation Using (*R*)-Rf-BINAP

The hydrogenation reaction was carried out as for T6 above. At the end of reaction, the catalysis mixture was removed from the autoclave by syringe using a positive flow of nitrogen and placed in an ampoule. The product was distilled under vacuum at 90 °C until a thick red-brown oil remained in the ampoule. This oil was reused in catalysis.

The distilled product was separated from the dichloromethane reaction solvent by further distillation and the percentage conversion and *ee* determined. δ<sub>H</sub> (C<sub>6</sub>D<sub>6</sub>) 1.95 (3H, d, <sup>3</sup>J<sub>HH</sub> 6 Hz, CH<sub>3</sub>), 3.21 (2H, d, <sup>3</sup>J<sub>HH</sub> 6 Hz, CH<sub>2</sub>), 4.40 (3H, s, OCH<sub>3</sub>), 4.79 (1H, s, OH), 4.97 (1H, um, CH). Run

1: > 95 % conversion, 74 % *ee*; Run 2: > 95 % conversion, 20 % *ee*; Run 3: > 95 % conversion, 0 % *ee*.

### 6.2.6 Solid Separation and Ligand Reuse

#### General Procedure for Product Separation and Ligand Recovery

A 1 cm diameter column with a cotton wool plug was filled to 3 cm in length with silica gel or FRP silica gel. The reaction mixture to be separated was concentrated *in vacuo* and then placed onto the top of the column of silica and eluted with methanol to obtain the clean organic product. Recovery of oxidised ligand was then achieved by elution with dichloromethane.

For anaerobic separations, silica gel or FRP silica gel were dried and degassed under high vacuum at 150 °C for 24 hours. These solids were then added to a 1 cm diameter column and filled to 3 cm in length in a dry box under nitrogen. The reaction mixture to be separated was concentrated *in vacuo*, passed through the column of silica and eluted with dry and degassed methanol under nitrogen. Recovery of non-oxidised ligand was then achieved by elution with dry and degassed dichloromethane.

#### Separation of a Ru/(*R*)-BINAP System Aerobically (S1)

The general separation procedure was followed using a Ru/(*R*)-BINAP catalytic run, which had been formed using the method described in the general catalytic procedure and T4. Methyl 3-hydroxybutyrate was collected in > 95 % conversion and 82 % *ee*.  $\delta_{\text{H}}$  ( $\text{C}_6\text{D}_6$ ) 1.94 (3H, d,  $^3J_{\text{HH}}$  6 Hz,  $\text{CH}_3$ ), 3.18 (2H, d,  $^3J_{\text{HH}}$  6 Hz,  $\text{CH}_2$ ), 4.41 (3H, s,  $\text{OCH}_3$ ), 4.81 (1H, s, OH), 4.97 (1H, um, CH).

Elution with dichloromethane and removal of the solvent *in vacuo* yielded (*R*)-BINAP oxide.  $^{31}\text{P}$  30.75 (s).  $[\alpha]_{\text{D}}$  ( $\text{CHCl}_3$ ) 150.3 ° (c = 0.3). (Enantiomerically pure (*R*)-BINAP oxide prepared by oxidation of (*R*)-BINAP -  $[\alpha]_{\text{D}}$  ( $\text{CHCl}_3$ ) 157.3 ° (c = 1.4).

#### Separation of a Ru/(*R*)-Rf-BINAP System Aerobically (S2)

The general separation procedure using FRP silica gel was followed using a Ru/(*R*)-Rf-BINAP catalytic run, which had been formed using the method described in the general catalytic procedure and T6. Methyl 3-hydroxybutyrate was collected in > 95 % conversion and 84 % *ee*.  $\delta_{\text{H}}$  ( $\text{C}_6\text{D}_6$ ) 1.94 (3H, d,  $^3J_{\text{HH}}$  6 Hz,  $\text{CH}_3$ ), 3.18 (2H, d,  $^3J_{\text{HH}}$  6 Hz,  $\text{CH}_2$ ), 4.41 (3H, s,  $\text{OCH}_3$ ), 4.81 (1H, s, OH), 4.97 (1H, um, CH).

Elution with dichloromethane and removal of the solvent *in vacuo* yielded (*R*)-Rf-BINAP oxide.  $\delta_{\text{P}}$  30.73 (s)  $[\alpha]_{\text{D}}$  ( $\text{CHCl}_3$ ) 90.2 ° (c = 0.3). (Enantiomerically pure (*R*)-Rf-BINAP oxide prepared by oxidation of (*R*)-Rf-BINAP -  $[\alpha]_{\text{D}}$  ( $\text{CHCl}_3$ ) 95.6 ° (c = 1.1).

### Separation of a Ru/(*R*)-BINAP System Under Anaerobic Conditions (S3)

The general separation procedure for anaerobic separations was followed using a Ru/(*R*)-BINAP catalytic run, which had been formed using the method described in the general catalytic procedure and T4. Methyl 3-hydroxybutyrate was collected by elution with methanol in > 95 % conversion and 82 % *ee*.  $\delta_{\text{H}}$  ( $\text{C}_6\text{D}_6$ ) 1.94 (3H, d,  $^3J_{\text{HH}}$  6 Hz,  $\text{CH}_3$ ), 3.18 (2H, d,  $^3J_{\text{HH}}$  6 Hz,  $\text{CH}_2$ ), 4.41 (3H, s,  $\text{OCH}_3$ ), 4.81 (1H, s, OH), 4.97 (1H, um, CH).

Elution with dichloromethane and removal of the solvent *in vacuo* yielded (*R*)-BINAP. (45 mg, 82 % recovery)  $m/z$  (FAB) 623  $[\text{MH}]^+$  (8 %).  $\delta_{\text{H}}$  6.75 – 7.88 (32 H, complex aromatic region, binaphthyl backbone and  $\text{PPh}_2$  groups).  $\delta_{\text{P}}$  -15.50 (s).  $[\alpha]_{\text{D}}$  ( $\text{CHCl}_3$ ) 218 ° ( $c = 0.7$ ). (Enantiomerically pure (*R*)-BINAP -  $[\alpha]_{\text{D}}$  ( $\text{CHCl}_3$ ) 224.0 ° ( $c = 1.2$ ).

The ligand was reused in one further catalytic run using the general catalytic procedure and T4. Using the general anaerobic separation methodology, (*R*)-methyl 3-hydroxybutyrate was isolated in > 95 % yield and 68 % *ee*.  $\delta_{\text{H}}$  ( $\text{C}_6\text{D}_6$ ) 1.94 (3H, d,  $^3J_{\text{HH}}$  6 Hz,  $\text{CH}_3$ ), 3.18 (2H, d,  $^3J_{\text{HH}}$  6 Hz,  $\text{CH}_2$ ), 4.41 (3H, s,  $\text{OCH}_3$ ), 4.81 (1H, s, OH), 4.97 (1H, um, CH).

Elution with dichloromethane and removal of the solvent *in vacuo* yielded (*R*)-BINAP (29 mg, 65 % recovery).  $m/z$  (FAB) 623  $[\text{MH}]^+$  (8 %).  $\delta_{\text{H}}$  6.77 – 7.80 (32 H, complex aromatic region, binaphthyl backbone and  $\text{PPh}_2$  groups).  $\delta_{\text{P}}$  -15.56 (s).  $[\alpha]_{\text{D}}$  ( $\text{CHCl}_3$ ) 203 ° ( $c = 0.4$ ). (Enantiomerically pure (*R*)-BINAP -  $[\alpha]_{\text{D}}$  ( $\text{CHCl}_3$ ) 224.0 ° ( $c = 1.2$ ).

### Separation of a Ru/(*R*)-Rf-BINAP System Under Anaerobic Conditions (S4)

The general separation procedure for anaerobic separations was followed using FRP silica gel after a Ru/(*R*)-Rf-BINAP catalytic run, which had been formed using the method described in the general catalytic procedure and T6. (*R*)-Methyl 3-hydroxybutyrate was collected in > 95 % conversion and 84 % *ee* from the methanol fraction.  $\delta_{\text{H}}$  ( $\text{C}_6\text{D}_6$ ) 1.94 (3H, d,  $^3J_{\text{HH}}$  6 Hz,  $\text{CH}_3$ ), 3.18 (2H, d,  $^3J_{\text{HH}}$  6 Hz,  $\text{CH}_2$ ), 4.41 (3H, s,  $\text{OCH}_3$ ), 4.81 (1H, s, OH), 4.97 (1H, um, CH).

Elution with dichloromethane and removal of the solvent *in vacuo* yielded (*R*)-Rf-BINAP (99 mg, 89 % recovery).  $m/z$  ( $\text{ES}^+$ ) 1259  $[\text{MH}]^+$  (5 %).  $\delta_{\text{H}}$  6.82 – 7.39 (20H, m, Ph), 6.76 (2H, d,  $^3J_{\text{HH}}$  9.4 Hz, ArH), 7.36 (2H, d,  $^3J_{\text{HH}}$  8.5 Hz, ArH), 7.52 (2H, d,  $^3J_{\text{HH}}$  8.0 Hz, ArH), 7.93 (2H, d,  $^3J_{\text{HH}}$  8.5 Hz, ArH), 8.02 (2H, s, ArH).  $\delta_{\text{F}}$  -81.28 (6F, t,  $^4J_{\text{FF}}$  10.6 Hz,  $\text{CF}_3$ ), -110.71 (4F, m,  $\text{CF}_2$ ), -121.82 (4F, m,  $\text{CF}_2$ ), -121.82 (4F, m,  $\text{CF}_2$ ), -123.17 (4F, m,  $\text{CF}_2$ ), -126.51 (4F, m,  $\text{CF}_2$ ).  $\delta_{\text{P}}$  -13.71 (s).  $[\alpha]_{\text{D}}$  ( $\text{C}_6\text{H}_6$ ) 97.5 ° ( $c = 0.7$ ). ((*R*)-Rf-BINAP Ligand prepared above ((*R*)-2.6) -  $[\alpha]_{\text{D}}$  ( $\text{C}_6\text{H}_6$ ) 104.2 ° ( $c = 1.0$ ).

The ligand was reused in a further catalytic run/separation cycle. (*R*)-Methyl 3-hydroxybutyrate was collected in > 95 % conversion and 72 % *ee*.  $\delta_{\text{H}}$  ( $\text{C}_6\text{D}_6$ ) 1.94 (3H, d,  $^3J_{\text{HH}}$  6 Hz,  $\text{CH}_3$ ), 3.18 (2H, d,  $^3J_{\text{HH}}$  6 Hz,  $\text{CH}_2$ ), 4.41 (3H, s,  $\text{OCH}_3$ ), 4.81 (1H, s, OH), 4.97 (1H, um, CH).

68 mg of (*R*)-Rf-BINAP was recovered (69 % recovery of original).  $m/z$  ( $ES^+$ ) 1259 [ $MH$ ] $^+$  (12 %).  $\delta_H$  6.82 – 7.39 (20H, m, Ph), 6.76 (2H, d,  $^3J_{HH}$  9.4 Hz, ArH), 7.36 (2H, d,  $^3J_{HH}$  8.5 Hz, ArH), 7.52 (2H, d,  $^3J_{HH}$  8.0 Hz, ArH), 7.93 (2H, d,  $^3J_{HH}$  8.5 Hz, ArH), 8.02 (2H, s, ArH).  $\delta_F$  –81.28 (6F, t,  $^4J_{FF}$  10.6 Hz,  $CF_3$ ), –110.71 (4F, m,  $CF_2$ ), –121.82 (4F, m,  $CF_2$ ), –121.82 (4F, m,  $CF_2$ ), –123.17 (4F, m,  $CF_2$ ), –126.51 (4F, m,  $CF_2$ ).  $\delta_P$  –13.71 (s).  $[\alpha]_D$  ( $C_6H_6$ ) 97.5 ° ( $c = 0.7$ ). ((*R*)-Rf-BINAP Ligand prepared above ((*R*)-2.6) -  $[\alpha]_D$  ( $C_6H_6$ ) 104.2 ° ( $c = 1.0$ )).

The recovered ligand was reused in one final catalytic run/separation cycle. (*R*)-Methyl 3-hydroxybutyrate was collected in > 95 % conversion and 68 % *ee*.  $\delta_H$  ( $C_6D_6$ ) 1.94 (3H, d,  $^3J_{HH}$  6 Hz,  $CH_3$ ), 3.18 (2H, d,  $^3J_{HH}$  6 Hz,  $CH_2$ ), 4.41 (3H, s,  $OCH_3$ ), 4.81 (1H, s, OH), 4.97 (1H, um, CH).

37 mg of (*R*)-Rf-BINAP was recovered (54 % recovery of original).  $m/z$  ( $ES^+$ ) 1259 [ $MH$ ] $^+$  (3 %).  $\delta_H$  6.82 – 7.34 (20H, m, Ph), 6.74 (2H, d,  $^3J_{HH}$  9.4 Hz, ArH), 7.36 (2H, d,  $^3J_{HH}$  8.5 Hz, ArH), 7.54 (2H, d,  $^3J_{HH}$  8.0 Hz, ArH), 7.94 (2H, d,  $^3J_{HH}$  8.5 Hz, ArH), 8.03 (2H, s, ArH).  $\delta_F$  –81.32 (6F, t,  $^4J_{FF}$  10.5 Hz,  $CF_3$ ), –110.70 (4F, m,  $CF_2$ ), –121.82 (4F, m,  $CF_2$ ), –121.82 (4F, m,  $CF_2$ ), –123.17 (4F, m,  $CF_2$ ), –126.56 (4F, m,  $CF_2$ ).  $\delta_P$  –13.77 (s).  $[\alpha]_D$  ( $C_6H_6$ ) 91.3 ° ( $c = 0.5$ ). ((*R*)-Rf-BINAP Ligand prepared above ((*R*)-2.6) -  $[\alpha]_D$  ( $C_6H_6$ ) 104.2 ° ( $c = 1.0$ )).

### 6.3 Experimental Details for Chapter Three

#### 6.3.1 Synthesis of MonoPhos and Light Fluorous MonoPhos Molecules

##### Preparation of (*R*)-1,1'-bi-2-naphthyl-dimethylphosphoramidite ((*R*)-MonoPhos) ((*R*)-3.1)

(*R*)-1,1'-bi-2-naphthol (2.00 g, 7 mmol) was dissolved in dry diethyl ether (30 ml) and HMPT (1.0 ml, 7 mmol) added *via* syringe. The mixture was stirred under nitrogen for 30 minutes after which time the product precipitated out of solution as a white powder, which was collected by filtration (2.49 g, 99 %). M.p. 117 – 119 °C. *m/z* (ES<sup>+</sup>) 360 [MH]<sup>+</sup> (93 %). [α]<sub>D</sub> (CHCl<sub>3</sub>) -504.3 ° (c = 1.2). Elemental analysis (expected (found)) C 73.54 (73.60), H 5.01 (4.98), N 3.90 (3.84). δ<sub>H</sub> 2.48 (6H, d, <sup>3</sup>J<sub>PH</sub> 9.2 Hz, CH<sub>3</sub>) 7.16 – 7.36 (7H, complex aromatic region, ArH), 7.42 (1H, dd, <sup>3</sup>J<sub>HH</sub> 8.3 Hz, <sup>4</sup>J<sub>HH</sub> 0.7 Hz, ArH), 7.82 (2H, d, <sup>3</sup>J<sub>HH</sub> 9.0 Hz, ArH), 7.83 (1H, d, <sup>3</sup>J<sub>HH</sub> 9.4 Hz, ArH), 7.88 (1H, d, <sup>3</sup>J<sub>HH</sub> 9.0 Hz, ArH). δ<sub>P</sub> {<sup>1</sup>H} 148.68 (s).

##### Preparation of (*S*)-1,1'-bi-2-naphthyl-dimethylphosphoramidite ((*S*)-MonoPhos) ((*S*)-3.1)

The title compound was prepared in the same manner as (*R*)-3.1 above using (*S*)-1,1'-bi-2-naphthol (2.01 g, 7 mmol). The product was again collected directly by filtration from the reaction mixture (2.47 g, 98 %). M.p. 118-119 °C. *m/z* (ES<sup>+</sup>) 360 [MH]<sup>+</sup> (64 %). [α]<sub>D</sub> (CHCl<sub>3</sub>) 504.5 ° (c = 0.9). Elemental analysis (expected (found)) C 73.54 (73.62), H 5.01 (4.92), N 3.90 (3.83). δ<sub>H</sub> 2.48 (6H, d, <sup>3</sup>J<sub>PH</sub> 9.2 Hz, CH<sub>3</sub>) 7.16 – 7.36 (complex aromatic region, 7H, ArH), 7.42 (1H, dd, <sup>3</sup>J<sub>HH</sub> 8.3 Hz, <sup>4</sup>J<sub>HH</sub> 0.7 Hz, ArH), 7.82 (2H, d, <sup>3</sup>J<sub>HH</sub> 9.0 Hz, ArH), 7.83 (1H, d, <sup>3</sup>J<sub>HH</sub> 9.4 Hz, ArH), 7.88 (1H, d, <sup>3</sup>J<sub>HH</sub> 9.0 Hz, ArH). δ<sub>P</sub> {<sup>1</sup>H} 148.71 (2P, s, PNMe<sub>2</sub>).

##### Preparation of (*R*)-6,6'-bis-(perfluoro-*n*-hexyl)-1,1'-bi-2-naphthyl-dimethylphosphoramidite ((*R*)-Rf-MonoPhos) ((*R*)-3.2)

(*R*)-6,6'-bis-(perfluoro-*n*-hexyl)-1,1'-bi-2-naphthol (2.04 g, 2.2 mmol) was dissolved in dry and degassed diethyl ether and HMPT (0.52 ml, 2.2 mmol) added *via* syringe. The mixture was then stirred for 30 minutes under nitrogen. The solvent was removed under reduced pressure to yield a yellow oil which was washed with acetonitrile (3 x 25 ml) and triturated with dichloromethane to yield an off-white solid. (1.49 g, 68 %). M.p. 118 – 120 °C. *m/z* (FAB) 996 [MH]<sup>+</sup> (8 %). [α]<sub>D</sub> (CHCl<sub>3</sub>) -205 ° (c = 2.3). Elemental analysis (expected (found)) C 41.01 (40.86), H 1.61 (1.58), N 1.41 (1.42). δ<sub>H</sub> 2.51 (6H, d, <sup>3</sup>J<sub>PH</sub> 9.2 Hz, CH<sub>3</sub>) 7.31 (2H, s, ArH), 7.38 (2H, s, ArH), 7.45 (1H, d, <sup>3</sup>J<sub>HH</sub> 8.7 Hz, ArH), 7.56 (1H, d, <sup>3</sup>J<sub>HH</sub> 8.3 Hz, ArH), 7.96 (1H, d, <sup>3</sup>J<sub>HH</sub> 8.7 Hz, ArH), 8.05 (1H, d, <sup>3</sup>J<sub>HH</sub> 8.7 Hz, ArH), 8.15 (1H, s, ArH), 8.17 (1H, s, ArH). δ<sub>F</sub> -81.27 (6F, t, <sup>4</sup>J<sub>FF</sub> 10.6 Hz, CF<sub>3</sub>), -110.59 (4F, tm, <sup>4</sup>J<sub>FF</sub> 13.9 Hz, α-CF<sub>2</sub>), -121.89 (4F, um, CF<sub>2</sub>), -121.89 (4F, um, CF<sub>2</sub>), -123.22 (4F, um, CF<sub>2</sub>), -128.14 (4F, um, CF<sub>2</sub>). δ<sub>P</sub> {<sup>1</sup>H} 149.95 (s).

### Preparation of (*S*)-6,6'-bis-(perfluoro-*n*-hexyl)-1,1'-bi-2-naphthyl-dimethylphosphoramidite ((*S*)-Rf-MonoPhos) ((*S*)-3.2)

The title compound was prepared as for (*R*)-3.2 above using (*S*)-6,6'-bis-(perfluoro-*n*-hexyl)-1,1'-bi-2-naphthol (2.02 g, 2.2 mmol) and HMPT (0.52 ml, 2.2 mmol). The product was collected as an off-white solid after trituration (1.56 g, 71 %). M.p. 118 – 120 °C. *m/z* (FAB) 996 [MH]<sup>+</sup> (7 %). [α]<sub>D</sub> (CHCl<sub>3</sub>) 195.8 ° (c = 1.6). Elemental analysis (expected (found)) C 41.01 (41.00), H 1.61 (1.48), N 1.41 (1.37). δ<sub>H</sub> 2.51 (6H, d, <sup>3</sup>J<sub>PH</sub> 9.2 Hz, CH<sub>3</sub>) 7.31 (2H, s, ArH), 7.38 (2H, s, ArH), 7.45 (1H, d, <sup>3</sup>J<sub>HH</sub> 8.7 Hz, ArH), 7.56 (1H, d, <sup>3</sup>J<sub>HH</sub> 8.3 Hz, ArH), 7.96 (1H, d, <sup>3</sup>J<sub>HH</sub> 8.7 Hz, ArH), 8.05 (1H, d, <sup>3</sup>J<sub>HH</sub> 8.7 Hz, ArH), 8.15 (1H, s, ArH), 8.17 (1H, s, ArH). δ<sub>F</sub> -81.27 (6F, t, <sup>4</sup>J<sub>FF</sub> 10.6 Hz, CF<sub>3</sub>), -110.58 (4F, <sup>4</sup>J<sub>FF</sub> 13.9 Hz, α-CF<sub>2</sub>), -121.88 (4F, um, CF<sub>2</sub>), -121.88 (4F, um, CF<sub>2</sub>), -123.22 (4F, um, CF<sub>2</sub>), -126.56 (4F, um, CF<sub>2</sub>). δ<sub>P</sub> {<sup>1</sup>H} 149.95 (s).

### General Procedure for the Determination of MonoPhos Partition Coefficients

A known quantity of ligand was stirred for 20 minutes in dry and degassed toluene (2.0 ml) and PP3 (2.0 ml). The mixture was then allowed to stand for 20 minutes before 1.0 ml of each layer was collected *via* syringe and dried to constant mass under vacuum. The partition coefficient was determined by comparison of the amount of ligand by weight in each fraction.

#### Determination of (*S*)-MonoPhos Partition Coefficient

(*S*)-MonoPhos (52 mg) was used. 16 mg of ligand was found in the 1.0 ml of toluene phase. The PP3 sample contained no ligand. The ligand was not completely soluble in either phase. Partition coefficient: 100 % in toluene phase, 62 % solubilised.

#### Determination of (*S*)-Rf-MonoPhos Partition Coefficient

(*S*)-Rf-MonoPhos (76 mg) was used. 17 mg of ligand was found in the 1.0 ml of toluene phase by mass. 21 mg was found in the 1 ml of PP3 phase. Partition coefficient: 55 % in fluoruous phase.

### 6.3.2 Preparation of Coordination Complexes

#### Preparation of *cis*-[PtCl<sub>2</sub>((*R*)-MonoPhos)<sub>2</sub>] ((*R*)-3.3)

*Cis*-[PtCl<sub>2</sub>(MeCN)<sub>2</sub>] (0.08 g, 2.3 x 10<sup>-4</sup> mol) and (*R*)-MonoPhos (0.166 g, 4.6 x 10<sup>-4</sup> mol) were dissolved in dry and degassed dichloromethane (25 ml) and stirred over night under nitrogen. The solvent was removed under reduced pressure and the crude product recrystallised from 1:10 dichloromethane/hexane. The precipitate was dried under vacuum to yield the product as a pale yellow solid (0.119 g, 53 %). M.p. 228 – 230 °C (dec). *m/z* (FAB) 949 [M-Cl]<sup>+</sup> (41 %). [α]<sub>D</sub>

(CHCl<sub>3</sub>) 119.2 ° (c = 1.2). Elemental analysis (expected (found)) C 53.66 (53.46), H 3.66 (3.65), N 2.85 (2.81).  $\delta_{\text{H}}$  2.13 (12H, d,  $^3J_{\text{PH}}$  9.2 Hz, CH<sub>3</sub>), 7.00 – 7.55 (14H, Complex aromatic region, ArH), 7.88 (4H, d,  $^3J_{\text{HH}}$  8.0 Hz, ArH), 7.93 (2H, d,  $^3J_{\text{HH}}$  8.7 Hz, ArH), 7.96 (2H, d,  $^3J_{\text{HH}}$  8.5 Hz, ArH), 8.20 (2H, d,  $^3J_{\text{HH}}$  8.7 Hz, ArH)  $\delta_{\text{P}}$  {<sup>1</sup>H} 93.22 (ss,  $^1J_{\text{Pt-P}}$  5604 Hz).

#### Preparation of *cis*-[PtCl<sub>2</sub>((*S*)-MonoPhos)<sub>2</sub>] ((*S*)-3.3)

The title compound was prepared following the same procedure as for (*R*)-3.3 above using (*S*)-MonoPhos (0.166 g, 4.6 x 10<sup>-4</sup> mol). The product was collected as a pale yellow solid. (0.113 g, 50 %). M.p. > 228 – 230 °C (dec). m/z (FAB) 949 [M-Cl]<sup>+</sup> (73 %). [ $\alpha$ ]<sub>D</sub> (CHCl<sub>3</sub>) -115.9 ° (c = 1.5). Elemental analysis (expected (found)) C 53.66 (53.67), H 3.66 (3.62), N 2.85 (2.81).  $\delta_{\text{H}}$  2.13 (12H, d,  $^3J_{\text{PH}}$  9.2 Hz, CH<sub>3</sub>), 7.00 – 7.55 (14H, Complex aromatic region, ArH), 7.88 (4H, bd,  $^3J_{\text{HH}}$  7.3 Hz, ArH), 7.94 (2H, d,  $^3J_{\text{HH}}$  9.0 Hz, ArH), 7.95 (2H, d,  $^3J_{\text{HH}}$  9.0 Hz, ArH), 8.20 (2H, d,  $^3J_{\text{HH}}$  8.7 Hz, ArH)  $\delta_{\text{P}}$  {<sup>1</sup>H} 93.23 (ss,  $^1J_{\text{Pt-P}}$  5604 Hz).

#### Preparation of *cis*-[PtCl<sub>2</sub>((*R*)-Rf-MonoPhos)<sub>2</sub>] ((*R*)-3.4)

*Cis*-[PtCl<sub>2</sub>(MeCN)<sub>2</sub>] (0.04 g, 1.2 x 10<sup>-4</sup> mol) and (*R*)-Rf-MonoPhos (0.229 g, 2.3 x 10<sup>-4</sup> mol) were dissolved in dry and degassed dichloromethane (25 ml) and stirred over night under nitrogen. The solvent was removed under reduced pressure. The residue was recrystallised from 1:10 dichloromethane/petroleum ether (b.p. 40 – 60 °C) and dried under vacuum to yield the product as a pale yellow solid (0.122 g, 45 %). M.p. 147 °C (dec.). m/z (FAB) 2222 [M-Cl]<sup>+</sup> (29 %). [ $\alpha$ ]<sub>D</sub> (CHCl<sub>3</sub>) 84.9 ° (c = 1.2). Elemental analysis (expected (found)) C 36.17 (35.94), H 1.42 (1.30), N 1.24 (1.35).  $\delta_{\text{H}}$  2.18 (12H, d,  $^3J_{\text{PH}}$  10.8 Hz, CH<sub>3</sub>), 7.40 – 7.52 (10H, um, ArH), 8.10 (2H, d,  $^3J_{\text{HH}}$  8.8 Hz, ArH), 8.18 (2H, d,  $^3J_{\text{HH}}$  9.2 Hz, ArH), 8.22 (4H, d,  $^3J_{\text{HH}}$  9.1 Hz, ArH), 8.36 (2H, d,  $^3J_{\text{HH}}$  8.5 Hz, ArH).  $\delta_{\text{F}}$  -80.75 (12F, t,  $^4J_{\text{FF}}$  8.6 Hz, CF<sub>3</sub>), -110.35 (8F, um,  $\alpha$ -CF<sub>2</sub>), -121.31 (8F, um, CF<sub>2</sub>), -121.58 (8F, um, CF<sub>2</sub>), -122.72 (8F, um, CF<sub>2</sub>), -126.06 (8F, um, CF<sub>2</sub>).  $\delta_{\text{P}}$  {<sup>1</sup>H} 95.32 (ss,  $^1J_{\text{PtP}}$  5582 Hz).

#### Preparation of *cis*-[PtCl<sub>2</sub>((*S*)-Rf-MonoPhos)<sub>2</sub>] ((*S*)-3.4)

The product was prepared as above using (*S*)-Rf-MonoPhos (0.229 g, 2.3 x 10<sup>-4</sup> mol). The product was collected as an off-white solid (0.132 g, 49 %). M.p. 145 °C (dec.). m/z (FAB) 2221 [M-Cl]<sup>+</sup> (100 %). [ $\alpha$ ]<sub>D</sub> (CHCl<sub>3</sub>) -79.9 ° (c = 1.1). Elemental analysis (expected (found)) C 36.17 (35.94), H 1.42 (1.40), N 1.24 (1.17).  $\delta_{\text{H}}$  2.17 (12H, d,  $^3J_{\text{PH}}$  10.8 Hz, CH<sub>3</sub>), 7.40 – 7.52 (8H, um, ArH), 8.10 (4H, d,  $^3J_{\text{HH}}$  9.0 Hz, ArH), 8.17 (2H, d,  $^3J_{\text{HH}}$  9.1 Hz, ArH), 8.22 (4H, d,  $^3J_{\text{HH}}$  9.3 Hz, ArH), 8.36 (2H, d,  $^3J_{\text{HH}}$  8.7 Hz, ArH).  $\delta_{\text{F}}$  -80.76 (12F, t,  $^4J_{\text{FF}}$  8.6 Hz, CF<sub>3</sub>), -110.36 (8F, um  $\alpha$ -CF<sub>2</sub>), -121.37 (8F, um, CF<sub>2</sub>), -121.58 (8F, um, CF<sub>2</sub>), -122.72 (8F, um, CF<sub>2</sub>), -127.78 (8F, um, CF<sub>2</sub>).  $\delta_{\text{P}}$  {<sup>1</sup>H} 95.36 (ss,  $^1J_{\text{PtP}}$  5578 Hz).

### Preparation of *trans*-[PdCl<sub>2</sub>((*R*)-MonoPhos)<sub>2</sub>] ((*R*)-3.5)

[PdCl<sub>2</sub>(MeCN)<sub>2</sub>] (0.08 g, 3.1 × 10<sup>-4</sup> mol) and (*R*)-MonoPhos (0.223 g, 6.2 × 10<sup>-4</sup> mol) were dissolved in dichloromethane (10 ml) and stirred for 1 hour under nitrogen. The product was collected directly from the reaction mixture as a bright orange solid by filtration (0.152 g, 55 %). M.p. 220 °C (dec.). m/z (FAB) 859 [M-Cl]<sup>+</sup> (32 %), 824 [M-2Cl]<sup>+</sup> (5 %). [α]<sub>D</sub> (CHCl<sub>3</sub>) -127.5 ° (c = 1.2). Elemental analysis (expected (found)) C 58.99 (58.89), H 4.02 (3.96), N 3.13 (3.02). δ<sub>H</sub> 2.15 (12H, vt, *J*<sub>PH</sub> 10.6 Hz, CH<sub>3</sub>), 7.23 – 7.48 (6H, um, ArH), 7.89 (2H, d, <sup>3</sup>*J*<sub>HH</sub> 7.55 Hz, ArH), 7.94 (2H, d, <sup>3</sup>*J*<sub>HH</sub> 8.45 Hz, ArH), 8.02 (1H, d, <sup>3</sup>*J*<sub>HH</sub> 8.7 Hz, ArH), 8.28 (1H, d, <sup>3</sup>*J*<sub>HH</sub> 8.73 Hz, ArH). δ<sub>P</sub> {<sup>1</sup>H} 118.49 (s). IR (nujol) 354.1 cm<sup>-1</sup> (*trans*-Pd-Cl).

### Preparation of *trans*-[PdCl<sub>2</sub>((*S*)-MonoPhos)<sub>2</sub>] ((*S*)-3.5)

The title compound was prepared and isolated similarly to compound (*R*)-3.5 above using (*S*)-MonoPhos (0.223 g, 2.2 × 10<sup>-4</sup> mol). (0.155 g, 56 %). M.p. 220 °C (dec.). m/z (FAB) 859 [M-Cl]<sup>+</sup> (37 %), 824 [M-2Cl]<sup>+</sup> (4 %). [α]<sub>D</sub> (CHCl<sub>3</sub>) 134.5 ° (c = 1.2). Elemental analysis (expected (found)) C 58.99 (59.04), H 4.02 (3.87), N 3.13 (3.07). δ<sub>H</sub> 2.15 (6H, vt, *J*<sub>PH</sub> 10.6 Hz, CH<sub>3</sub>), 7.22 – 7.48 (12H, um, ArH), 7.89 (4H, d, <sup>3</sup>*J*<sub>HH</sub> 7.6 Hz, ArH), 7.94 (4H, d, <sup>3</sup>*J*<sub>HH</sub> 8.4 Hz, ArH), 8.02 (2H, d, <sup>3</sup>*J*<sub>HH</sub> 8.7 Hz, ArH), 8.28 (2H, d, <sup>3</sup>*J*<sub>HH</sub> 8.7 Hz, ArH). δ<sub>P</sub> {<sup>1</sup>H} 118.47 (s). IR (nujol) 354.5 cm<sup>-1</sup> (*trans*-Pd-Cl).

### Preparation of *trans*-[PdCl<sub>2</sub>((*R*)-Rf-MonoPhos)<sub>2</sub>] ((*R*)-3.6)

[PdCl<sub>2</sub>(MeCN)<sub>2</sub>] (0.02 g, 7.7 × 10<sup>-5</sup> mol) and Rf-MonoPhos (0.153 g, 1.54 × 10<sup>-4</sup> mol) were dissolved in dichloromethane (15 ml) and stirred for 1 hour under nitrogen. The solvent was removed under reduced pressure and the crude product recrystallised from 1:10 dichloromethane/hexane to yield a pale yellow solid. (0.098 g, 57 %). M.p. 145 – 147 °C. m/z (FAB) 2132 [M-Cl]<sup>+</sup> (10 %). [α]<sub>D</sub> (CHCl<sub>3</sub>) -76.3 ° (c = 1.4). Elemental analysis (expected (found)) C 37.66 (37.51), H 1.48 (1.40), N 1.29 (1.30). δ<sub>H</sub> 2.17 (12H, d, <sup>3</sup>*J*<sub>PH</sub> 10.4 Hz, CH<sub>3</sub>), 7.41 – 7.51 (10H, um, ArH), 8.11 (2H, d, <sup>3</sup>*J*<sub>HH</sub> 9.1 Hz, ArH), 8.21 (2H, um, ArH), 8.23 (4H, d, <sup>3</sup>*J*<sub>HH</sub> 9.3 Hz, ArH), 8.42 (2H, d, <sup>3</sup>*J*<sub>HH</sub> 8.8 Hz, ArH). δ<sub>F</sub> -80.73 (12F, t, <sup>4</sup>*J*<sub>FF</sub> 10.1 Hz, CF<sub>3</sub>), -110.77 (8F, um, α-CF<sub>2</sub>), -121.79 (8F, um, CF<sub>2</sub>), -122.20 (8F, um, CF<sub>2</sub>), -123.18 (8F, um, CF<sub>2</sub>), -125.90 (8F, um, CF<sub>2</sub>). δ<sub>P</sub> {<sup>1</sup>H} 119.93 (s). IR (nujol) 356.0 cm<sup>-1</sup> (*trans*-Pd-Cl).

### Preparation of *trans*-[PdCl<sub>2</sub>((*S*)-Rf-MonoPhos)<sub>2</sub>] ((*S*)-3.6)

The product was prepared as for compound 3.6 using (*S*)-Rf-MonoPhos (0.153 g, 1.54 x 10<sup>-4</sup> mol). (0.101 g, 60 %). M.p. 144 – 146 °C. m/z (FAB) 2132 [M-Cl]<sup>+</sup> (23 %). [α]<sub>D</sub> (CHCl<sub>3</sub>) 86.1° (c = 1.4). Elemental analysis (expected (found)) C 37.66 (37.69), H 1.48 (1.38), N 1.29 (1.28). δ<sub>H</sub> 2.17 (12H, vt, *J*<sub>PH</sub> 10.6 Hz, CH<sub>3</sub>), 7.44 – 7.51 (10H, um ArH), 8.10 (2H, d, <sup>3</sup>*J*<sub>HH</sub> 8.8 Hz, ArH), 8.19 (2H, um, ArH), 8.22 (4H, d, <sup>3</sup>*J*<sub>HH</sub> 9.5 Hz, ArH), 8.42 (2H, d, <sup>3</sup>*J*<sub>HH</sub> 9.1 Hz, ArH). δ<sub>F</sub> -80.73 (12F, t, <sup>4</sup>*J*<sub>FF</sub> 9.0 Hz, CF<sub>3</sub>), -110.40 (8F, um, α-CF<sub>2</sub>), -121.30 (8F, um, CF<sub>2</sub>), -121.57 (8F, um, CF<sub>2</sub>), -122.71 (8F, um, CF<sub>2</sub>), -127.21 (8F, um, CF<sub>2</sub>). δ<sub>P</sub> {<sup>1</sup>H} 119.94 (s). IR (nujol) 356.1 cm<sup>-1</sup> (*trans*-Pd-Cl).

### Preparation of [RhCp\*Cl<sub>2</sub>((*R*)-MonoPhos)] ((*R*)-3.7)

[RhCp\*Cl<sub>2</sub>]<sub>2</sub> (0.08 g, 1.3 x 10<sup>-4</sup> mol) and (*R*)-MonoPhos (0.093 g, 2.6 x 10<sup>-4</sup> mol) were dissolved in dichloromethane and stirred for one hour. The solvent was removed under reduced pressure and the solid obtained redissolved in a small volume of dichloromethane (3 ml). The product was precipitated from solution by addition of petroleum ether (b.p. 40 – 60 °C), collected by filtration and dried *in vacuo* to yield a red-orange solid (0.152 g, 88 %). M.p. 228 – 230 °C. m/z (FAB) 632 [M-Cl]<sup>+</sup> (100 %), 597 [M-2Cl]<sup>+</sup> (9 %). [α]<sub>D</sub> (CHCl<sub>3</sub>) 43.4° (c = 3.1). Elemental analysis (Expected (Found)) C 57.49 (57.69), H 4.94 (4.99), N 2.10 (1.99). δ<sub>H</sub> (253 K) 1.56 (15H, d, *J*<sub>PH</sub> 3.9 Hz, Cp\*H), 2.51 (6H, d, <sup>3</sup>*J*<sub>PH</sub> 9.8 Hz, CH<sub>3</sub>), 7.24 (4H, um, ArH), 7.47 (4H, um, ArH), 7.98 (1H, d, <sup>3</sup>*J*<sub>HH</sub> 9.4 Hz, ArH), 8.00 (2H, d, <sup>3</sup>*J*<sub>HH</sub> 9.4 Hz, ArH), 8.05 (1H, d, <sup>3</sup>*J*<sub>HH</sub> 8.9 Hz, ArH). δ<sub>P</sub> {<sup>1</sup>H} (253 K) 141.74 (d, <sup>1</sup>*J*<sub>P-Rh</sub> 223 Hz).

### Preparation of [RhCp\*Cl<sub>2</sub>((*S*)-MonoPhos)] ((*R*)-3.7)

The same procedure was carried out as for compound (*R*)-3.7 above using (*S*)-MonoPhos (0.093 g, 2.6 x 10<sup>-4</sup> mol). The product was collected again as a red-orange solid (0.142 g, 82 %). M.p. 229 – 230 °C. m/z (FAB) 632 [M-Cl]<sup>+</sup> (100 %), 597 [M-2Cl]<sup>+</sup> (7 %). [α]<sub>D</sub> (CHCl<sub>3</sub>) -39.7 (c = 1.3). Elemental analysis (Expected (Found)) C 57.53 (57.69), H 4.91 (4.99), N 2.01 (1.99). δ<sub>H</sub> (253 K) 1.55 (15H, d, *J*<sub>PH</sub> 3.9 Hz, Cp\*H), 2.50 (6H, d, <sup>3</sup>*J*<sub>PH</sub> 9.9 Hz, CH<sub>3</sub>), 7.29 (4H, um, ArH), 7.44 (4H, um, ArH), 7.98 (1H, d, <sup>3</sup>*J*<sub>HH</sub> 9.4 Hz, ArH), 8.01 (2H, d, <sup>3</sup>*J*<sub>HH</sub> 9.4 Hz, ArH), 8.06 (1H, d, <sup>3</sup>*J*<sub>HH</sub> 8.9 Hz, ArH). δ<sub>P</sub> {<sup>1</sup>H} (253 K) 141.72 (d, <sup>1</sup>*J*<sub>P-Rh</sub> 223 Hz).

### Preparation of [RhCp\*Cl<sub>2</sub>((*R*)-Rf-MonoPhos)] ((*R*)-3.8)

[RhCp\*Cl<sub>2</sub>]<sub>2</sub> (0.04 g, 6.5 x 10<sup>-5</sup> mol) and (*R*)-Rf-MonoPhos (0.129 g, 1.3 x 10<sup>-4</sup> mol) were dissolved in dichloromethane and stirred for one hour. The solvent was removed under reduced pressure and the solid obtained recrystallised from dichloromethane/hexane. The product was collected as a red-orange powder (0.137 g, 81 %). M.p. 96 – 98 °C. m/z (FAB) 1269 [M-Cl]<sup>+</sup> (38

%).  $[\alpha]_D$  (CHCl<sub>3</sub>) 15.9 (c = 1.2). Elemental analysis (Expected (Found)) C 40.49 (40.37), H 2.38 (2.39), N 1.07 (0.98).  $\delta_H$  (253 K) 1.63 (15H, d,  $J_{PH}$  5.1 Hz, Cp\*H), 2.54 (6H, d,  $^3J_{PH}$  10.1 Hz, CH<sub>3</sub>), 7.30 (1H, d,  $^3J_{HH}$  9.0 Hz, ArH), 7.38 (2H, d,  $^3J_{HH}$  8.6 Hz, ArH), 7.44 (1H, d,  $^3J_{HH}$  9.4 Hz, ArH), 7.58 (1H, d,  $^3J_{HH}$  9.0 Hz, ArH), 7.60 (1H, d,  $^3J_{HH}$  8.7 Hz, ArH), 8.16 (1H, d,  $^3J_{HH}$  8.9 Hz, ArH), 8.21 (1H, d,  $^3J_{HH}$  9.1 Hz, ArH), 8.28 (1H, s, ArH), 8.31 (1H, s, ArH).  $\delta_F$  (253 K) -81.19 (6F, t,  $^4J_{FF}$  10.6 Hz, CF<sub>3</sub>), -110.65 (4F, um,  $\alpha$ -CF<sub>2</sub>), -121.82 (4F, um, CF<sub>2</sub>), -121.82 (4F, um, CF<sub>2</sub>), -123.18 (4F, um, CF<sub>2</sub>), -126.52 (4F, um, CF<sub>2</sub>).  $\delta_P\{^1H\}$  (253 K) 143.39 (d,  $^1J_{P-Rh}$  225 Hz).

### Preparation of [RhCp\*Cl<sub>2</sub>((S)-Rf-MonoPhos)] ((S)-3.8)

Procedure 3.8 was carried out again using (S)-Rf-MonoPhos (0.129 g,  $1.3 \times 10^{-4}$  mol) and [RhCp\*Cl<sub>2</sub>]<sub>2</sub> (0.04 g,  $6.5 \times 10^{-5}$  mol). The product was collected as a red powder (0.144 g, 85 %). M.p. 96 – 97 °C. m/z (FAB) 1269 [M-Cl]<sup>+</sup> (40 %).  $[\alpha]_D$  (CHCl<sub>3</sub>) -22.1 ° (c = 1.2). Elemental analysis (Expected (Found)) C 40.31 (40.37), H 2.38 (2.27), N 1.11 (1.02).  $\delta_H$  (253 K) 1.64 (15H, d,  $J_{PH}$  5.3 Hz, Cp\*H), 2.53 (6H, d,  $^3J_{PH}$  10.2 Hz, CH<sub>3</sub>), 7.30 (1H, d,  $^3J_{HH}$  8.9 Hz, ArH), 7.39 (2H, d,  $^3J_{HH}$  8.7 Hz, ArH), 7.44 (1H, d,  $^3J_{HH}$  9.4 Hz, ArH), 7.59 (1H, d,  $^3J_{HH}$  9.0 Hz, ArH), 7.61 (1H, d,  $^3J_{HH}$  8.8 Hz, ArH), 8.16 (1H, d,  $^3J_{HH}$  8.8 Hz, ArH), 8.24 (1H, d,  $^3J_{HH}$  9.1 Hz, ArH), 8.29 (1H, s, ArH), 8.31 (1H, s, ArH).  $\delta_F$  (253 K) -81.11 (6F, t,  $^4J_{FF}$  10.2 Hz, CF<sub>3</sub>), -110.65 (4F, um,  $\alpha$ -CF<sub>2</sub>), -121.86 (4F, um, CF<sub>2</sub>), -121.86 (4F, um, CF<sub>2</sub>), -123.18 (4F, um, CF<sub>2</sub>), -126.52 (4F, um, CF<sub>2</sub>).  $\delta_P\{^1H\}$  (253 K) 143.37 (d,  $^1J_{P-Rh}$  225.3 Hz).

### 6.3.3 Catalytic Testing

#### General Procedure for the Hydrogenation of Dimethyl Itaconate

[Rh(cod)<sub>2</sub>]BF<sub>4</sub> catalyst precursor (16 mg,  $4 \times 10^{-5}$  mol) and the MonoPhos ligand ( $8.6 \times 10^{-5}$  mol) were dissolved in dry and degassed ethyl acetate (10 ml) and dimethyl itaconate added (123 mg, 0.8 mmol). The resulting solution was briefly placed under vacuum before being placed under 1 atm of hydrogen gas and stirred for 20 hours.

The mixture was concentrated *in vacuo* and passed through a short plug of silica gel. The solvent was then removed under reduced pressure to yield dimethyl succinate. Percentage conversion was determined by <sup>1</sup>H NMR analysis and product *ee* determined by chiral HPLC (Diacel Chiralcel OD-H, 8 % IPA in hexane, 1 ml/min. Sample loop: 6  $\mu$ l. Detector: 220 nm. (S)-dimethyl succinate, R<sub>t</sub> 4.37 min, (R)-dimethyl succinate, R<sub>t</sub> 6.33 min) or chiral GC (Shimadzu GC-17A, Supelco Beta Dex 225 Fused Silica Capillary Column, 30m x 0.25 mm (od) x 0.25  $\mu$ m (film thickness). 100 °C for 25 min, 20 °C/min to 200 °C, hold 5 min. Injector: 220 °C, detector: 300 °C. Flow rate: 1.1 ml/min. (S)-dimethyl succinate, R<sub>t</sub> 15.27 min, (R)-dimethyl succinate, R<sub>t</sub> 15.74 min).

**Asymmetric Hydrogenation Using (*R*)-MonoPhos (T12)**

The general procedure was followed using (*R*)-MonoPhos (31 mg,  $8.6 \times 10^{-5}$  mol). Three separate catalytic runs were carried out and the product collected as a yellow oil in each case.  $\delta_{\text{H}}$  1.14 (3H, d,  $^3J_{\text{HH}}$  7.3 Hz, CH<sub>3</sub>), 2.32 (1H, dd,  $^2J_{\text{HH}}$  17.8 Hz,  $^3J_{\text{HH}}$  7.2 Hz, CH<sub>2</sub>), 2.68 (1H, dd,  $^2J_{\text{HH}}$  18.1 Hz,  $^3J_{\text{HH}}$  7.9 Hz, CH<sub>2</sub>), 2.83 (1H, um, CH), 3.60 (3H, s, CH<sub>3</sub>), 3.62 (3H, s, CH<sub>3</sub>).  $m/z$  (ES<sup>+</sup>) 160 [M]<sup>+</sup> (15 %). Run 1, 93 % conversion, 78 % *ee*; Run 2, 97 % conversion, 90 % *ee*; Run 3, 95 % conversion, 98 % *ee*.

**Asymmetric Hydrogenation Using (*S*)-MonoPhos (T13)**

The general procedure was followed using (*S*)-MonoPhos (31 mg,  $8.6 \times 10^{-5}$  mol). Three separate catalytic runs were carried out and the product collected as a yellow oil in each case.  $\delta_{\text{H}}$  1.14 (3H, d,  $^3J_{\text{HH}}$  7.3 Hz, CH<sub>3</sub>), 2.32 (1H, dd,  $^2J_{\text{HH}}$  17.8 Hz,  $^3J_{\text{HH}}$  7.2 Hz, CH<sub>2</sub>), 2.68 (1H, dd,  $^2J_{\text{HH}}$  18.1 Hz,  $^3J_{\text{HH}}$  7.9 Hz, CH<sub>2</sub>), 2.83 (1H, um, CH), 3.60 (3H, s, CH<sub>3</sub>), 3.62 (3H, s, CH<sub>3</sub>).  $m/z$  (ES<sup>+</sup>) 160 [M]<sup>+</sup> (10 %). Run 1, 92 % conversion, 95 % *ee*; Run 2, 98 % conversion, 95 % *ee*; Run 3, 95 % conversion, 95 % *ee*.

**Asymmetric Hydrogenation Using (*R*)-Rf-MonoPhos (T14)**

The general procedure was followed using (*R*)-Rf-MonoPhos (86 mg,  $8.6 \times 10^{-5}$  mol). Three separate catalytic runs were carried out and the product collected as a yellow oil in each case.  $\delta_{\text{H}}$  1.14 (3H, d,  $^3J_{\text{HH}}$  7.3 Hz, CH<sub>3</sub>), 2.32 (1H, dd,  $^2J_{\text{HH}}$  17.8 Hz,  $^3J_{\text{HH}}$  7.2 Hz, CH<sub>2</sub>), 2.68 (1H, dd,  $^2J_{\text{HH}}$  18.1 Hz,  $^3J_{\text{HH}}$  7.9 Hz, CH<sub>2</sub>), 2.83 (1H, um, CH), 3.60 (3H, s, CH<sub>3</sub>), 3.62 (3H, s, CH<sub>3</sub>).  $m/z$  (ES<sup>+</sup>) 160 [M]<sup>+</sup> (15 %). Run 1, 90 % conversion, 90 % *ee*; Run 2, 90 % conversion, 85 % *ee*; Run 3, 90 % conversion, 75 % *ee*.

**Asymmetric Hydrogenation Using (*S*)-Rf-MonoPhos (T15)**

The general procedure was followed using (*S*)-Rf-MonoPhos (86 mg,  $8.6 \times 10^{-5}$  mol). Three separate catalytic runs were carried out and the product collected as a yellow oil in each case.  $\delta_{\text{H}}$  1.14 (3H, d,  $^3J_{\text{HH}}$  7.3 Hz, CH<sub>3</sub>), 2.32 (1H, dd,  $^2J_{\text{HH}}$  17.8 Hz,  $^3J_{\text{HH}}$  7.2 Hz, CH<sub>2</sub>), 2.68 (1H, dd,  $^2J_{\text{HH}}$  18.1 Hz,  $^3J_{\text{HH}}$  7.9 Hz, CH<sub>2</sub>), 2.83 (1H, um, CH), 3.60 (3H, s, CH<sub>3</sub>), 3.62 (3H, s, CH<sub>3</sub>).  $m/z$  (ES<sup>+</sup>) 160 [M]<sup>+</sup> (19 %). Run 1, 84 % conversion, 85 % *ee*; Run 2, 86 % conversion, 95 % *ee*; Run 3, 85 % conversion, 90 % *ee*.

### 6.3.4 Solid Phase Separation

#### General Procedure for the Separation of MonoPhos-Based Catalysts from Dimethyl Succinate

Silica gel or FRP silica gel were dried and degassed under high vacuum at 150 °C for 24 hours. In a dry box under nitrogen, the silica gel was then added to length of 3 cm to a column 1 cm in diameter. After a catalytic run using (*R*)-MonoPhos or (*R*)-Rf-MonoPhos the reaction mixture was concentrated under reduced pressure and added to the top of the column under nitrogen. The product was then eluted with dry and degassed ethyl acetate. Recovery of a catalytically active species and/or the ligand was not possible using any solvent.

### 6.3.5 Supported Catalysis

#### General Procedure for Catalysis Using a Supported Catalyst

[Rh(cod)<sub>2</sub>]BF<sub>4</sub> (16 mg, 4 × 10<sup>-5</sup> mol) and (*R*)-Rf-MonoPhos were stirred in dry and degassed dichloromethane containing 250 mg of dry and degassed FRP silica gel for 30 minutes. The solvent was then removed under reduced pressure and the silica dried under high vacuum. Dimethyl itaconate (123 mg, 0.8 mmol) was added under nitrogen and dry and degassed ethyl acetate (10 ml) added as solvent. The mixture was briefly placed under vacuum before being placed under 1 atm of hydrogen gas and stirred for 20 hours.

The reaction mixture was filtered in a dry box under nitrogen and the silica gel recovered and reused in a subsequent reaction. The product was obtained in 5 % overall conversion with high ligand contamination. The *ee* was not determined. The supported catalyst proved to be inactive in further catalysis.

### 6.3.6 Synthesis of Heavy Fluorous (*R*)-Rf<sub>4</sub>-MonoPhos and Complexes

#### Preparation of (*R*)-2,2'-dihexyloxy-1,1'-binaphthyl ((*R*)-3.9)

(*R*)-1,1'-Bi-2-naphthol (6.01 g, 21 mmol), potassium carbonate (16.0 g) and 1-bromohexane (10.0 ml, 71.3 mmol) were dissolved in acetone (100 ml) and heated to reflux under nitrogen for 72 hours. Upon cooling to room temperature, water was added (75 ml) and the mixture extracted with hexane. The organic layer was washed with brine (50 ml), dried (MgSO<sub>4</sub>), filtered and the solvent removed under reduced pressure to yield a yellow oil. Methanol was added to the oil (75 ml) and the mixture stirred for 30 minutes, whereupon white crystals of product crashed out of solution. Filtration of the suspension yielded the product as white crystals (7.29 g, 76 %). M.p. 42 – 43 °C. *m/z* (ES<sup>+</sup>) 455 [M]<sup>+</sup> 66 %. [α]<sub>D</sub> (THF) 36.1 ° (c = 1.0). δ<sub>H</sub> 0.71 (6H, t, <sup>3</sup>J<sub>HH</sub> 6.9 Hz, CH<sub>3</sub>), 0.94 (12H, m, (CH<sub>2</sub>)<sub>3</sub>), 1.33 (4H, m, CH<sub>2</sub>), 3.86 (4H, m, CH<sub>2</sub>), 6.88 – 8.44 (12H, complex aromatic region, ArH). δ<sub>C</sub> 12.87 (CH<sub>3</sub>), 21.39 (CH<sub>2</sub>), 24.24 (CH<sub>2</sub>), 28.32 (CH<sub>2</sub>), 30.27 (CH<sub>2</sub>), 68.66 (OCH<sub>2</sub>),

114.77 (CH), 119.68 (C), 122.29 (CH), 124.45 (CH), 124.93 (CH), 126.70 (CH), 127.95 (CH), 128.21 (C), 133.19 (C), 153.49 (C).

#### Preparation of (*R*)-4,4'-6,6'-tetrabromo-2,2'-dihexyloxy-1,1'-binaphthyl ((*R*)-3.10)

2,2'-Dihexyloxy-1,1'-binaphthyl (2.05 g, 4.41 mmol) was dissolved in acetic acid (50 ml) and elemental bromine (7.05 g, 44.1 mmol) added dropwise to the solution over thirty minutes at room temperature. The mixture was then stirred overnight.

Sodium bisulphite was added to quench the excess bromine and the product filtered off. The solid was washed with NaHCO<sub>3</sub> solution (5 x 50 ml), brine (50 ml) and hexane (50 ml), and dried under reduced pressure to yield the product as an off-white powder (2.12 g, 63 %). M.p. 98 – 100 °C. m/z (FAB) 770 [M]<sup>+</sup> (15 %). [α]<sub>D</sub> (CHCl<sub>3</sub>) –6.9 ° (c = 1.4). δ<sub>H</sub> 0.68 (6H, t, <sup>3</sup>J<sub>HH</sub> 6.8 Hz, CH<sub>3</sub>), 0.98 (12H, m, (CH<sub>2</sub>)<sub>3</sub>), 1.29 (4H, m, CH<sub>2</sub>), 3.82 (4H, m, CH<sub>2</sub>), 6.89 (2H, d, <sup>3</sup>J<sub>HH</sub> 9.2 Hz, 8-ArH), 7.24 (2H, dd, <sup>3</sup>J<sub>HH</sub> 9.0 Hz, <sup>4</sup>J<sub>HH</sub> 1.8 Hz, 7-ArH), 7.63 (2H, s, 3-ArH), 8.32 (2H, d, <sup>4</sup>J<sub>HH</sub> 1.8 Hz, 5-ArH). δ<sub>C</sub> 13.87 (CH<sub>3</sub>), 22.45 (CH<sub>2</sub>), 25.29 (CH<sub>2</sub>), 29.06 (CH<sub>2</sub>), 31.19 (CH<sub>2</sub>), 69.78 (OCH<sub>2</sub>), 110.31 (C), 119.17 (C), 120.32 (CH), 122.37 (C), 127.31 (CH), 128.81 (C), 129.35 (CH), 130.54 (CH), 133.06 (C), 154.37 (C).

#### Preparation of (*R*)-4,4'-6,6'-tetrabromo-1,1'-bi-2-naphthol ((*R*)-3.11)

(*R*)-4,4'-6,6'-Tetrabromo-2,2'-dihexyloxy-1,1'-binaphthyl (2.51 g, 3.3 mmol) was dissolved in dry and degassed dichloromethane (100 ml) and cooled to –78 °C. To the solution, BBr<sub>3</sub> (0.2 ml, 2.2 mmol) in dry dichloromethane (20 ml) was added dropwise over five minutes and the solution stirred for 1 hour at –78 °C before being allowed to warm to room temperature over night.

With extreme care, the mixture was hydrolysed with water and the organic layer separated. The organic layer was washed twice with water (50 ml), dried (MgSO<sub>4</sub>), filtered and the solvent removed under reduced pressure to obtain the product as an off-white solid (1.52 g, 77 %). M.p. 184 – 186 °C. m/z (ES-) 601 [M]<sup>–</sup> (100 %). [α]<sub>D</sub> (CHCl<sub>3</sub>) –28.4 (c = 2.0). δ<sub>H</sub> 6.84 (2H, d, <sup>3</sup>J<sub>HH</sub> 9.4 Hz, 8-ArH), 7.26 (2H, dd, <sup>3</sup>J<sub>HH</sub> 9.0 Hz, <sup>4</sup>J<sub>HH</sub> 1.8 Hz, 7-ArH), 7.67 (2H, s, 3-ArH), 8.38 (2H, d, <sup>4</sup>J<sub>HH</sub> 1.8 Hz, 5-ArH). δ<sub>C</sub> 110.30 (C), 119.93 (C), 123.05 (CH), 124.89 (C), 126.16 (CH), 129.43 (C), 130.13 (CH), 131.96 (CH), 132.39 (C), 152.53 (C)

#### Preparation of (*R*)-4,4'-6,6'-tetra(perfluoro-*n*-hexyl)-1,1'-bi-2-naphthol ((*R*)-3.12)

(*R*)-4,4'-6,6'-Tetrabromo-1,1'-bi-2-naphthol (2.53 g, 4.2 mmol) activated copper powder (3.02 g, 47 mmol), 2,2'-bipyridine (0.24 g, 1.5 mmol), perfluoro-*n*-hexyl iodide (15.01 g, 33.6 mmol), DMSO (75 ml) and fluorobenzene (25 ml) were mixed together and heated to 130 °C for 4 days. Upon cooling, the mixture was diluted with water (300 ml) and ethyl acetate added (200 ml).

The slurry was filtered and the organic layer separated from the aqueous phase. The aqueous layer was extracted twice with ethyl acetate (2 x 100 ml) and the organic layers combined, washed with 1 M HCl (2 x 100 ml), water (3 x 100 ml) and saturated sodium chloride solution (2 x 100 ml) and dried over magnesium sulphate. The suspension was filtered and the solvent removed under reduced pressure to yield a brown oil. The crude product was purified by column chromatography (8.5:1.5 EtOAc:hexane) to yield a yellow oil (3.65 g, 56 %).  $m/z$  (ES<sup>-</sup>) 1557 [M-H]<sup>-</sup> (100 %).  $[\alpha]_D$  (EtOAc) 13.2 ° (c = 2.3). Elemental analysis (expected(found)) C 33.89 (33.85), H 0.64 (0.60).  $\delta_H$  5.96 (2H, bs, OH), 7.20 (2H, d,  $^3J_{HH}$  9.0 Hz, 8-ArH), 7.46 (2H, d,  $^3J_{HH}$  8.8 Hz, 7-ArH), 7.80 (2H, s, 3-ArH), 8.48 (2H, bs, 5-ArH).  $\delta_F$  -80.89 (6F, t,  $^4J_{FF}$  10.7 Hz, CF<sub>3</sub>), -80.98 (6F, t,  $^4J_{FF}$  10.5 Hz, CF<sub>3</sub>), -104.62 (2F, um,  $\alpha$ -CF<sub>2</sub>), -110.65 (4F, um,  $\alpha$ -CF<sub>2</sub>), -119.71 (4F, um, CF<sub>2</sub>), -121.43 (8F, um, CF<sub>2</sub>), -122.0 (4F, um, CF<sub>2</sub>), -122.68 (4F, um, CF<sub>2</sub>), -122.86 (4F, um, CF<sub>2</sub>), -126.13 (4F, um, CF<sub>2</sub>), -126.29 (4F, um, CF<sub>2</sub>).  $\delta_C$  116.84 (t,  $^2J_{CF}$  12.9 Hz, C), 120.66 (CH), 120.89 (t,  $^2J_{CF}$  11.9 Hz, C), 124.48 (CH), 124.85 (CH), 125.12 (CH), 127.13 (C), 130.32 (C), 135.50 (C), 153.15 (C)

#### Determination of enantiomeric excess of (*R*)-4,4'-6,6'-tetra(perfluoro-*n*-hexyl)-1,1'-bi-2-naphthol ((*R*)-3.13)

(*R*)-4,4'-6,6'-tetra(perfluoro-*n*-hexyl)-1,1'-bi-2-naphthol (0.31 g,  $2 \times 10^{-4}$  mol) and (*S*)-(+)-10-camphorsulphonyl chloride (0.10 g,  $4 \times 10^{-4}$  mol) were stirred in dry dichloromethane (10 ml) and triethylamine (0.5 ml,  $8 \times 10^{-4}$  mol) added *via* syringe. The mixture was stirred for one hour and then refluxed for four hours under nitrogen.

The reaction mixture was allowed to cool before 1M HCl solution (20 ml) was added and the organic layer separated, dried, filtered and the solvent removed *in vacuo* to yield a yellow oil. The <sup>1</sup>H NMR spectrum of the oil was compared to the <sup>1</sup>H NMR spectra of the diastereomers formed from the reaction between (*R*)- and (*S*)-1,1'-bi-2-naphthol (57 mg,  $2 \times 10^{-4}$  mol) and (*S*)-(+)-10-camphorsulphonyl chloride (100 mg,  $4 \times 10^{-4}$  mol) using the same reaction conditions. The spectra showed the title compound was in 90 % enantiomeric excess (0.35 g, 88 % (impure)).  $m/z$  (FAB) 1948 [M]<sup>+</sup> (3 %). (*S,S*)-2,2'-bis(camphorsulphonyl)-1,1'-binaphthyl ester  $\delta_H$  2.65 (1H, dd,  $J_{HH}$  35.0 Hz,  $J_{HH}$  3.0 Hz) (*S,R*)-2,2'-bis(camphorsulphonyl)-1,1'-binaphthyl ester  $\delta_H$  2.75 (1H, dd,  $J_{HH}$  96.1 Hz,  $J_{HH}$  4.0 Hz). 4,4'-6,6'-tetra(perfluoro-*n*-hexyl)-2,2'-bis(camphorsulphonyl)-1,1'-binaphthyl ester  $\delta_H$  2.81 (1H, dd,  $^3J_{HH}$  101.1 Hz,  $^4J_{HH}$  4.2 Hz).

#### Preparation of (*R*)-4,4'-6,6'-tetra(perfluoro-*n*-hexyl)-1,1'-bi-2-naphthyl-dimethylphosphoramidite ((*R*)-Rf<sub>4</sub>-MonoPhos) ((*R*)-3.14)

(*R*)-4,4'-6,6'-tetra(perfluoro-*n*-hexyl)-1,1'-bi-2-naphthol (1.01 g,  $6.5 \times 10^{-4}$  mol) was dissolved in dry and degassed ethyl acetate and HMPT (0.15 ml,  $6.5 \times 10^{-4}$ ) added *via* syringe. The

mixture was stirred for 30 minutes and then the solvent removed under reduced pressure. The residue was washed with acetonitrile, re-dissolved in dichloromethane and the solvent removed under reduced pressure to yield a yellow semi-solid.  $m/z$  (FAB) 1632  $[MH]^+$  (6 %).  $[\alpha]_D$  ( $CHCl_3$ ) – 71.6 ° ( $c = 2.4$ ). Elemental analysis (expected(found)) C 33.84 (33.60), H 0.86 (0.76), N 0.86 (0.77).  $\delta_H$  2.44 (6H, d,  $^3J_{PH}$  9.2 Hz,  $CH_3$ ) 7.24 – 7.40 (4H, um, 8-ArH and 7-ArH), 7.73 (1H, s, 3-ArH), 7.84 (1H, s, 3-ArH), 8.68 (2H, bs, 5-ArH).  $\delta_F$  –80.92 (6F, t,  $^4J_{FF}$  10.7 Hz,  $CF_3$ ), –81.03 (6F, t,  $^4J_{FF}$  10.5 Hz,  $CF_3$ ), –104.67 (2F, um,  $\alpha$ - $CF_2$ ), –110.67 (4F, um,  $\alpha$ - $CF_2$ ), –119.76 (4F, um,  $CF_2$ ), –121.41 (8F, um,  $CF_2$ ), –122.0 (4F, um,  $CF_2$ ), –122.66 (4F, um,  $CF_2$ ), –122.89 (4F, um,  $CF_2$ ), –126.18 (4F, um,  $CF_2$ ), –126.34 (4F, um,  $CF_2$ ).  $\delta_P$  152.75 (1P, s,  $PNMe_2$ ).

#### Preparation of $[PdCl_2((R)\text{-Rf}_4\text{-MonoPhos})_2]$ ((R)-3.15)

(R)-Rf<sub>4</sub>-MonoPhos (0.32 g,  $2 \times 10^{-4}$  mol) and  $[PdCl_2(MeCN)_2]$  (26 mg, 0.1 mmol) were dissolved in dry and degassed dichloromethane and stirred for 2 hours. The solvent was removed under reduced pressure and the residue recrystallised from 1:10 dichloromethane/hexane (80 mg, 23 %).  $m/z$  (FAB) 3477  $[M-Cl]^+$  (12 %).  $\delta_H$  2.44 (6H, d,  $^3J_{PH}$  9.2 Hz,  $CH_3$ ) 2.46 (6H, d,  $^3J_{PH}$  9.2 Hz,  $CH_3$ ), 7.20 – 7.42 (8H, um, 8-ArH and 7-ArH), 7.74 (2H, s, 3-ArH), 7.84 (1H, s, 3-ArH), 7.87 (1H, s, 3-ArH), 8.68 (4H, bs, 5-ArH).  $\delta_F$  –80.77 (12F, t,  $^4J_{FF}$  10.7 Hz,  $CF_3$ ), –80.86 (12F, t,  $^4J_{FF}$  10.5 Hz,  $CF_3$ ), –103.79 (4F, um,  $\alpha$ - $CF_2$ ), –104.53 (4F, um,  $\alpha$ - $CF_2$ ), –110.82 (8F, bm,  $\alpha$ - $CF_2$ ), –119.39 (4F, um,  $CF_2$ ), –119.69 (4F, um,  $CF_2$ ), –121.35 (16F, um,  $CF_2$ ), –122.21 (4F, um,  $CF_2$ ), –122.81 (4F, um,  $CF_2$ ), –124.44 (16F, um,  $CF_2$ ), –126.19 (16F, um,  $CF_2$ ).  $\delta_P$  122.89 (2P, s,  $PNMe_2$ ).

#### Preparation of $[RhCp^*Cl_2((R)\text{-Rf}_4\text{-MonoPhos})]$ ((R)-3.16)

(R)-Rf<sub>4</sub>-MonoPhos (0.30 g,  $2 \times 10^{-4}$  mol) and  $[RhCp^*Cl_2]_2$  (62 mg, 0.1 mmol) were dissolved in dry and degassed dichloromethane and stirred for 2 hours. The solvent was removed under reduced pressure and the residue recrystallised from 1:10 dichloromethane/hexane (122 mg, 31 %).  $m/z$  (FAB) 1942  $[M-Cl]^+$  (22 %).  $\delta_H$  (253 K) 1.56 (15H, d,  $J_{PH}$  3.9 Hz,  $Cp^*H$ ), 2.51 (6H, d,  $^3J_{PH}$  9.6 Hz,  $CH_3$ ), 7.19 (1H, d,  $^3J_{HH}$  8.5 Hz, 8-ArH), 7.30 (1H, d,  $^3J_{HH}$  8.7 Hz, 8-ArH), 7.34 (1H, d,  $^3J_{HH}$  9.1 Hz, 7-ArH), 7.48 (1H, d,  $^3J_{HH}$  9.3 Hz, 7-ArH), 7.86 (2H, bs, 3-ArH), 8.49 (1H, bs, 5-ArH), 8.54 (1H, bs, 5-ArH).  $\delta_F$  –80.92 (6F, t,  $^4J_{FF}$  10.2 Hz,  $CF_3$ ), –81.03 (6F, t,  $^4J_{FF}$  10.5 Hz,  $CF_3$ ), –103.67 (2F, um,  $\alpha$ - $CF_2$ ), –104.34 (2F, um,  $\alpha$ - $CF_2$ ), –110.80 (4F, um,  $\alpha$ - $CF_2$ ), –119.17 (2F, um,  $CF_2$ ), –119.66 (2F, um,  $CF_2$ ), –121.38 (4F, um,  $CF_2$ ), –121.84 (4F, um,  $CF_2$ ), –121.99 (4F, um,  $CF_2$ ), –122.57 (4F, um,  $CF_2$ ), –122.78 (4F, um,  $CF_2$ ), –126.00 (4F, um,  $CF_2$ ), –126.17 (4F, um,  $CF_2$ ).  $\delta_P$   $\{^1H\}$  (253 K) 146.57 (d,  $^1J_{P-Rh}$  229 Hz,  $PNMe_2$ ).

**Procedure for the Determination of (*R*)-Rf<sub>4</sub>-MonoPhos Partition Coefficient**

(*R*)-Rf<sub>4</sub>-MonoPhos (60 mg) was stirred for 20 minutes in dry and degassed toluene (2.0 ml) and PP3 (2.0 ml). The mixture was then allowed to stand for 20 minutes before 1.0 ml of each layer was collected *via* syringe and dried to constant mass under vacuum. The partition coefficient was determined by comparison of the amount of ligand by weight in each fraction. 1 mg was found in the 1 ml toluene phase. 29 mg was found in the 1 ml PP3 phase. Partition coefficient: 97 % in fluoros phase.

**Catalytic Procedure for Asymmetric Hydrogenation under Fluorous Biphasic Conditions**

[Rh(cod)<sub>2</sub>]BF<sub>4</sub> (16 mg, 4 × 10<sup>-5</sup> mol) and (*R*)-Rf<sub>4</sub>-MonoPhos (140 mg, 8.5 × 10<sup>-5</sup> mol) were stirred in dry and degassed PP3 (6 ml) and ethyl acetate (6 ml) for 30 minutes. Dimethyl itaconate (123 mg, 8 × 10<sup>-4</sup> mol) was then added in a glove box under nitrogen and the mixture stirred for a further ten minutes before being placed briefly under vacuum. Hydrogen gas (1 bar) was then added and the reaction mixture stirred for 20 hours.

The organic and fluoros layers were separated in a glove box and the fluoros layer used in further catalysis. The solvent was removed from the organic layer *in vacuo* to yield the product as a pale yellow oil. The amount of leached rhodium was determined by ICP analysis of an acid wash of the product redissolved in dichloromethane. Product *ee* was determined by chiral GC (Beta Dex 225, 30m × 0.25 mm (od) × 0.25 μm (film thickness). 100 °C for 25 min, 20 °C/min to 200 °C, hold 5 min. Injector: 220 °C, detector: 300 °C. Flow rate: 1.1 ml/min). *m/z* (ES+) 160 [M]<sup>+</sup> (15 %). NMR Run 1: 53 % conversion, 25 % *ee*, 2.23 ppm Rh (0.6 %); Run 2: 80 % conversion, 22 % *ee*, 1.21 ppm Rh (0.3 %); Run 3: 70 % conversion, 15 % *ee*, 0.37 ppm Rh (0.09 %); Run 4: 80 % conversion, 15 % *ee*, 0.18 ppm Rh (0.04 %); Total rhodium loss: 1.03 % after four runs.

## 6.4 Experimental Details for Chapter Four

### 6.4.1 General Procedure for the Determination of BINOL Partition Coefficients

A known mass of BINOL ligand was stirred for 20 minutes in dry and degassed toluene (2.0 ml) and PP3 (2.0 ml). The mixture was then allowed to stand for 20 minutes before 1.0 ml of each layer was collected *via* syringe and dried to constant mass under vacuum. The partition coefficient was determined by comparison of the amount of ligand by weight in each fraction.

#### Determination of (*R*)-BINOL Partition Coefficient

(*R*)-BINOL (71 mg) was used. 23 mg of ligand was found in the 1 ml of toluene phase by mass. The PP3 sample contained no ligand. The ligand was not completely soluble in either phase. Partition coefficient: 100 % in toluene phase, 65 % solubilised.

#### Determination of (*R*)-Rf-BINOL Partition Coefficient

(*R*)-Rf-BINOL (63 mg) was used. 22 mg of ligand was found in the 1 ml of toluene phase. 8 mg of ligand was found in the 1 ml of PP3 phase. Partition coefficient: 73 % in toluene phase.

### 6.4.2 Catalytic Testing

#### General Catalysis Procedure for the Asymmetric Addition of Diethylzinc to Benzaldehyde

Ti(O<sup>*i*</sup>Pr)<sub>4</sub> (157 μl, 0.32 mmol) and BINOL (0.21 mmol, 0.2 eq) were stirred in dichloromethane (10 ml) for one hour. An additional portion of Ti(O<sup>*i*</sup>Pr)<sub>4</sub> was then added (314 μl, 0.64 mmol) and benzaldehyde added (107 μl, 1.2 mmol).

The solution was cooled to -20 °C and diethylzinc added (3.12 mmol, 3.12 ml of 1M solution in hexane). The mixture was stirred for five hours and then quenched with 1M hydrochloric acid (50 ml). The mixture was extracted with diethyl ether, dried, filtered and the solvent removed *in vacuo* to yield the product as a colourless oil contaminated with BINOL ligand. Pure product was obtained by simple decantation from the solid ligand. Product *ee* was determined using chiral GC (CYDEX-B 30m, 90 °C for 24 min, 45 °C/min to 135 °C, hold 5 min. Injector: 220 °C, detector: 250 °C. Flow rate: 3 ml/min).

#### Asymmetric Addition using (*R*)-BINOL (T16)

The general catalysis procedure was followed using (*R*)-BINOL as ligand (0.21 mmol, 60 mg). The product was collected as a colourless oil contaminated with (*R*)-BINOL. *m/z* (ES<sup>+</sup>) 135 [M-H]<sup>+</sup> (90 %). δ<sub>H</sub> 0.81 (3H, t, <sup>3</sup>J<sub>HH</sub> 7.2 Hz, CH<sub>3</sub>), 1.69 (2H, um, CH<sub>2</sub>), 1.98 (1H, bs, OH), 4.47 (1H, t, <sup>3</sup>J<sub>HH</sub> 6.6 Hz, CH), 7.16 – 7.29 (6H, um, PhH). Run 1: 90 % conversion, 86 % *ee*; Run 2: 85 % conversion, 90 % *ee*; Run 3: 90 % conversion, 90 % *ee*.

### Asymmetric Addition using (*R*)-Rf-BINOL (T17)

The general catalysis procedure was followed using (*R*)-Rf-BINOL as ligand (0.21 mmol, 194 mg). The product was collected as a colourless oil. *m/z* (ES+) 135 [M-H]<sup>+</sup> (90 %).  $\delta_{\text{H}}$  0.81 (3H, t,  $^3J_{\text{HH}}$  7.2 Hz, CH<sub>3</sub>), 1.69 (2H, um, CH<sub>2</sub>), 1.98 (1H, bs, OH), 4.47 (1H, t,  $^3J_{\text{HH}}$  6.6 Hz, CH), 7.16 – 7.29 (5H, um, PhH). Run 1: 90 % conversion, 77 % *ee*; Run 2: 86 % conversion, 70 % *ee*; Run 3: 88 % conversion, 75 % *ee*.

### 6.4.3 General Procedure for Attempted Separation of BINOL and 1-Phenyl-propan-1-ol

The crude product and BINOL post-reaction mixture in diethyl ether was concentrated *in vacuo* and placed on the top of a 3 cm long column of silica gel or FRP silica gel 1 cm in diameter. Acetonitrile and hexane were then tested as elutants. The product was collected along with BINOL ligand or Rf-BINOL ligand in all cases.

### 6.4.4 Asymmetric Addition of Diethylzinc to Benzaldehyde using (*R*)-Rf<sub>4</sub>-BINOL

The general catalytic procedure was followed using (*R*)-Rf<sub>4</sub>-BINOL (327 mg, 0.21 mmol) and dry and degassed ethyl acetate as solvent. Separation of ligand and product after acid work-up was attempted using the general separation procedure given above and the product collected with ligand contamination. Percentage conversion was determined by <sup>1</sup>H NMR analysis and product *ee* was determined by chiral GC. *m/z* (ES+) 135 [M-H]<sup>+</sup> (88 %).  $\delta_{\text{H}}$  0.82 (3H, t,  $^3J_{\text{HH}}$  7.2 Hz, CH<sub>3</sub>), 1.68 (2H, um, CH<sub>2</sub>), 2.02 (1H, bs, OH), 4.49 (1H, t,  $^3J_{\text{HH}}$  6.6 Hz, CH), 7.15 – 7.28 (5H, um, PhH).

The ligand retained on the FRP silica gel column was recovered by elution with ethyl acetate, the solvent removed *in vacuo* and the ligand reused in further catalysis. Partial retention of the ligand was, once again, observed with the product obtained after elution with acetonitrile showing ligand contamination by <sup>1</sup>H and <sup>19</sup>F NMR. Run 1: 65 % conversion, 33 % *ee*; Run 2: 60 % conversion, 28 % *ee*.

### 6.4.5 General Catalysis Procedure for the Addition of Allyltri-*n*-butyltin to Benzaldehyde

To a solution of Ti(O<sup>*i*</sup>Pr)<sub>4</sub> (0.3 ml in 20 ml hexane, 2 ml, 0.1 mmol), was added the BINOL ligand (0.2 mmol) and the mixture stirred for one hour. The mixture was then cooled to 0 °C and benzaldehyde (0.1 ml, 1 mmol) added. The mix was stirred for 10 minutes and then allyltri-*n*-butyltin added (0.34 ml, 1.1 mmol) and the reaction mixture held at 0 °C for six hours.

The solvent was removed under reduced pressure and the crude mixture then used in the general separation procedure.

### Procedure for the Determination of 4-Phenyl-1-buten-4-ol Product *ee*

Mosher's acid chloride (250 mg in 10 ml DCM, 990  $\mu\text{M}$ , 2 ml, 0.2 mmol) and pyridine (0.2 ml, 2.5 mmol) were added to a flame-dried flask under nitrogen. To this mixture, 4-phenyl-1-buten-4-ol (29  $\mu\text{l}$ , 0.2 mmol) was added and the reaction mixture stirred for 30 minutes.

1M hydrochloric acid was added (3 ml) and the biphasic mixture transferred to a separating funnel. The organic phase was separated and washed with  $\text{NaHCO}_3$  (10 ml) and water (10 ml), dried ( $\text{MgSO}_4$ ), filtered and the solvent removed *in vacuo* to yield a colourless oil which was analysed by chiral GC for diastereomeric content (CYDEX-B, 180  $^\circ\text{C}$  for 20 min. Injector: 220  $^\circ\text{C}$ , detector: 250  $^\circ\text{C}$ . Flow rate: 2 ml/min (*R*)-4-phenyl-1-buten-4-ol, Mosher's acid ester  $R_t$  8.81 min, (*S*)-4-phenyl-1-buten-4-ol, Mosher's acid ester,  $R_t$  13.00 min).

### $^{119}\text{Sn}\{^1\text{H}\}$ NMR of Material Recovered from Column before Acid Wash

The reaction using non-fluorous BINOL as ligand produced crystals that were identified by X-ray analysis to be a Sn-BINOL polymer (see Appendix).  $^{119}\text{Sn}$  NMR of these crystals was obtained.  $\delta_{\text{Sn}}$  (400 MHz NMR spectrometer at 149.21 MHz) 105.47 (2Sn, s), 115.63 (1Sn, s).

Crystals of a Sn-Rf-BINOL polymer could not be obtained, but  $^{119}\text{Sn}$  NMR showed the residue contained Sn atoms in similar environments.  $\delta_{\text{Sn}}$  (400 MHz NMR spectrometer at 149.21 MHz) 106.20 (2Sn, s), 123.05 (1Sn, s).

### Asymmetric Addition of Allyltri-*n*-butyltin Using (*R*)-BINOL (T18)

The general catalysis procedure was followed using (*R*)-BINOL (57 mg, 0.2 mmol) as ligand. The product was collected as a colourless oil contaminated with BINOL material.  $m/z$  ( $\text{ES}^+$ ) 149 [ $\text{MH}$ ] $^+$  (23 %).  $\delta_{\text{H}}$  2.32 (1H, bs, OH), 2.54 (2H, um,  $\text{CH}_2$ ), 4.74 (1H, dd,  $^3J_{\text{HH}}$  5.8 Hz,  $^3J_{\text{HH}}$  7.0 Hz, CH), 5.15 (1H, um,  $=\text{CH}_2$ ), 5.20 (1H, dum,  $^3J_{\text{HH}}$  9.0 Hz,  $=\text{CH}_2$ ), 5.84 (1H, um, HC=), 7.24 – 7.39 (5H, um, PhH). Run 1: 90 % conversion, 82 % *ee*; Run 2: 90 % conversion, 78 % *ee*; Run 3: 88 % conversion, 78 % *ee*.

### Asymmetric Addition of Allyltri-*n*-butyltin Using (*R*)-Rf-BINOL (T19)

The general catalysis procedure was followed using (*R*)-Rf-BINOL (184 mg, 0.2 mmol) as ligand. The product was collected as a colourless oil.  $m/z$  ( $\text{ES}^+$ ) 149 [ $\text{MH}$ ] $^+$  (26 %).  $\delta_{\text{H}}$  2.32 (1H, bs, OH), 2.54 (2H, um,  $\text{CH}_2$ ), 4.74 (1H, dd,  $^3J_{\text{HH}}$  5.8 Hz,  $^3J_{\text{HH}}$  7.0 Hz, CH), 5.15 (1H, um,  $=\text{CH}_2$ ), 5.20 (1H, dum,  $^3J_{\text{HH}}$  9.0 Hz,  $=\text{CH}_2$ ), 5.84 (1H, um, HC=), 7.24 – 7.39 (5H, um, PhH). Run 1: 86 % conversion, 74 % *ee*; Run 2: 90 % conversion, 78 % *ee*; Run 3: 88 % conversion, 74 % *ee*.

#### 6.4.6 General Procedure for the Separation of BINOL and 4-phenyl-1-buten-4-ol

A standard reaction mixture was concentrated *in vacuo* and the residue placed onto the top of a column of silica gel, FRP silica gel, C<sub>8</sub>-reverse phase silica gel or powdered PTFE (3 cm long, 1 cm diameter). Acetonitrile was then used as elutant to recover the product. Diethyl ether was used as the second elutant to recover any ligand not eluted with the acetonitrile phase. This was washed with 6 M HCl, the organic layer separated and dried and the solvent removed under reduced pressure to yield free BINOL. Only when FRP silica gel and (*R*)-Rf-BINOL were used was complete separation of the ligand and product possible. After acid washes of the diethyl ether fraction and removal of the solvent, the recovered (*R*)-Rf-BINOL was used in three further catalytic runs following the same catalysis procedure. The general separation procedure was then used to recover the ligand and separate the 4-phenyl-1-buten-4-ol product. After each run, the product was washed with 6M hydrochloric acid and the Sn and Ti levels determined by ICP analysis of the wash. Figures in brackets indicate percentage of metal added at the outset which is present in the product. Run 1: 85 % conversion, 66 % *ee*. Sn: 1.24 ppm, (0.02 %) Ti: 2.21 ppm, (0.88 %); Run 2: 85 % conversion, 63 % *ee*. Sn: 0.75 ppm, (0.01 %) Ti: 1.99 ppm, (0.83 %); Run 3: 82 % conversion, 58 % *ee*. Sn: 2.73 ppm, (0.04 %) Ti: 2.86 ppm, (1.19 %); Run 4: 78 % conversion, 58 % *ee*. Sn: 4.40 ppm, (0.07 %) Ti: 4.65 ppm, (1.93 %).

## 6.5 Experimental Details for Chapter Five

### 6.5.1 Synthesis of Palladium(II)-Diaqua Catalysts

#### Preparation of [Pd(H<sub>2</sub>O)<sub>2</sub>((R)-BINAP)][BF<sub>4</sub>]<sub>2</sub> ((R)-5.1)

[PdCl<sub>2</sub>((R)-BINAP)] (0.51 g, 0.64 mmol) and AgBF<sub>4</sub> (0.27 g, 1.38 mmol) were stirred in wet acetone (5 % v/v water/acetone) for one hour. The solution was filtered through celite to remove insoluble silver chloride and dried (MgSO<sub>4</sub>). The solvent was removed *in vacuo* to yield the product as a yellow-green solid. (0.58 g, 97 %). m/z (ES<sup>+</sup>) 746 [M-2BF<sub>4</sub>-H<sub>2</sub>O]<sup>+</sup> (92 %). [α]<sub>D</sub> (CHCl<sub>3</sub>) 402.7 ° (c = 1.8). Elemental analysis (expected (found)) C 56.29 (55.97), H 3.84 (3.58). δ<sub>H</sub> 3.28 (4H, bs, H<sub>2</sub>O), 6.63 (2H, d, <sup>3</sup>J<sub>HH</sub> 8.5 Hz, ArH), 6.80 (2H, bs, ArH), 6.96 (2H, t, <sup>3</sup>J<sub>HH</sub> 7.3 Hz, ArH), 7.12 (2H, t, <sup>3</sup>J<sub>HH</sub> 7.9 Hz, ArH), 7.43 (2H, t, <sup>3</sup>J<sub>HH</sub> 8.2 Hz, ArH), 7.55 (20H, um, PhH), 7.59 (2H, d, <sup>3</sup>J<sub>HH</sub> 7.4 Hz, ArH). δ<sub>F</sub> -151.68 (s, BF<sub>4</sub>). δ<sub>P</sub> {<sup>1</sup>H} 33.91 (s).

#### Preparation of [Pd(H<sub>2</sub>O)<sub>2</sub>((R)-Rf-BINAP)][BF<sub>4</sub>]<sub>2</sub> ((R)-5.2)

The title compound was prepared similarly to compound (R)-5.1 above using [PdCl<sub>2</sub>((R)-Rf-BINAP)] (0.48 g, 0.33 mmol) and AgBF<sub>4</sub> (0.14 g, 0.70 mmol). The product was collected as a yellow-green solid. (0.50 g, 96 %). M.p. 76 – 78 °C. m/z (FAB) 1471 [M]<sup>+</sup> (1 %). [α]<sub>D</sub> (CHCl<sub>3</sub>) 155.1 (c = 0.9). δ<sub>H</sub> 2.47 (4H, bs, H<sub>2</sub>O), 6.70 (2H, d, <sup>3</sup>J<sub>HH</sub> 8.8 Hz, ArH), 6.88 (2H, um, ArH), 7.27 (2H, d, <sup>3</sup>J<sub>HH</sub> 8.8 Hz, ArH), 7.59 (8H, um, PhH), 7.76 (12H, um, PhH), 7.80 (2H, bs, ArH), 7.91 (2H, bs, ArH). δ<sub>F</sub> -80.66 (6F, t, <sup>4</sup>J<sub>FF</sub> 9.3 Hz, CF<sub>3</sub>), -110.77 (4F, um, α-CF<sub>2</sub>), -120.78 (4F, um, CF<sub>2</sub>), -121.23 (4F, um, CF<sub>2</sub>), -122.66 (4F, um, CF<sub>2</sub>), -126.01 (4F, um, CF<sub>2</sub>) -149.14 (s, BF<sub>4</sub>). δ<sub>P</sub> {<sup>1</sup>H} 33.44 (s).

#### Preparation of [Pd(H<sub>2</sub>O)<sub>2</sub>((R)-MonoPhos)<sub>2</sub>][BF<sub>4</sub>]<sub>2</sub> ((R)-5.3)

The title compound was prepared similarly to compound (R)-5.1 above using *trans*-[PdCl<sub>2</sub>((R)-MonoPhos)<sub>2</sub>] (0.45 g, 0.50 mmol) and AgBF<sub>4</sub> (0.22 g, 1.1 mmol). The product was collected as a yellow-brown solid. (0.42 g, 81 %). M.p. 150 – 152 °C. m/z (FAB) 860 [M-2BF<sub>4</sub>]<sup>+</sup> (25 %). [α]<sub>D</sub> (CHCl<sub>3</sub>) 329.8 (c = 1.6). δ<sub>H</sub> 2.44 (4H, bs, H<sub>2</sub>O), 2.54 (12H, d, <sup>3</sup>J<sub>PH</sub> 9.9 Hz, NMe<sub>2</sub>), 7.21 (4H, um, ArH), 7.36 (8H, um, ArH), 7.42 (2H, dd, <sup>3</sup>J<sub>HH</sub> 8.8 Hz, <sup>4</sup>J<sub>HH</sub> 0.9 Hz, ArH), 7.52 (2H, dd, <sup>3</sup>J<sub>HH</sub> 8.8 Hz, <sup>4</sup>J<sub>HH</sub> 1.0 Hz, ArH), 7.85 (4H, dd, <sup>3</sup>J<sub>HH</sub> 8.1 Hz, <sup>4</sup>J<sub>HH</sub> 3.8 Hz, ArH), 7.92 (4H, dd, <sup>3</sup>J<sub>HH</sub> 9.1 Hz, <sup>4</sup>J<sub>HH</sub> 5.9 Hz, ArH). δ<sub>F</sub> -150.1 (8F, s, BF<sub>4</sub>). δ<sub>P</sub> {<sup>1</sup>H} 14.26 (2P, s, PNMe<sub>2</sub>).

### General Procedure for the Palladium(II) Catalysed Condensation Reaction

Following the literature procedure,<sup>5</sup> benzaldehyde (0.24 ml, 2.4 mmol), 1-phenyl-1-trimethylsilyloxyethane (0.73 ml, 3.5 mmol) and the palladium(II)-diaqua catalyst (1.2 × 10<sup>-4</sup> mol)

were stirred in wet DMF (5 ml, 0.2 eq water, 9  $\mu$ l) at room temperature for 20 hours. The DMF solvent was removed by distillation under reduced pressure and diethyl ether added (10 ml).

#### Catalysis using $[\text{Pd}(\text{H}_2\text{O})_2((R)\text{-BINAP})][\text{BF}_4]_2$ (T20)

The general procedure was followed using  $[\text{Pd}(\text{H}_2\text{O})_2((R)\text{-BINAP})][\text{BF}_4]_2$  (110 mg,  $1.2 \times 10^{-4}$  mol). The crude product was isolated by filtration of the catalyst after precipitation using diethyl ether. The organic layer was washed with 1M HCl (20 ml), dried ( $\text{MgSO}_4$ ), filtered and the solvent removed *in vacuo* to yield a yellow oil.  $\delta_{\text{H}}$  3.38 (1H, d,  $^3J_{\text{HH}}$  1.2 Hz,  $\text{CH}_2$ ), 3.40 (1H, d,  $^3J_{\text{HH}}$  4.6 Hz,  $\text{CH}_2$ ), 5.38 (1H, dd,  $^3J_{\text{HH}}$  7.5 Hz,  $^4J_{\text{HH}}$  4.2 Hz, CH), 7.32 – 7.66 (7H, um, PhH), 8.00 (3H, um, PhH).

The recovered catalyst was used in two further catalytic runs following the same general catalysis procedure outlined above. Product conversion was determined by  $^1\text{H}$  NMR analysis and *ee* was determined by conversion of the product into the Mosher's acid esters and analysis of the formed diastereomers by  $^1\text{H}$  NMR analysis. Palladium leaching was determined by washing the product with 6M HCl followed by ICP analysis of the washings.  $\delta_{\text{H}}$  3.32 (2H, um, (*S,R*)-diastereomer), 3.39 (2H, um, starting material) 3.46 (2H, um, (*R,R*)-diastereomer). Run 1: conversion: > 95 %, *ee*: 50 %, 1.09 ppm Pd (0.06 %); Run 2: conversion: 90 %, *ee*: 22 %, 0.48 ppm Pd (0.03 %); Run 3: conversion: 88 %, *ee*: 0 %.

#### Catalysis using $[\text{Pd}(\text{H}_2\text{O})_2((R)\text{-Rf-BINAP})][\text{BF}_4]_2$ (T21)

The general procedure was followed using  $[\text{Pd}(\text{H}_2\text{O})_2((R)\text{-Rf-BINAP})][\text{BF}_4]_2$  (185 mg,  $1.2 \times 10^{-4}$  mol). The diethyl ether extract was concentrated *in vacuo* and placed onto the top of a column of FRP silica gel (3 cm long, 1 cm diameter). Toluene was used to elute the crude product and the elutant was washed with 1M HCl, dried ( $\text{MgSO}_4$ ), filtered and the solvent removed under reduced pressure to yield the product as a yellow oil.  $\delta_{\text{H}}$  3.38 (1H, d,  $^3J_{\text{HH}}$  1.2 Hz,  $\text{CH}_2$ ), 3.40 (1H, d,  $^3J_{\text{HH}}$  4.6 Hz,  $\text{CH}_2$ ), 5.38 (1H, dd,  $^3J_{\text{HH}}$  4.2 Hz,  $^4J_{\text{HH}}$  7.5 Hz, CH), 7.32 – 7.66 (7H, um, PhH), 8.00 (3H, um, PhH).

The catalyst was then eluted from the column using acetone. The solvent was removed *in vacuo* and the recovered material used in two further catalytic runs. Percentage conversion was determined by  $^1\text{H}$  NMR analysis and percentage *ee* was determined by conversion of the product into the Mosher's acid esters and analysis of the formed diastereomers by  $^1\text{H}$  NMR analysis. Palladium leaching was determined by washing the product with 6M HCl followed by ICP analysis of the washings.  $\delta_{\text{H}}$  3.32 (2H, um, (*S,R*)-diastereomer), 3.39 (2H, um, starting material) 3.46 (2H, um, (*R,R*)-diastereomer). Run 1: conversion: > 95 %, *ee*: 48 %, 1.07 ppm Pd (0.06 %); Run 2:

conversion: 90 %, *ee*: 56 %, 0.50 ppm Pd (0.03 %); Run 3: conversion: 88 %, *ee*: 54 %, 0.22 ppm Pd (0.02 %).

#### Attempted Catalysis using $[\text{Pd}(\text{H}_2\text{O})_2((R)\text{-MonoPhos})_2][\text{BF}_4]_2$ (T22)

The general procedure was followed using  $[\text{Pd}(\text{H}_2\text{O})_2((R)\text{-MonoPhos})_2][\text{BF}_4]_2$  (128mg,  $1.2 \times 10^{-4}$  mol). The catalyst was recovered by precipitation using diethyl ether followed by filtration and the organic solvent was washed with 1M HCl, dried ( $\text{MgSO}_4$ ), filtered and the solvent removed under reduced pressure to yield a yellow oil. Analysis of the recovered material by  $^1\text{H}$  NMR spectroscopy showed the catalyst was inactive for this catalytic transformation.

#### 6.6 References for Chapter Six

1. Andrews, M. A., Chang, C.-T., Cheng, C.-W. F., Emge, T. J., Kelly, K. P., Koetzle, T. F., *J. Am. Chem. Soc.*, 106, **1984**, 5913.
2. Mueller, T. E., Green, J. C., Mingos, D. M. P., McPartlin, L. M., Whittingham, C., *J. Organomet. Chem.*, 551, **1998**, 313.
3. Busby, R., Hursthouse, M. B., Jarrett, P. S., Lehmann, C. W., Malik, K. M. A., Phillips, C., *J. Chem Soc., Dalton Trans.*, **1993**, 3767.
4. Celentano, G., BenincorCelentano, G., Benincori, T., Radaelli, S., Sada, M., Sannicolo, F., *J. Organomet. Chem.*, 643/644, **2002**, 424.
5. Fujii, A., Sodeoka, M., *Tetrahedron Lett.*, 40 **1999**, 8011.

## Appendix

A 1

Crystal Data and Structure Refinement for (R)-4,6-bis(perfluoro-n-hexyl)-2,2-dicyanobenzenesulfone (trihomology)-1,1'-bis(phthalyl)

Identification code

02011

Empirical formula

C<sub>38</sub>H<sub>10</sub>F<sub>32</sub>O<sub>6</sub>S<sub>2</sub>

Formula weight

1730.54

Temperature

150(2) K

Wavelength

0.71073 Å

Crystal system

Orthorhombic

Space group

P2<sub>1</sub>2<sub>1</sub>2<sub>1</sub>

Unit cell dimensions

a = 10.14(4) Å

b = 30.7(2) Å

c = 10.14(4) Å

β = 90°

V = 3114.0(4) Å<sup>3</sup>

Z = 4

Volume



Density (calculated)

1.574 g/cm<sup>3</sup>

Crystal description

Prism, colorless

Weight

0.270 g

Crystal size

0.41 × 0.26 × 0.11 mm<sup>3</sup>

Theta range for data collection

2.23 to 24.95°

Index ranges

-10 ≤ h ≤ 10, -10 ≤ k ≤ 10, -41 ≤ l ≤ 41

Reflections collected

28427

Independent reflections

7409 [R(int) = 0.0516]

Refinement method

Full-matrix least-squares on F<sup>2</sup>

Data / restraints / parameters

7409 / 3 / 776

Goodness-of-fit on F<sup>2</sup>

1.025

Final R indices [I > 2σ(I)]

R<sub>1</sub> = 0.0372, wR<sub>2</sub> = 0.0973

R indices (all data)

R<sub>1</sub> = 0.0395, wR<sub>2</sub> = 0.0996

Absolute structure parameter

0.12(4)

Largest diff. peak and hole

0.275 and -0.275 e/Å<sup>3</sup>

# Appendix

“An expert is someone who has made all the mistakes that can be made, but in a very narrow field.”

- Niels Bohr

## Appendix

### A 1

#### Crystal Data and Structure Refinement for (*R*)-6,6'-bis(perfluoro-*n*-hexyl)-2,2'-di(trifluoromethane-sulphonyloxy)-1,1'-binaphthyl

Identification code	03011	
Empirical formula	C <sub>34</sub> H <sub>10</sub> F <sub>32</sub> O <sub>6</sub> S <sub>2</sub>	
Formula weight	1186.54	
Temperature	150(2) K	
Wavelength	0.71073 Å	
Crystal system	Orthorhombic	
Space group	Pna2(1)	
Unit cell dimensions	a = 14.0758(14) Å	α = 90°.
	b = 8.5515(8) Å	β = 90°.
	c = 34.940(3) Å	γ = 90°.
Volume	4205.7(7) Å <sup>3</sup>	
Z	4	
Density (calculated)	1.874 Mg/m <sup>3</sup>	
Absorption coefficient	0.314 mm <sup>-1</sup>	
F(000)	2328	
Crystal size	0.41 x 0.26 x 0.11 mm <sup>3</sup>	
Theta range for data collection	2.33 to 24.99°.	
Index ranges	-16 ≤ h ≤ 16, -10 ≤ k ≤ 10, -41 ≤ l ≤ 41	
Reflections collected	28427	
Independent reflections	7409 [R(int) = 0.0516]	
Refinement method	Full-matrix least-squares on F <sup>2</sup>	
Data / restraints / parameters	7409 / 3 / 776	
Goodness-of-fit on F <sup>2</sup>	1.025	
Final R indices [I > 2σ(I)]	R1 = 0.0721, wR2 = 0.1875	
R indices (all data)	R1 = 0.0851, wR2 = 0.2006	
Absolute structure parameter	0.36(14)	
Largest diff. peak and hole	0.525 and -0.415 e.Å <sup>-3</sup>	

## A 2

## Crystal data and structure refinement for Rf-BINAP

Identification code	2066	
Empirical formula	C <sub>56</sub> H <sub>30</sub> F <sub>26</sub> P <sub>2</sub>	
Formula weight	1258.74	
Temperature	150(2) K	
Wavelength	0.71073 Å	
Crystal system	Monoclinic	
Space group	C2/c	
Unit cell dimensions	a = 19.456(3) Å	α = 90°.
	b = 8.2838(9) Å	β = 101.212(4)°.
	c = 31.886(4) Å	γ = 90°.
Volume	5040.9(11) Å <sup>3</sup>	
Z	4	
Density (calculated)	1.659 Mg/m <sup>3</sup>	
Absorption coefficient	0.224 mm <sup>-1</sup>	
F(000)	2520	
Crystal size	0.34 x 0.16 x 0.14 mm <sup>3</sup>	
Theta range for data collection	1.30 to 26.00°.	
Index ranges	-23 ≤ h ≤ 23, -10 ≤ k ≤ 10, -39 ≤ l ≤ 39	
Reflections collected	19219	
Independent reflections	4947 [R(int) = 0.0309]	
Refinement method	Full-matrix least-squares on F <sup>2</sup>	
Data / restraints / parameters	4947 / 0 / 379	
Goodness-of-fit on F <sup>2</sup>	1.034	
Final R indices [I > 2σ(I)]	R1 = 0.0582, wR2 = 0.1658	
R indices (all data)	R1 = 0.0679, wR2 = 0.1736	
Largest diff. peak and hole	2.636 and -0.427 e.Å <sup>-3</sup>	

## A 3

Crystal Data and Structure Refinement for [PdCl<sub>2</sub>((*R*)-BINAP)]

Identification code	04096	
Empirical formula	C <sub>45</sub> H <sub>34</sub> Cl <sub>4</sub> P <sub>2</sub> Pd	
Formula weight	884.86	
Temperature	150(2) K	
Wavelength	0.71073 Å	
Crystal system	Monoclinic	
Space group	P2(1)/n	
Unit cell dimensions	a = 17.236(13) Å	α = 90°.
	b = 12.927(10) Å	β = 91.716(12)°.
	c = 17.238(14) Å	γ = 90°.
Volume	3839(5) Å <sup>3</sup>	
Z	4	
Density (calculated)	1.531 Mg/m <sup>3</sup>	
Absorption coefficient	0.878 mm <sup>-1</sup>	
F(000)	1792	
Crystal size	0.31 x 0.10 x 0.06 mm <sup>3</sup>	
Theta range for data collection	1.65 to 23.43°.	
Index ranges	-19 ≤ h ≤ 18, -14 ≤ k ≤ 14, -19 ≤ l ≤ 19	
Reflections collected	22347	
Independent reflections	5501 [R(int) = 0.2600]	
Refinement method	Full-matrix least-squares on F <sup>2</sup>	
Data / restraints / parameters	5501 / 0 / 390	
Goodness-of-fit on F <sup>2</sup>	0.915	
Final R indices [I > 2σ(I)]	R1 = 0.0883, wR2 = 0.1567	
R indices (all data)	R1 = 0.1993, wR2 = 0.1929	
Largest diff. peak and hole	1.185 and -0.723 e.Å <sup>-3</sup>	

## A 4

Crystal Data and Structure Refinement for [RhCp\*Cl<sub>2</sub>((S)-MonoPhos)]

Identification code	2131
Empirical formula	C <sub>32.50</sub> H <sub>34</sub> Cl <sub>3</sub> N O <sub>2</sub> P Rh
Formula weight	710.84
Temperature	150(2) K
Wavelength	0.71073 Å
Crystal system	Orthorhombic
Space group	P2(1)2(1)2
Unit cell dimensions	a = 17.8135(7) Å      α = 90°. b = 22.7127(9) Å      β = 90°. c = 7.6566(3) Å      γ = 90°.
Volume	3097.8(2) Å <sup>3</sup>
Z	4
Density (calculated)	1.524 Mg/m <sup>3</sup>
Absorption coefficient	0.893 mm <sup>-1</sup>
F(000)	1452
Crystal size	0.18 x 0.16 x 0.11 mm <sup>3</sup>
Theta range for data collection	1.79 to 25.00°.
Index ranges	-21 ≤ h ≤ 21, -27 ≤ k ≤ 26, -9 ≤ l ≤ 8
Reflections collected	22576
Independent reflections	5439 [R(int) = 0.0329]
Refinement method	Full-matrix least-squares on F <sup>2</sup>
Data / restraints / parameters	5439 / 0 / 360
Goodness-of-fit on F <sup>2</sup>	1.076
Final R indices [I > 2σ(I)]	R1 = 0.0318, wR2 = 0.0826
R indices (all data)	R1 = 0.0326, wR2 = 0.0833
Largest diff. peak and hole	1.038 and -0.891 e.Å <sup>-3</sup>

## A 5

**Crystal Data and Structure Refinement for (*R*)-4,4'-6,6'-tetrabromo-2,2'-dihexyloxy-1,1'-binaphthyl**

Identification code	02107	
Empirical formula	C <sub>32</sub> H <sub>34</sub> Br <sub>4</sub> O <sub>2</sub>	
Formula weight	770.23	
Temperature	150(2) K	
Wavelength	0.71073 Å	
Crystal system	Orthorhombic	
Space group	Pna2(1)	
Unit cell dimensions	a = 13.9754(8) Å	α = 90°.
	b = 8.2239(5) Å	β = 90°.
	c = 26.5405(15) Å	γ = 90°.
Volume	3050.4(3) Å <sup>3</sup>	
Z	4	
Density (calculated)	1.677 Mg/m <sup>3</sup>	
Absorption coefficient	5.305 mm <sup>-1</sup>	
F(000)	1528	
Crystal size	0.22 x 0.20 x 0.17 mm <sup>3</sup>	
Theta range for data collection	1.53 to 25.00°.	
Index ranges	-16 ≤ h ≤ 16, -9 ≤ k ≤ 9, -31 ≤ l ≤ 31	
Reflections collected	20769	
Independent reflections	5373 [R(int) = 0.0599]	
Refinement method	Full-matrix least-squares on F <sup>2</sup>	
Data / restraints / parameters	5373 / 1 / 339	
Goodness-of-fit on F <sup>2</sup>	0.844	
Final R indices [I > 2σ(I)]	R <sub>1</sub> = 0.0436, wR <sub>2</sub> = 0.0891	
R indices (all data)	R <sub>1</sub> = 0.0764, wR <sub>2</sub> = 0.0966	
Absolute structure parameter	-0.001(17)	
Largest diff. peak and hole	0.834 and -0.414 e.Å <sup>-3</sup>	

## A 6

**Crystal Data and Structure Refinement for Sn-BINOL Polymer**

Identification code	04004	
Empirical formula	C <sub>32</sub> H <sub>39</sub> O <sub>2</sub> Sn	
Formula weight	574.32	
Temperature	150(2) K	
Wavelength	0.71073 Å	
Crystal system	Monoclinic	
Space group	P2(1)	
Unit cell dimensions	a = 11.2787(12) Å	α = 90°.
	b = 11.6990(13) Å	β = 115.519(2)°.
	c = 11.6960(13) Å	γ = 90°.
Volume	1392.7(3) Å <sup>3</sup>	
Z	2	
Density (calculated)	1.370 Mg/m <sup>3</sup>	
Absorption coefficient	0.943 mm <sup>-1</sup>	
F(000)	594	
Crystal size	0.26 x 0.12 x 0.06 mm <sup>3</sup>	
Theta range for data collection	1.93 to 25.99°.	
Index ranges	-13 ≤ h ≤ 13, -14 ≤ k ≤ 14, -14 ≤ l ≤ 14	
Reflections collected	10765	
Independent reflections	5207 [R(int) = 0.0232]	
Refinement method	Full-matrix least-squares on F <sup>2</sup>	
Data / restraints / parameters	5207 / 1 / 320	
Goodness-of-fit on F <sup>2</sup>	1.078	
Final R indices [I > 2σ(I)]	R1 = 0.0449, wR2 = 0.1198	
R indices (all data)	R1 = 0.0458, wR2 = 0.1205	
Absolute structure parameter	0.03(3)	
Largest diff. peak and hole	3.885 and -0.746 e.Å <sup>-3</sup>	

A 7

**Inorganic Seminar Programme (Autumn/Winter 2001)**

<b>Date</b>	<b>Title</b>	<b>Speaker</b>
1 <sup>st</sup> Oct.	<i>Enabling Technologies for Biology and Medicine Arising From Endeavours in Total Synthesis</i>	<b>Prof. K. C. Nicolaou</b> <i>Scripps Research Institute</i>
4 <sup>th</sup> Oct.	<i>Basic Instinct: New Synthetic Adventures with Chiral Bases</i>	<b>Dr. P. O'Brien</b> <i>University of York</i>
10 <sup>th</sup> Oct.	<i>Stable Carbenes and Diradicals: New Stabilisation and Bonding Modes</i>	<b>Dr. D. Bourrison</b> <i>Toulouse, France</i>
15 <sup>th</sup> Oct.	<i>Introductory Session</i>	<b>Dr. P. Dyer</b> <i>University of Leicester</i>
22 <sup>nd</sup> Oct.	<i>Sex and Bugs and Rock 'N' Roll</i>	<b>Dr. A. Hooper</b> <i>Rothamstead</i>
29 <sup>th</sup> Oct.	<i>Literature Discussion Session</i>	<b>Ms. N. Patel</b> <b>Mr. M. Hanton</b>
5 <sup>th</sup> Nov.	<i>Literature Discussion Session</i>	<b>Mr. P. Griffith</b> <b>Mr. D. Harding</b>
14 <sup>th</sup> Nov.	<i>Designing Catalysts for Polymer Synthesis</i> <i>RSC Joseph Chatt Lecture</i>	<b>Prof. V. C. Gibson</b> <i>Imperial College</i>
26 <sup>th</sup> Nov.	<i>Literature Discussion Session</i>	<b>Mr. G. Barth</b> <b>Mr. M. Dix</b>
3 <sup>rd</sup> Dec.	<i>Organometallic Synthesis, Catalysis and Green Chemistry</i> <i>Research in Leicester</i>	<b>Dr. G. Solan</b> <b>Dr. P. Dyer</b>
10 <sup>th</sup> Dec.	<i>The Electronic Structure of the Active Sites of Molybdoenzymes</i>	<b>Dr. J. McMaster</b> <i>Univ. of Nottingham</i>

## A 8

## Inorganic Seminar Programme (Winter/Spring 2002)

<b>Date</b>	<b>Title</b>	<b>Speaker</b>
21 <sup>st</sup> Jan.	<i>Literature Discussion Session</i>	<b>Mr. C. Davies</b> <b>Mr. J. Sherrington</b> <b>Mr. T. Reeve</b> <i>Chair: Mr. B. Croxtall</i> <i>Main questioners:</i> <b>Miss N. Patel</b> <b>Miss S. Kandola</b> <b>Mr. S. Suhard</b>
28 <sup>th</sup> Jan.	<i>"The Application of Very Low Temperature Crystallography to Chemical Problems"</i>	<b>Prof. J. Howard</b> <i>University of Durham</i>
4 <sup>th</sup> Feb.	<i>1<sup>st</sup> Year Outlines</i>	<b>Miss A. Hickman</b> <b>Miss K. Sharpe</b> <b>Mr. J. Pelletier</b>
11 <sup>th</sup> Feb.	<i>"High Activity Catalysts for C-C Bond Formation"</i>	<b>Dr R. Bedford</b> <i>University of Exeter</i>
18 <sup>th</sup> Feb.	<i>1<sup>st</sup> Year Outlines</i>	<b>Mr. A. West</b> <b>Miss R. Chaggar</b> <b>Mr. O. Duaij</b>
25 <sup>th</sup> Feb.	<i>"The New World of Phospha-Organometallic Chemistry"</i>	<b>Prof. J. Nixon</b> <i>University of Sussex</i>
4 <sup>th</sup> March	<i>"Compounds with Novel Boron-containing Ligands: Transition Metal Complexes of Boron and [1]Bora-metallophenanes"</i>	<b>Dr. H. Braunschweig</b> <i>Imperial College</i>
11 <sup>th</sup> March	<i>Literature Discussion Session</i>	<b>Mr. B. Croxtall</b> <b>Mr. S. Suhard</b> <b>Miss S. Kandola</b> <i>Chair: Miss N. Patel</i> <i>Main questioners:</i> <b>Mr. C. Davies</b> <b>Mr. T. Reeve</b> <b>Mr. M. Hanton</b>
18 <sup>th</sup> March	<i>Inorganic Chemistry Research at Leicester (II)</i>	<b>Dr D. Davies</b> <b>Dr E. Raven</b> <i>University of Leicester</i>

A 9

**Inorganic Seminar Programme (Spring/Summer 2002)**

<b>Date</b>	<b>Title</b>	<b>Speaker</b>
29 <sup>th</sup> April	Literature Discussion Session	<b>Mr A. West</b> <b>Miss R. Chaggar</b> <b>Miss A. Hickman</b> <b>Chair: Miss N. Patel</b> <b>Main questioners:</b> <b>Mr O. Duaij</b> <b>Mr J. Pelletier</b> <b>Miss K. Sharp</b>
8 <sup>th</sup> May	“Ferrocene-Ligand Design”	<b>Dr N. Long</b> <i>Imperial College</i>
13 <sup>th</sup> May	Literature Discussion Session	<b>Mr O. Duaij</b> <b>Mr J. Pelletier</b> <b>Miss K. Sharp</b> <b>Chair: Miss S. Kandola</b> <b>Main questioners:</b> <b>Miss A. Hickman</b> <b>Mr A. West</b> <b>Miss R. Chaggar</b>
20 <sup>th</sup> May	Transition Metal Catalysis	<b>Dr M. Coles</b> <i>University of Sussex</i>
27 <sup>th</sup> May	3 <sup>rd</sup> Year Talk	<b>Mr M. Hanton</b> <i>University of Leicester</i>
10 <sup>th</sup> June	3 <sup>rd</sup> Year Talk	<b>Miss N. Patel</b> <i>University of Leicester</i>
17 <sup>th</sup> June	3 <sup>rd</sup> Year Talk	<b>Mr J. Sherrington</b> <i>University of Leicester</i>
24 <sup>th</sup> June	3 <sup>rd</sup> Year Talk	<b>Mr B. Croxtall</b> <i>University of Leicester</i>

## A 10

**Inorganic Seminar Programme (Autumn/Winter 2002)**

<b>Date</b>	<b>Title</b>	<b>Speaker</b>
16 <sup>th</sup> Oct.	<i>Theoretical and Experimental Studies of NO-Containing Complexes</i>	<b>Dr. Timothy Wright</b> <i>University of Sussex</i>
21 <sup>st</sup> Oct.	<i>Adventures in Organometallic Polymer Chemistry</i>	<b>Prof. Paul Raithby</b> <i>University of Bath</i>
28 <sup>th</sup> Oct.	<i>Transition Metal Complexes and their Interaction with DNA</i>	<b>Dr. C. Metcalfe</b> <i>University of Leicester</i>
4 <sup>th</sup> Nov.	<i>Leicester Half-Day Catalysis Symposium</i>	<b>Prof. Robert Grubbs</b> <b>Prof. Roger Sheldon</b> <b>Professor Martin Wills</b> <b>Dr. David Davies</b>
13 <sup>th</sup> Nov.	<i>Materials Synthesis using Supercritical and Dense Gas Solvents</i>	<b>Dr. Andrew Cooper</b> <i>University of Liverpool</i>
18 <sup>th</sup> Nov.	<i>Synthesis of Conjugated Polymers for Polarised Electroluminescence</i>	<b>Dr. Mike Turner</b> <i>University of Sheffield</i>
9 <sup>th</sup> Dec.	<i>The Role of Transition Metal Boryl Complexes in Catalysed Borylations</i>	<b>Prof. Todd Marder</b> <i>University of Durham</i>

## A 11

**Inorganic Seminar Programme (Spring/Summer 2003)**

<b>Date</b>	<b>Title</b>	<b>Speaker</b>
10 <sup>th</sup> Feb.	<i>Metal Alkyne Complexes in Asymmetric Synthesis</i>	<b>Dr. Steve Christie</b> <i>University of Loughborough</i>
26 <sup>th</sup> Feb.	<i>Very Active Planar Chiral Catalysts for Asymmetric Synthesis</i>	<b>Dr. Chris Richards</b> <i>University of London</i>
3 <sup>rd</sup> March	<i>Exploiting the Potential of Carbon Dioxide in synthetic Organic Chemistry</i>	<b>Dr. Chris Rayner</b> <i>University of Leeds</i>
11 <sup>th</sup> March	<i>Literature Discussion Session</i>	<b>Mr. B. Croxtall</b> <b>Mr. S. Suhard</b> <b>Miss S. Kandola</b> <i>Chair: Miss N. Patel</i> <b>Main questioners:</b> <b>Mr. C. Davies</b> <b>Mr. T. Reeve</b> <b>Mr. M. Hanton</b>
17 <sup>th</sup> March	<i>Molecular Design of Precursors for the CVD of Electronic Materials</i>	<b>Dr. Claire Carmalt</b> <i>University College London</i>
18 <sup>th</sup> March	<i>Inorganic Chemistry Research at Leicester (II)</i>	<b>Dr D. Davies</b> <b>Dr E. Raven</b> <i>University of Leicester</i>
12 <sup>th</sup> May	<i>Functionalised N-Heterocyclic Carbene Ligands in Organometallic Chemistry and Catalysis</i>	<b>Dr. A. Danopoulos</b> <i>University of Southampton</i>
28 <sup>th</sup> May	<i>Synthesis of Heterocycles Using Copper and Cerium-Mediated Radical Cyclisations</i>	<b>Dr. Andrew Clarke</b> <i>University of Warwick</i>
2 <sup>nd</sup> June	<i>Shedding Light on Biological Systems: The Development of Dinuclear Lanthanide Probes</i>	<b>Dr. Sarah Heath</b> <i>University of Manchester</i>
9 <sup>th</sup> June	<i>Catalytic Asymmetric Acylation – Studies Towards the Total Synthesis of Polyol Sesquiterpenes</i>	<b>Sr. Alan Spivey</b> <i>Imperial College</i>

A 12

**Inorganic Seminar Programme (Autumn/Winter 2003)**

<b>Date</b>	<b>Title</b>	<b>Speaker</b>
6 <sup>th</sup> Oct.	<i>Palladium and Platinum Metallocycles for Organic Synthesis</i>	<b>Dr. Chris Richards</b> <i>Queen Mary, University of London</i>
8 <sup>th</sup> Oct.	<i>NMR and Proteins</i>	<b>Prof. Iain Campbell</b> <i>University of Oxford</i>
20 <sup>th</sup> Oct.	<i>Unusual Complex Oxides and Sulphides</i>	<b>Dr. Sandie Dann</b> <i>University of Loughborough</i>
27 <sup>th</sup> Oct.	<i>Natural and Non-natural Products: Total Synthesis and Biological Applications</i>	<b>Dr. Chris Hayes</b> <i>University of Nottingham</i>
3 <sup>rd</sup> Nov.	<i>Controlling Electrons and Molecules Using Light</i>	<b>Prof. Helen Fielding</b> <i>U.C.L</i>
14 <sup>th</sup> Nov.	<i>Green Solvents for Catalysis – From Molecular Understanding to Process Design</i>	<b>Prof. dr. Walter Leitner</b> <i>Greiss Lecture</i>
17 <sup>th</sup> Nov.	<i>Physics at Leicester</i>	<b>Prof. Chris Binns</b> <i>University of Leicester</i>
24 <sup>th</sup> Nov.	<i>Scope and Potential of Chiral Electrophiles in Stereoselective Synthesis</i>	<b>Prof. Thomas Wirth</b> <i>Cardiff University</i>
8 <sup>th</sup> Dec.	<i>Bird Navigation: A Photochemical Magnetic Compass?</i>	<b>Prof. Peter Hore</b> <i>University of Oxford</i>

## A 13

**Inorganic Seminar Programme (Spring/Summer 2004)**

<b>Date</b>	<b>Title</b>	<b>Speaker</b>
12 <sup>th</sup> Jan.	<i>Exploiting Silicon Reagents in Asymmetric Reactions</i>	<b>Dr. Liam Cox</b> <i>University of Birmingham</i>
12 <sup>th</sup> Jan.	<i>Recent Developments in the Chemistry of Antimony Ligands</i>	<b>Prof. Bill Levason</b> <i>University of Southampton</i>
2 <sup>nd</sup> Feb.	<i>Synthesis of Biologically Active Compounds</i>	<b>Dr. Adam Nelson</b> <i>University of Leeds</i>
9 <sup>th</sup> Feb.	<i>Stoichiometric and Catalytic Ruthenium Carbene Species</i>	<b>Dr. Michael Whitlesey</b> <i>University of Bath</i>
23 <sup>rd</sup> Feb.	<i>3<sup>rd</sup> Leicester Half-Day Catalysis Symposium</i>	<b>Prof. P. Braunstein</b> <b>Prof. Sue Gibson</b> <b>Dr. P. Kamer</b> <b>Dr. Gregory Solan</b>
1 <sup>st</sup> March	<i>Stereoselective Synthesis of Cyclic Amines using Chiral Organolithium Species</i>	<b>Dr. Iain Coldham</b> <i>University of Sheffield</i>
15 <sup>th</sup> March	<i>Connectivity of Functionalised Nanoparticles and their Arrays</i>	<b>Prof. David Schiffrin</b> <i>University of Liverpool</i>
29 <sup>th</sup> March	<i>Synthesis and Reactivity of Organometallic Complexes</i>	<b>Dr. Polly Arnold</b> <i>University of Nottingham</i>
26 <sup>th</sup> April	<i>Polyfunctional Heterocycles and Macrocycles</i>	<b>Dr. Graham Sandford</b> <i>University of Durham</i>
10 <sup>th</sup> May	<i>Torocyclic Ligands</i>	<b>Dr. Dominic Wright</b> <i>University of Cambridge</i>
17 <sup>th</sup> May	<i>Ion Mobility Spectrometry – a Little-known Technique</i>	<b>Dr. Andy Bell</b> <i>DSTL, Porton Down</i>
31 <sup>st</sup> May	<i>New Asymmetric Routes to Chiral Heterocycles</i>	<b>Dr. Steve Allin</b> <i>University of Loughborough</i>
7 <sup>th</sup> June	<i>Catalysis with Chiral Metal Complexes</i>	<b>Dr. Peter Scott</b> <i>University of Warwick</i>

## A 14

**Conferences Attended**

<b>Date</b>	<b>Conference</b>	<b>Location</b>
Nov. 2001	SCi Conference	London
April 2002	Merck CASE conference	Southampton
April 2002	Organic Synthesis Meeting	Bristol Univ.
July 2002	Coordination Chemistry Discussion Group	Loughborough Univ.
September 2002	2 <sup>nd</sup> Postgrad. Fluorine Subject Group Meeting	Manchester
12-16 <sup>th</sup> Oct. 2002	Green Solvents for Catalysis	Bruchsal, Germany
11-15th Jan. 2003	Winter School in Organic Reactivity	Bressanone, Italy
April 2003	Merck CASE conference	Southampton
April 2003	Organic Synthesis Meeting	Bristol Univ.
June 2003	Dalton Meeting	Univ. of Nottingham
4-5 <sup>th</sup> Sep. 2003	3 <sup>rd</sup> Postgrad. Fluorine Subject Group Meeting	St. Andrews Univ.
27-31 <sup>st</sup> Mar. 2004	British Council INYS Meeting	Prague, Czech Rep.
April 2004	Organic Synthesis Meeting	Bristol Univ.
April 2004	Merck CASE Conference	Southampton
April 2004	CRYSTAL Faraday Meeting	Leicester
4-9 <sup>th</sup> July 2004	Gordon Conference on Green Chemistry	Bristol, Rhode Is., USA
2-3 <sup>rd</sup> Sep. 2004	4 <sup>th</sup> Postgrad. Fluorine Subject Group Meeting	Durham Univ.

A 15

**Presentations****Merck CASE Conference, Southampton, April 2002:**

Poster entitled Asymmetric Catalysis Using the Light Fluorous Approach

**Green Solvents For Catalysis, Bruchsal, Germany, 12-16<sup>th</sup> Oct. 2002:**

Poster entitled Asymmetric Catalysis Using Light Fluorous Ligands

**Winter School in Organic Reactivity, Bressanone, Italy, 11-15<sup>th</sup> Jan. 2003:**

Poster entitled Testing and Recovery of Light Fluorous Asymmetric Catalysts

**Merck CASE Conference, Southampton, April 2003:**

Presentation entitled Ruthenium/BINAP Systems and the Light Fluorous Approach to Catalyst Recovery

**Postgraduate Fluorine Meeting, St. Andrews, Scotland, 4-5<sup>th</sup> Sep. 2003:**

Presentation entitled Ruthenium/BINAP Systems and the Light Fluorous Approach to Catalyst Recovery

**British Council International Networking of Young Scientist Meeting, Prague, Czech Republic, 27-31<sup>st</sup> Mar., 2004**

Presentation entitled Asymmetric Catalysis Using the Light Fluorous Approach

**Merck CASE Conference, Southampton, April 2004**

Presentation entitled Asymmetric Catalysis Using the Light Fluorous Approach

**CRYSTAL Faraday Meeting, Leicester, April 2004**

Poster entitled Reactions and Recovery of Light Fluorous Asymmetric Catalysts

## A 16

**Publications and Awards**

Winner of Italian Chemical Society/University of Padova competition to attend Winter School in Organic Reactivity, Bressanone, Italy, 2003.

Winner of British Council competition to attend International Networking of Young Scientist Meeting in Prague, Czech Republic, March 2004.

Winner of Presentation prize, Merck CASE Conference, April 2004.

Winner of CRYSTAL Faraday essay competition to attend Gordon Conference on Green Chemistry in Bristol, Rhode Island, July 2004.

Winner of Marriott Studentship writing placement at Chemistry World (Royal Society of Chemistry member magazine), Cambridge, July-August 2004.

Winner of runner-up prize in the Daily Telegraph/BASF Young Science Writer awards, August 2004.

D. J. Adams, D. Gudmunsen, E. G. Hope, A. M. Stuart, A. West, *J. Fluorine Chem.*, 121, 2003, 213-217.

D. J. Adams, W. Chen, E. G. Hope, S. Lange, A. M. Stuart, A. West, J. Xiao, *Green Chem.*, 5, 2003, 118-122.

Contributing author for the publication:

Gładysz, John A. / Curran, Dennis P. / Horvath, Istvan T. (eds.), *Handbook of Fluorous Chemistry*, Wiley VCH., 1. Edition - June 2004.

E. G. Hope, A. M. Stuart, A. J. West, *Green Chem.*, 6, 2004, 345.

A. J. West, *Chemistry World*, September 2004 (numerous articles)

J. Vaughan-Spickers, M. Pellatt, E. G. Hope, A. M. Stuart, A. J. West, *International Patent*, applied for

E. G. Hope, A. M. Stuart, A. J. West, *Polyhedron*, In Preparation

A 17

**Lecture Courses Attended (2001-2002)**

<b>Title</b>	<b>Convenor</b>	<b>Term</b>	<b>Credits</b>
Inorganic Rings and Chains	Dr. P. Dyer	1	5
Supercritical Phenomena	Dr. A. Abbott	2	5
Clusters	Dr. G. Solan	2	5